

# **The role of cardiolipin in the regulation of mitochondria-dependent apoptosis**

*François Gonzalvez, M.Sc.*

*December 2007*

**This thesis is submitted to the University of Glasgow in accordance with the requirements for the degree of Doctor of Philosophy in the Faculty of Medicine Graduate School**

The Beatson Institute for Cancer Research  
Garscube Estate  
Switchback Road  
Bearsden, Glasgow

Faculty of Medicine Graduate School  
University of Glasgow

*A ma famille*  
*(To my family)*

## ABSTRACT

Mitochondria are known as the powerhouse of the cell due to their central role in energy generation and as the site of key metabolic pathways. Over the past 15 years, it has become unequivocally clear that most pro-apoptotic stimuli require a mitochondria-dependent step, involving the permeabilisation of the mitochondrial outer membrane to apoptogenic factors, such as cytochrome *c* and Smac/DIABLO. The release of these factors into the cytosol is tightly regulated by proteins of the Bcl-2 family and results in the activation of the caspase cascade, leading to cell death. This event is considered as a point of no return in the apoptotic pathway and is often inhibited in cancer.

Cardiolipin (CL) is a mitochondria-specific phospholipid that contains four acyl-chains. CL has been implicated in many of the mitochondria-dependent steps that lead to the release of apoptogenic factors including interaction with the Bcl-2 family protein tBid, Bax-dependant mitochondrial outer membrane permeabilization and cytochrome *c* release. Despite this growing body of evidence, the mechanism by which CL and its fatty acyl chain composition regulate mitochondrial apoptotic pathways remains unresolved, mostly due to the lack of cellular model. Tafazzin is a mitochondrial enzyme, which is mutated in Barth syndrome (BTHS) and is involved in the maturation process of CL. In BTHS, loss of tafazzin activity results in a decrease in mature CL, making it a good model to investigate the role of CL in apoptosis.

Using BTHS patients-derived lymphoblastoid cells and HeLa cells in which *tafazzin* was stably knocked-down using RNA interference, this study provides the first evidence that mature CL are required for an efficient extrinsic apoptotic pathway in type II cells. Further investigation of the impaired apoptotic pathway revealed that the major block is in the activation of caspase-8. In this work, mature CL was identified as a crucial component of a mitochondrial platform required for caspase-8 translocation, oligomerization and activation following Fas signalling in type II cells. These results support a model in which once the first cleavage of procaspase-8 occurs at the DISC, the p43/p10 heteromer product translocates and inserts into the mitochondrial membrane in a CL-dependant manner. In the mitochondria, caspase-8 further oligomerizes and auto-cleaves to adopt its fully active form p18/p10.

Additionally, it is shown here that mature CL is required for the physiological association of full-length Bid, the major caspase-8 cleavage substrate, with mitochondria. Thus, Bid is directly available for active caspase-8 on the mitochondrial surface where it cleaves into tBid, which in turn inserts into the mitochondrial outer membrane and induces cytochrome *c* release. Therefore, by tethering full-length Bid on mitochondria and by providing an activation site for caspase-8 following Fas signalling, CL brings together both the enzyme and its substrate and provides a platform from which the mitochondrial phase of apoptosis is launched.

In summary, the data presented in this thesis provide the first evidence that mature CL participates in a new mitochondrial associated platform, called the “mitosome”, required for the activation of caspase-8 in type II cells.

## ACKNOWLEDGEMENTS

During the four years of my PhD I have been sponsored by Cancer Research UK, for which I am really grateful.

I would like to thank my supervisor, Eyal Gottlieb, for all the help and support during my time in the lab. Also, for giving me the opportunity to express myself and to defend my ideas. You told me one day that “we work better under pressure” and I realize now that you were definitely right.

I am also really grateful to my advisor, Kevin Ryan, for his constant advice and guidance all along my PhD. I would especially like to thank Patrice Petit for transmitting his passion of science and for always supporting me. I wish to thank all the past and present colleagues of R12. A big HUG and THANK YOU for Mary Sweetie, Elaine, Zinezine, Lisa, Dan and Raoulito. This journey would have never been the same without you guys. During my time in the Beaston I had the chance to meet and to work with the best people, and I am grateful for their kindness and friendship.

I would like to thank Susie for her continued love and support. Well done you! Many thanks to the Grahams for adopting me into their clan. I promise I will wear the kilt soon.

Finally, I would like to dedicate all this work to my parents who have always believed in me.

## DECLARATION

I hereby declare that all the work presented in this thesis is the result of my own independent investigation unless otherwise stated.

This work has not already been accepted for any degree, and is not being currently submitted for any other degree.

François Gonzalvez

# TABLE OF CONTENTS

<b>ABSTRACT</b> .....	<b>3</b>
<b>ACKNOWLEDGEMENTS</b> .....	<b>5</b>
<b>DECLARATION</b> .....	<b>6</b>
<b>TABLE OF CONTENTS</b> .....	<b>7</b>
<b>LIST OF FIGURES AND TABLES</b> .....	<b>10</b>
<b>ABBREVIATIONS</b> .....	<b>12</b>
<b>CHAPTER 1 INTRODUCTION</b> .....	<b>15</b>
1.1 <i>Apoptosis: historical overview and definition</i> .....	16
1.2 <i>Morphological classification of cell death</i> .....	16
1.3 <i>Significance of apoptosis</i> .....	18
1.4 <i>Dysregulation of apoptosis and pathology</i> .....	19
1.5 <i>Apoptotic signalling pathway</i> .....	20
1.5.1 Activation of apoptosis.....	20
1.5.2 Death receptors extrinsic pathway .....	22
1.5.3 Mitochondrial intrinsic pathway .....	26
1.5.4 Mitochondria: central executioner of apoptosis .....	28
1.5.5 Bid and the type II death receptor signalling pathway .....	36
1.5.6 Caspase family .....	37
1.6 <i>Cardiolipin in apoptosis</i> .....	43
1.6.1 Cardiolipin synthesis .....	43
1.6.2 Barth syndrome .....	46
1.6.3 Cardiolipin localization in mitochondria.....	47
1.6.4 The role of cardiolipin in bioenergetics .....	48
1.6.5 Cardiolipin maintains the structure of the mitochondrial inner membrane .....	49
1.6.6 Cardiolipin in relation to apoptosis .....	50
1.7 <i>Apoptosis: a target in cancer therapy</i> .....	56
1.7.1 Targeting the TRAIL pathway .....	56
1.7.2 Targeting the IAPs.....	57
1.7.3 Targeting the Bcl-2 family proteins .....	58
1.8 <i>Aims</i> .....	58
<b>CHAPTER 2 MATERIALS AND EXPERIMENTAL PROCEDURES</b> .....	<b>59</b>
2.1 <i>Materials</i> .....	60
2.1.1 General reagents .....	60
2.1.2 Primers sequences .....	61
2.1.3 Antiserum .....	62
2.1.4 RNA interference oligonucleotides sequences.....	63
2.2 <i>Experimental procedures</i> .....	63

2.2.1 Plasmid constructs .....	63
2.2.2 Bacterial transformation .....	65
2.2.3 Tissue culture .....	65
2.2.4 Transfection of cell lines .....	67
2.2.5 Retroviruses infection of lymphoblastoid cell lines .....	68
2.2.6 Establishment of stable transfected HeLa cell lines .....	68
2.2.7 Preparation of cell lysates for protein analysis .....	69
2.2.8 Protein sample preparation .....	69
2.2.9 SDS-PAGE .....	70
2.2.10 Western blotting .....	70
2.2.11 RNA interference .....	71
2.2.12 RNA extraction .....	71
2.2.13 Reverse Transcriptase - Polymerase Chain Reaction (RT-PCR) .....	72
2.2.14 Quantitative Real Time Polymerase Chain Reaction (qRT-PCR) .....	72
2.2.15 Induction of cell death .....	73
2.2.16 Assessment of cell death .....	73
2.2.17 Mitochondrial membrane potential assay .....	74
2.2.18 Monitoring of caspase activities .....	74
2.2.19 Transmission electron microscopy .....	75
2.2.20 Fluorescent microscopy .....	75
2.2.21 Preparation of mitochondrial fractions from anti-Fas antibody treated HeLa cells .....	76
2.2.22 Isolation of mitochondria for in vitro assay .....	76
2.2.23 Oxygen consumption monitoring .....	76
2.2.24 In vitro cytochrome c release assay .....	77
2.2.25 In vitro Bak oligomerization assay .....	77
2.2.26 Mitochondrial-caspase-8 oligomerization assay .....	78
2.2.27 Mitochondrial membranes insertion assay .....	78
2.2.28 CL and MLCL analysis .....	78
<b>CHAPTER 3 ROLE OF CL IN APOPTOSIS .....</b>	<b>80</b>
3.1 <i>Introduction</i> .....	81
3.2 <i>Results</i> .....	82
3.2.1 Characterisation of BTHS lymphoblastoid cells .....	82
3.2.2 Knocking-down tafazzin decreases CL level and protects cells from extrinsic apoptosis. ....	94
3.2.3 Full-length tafazzin is required for CL remodelling and Fas-induced apoptosis. ....	105
3.3 <i>Discussion</i> .....	113
<b>CHAPTER 4 MECHANISM OF APOPTOSIS RESISTANCE IN TAFAZZIN- DEFICIENT CELLS .....</b>	<b>118</b>
4.1 <i>Introduction</i> .....	119
4.2 <i>Results</i> .....	119
4.2.1 Inhibition of mitochondrial apoptosis in tafazzin-deficient cells .....	119
4.2.2 Tafazzin-deficient mitochondria are able to release cytochrome c in vitro .....	127
4.2.3 tBid interacts with and releases cytochrome c from tafazzin-deficient mitochondria .....	129
4.2.4 Inhibition of caspase-8 activity in tafazzin-deficient cells .....	133

4.2.5 Mitochondrial caspase-8 translocation is inhibited in tafazzin-deficient cells.....	138
4.2.6 Mitochondrial caspase-8 translocation is an early apoptotic event independent of Bid .....	142
4.3 <i>Discussion</i> .....	142
<b>CHAPTER 5 ACTIVATION OF CASPASE-8 AT THE MITOCHONDRIAL MEMBRANE: THE ACTIVATING PLATFORM MODEL.....</b>	<b>148</b>
5.1 <i>Introduction</i> .....	149
5.2 <i>Results</i> .....	150
5.2.1 Caspase-8 oligomerizes on mitochondrial-membranes following Fas activation .....	150
5.2.2 Active caspase-8 induces cytochrome c release in a CL dependant manner .....	150
5.2.3 Caspase-8 induced cytochrome c release is regulated by the Bcl-2 family proteins .....	154
5.2.4 Active caspase-8 induced cytochrome c release through the cleavage of mitochondrial-associated Bid .....	156
5.2.5 CL is required for the physiological association of full-length Bid with the mitochondria.....	156
5.3 <i>Discussion</i> .....	159
<b>CHAPTER 6 GENERAL DISCUSSION AND SUMMARY .....</b>	<b>163</b>
<b>APPENDIX I .....</b>	<b>169</b>
<b>REFERENCES .....</b>	<b>179</b>

## LIST OF FIGURES AND TABLES

Figure 1-1: Extrinsic and intrinsic pathway of apoptosis.....	21
Figure 1-2: The Death Inducing Signalling Complex. ....	24
Figure 1-3: Mitochondrial oxidative phosphorylation.....	27
Figure 1-4: The Bcl-2 family of proteins (adapted from Cory <i>et al</i> , 2003). ....	31
Figure 1-5: Domain organization of human caspases. ....	38
Figure 1-6: Molecular structure of cardiolipin. ....	44
Figure 1-7: Remodelling cycle of cardiolipin. ....	45
Figure 1-8: Cardiolipin at the mitochondrial contact sites. ....	48
Figure 1-9: Dissociation of cardiolipin-cytochrome <i>c</i> interaction during apoptosis....	52
Figure 1-10: Cardiolipin serves as a docking platform for the Bcl-2 proteins tBid. ....	53
Figure 1-11: Cardiolipin and permeabilization of the mitochondrial outer membrane. ....	55
Figure 3-1: Alteration of CL composition in Barth syndrome (BTHS) lymphoblastoid cells.....	84
Figure 3-2: Mitochondria from BTHS patients present an abnormal morphology.....	86
Figure 3-3: Defective OXPHOS in BTHS mitochondria. ....	88
Figure 3-4: BTHS cells are resistant to extrinsic apoptotic stimuli. ....	91
Figure 3-5: BTHS cells are sensitive to intrinsic apoptotic stimuli. ....	93
Figure 3-6: HeLa cells display a type II response to Fas-induced apoptosis.....	95
Figure 3-7: Tafazzin localizes to the mitochondria and is efficiently ablated by a specific <i>tafazzin</i> siRNA.....	97
Figure 3-8: Transient depletion of tafazzin using siTaz does not affect the level of CL and the sensitivity to Fas-mediated apoptosis. ....	100
Figure 3-9: Stably knockdown of tafazzin in HeLa cells using short hairpin RNA plasmid (shTaz). ....	102
Figure 3-10: Barth-syndrome like model in HeLa cells.....	104
Figure 3-11: Tafazzin-deficient HeLa cells are resistant to apoptosis. ....	106
Figure 3-12: Retroviral infection of lymphoblastoid cells. ....	108
Figure 3-13: Tafazzin $\Delta 5$ does not restore the CL composition and the sensitivity of BTHS cells to Fas-mediated apoptosis.....	109
Figure 3-14: Full length tafazzin restores the CL composition and sensitises HeLa tafazzin-deficient cells to Fas-mediated apoptosis. ....	111
Figure 4-1: Inhibition of caspase-3 activation in tafazzin-deficient HeLa cells. ....	120
Figure 4-2: Inhibition of mitochondrial membrane depolarization in Tafazzin-deficient HeLa cells.....	122
Figure 4-3: Inhibition of cytochrome <i>c</i> release in Tafazzin-deficient HeLa cells. ....	124
Figure 4-4: Inhibition of Smac/DIABLO release in tafazzin-deficient HeLa cells. ....	126
Figure 4-5: BTHS mitochondria are capable of releasing cytochrome <i>c</i> in response to BidBH3 peptide.....	128

<b>Figure 4-6: tBid induces Bak oligomerization and cytochrome c release in BTHS mitochondria.....</b>	<b>130</b>
<b>Figure 4-7: tBid interacts with mitochondria and induces Bak-oligomerization and subsequent cytochrome c release in tafazzin-deficient mitochondria.....</b>	<b>132</b>
<b>Figure 4-8: Inhibition of Bid cleavage in tafazzin-deficient cells. ....</b>	<b>134</b>
<b>Figure 4-9: Inhibition of caspase-8 activity in tafazzin-deficient cells. ....</b>	<b>136</b>
<b>Figure 4-10: Inhibition of caspase-8 cleavage in tafazzin-deficient cells. ....</b>	<b>137</b>
<b>Figure 4-11: Tafazzin is required for the autoprocessing of caspase-8 on the mitochondria.....</b>	<b>139</b>
<b>Figure 4-12: The p18 and p43 subunits of caspase-8 integrate into the mitochondrial membranes after Fas activation. ....</b>	<b>141</b>
<b>Figure 4-13: Mitochondrial caspase-8 translocation is independent of Bid.....</b>	<b>143</b>
<b>Figure 5-1: Caspase-8 oligomerizes in the mitochondrial membranes in response to Fas-activation. ....</b>	<b>151</b>
<b>Figure 5-2: Mitochondrial active caspase-8 induces cytochrome c release in a CL-dependant manner. ....</b>	<b>153</b>
<b>Figure 5-3: Caspase-8 induced-cytochrome c release is regulated by the Bcl-2 family proteins. ....</b>	<b>155</b>
<b>Figure 5-4: Caspase-8 cleaves mitochondrial-associated Bid and induces cytochrome c release.....</b>	<b>157</b>
<b>Figure 5-5: CL is required for the physiological association of full-length Bid with the mitochondria and for presenting Bid to active caspase-8.....</b>	<b>158</b>
<b>Figure 6-1: The “mitosome” model in type II cells. ....</b>	<b>166</b>
<b>Table 1 Primer sequences</b>	<b>61</b>
<b>Table 2 Primary antibodies list</b>	<b>62</b>
<b>Table 3 Secondary antibodies list</b>	<b>63</b>
<b>Table 4 RNA interference targeting sequences</b>	<b>63</b>

## ABBREVIATIONS

Ab	Antibody
ADP	Adenosine Diphosphate
AIF	Apoptosis Inducing Factor
ALPS	Autoimmune Lymphoproliferative Syndrome
ANT	Adenylic Nucleotide Translocator
ATP	Adenosine Triphosphate
BAR	Bifunctional Apoptosis Regulator
BH	Bcl-2 Homology
Bid	BH3-Interacting Domain death agonist
BidBH3	BH3 domain of Bid
BIR	Baculovirus IAP Repeat
BMH	<i>Bis</i> -MaleimidoHexane
BSA	Bovin Serum Albumin
BTHS	Barth Syndrome
CARD	Caspase Recruitment Domain
CCCP	Carbonyl Cyanide <i>m</i> -Chloro Phenyl hydrazone
CDP	Cytidine Diphosphate
CED	Cell Death gene
CHO	Chinese Hamster Ovary
CL	Cardiolipin
COXIV	Subunit 4 of the respiratory complex IV
DD	Death Domain
DED	Death Effector Domain
DISC	Death Inducing Signalling Complex
DMSO	Dimethylsulphoxide
DNA	Deoxyribose Nucleic Acid
$\Delta\psi_m$	Mitochondrial membrane potential
DR	Death Receptor
DTT	Dithiothreitol
EDAR	Ectodysplasin A Receptor
EndoG	Endonuclease G
ER	Endoplasmic Reticulum

FACS	Fluorescence Activated Cell Sorting
FADD	Fas-Associated Death Domain
FADH2	Flavin Adenine Dinucleotide
FasL	Fas Ligand
FLASH	FLICE-Associated huge protein
FLICE	FADD-Homologous ICE/CED3-like protease
FLIP	FLICE-inhibitory protein
GFP	Green Fluorescent Protein
G418	Geneticin
GTP	Guanine Triphosphate
HPLC	High Performance Liquid Chromatography
HPV	Humam Papilloma Virus
IAP	Inhibitor of Apoptosis
ICE	Interleukin-1 $\beta$ converting enzyme
IgG	Immunoglobulin G
IM	Inner Mitochondrial Membrane
IMD	Integrin-Mediated Death
LB medium	Luria-Bertani medium
MIB	Mitochondria Isolation Buffer
MEF	Mouse Embryonic Fibroblast
MLCL	Monolyso-cardiolipin
MOMP	Mitochondrial Outer Membrane Permeabilization
MS	Mass Spectrometry
NAD	Nicotinamide Adenine Dinucleotide
NADP	Nicotinamide Adenine Dinucleotide Phosphate
NF- $\kappa$ B	Nuclear factor $\kappa$ B
OXPHOS	Oxidative Phosphorylation
OM	Outer Mitochondrial Membrane
PA	Phosphatidic Acid
PARP	Poly-ADP Ribose Polymerase
PBS	Phosphate Buffer Saline
PC	Phosphatidyl-Choline
PCR	Polymerase Chain Reaction
Q-PCR	Real-Time PCR
RT-PCR	Reverse-Transcriptase PCR

PE	Phosphatidyl-Ethanolamine
PG	Phosphatidyl-Glycerol
PGP	Phosphatidyl-Glycerol-3-Phosphate
Pi	Inorganic Phosphate
PI	Propidium Iodide
PS	Phosphatidyl-Serine
PTP	Permeability Transition Pore
RCR	Respiratory Control Ratio
mRNA	Messenger Ribose Nucleic Acid
RNAi	RNA interference
scRNA	Non-targeting siRNA pool
shRNA	Short hairpin RNA
ROS	Reactive Oxygen Species
SDHB	Subunit B of the respiratory complex II
SDS	Sodium Dodecyl Sulfate
SMAC	Second Mitochondria-Derived Activator of Caspases
TAZ	<i>Tafazzin</i> gene
tBid	Truncated Bid
TCA	Tricarboxylic Acid
TEM	Transmission Electron Microscope
TMRE	Tetramethylrhodamine ethyl ester perchlorate
TNF	Tumour Necrosis Factor
TNFR	Tumour Necrosis Factor Receptor
TRAIL	TNF-Related Apoptosis-inducing ligand
VDAC	Voltage-Dependent Anion Channel

# **CHAPTER 1 INTRODUCTION**

# 1 Introduction

## 1.1 *Apoptosis: historical overview and definition*

The first recognition of physiological cell death mechanisms appeared in the mid-nineteenth century with the observation by Carl Vogt in 1842, that cells die during the development of the nervous system [1]. Developmental biologists then realized that cell death was essential for successful embryogenesis and metamorphosis, both in insects and mammals. In 1965, Lockshin and Williams established a new concept, programmed cell death, which was used to describe the controlled and sophisticated mechanism of cell-destruction occurring during insect development [2]. The term “apoptosis” was introduced in 1972 by Kerr and colleagues [3], who recognized that the morphological features of liver and lymphocyte cells dying, due to toxin or hormones, resembled that described for the developmental cell death by the embryologist Glucksmann earlier [4]. Apoptosis was named after an ancient Greek word, referring to the process of leaves falling from trees, to describe the novel cell death phenotype, morphologically distinct from classical necrosis. Apoptosis is now considered to be a genetically controlled process of cell death, essential for the development and life of multicellular organisms.

## 1.2 *Morphological classification of cell death*

A cell is considered dead when it has lost the integrity of the plasma membrane. Three distinct cell death morphologies have been defined in mammals: apoptosis, necrosis and autophagy. Apoptotic cells are characterized by stereotypical morphological changes [5]. The cell rounds up and shrinks and its chromatin condenses (piknosis) and fragments (karyorrhexis). The plasma membrane becomes blebbed and the cell is fragmented into membrane-enclosed structures, called apoptotic bodies, which contain cytosolic, nuclear and organelle material. *In vivo*, apoptotic bodies are recognized and engulfed by macrophages or other specialized phagocytes and thus removed from the tissue to avoid an inflammatory reaction. It is of note that in tissue culture, apoptotic cells progress into secondary necrosis resulting in the loss of membrane integrity. Those phenotypic features are the consequences of biochemical events, in particular the activation of endonucleases,

responsible for internucleosomal cleavage of the DNA (DNA ladder), and the activation of a family of cysteine-dependant aspartate-specific proteases, called caspases, that mediate the degradation of specific cellular proteins. Caspase activation constitutes one of the molecular features of the apoptotic pathway and is therefore frequently used as a marker of apoptosis. Another biochemical hallmark of apoptosis is the externalization of phosphatidyl-serine (PS) to the outer leaflet of the plasma membrane where it forms a recognition signal for phagocytes. Apoptosis is an energy-dependant process requiring ATP for optimal caspase activation.

Necrosis is characterized morphologically by an overall swelling of the cytoplasm (oncosis) and organelles and a rapid loss of the plasma membrane. *In vivo*, leaking of cellular contents after membrane rupture initiates an inflammation reaction in the affected-tissue. In contrast to apoptosis, necrosis has long been considered a non-programmed, passive, form of cell death initiated by cellular “accidents” such as toxic insults or physical damage. However, over the past few years, accumulating evidence in favour of a physiological role of necrosis suggests that its activation and process may also be tightly regulated [6]. Necrosis was described during bones development and it also participates in intestinal epithelial cell homeostasis [7, 8]. Moreover, the fact that inhibition of apoptosis can induce necrotic cell death [9] has indicated that necrosis, may in some circumstance, constitute a default and programmed-cell death mechanism which substitutes for failed apoptosis [6, 10].

Autophagy is morphologically defined by the formation of double membrane vesicles or autophagosomes that encapsulated cytosolic contents and organelles such as mitochondria [11]. Fusion of the autophagosome with the lysosome results in the degradation of its contents by lysosomal enzymes. These vesicles are distinguishable by electron microscopy from the endosomes, lysosomes or apoptotic blebs [11]. Autophagy was first characterized as a survival strategy employed by yeasts to survive nutrient deprivation, by providing amino acids and other essential components to the cells [12]. It is an evolutionary conserved mechanism that plays a role in the turnover and elimination of long-lived proteins and organelles [13]. Recent data indicate that autophagy is essential in the early development of *Drosophila*, *Caenorhabditis elegans* (*C.elegans*) and mice [14-16] but its precise role in this process remains to be defined. Silencing autophagic genes in mice and *C. elegans* increased cell death, supporting the idea that autophagy has a survival role

during early development. On the other hands, autophagic vesicles have also been observed in dying cells where the apoptotic pathway was inhibited [17, 18]. As described above for necrosis, autophagy may be another alternative pathway of cell death which could be unravelled when apoptosis is inhibited. Whether or not autophagy represents a proper mechanism of cell suicide, independent of caspases, or only a survival strategy is still a matter of debate.

Although these three types of cell death are morphologically very distinct, a growing body of evidence indicate that they are tightly interconnected and the existence of common molecular regulating pathways was suggested.

### **1.3 Significance of apoptosis**

Apoptosis is an evolutionary conserved and regulated mechanism of programmed cell death that plays a crucial role in the development and homeostasis of multicellular organisms by eliminating superfluous, aged, damaged and infected cells. During development, many cells are produced in excess and are eliminated by apoptosis to contribute to the morphogenesis of the different tissues and organs [19]. Cell death in the interdigital mesenchymal tissue for example, results in the formation of individualized digits in animals. Other examples include the ablation of tadpole tails during amphibian metamorphosis, massive neuronal cell death in the development of the brain, deletion of uterus and Wolffian duct during the formation of the male and female reproductive organs etc. Once, development is complete, the viability of multicellular organisms is constantly controlled by a balance between cell proliferation and cell death. In human body, one hundred thousands cells are removed every second by apoptosis and the same number is regenerated by mitosis [20]. In the immune system, apoptosis has an essential role not only in the development and maintenance of the immune repertoire, but also in the regulation of the immune response [21]. During their development, lymphocytes undergo stringent selection that results in the elimination of non functional and auto-reactive lymphocytes. In response to pathogens, the immune system rapidly activates and amplifies the number of antigen-specific lymphocytes via rapid cell division and inhibition of apoptosis. After pathogen clearance, the immune system restores its cellular homeostasis by selectively eliminating these activated lymphocytes. This phase requires the activation of the death receptor Fas (also known as CD95 or APO-

1) located at the plasma membrane and the resetting of the balance between pro- and anti-apoptotic molecules, resulting in the apoptosis of activated lymphocytes. In addition to controlling cell number, apoptosis can act to preserve tissue integrity. Aged or damaged cells with severe DNA damage that cannot be repaired undergo programmed cell death to avoid the replication of these mutations. Metazoans also use apoptosis as a mechanism of defence against viral infection. Early elimination of infected cells limits virus replication and spread to neighbouring cells. However, viruses have developed strategies to inhibit apoptosis of the host cell by expressing inhibitors of key components of the apoptotic program.

## **1.4 Dysregulation of apoptosis and pathology**

Since apoptosis is an essential mechanism required for the development and survival of metazoans, its dysregulation is involved in a plethora of human diseases [22]. Evidence indicate that insufficient apoptosis can be manifested as cancer, autoimmune lymphoproliferative syndrome (ALPS) and some metabolic disorders while accelerated cell death is evident in acute and chronic degenerative diseases, stroke, ischemic heart disease, acquired immunodeficiency, and infertility. However, the role of apoptosis in disease pathology is not always straightforward. For example, viral infections and autoimmune disorders have been correlated with either an excess or a lack in apoptotic cell death and cancer cells have the ability to evade the immune response by inducing apoptosis of immune cells.

It is now established that apoptosis plays a role in all facets of cancer development including tumour initiation, progression and during metastasis. The importance of apoptosis in cancer development emerged in the early 80s, when Tsujimoto and colleagues cloned and identified the *bcl-2* oncogene at the chromosome translocation t(14:18) in leukemic and follicular lymphoma cells [23, 24]. This translocation juxtaposes the *bcl-2* gene with the immunoglobulin heavy chain locus and results in the overexpression of *bcl-2*. In contrast to oncogenes identified at the time due to their ability to transform and immortalize cells, *bcl-2* appeared to localize to mitochondria and promote cell survival by inhibiting apoptosis [25-27].

p53 was the first tumour suppressor gene linked to apoptosis [28]. p53 mutations occur in the majority of human cancers and have been associated with advanced

tumour stage and with poor patient survival [29]. p53 was first established as a checkpoint protein involved in cell cycle arrest and maintaining genomic integrity after DNA damage [30]. The first evidence for a role of p53 in cell survival emerged in 1991 when Moshe Oren and colleagues demonstrated that reintroduction of wild type p53 into a murine myeloid leukaemic cell line could induce apoptosis [28]. Although the initial studies of bcl-2 and p53 established the importance of apoptosis in carcinogenesis, it is now clear that mutations in many apoptosis-regulators can lead to cancer. Therefore, in the past few years the identification of novel targets that reactivate apoptosis in cancer cells has been one of the major goals of cancer research. New promising targets and advance anti-cancer therapy based on the modulation of apoptosis were identified and will be discussed in *section 1.7*.

## **1.5 Apoptotic signalling pathway**

### **1.5.1 Activation of apoptosis**

Apoptosis can be triggered by a wide variety of physiological, pathogenic or cytotoxic stimuli. In mammal cells, induction of apoptosis occurs via two distinct pathways: extrinsic and intrinsic (**Figure 1-1**). The extrinsic pathway integrates extracellular signals through the binding of external ligands to death receptors located at the plasma membrane (e.g Tumour Necrosis Factor (TNF) receptor family, Fas and TNFR1). The intrinsic pathway is activated under conditions of intracellular stress (such as DNA damage, deprivation of survival signals and oxidative stress) and involves organelles to propagate death signals. Over a number of years, mitochondria have been identified as central executors of intrinsic apoptosis following a wide variety of death signals [31, 32]. Both extrinsic and intrinsic pathways lead to the activation of the cysteine-dependant aspartate-specific proteases, called caspases, which are responsible for the morphological features of apoptosis (*section 1.5.6*).

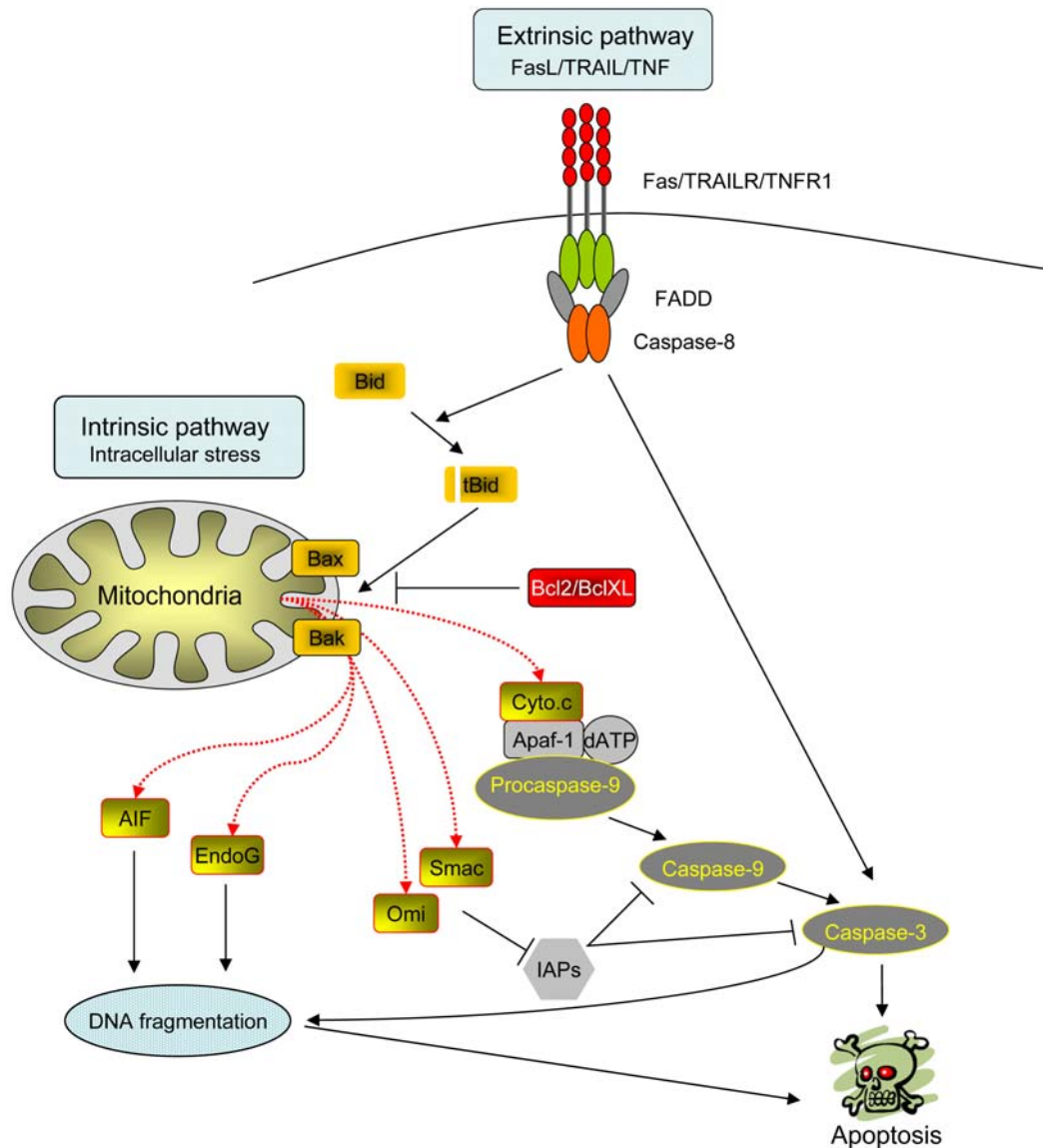


**Figure 1-1: Extrinsic and intrinsic pathway of apoptosis.**

The extrinsic apoptosis engage the cell surface death receptors such as TNFR1, Fas receptor or TRAIL. Engagement of these receptors by their specific ligand induces their trimerisation and leads to the assemblage of the DISC at the plasma membrane. In this complex, procaspase-8 is activated and in turn cleaves and activates the effector caspase-3 that degrades essential cellular proteins and confers the apoptotic morphological features. The intrinsic pathway involves mitochondria and is activated following a wide variety of intracellular stress such as DNA damage, oncogene activation, ER stress, growth factor deprivation, oxidative stress and others. Transduction of these signals requires the permeabilization of the mitochondrial outer membrane by proteins of the Bcl-2 family and results in the release of mitochondrial apoptogenic factors to the cytosol. Once released in the cytosol, these apoptogenic factors including cytochrome c, Smac/DIABLO, AIF, EndoG and Omi/Htra2 activate different cellular programs committing the cells to death. In type II cells, the BH3-only protein Bid relays the signals from the death receptors to the mitochondria and therefore links the extrinsic and intrinsic pathway.

## **1.5.2 Death receptors extrinsic pathway**

### **1.5.2.1 The death receptors family**

The death receptors (DR) belong to the TNF receptor superfamily and are involved in the transduction of either apoptotic or survival signals. DR are transmembrane proteins composed of cysteine-rich extracellular domains and a characteristic cytoplasmic region composed of around 80 residues called death domains (DD) essential for transmitting the death signal. To date, eight members have been described: TNF receptor 1 (also known as DR1), Fas receptor (also known as DR2, CD95 and APO-1), DR3 (APO-3), TNF-Related Apoptosis-Inducing Ligand receptor 1 (also known as TRAILR1 and DR4), TRAILR2 (also known as DR5 and KILLER), DR6, ectodysplasin A receptor (EDAR) and nerve growth factor receptor (NGFR) [33]. Two types of DR can be identified depending on their signalling complex. Fas receptor, TRAILR1 or TRAILR2 activation leads to the formation of the Death Inducing Signalling Complex (DISC) and results in the induction of apoptosis [34, 35]. The others, TNFR1, DR3, DR6 and EDAR recruit different set of molecules and transduce, in addition to apoptosis, other cellular responses including proliferation, differentiation and survival [36]. The binding of TNF to the TNFR1 can trigger the formation of the DISC but also the assembly of two other signalling platforms that ultimately result in the activation of two major transcription factors, the nuclear factor  $\kappa$ B (NF- $\kappa$ B) and c-Jun. These transcription factors are responsible for the expression of genes involved in diverse biological processes such as, cell growth and death, development, oncogenesis and immune responses [37]. To date, out of the DR family, the Fas receptor signalling pathway is the most well-characterized [35].

### **1.5.2.2 Fas receptor signalling pathway**

The Fas receptor is a widely expressed glycosylated transmembrane protein essential for the regulation of apoptosis in a large variety of tissues. As already mentioned, the Fas receptor signalling pathway participates in downregulation of the immune response by eliminating activated T and B lymphocytes after clearance of the pathogen, but it also plays an important role in the control of cellular homeostasis in other organs, such as liver [38]. Under physiological conditions, Fas-mediated

apoptosis is activated by the binding of the natural ligand, Fas Ligand (FasL) to its receptor Fas. FasL exists in two forms, a transmembrane form expressed on the surface of cells and a trimeric soluble form generated by the cleavage of the membrane-bound form by metalloproteases. Fas activation can also be artificially induced by the addition of anti-Fas antibodies (Ab) [39]. Ligation of FasL or anti-Fas Ab changes the conformation of the receptor and results in clustering of the receptor [40]. This oligomerization, likely a trimerization, is required for the recruitment of the DISC at the plasma membrane and for the engagement of the cell death machinery [41].

### 1.5.2.3 The Death Inducing Signalling Complex

The DISC was first described in 1995 by Krammer and Peter as a complex of proteins that were recruited to the activated Fas-receptor [41]. These proteins have been identified since and have been shown to associate within the complex via homotypic contacts involving the presence of specific domains (**Figure 1-2**). The DISC consists of oligomerized Fas receptor, the Fas-Associated Death Domain protein (FADD), the procaspase-8 (or procaspase-10) and the cellular FLICE-inhibitory protein (FLIP) [34]. After engagement of the Fas-receptor, FADD associates via its C-terminal death domain (DD) with the DD of the Fas-receptor. FADD contains another protein-protein interaction domain at its N-terminus: the Death Effector Domain (DED). FADD acts as an adaptor molecule within the complex and recruits the N-terminal DED domain of the procaspase-8, procaspase-10 and FLIP. Association of procaspase-8 to the DISC results in its activation. The mechanism whereby procaspase-8 is activated is still controversial and will be discussed in more details in the *section 1.5.6.5*. Then recruitment and activation of procaspase-8 leads to the cleavage and activation of the downstream effector caspases, such as caspase-3, and to the degradation of cellular proteins responsible for the apoptotic morphological features.

Procaspace-10 also contains a tandem of DED domains and can thus be recruited by FADD, however its role in apoptosis is not yet clear [42, 43]. Like its close homologue caspase-8, caspase-10 may serve as an initiator caspase in DR-mediated apoptosis and may drive forward the signal to the executioner caspases [44, 45]. No homologue of caspase-10 was found in mouse. In human, family-inherited inactive

mutant of caspase-10 was reported to be associated with autoimmune lymphoproliferative syndrome (ALPS) and cancer [46, 47].

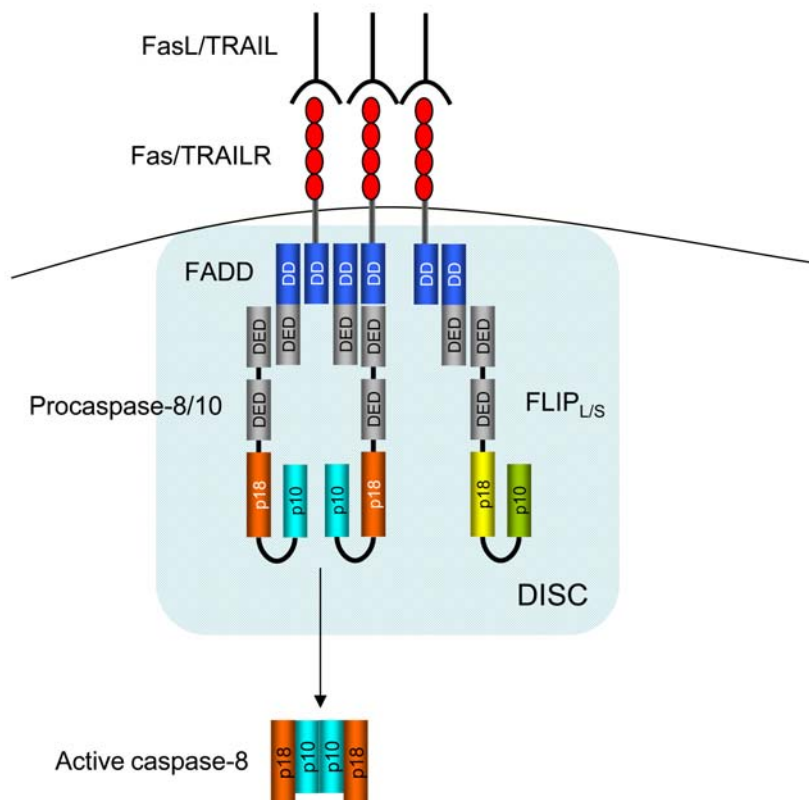


**Figure 1-2: The Death Inducing Signalling Complex.**

After ligation by their cognate ligands, death receptors oligomerize at the plasma membrane and recruit FADD through their cytosolic DD. FADD binds procaspase-8 (or procaspase-10) via its DED to form the death-inducing signalling complex (DISC). Clustering of procaspase-8 to the receptor results in its activation into the heterodimeric active caspase-8 form. FLIP competes with procaspase-8 for its recruitment to the receptor.

FLIP was originally identified as a viral death inhibitor v-FLIP expressed by the  $\gamma$ -herpes viruses to escape its elimination by infected cells [48]. v-FLIP consists of two tandem DEDs and therefore acts as a competitive inhibitor of caspase-8 for its association with FADD. To date, two cellular homologues have also been characterized in human, c-FLIP<sub>s</sub> (short form) and c-FLIP<sub>L</sub> (long form). c-FLIP<sub>s</sub>, like v-FLIP, functions as a dominant-negative inhibitor of caspase-8. However, c-FLIP<sub>L</sub> is a more complex protein that resembles the overall structure of caspase-8 but contains a mutated protease-like domain. This inactive homologue was reported to

inhibit Fas-mediated apoptosis by competing with caspase-8 for its recruitment to the DISC, but also to activate apoptosis by activating procaspase-8. The physiological relevance of c-FLIP and the mechanism whereby c-FLIP regulates Fas-mediated apoptosis at the DISC are still unclear and require more investigations.

Evidence for the physiological importance of the Fas-receptor pathway come from mouse strains and from human patients presenting a defect in genes encoding components of the DISC. Inactive mutations of the Fas locus in lymphoproliferation mice (lpr) or Fas knockout mice are associated with an excessive accumulation of CD4-/CD8- T cells (premature thymocytes), splenomegaly, massive enlargement of the lymph nodes, and a low level of platelets and red blood cells due to autoimmune reactions [49, 50]. In humans, a similar phenotype with dysfunctional Fas has been reported. Mutations in Fas receptor in children have been associated with autoimmune lymphoproliferative syndrome (ALPS) [51]. Therefore, Fas-mediated apoptosis is a fundamental process in the regulation of the immune system. The biological importance of the Fas pathway has also been highlighted by the similar phenotype of the FADD and caspase-8 knockout mice. Disruption of the FADD or caspase-8 genes in mice was lethal *in utero*, and was thought to be due to abnormalities in heart development and abdominal hemorrhage [52, 53]. FADD and caspase-8 deficient mouse embryonic fibroblasts (MEFs) are resistant to Fas- and TNF $\alpha$ -mediated apoptosis but are still sensitive to death induced by intrinsic stimuli such as DNA damage. Familial mutations of caspase-8 have also been associated with immunodeficiency in humans due to defects in T and B cells development [54]. In this context, caspase-8 deficiency is compatible with normal embryonic development but it leads to post-natal defects in the activation of naïve-lymphocytes. More recently, conditional deletion of caspase-8 in mice has revealed non-apoptotic functions of caspase-8 [55]. Caspase-8 was shown to be essential for the function of hematopoietic progenitors in bone marrow and for the differentiation of macrophages. The similarity in the phenotype of FADD and caspase-8 knockouts indicates that these two proteins are essential components of the Fas-mediated apoptosis machinery and also emphasizes the physiological importance of the extrinsic pathway in the regulation of the immune system. In addition, these data strongly indicate that FADD and caspase-8 play an essential role in cardiac and lymphohematopoietic development.

### **1.5.2.4 Type I and type II extrinsic pathways**

Depending on the cell type, two distinct Fas-signalling pathways can be activated after binding of either anti-Fas antibody or FasL [56, 57]. In type I cells, engagement of the Fas-receptor is followed by rapid DISC formation resulting in strong association and activation of procaspase-8 at the DISC. This directly activates caspase-3, which executes apoptosis. In these cells, caspase activation does not require a mitochondrial amplification step (cannot be blocked by Bcl-2 or Bcl-X<sub>L</sub>) though it does trigger mitochondrial alterations (such as cytochrome *c* release and mitochondrial depolarization). In type II cells, DISC formation and thus procaspase-8 association are low and activation of caspase-3 requires a mitochondrial-dependant step. In these cells, apoptosis is inhibited by Bcl-2 or Bcl-X<sub>L</sub>. The physiological relevance of these two apoptotic pathways has recently emerged *in vivo* using transgenic animals. Hepatocytes from mice expressing a human Bcl-2 transgene were completely protected from Fas-induced apoptosis whereas Bcl-2 transgenic T cells and thymocytes were still sensitive [58, 59]. Similar results were found in Bax/Bak double knockout mice and in Bid-deficient mice [60-62]. Moreover, overexpression of Bcl-X<sub>L</sub> in mice protected B cells against Fas-induced apoptosis [63]. All together, these data indicate that thymocytes and T cells are type I cells and hepatocytes and B cells behave like type II cells. These two pathways are equally represented in tumour cell lines [64]. Type I and type II tumour cells were shown to express different set of genes: mesenchymal-like genes in type I and epithelial-like genes in type II cells. However, the significance of these two pathways in normal cell lines and in carcinogenesis is still unclear.

### **1.5.3 Mitochondrial intrinsic pathway**

Mitochondria are intracellular double-membraned organelles that possess two well-defined compartments, an intermembrane space surrounded by the outer membrane and a matrix surrounded by the inner membrane. The inner membrane is folded into numerous cristae and under physiological conditions it is almost impermeable to ions, a property required for the energy-production process, oxidative phosphorylation. It has long been known that mitochondria are the ATP generating powerhouses of the cell and the site of other key metabolic pathways. However, in

the early 1990s it became clear that in addition to these critical life supporting roles, mitochondria play a central part in the execution of apoptotic cell death [27, 65-68].

### 1.5.3.1 Mitochondria: powerhouses of the cell

About 2 billion years ago, a symbiosis occurred between a primitive anaerobic eukaryote (proto eukaryotes) and an aerobic eubacteria. This alliance allowed each partner to exploit the energy opportunities of the rising atmospheric oxygen and gave birth to the ancestor of eukaryotic cells, the protoeukaryotes. The endosymbiotic eubacteria were to become mitochondria [69]. Mitochondria utilize oxygen to oxidize metabolic substrates and to generate energy in the form of ATP. This process, called oxidative phosphorylation (OXPHOS), forms the basis of cellular respiration. OXPHOS was first described in 1961 by Peter Mitchell as the chemiosmotic theory which earned him the Nobel Prize in chemistry in 1978. Mitchell suggested that the transfer of electrons through the different respiratory complexes generates an electrochemical gradient of protons, which constitute the driving force for ATP synthesis [70]. This hypothesis is now generally accepted as the fundamental principle of OXPHOS (**Figure 1-3**).

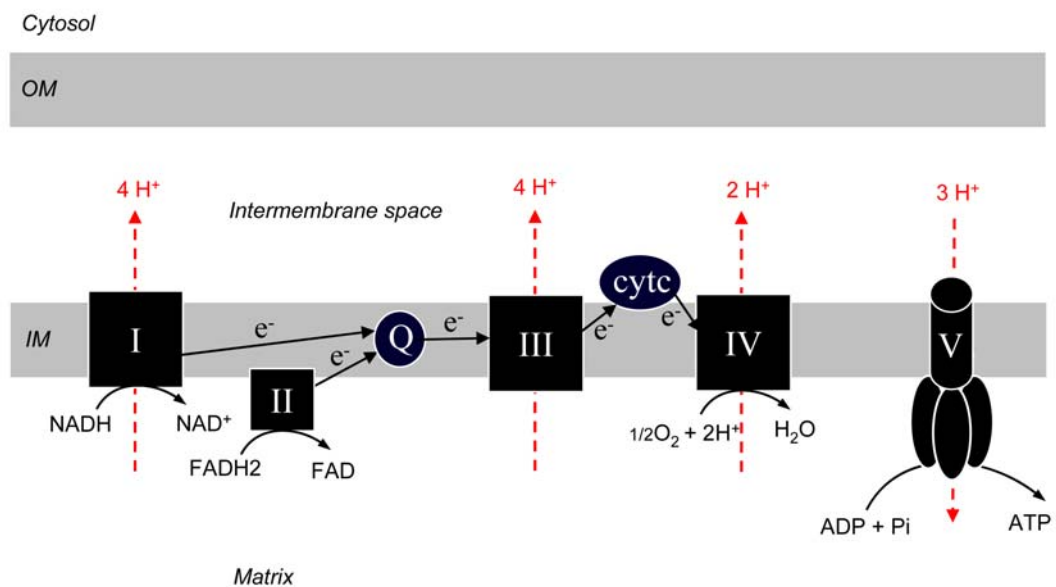


**Figure 1-3: Mitochondrial oxidative phosphorylation**

I, II, III, IV refer to the respiratory chain complexes. V denotes the ATP synthase. Q, coenzyme Q; cytc, cytochrome c; OM, outer mitochondrial membrane; IM, inner mitochondrial membrane; e<sup>-</sup>, electrons. The black arrows represent the transfer of electrons through the electron transport chain. The red arrows show the flux of protons across the mitochondrial inner membrane.

During OXPHOS, electrons are transferred from NADH or FADH<sub>2</sub> to the terminal acceptor, oxygen, via a series of oxidoreductive reactions through four respiratory chain complexes: NADH dehydrogenase (complex I), succinate dehydrogenase (complex II), cytochrome *c* reductase (complex III), and cytochrome *c* oxidase (complex IV) (**Figure 1-3**). Complex I and II transfer electrons from NADH and FADH<sub>2</sub> [products of the tricarboxylic acid cycle (TCA)], to ubiquinone, which is reduced to ubiquinol. The electrons are then transferred from ubiquinol to cytochrome *c* via complex III. Finally, complex IV transfers the electrons from reduced cytochrome *c* to oxygen, which is then reduced to water. These complexes are located within the mitochondrial inner membrane. During the electron transport, complex I, III and IV translocate protons into the mitochondrial intermembrane space establishing a proton gradient across the inner mitochondrial membrane. This generates both a pH gradient and an electric potential across the mitochondrial inner membrane, called the mitochondrial membrane potential ( $\Delta\psi_m$ ). The electrochemical gradient of protons is used by the ATP synthase complex (complex V) as the driving force to phosphorylate ADP. In total, oxidation of one NADH transfers two electrons to oxygen and leads to the expulsion of 10 protons into the mitochondrial intermembrane space, which generates between 2 and 3 ATP molecules. Under aerobic conditions, OXPHOS functions in combination with glycolysis and the TCA cycle, to generate approximately 36 molecules of ATP per molecule of glucose oxidized.

In addition to supplying energy to the cells, mitochondria carry out several essential metabolic reactions, including beta-oxidation of fatty acids and anabolic reactions such as amino acid, pyrimidine, heme, nucleotide and phospholipid synthesis. Moreover, mitochondria also participate in the calcium signalling and are the primary site of production of oxygen radicals.

## **1.5.4 Mitochondria: central executioner of apoptosis**

### **1.5.4.1 Historic overview**

A role for mitochondria in apoptosis was first suggested in the early 90's with the discoveries that the apoptotic-inhibitor Bcl-2 protein resides at the mitochondria and, that the presence of mitochondrial fractions is required for an efficient *in-vitro* apoptosis in *Xenopus laevis* oocyte extracts [27, 65]. This connection became more

evident when in 1995 Guido Kroemer demonstrated that cells undergoing apoptosis exhibited an early dissipation of their mitochondrial potential associated with production of reactive oxygen species [66, 67]. This evidence was quickly followed by the demonstration by Doug Green that cytosolic extracts from apoptotic cells were able to induce DNA fragmentation in a caspase-dependant and Bcl-2 inhibited manner [71]. Using a cell-free system, Xiadong Wang identified cytochrome *c* as the key factor required for apoptosis and proposed for the first time that mitochondria amplify apoptosis by releasing cytochrome *c* to the cytosol [68]. One year later, Don Newmeyer provided evidence that cytochrome *c* release from the mitochondria is controlled by Bcl-2 [72]. All these pioneering discoveries launched the fascinating mitochondria-mediated apoptotic research.

#### **1.5.4.2 Mitochondrial outer membrane permeabilization**

The mitochondrial intrinsic pathway is initiated following a wide variety of apoptotic stimuli including DNA damage, oncogene activation (such as Myc), endoplasmic reticulum (ER) stress, cytoskeletal damage, survival factor deprivation, DR engagement and others [31, 32]. Transduction of the apoptotic cascades requires the mitochondrial outer membrane permeabilization (MOMP) [73]. MOMP is an early pivotal event that leads to the release of proteins normally localized in the mitochondrial intermembrane space. Known as apoptogenic factors, these proteins include cytochrome *c* [68], Smac/DIABLO [74], HtrA2/Omi [75], AIF [76] and Endonuclease G [77] of which cytochrome *c* has been the most intensively studied. Once released to the cytosol, these apoptogenic factors activate different cellular programs committing the cells to death [78]. Therefore, MOMP is often considered as the point of no return in the mitochondrial apoptotic pathway [79]. The release of cytochrome *c*, Smac-DIABLO and HtrA2/Omi to the cytosol drives the activation of caspases [80, 81]. Some evidence suggests that this event is a rapid and synchronized process achieved by all the mitochondria of a given cell within five minutes [81]. In these permeabilized mitochondria, the electron transport chain remains functional and maintains the  $\Delta\psi_m$  until the activation of caspases [81, 82]. Apart from performing their pro-apoptotic function in the cytosol and nucleus, there are indications that once activated, caspases target the mitochondria and induce the degradation of respiratory complexes leading to the disruption of the electron transfer chain, loss of  $\Delta\psi_m$  and the production of reactive oxygen species [83, 84]. At the

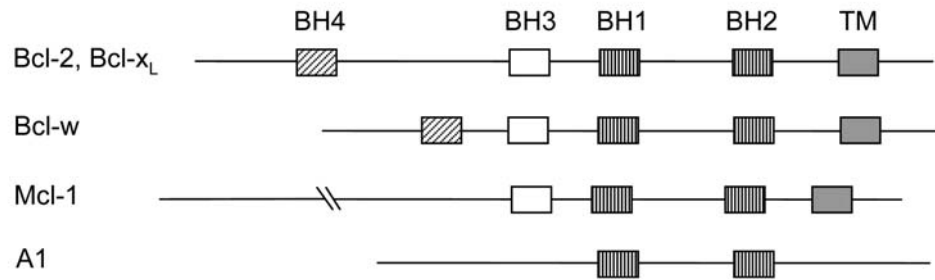
same time, caspase activation may also result in the release of the two other apoptogenic factors, AIF and Endonuclease G [80]. It is possible that the feedforward effect of caspases on the mitochondria is part of the induction of secondary necrosis described above.

Beside MOMP, the release of cytochrome *c* from mitochondria appears to be more complex than simply diffusing out through the porated mitochondrial outer membrane and is thought to involve changes in mitochondrial configuration. Most of the cytochrome *c* is entrapped within the mitochondrial cristae and therefore, remodelling of these cristae is required to allow a complete release of cytochrome *c* [85]. This remodelling is critically controlled by two mitochondrial proteins, the rhomboid intra-membrane protease PARL and the dynamin-related protein OPA1 [86, 87]. A decrease in  $\Delta\psi_m$  has also been shown to induce matrix remodelling and to increase the pool of cytochrome *c* available for release [88]. Furthermore, mitochondrial fission can occur at the same time as MOMP and the proteins regulating fusion or fission have been shown to regulate MOMP [89]. The process of MOMP, and cytochrome *c* release in particular, has been intensively investigated in the past ten years. However, the exact mechanism remains unclear.

#### 1.5.4.3 Bcl-2 family proteins

Bcl-2 family of proteins functions as a “life/death” switch that regulates MOMP and thus controls fate of cells. The Bcl-2 family of proteins are evolutionary conserved and are divided into three subfamilies according to their function and their homology shared within four Bcl-2-homology domains (designated BH1-4) (**Figure 1-4**). The anti-apoptotic members (Bcl-2, Bcl-X<sub>L</sub>, Bcl-w, Mcl-1 and A1 in humans) contain all four BH domains and they all repress the release of apoptogenic factors from mitochondria. The pro-apoptotic members promote MOMP and are subdivided into two groups, the multi-domains proteins (Bax, Bak and Bok) containing the 3 domains BH1-3 and the BH3 only proteins including eight members, Bid, Bad, Bim, Bik, Puma, Noxa, Bmf and Hrk [90].

## ANTI-APOPTOTIC PROTEINS



## PRO-APOPTOTIC PROTEINS

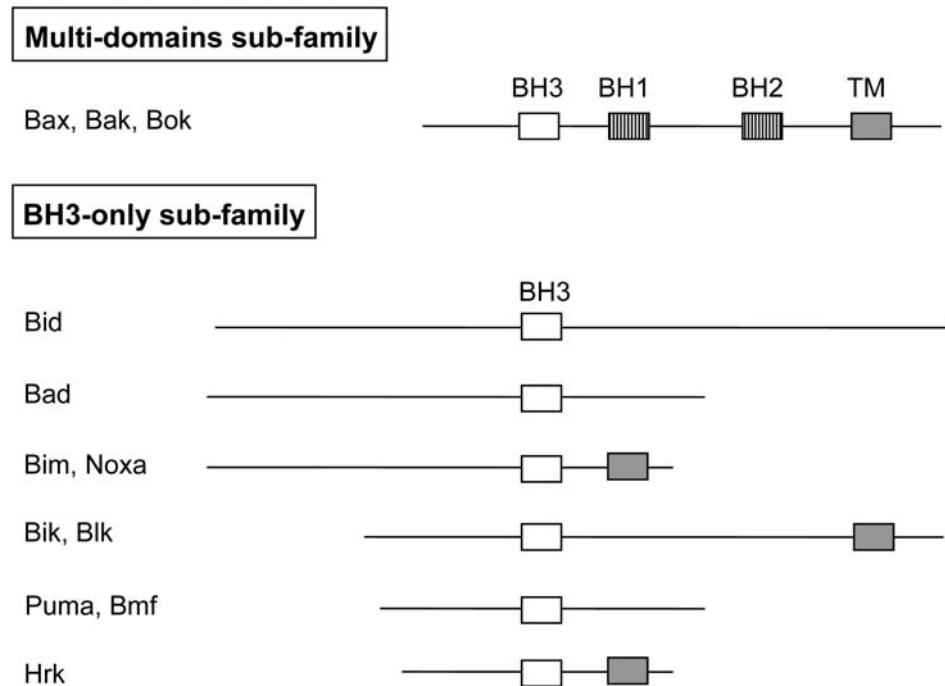


**Figure 1-4: The Bcl-2 family of proteins** (adapted from Cory *et al*, 2003).

Bcl-2 family is divided into anti-apoptotic members that promote cell survival and pro-apoptotic members. BH1 to BH4 (Bcl-2 homology domains 1-4) are regions which share relatively high similarity with Bcl-2. Many family members contain a carboxy-terminal hydrophobic transmembrane domain (TM) involved in the targeting of the proteins to intracellular membranes.

Structural studies of the Bcl-2 family members have provided many important insights into their mechanism of action during apoptosis. They all present a similar three dimensional structure consisting of 6 or 7 amphipathic alpha-helices folded into a globular domain [91]. The pro-survival members (Bcl-2 and Bcl-X<sub>L</sub>) present a

hydrophobic groove on their surface responsible for the binding of the BH3 domain of the pro-apoptotic members [92, 93]. This interaction neutralizes the pro-apoptotic members. The ability of the Bcl-2 proteins to hetero-dimerize among themselves provides the basis for the “life/death” rheostat [94]. The multi-domain pro-apoptotic proteins (Bax and Bak) are constitutively expressed, but in healthy cells they are kept inactive to avoid their lethal effect. The BH3 only proteins act as sentinels, upstream from the multi-domain members and they become activated in response to different cellular stresses specific for each member (e.g, DR engagement for Bid, ER stress for Bik, cytokine deprivation for Bim and Bad, DNA damage for Puma and Noxa etc.). Once activated, the BH3 only proteins further activate the multi-domain pro-apoptotic proteins required for MOMP. The mechanism of this activation is still debated. To date, two models have been proposed, the direct and the indirect activation model [95, 96]. It was proposed that depending on their affinity for the Bcl-2 family members, the BH3 only proteins are divided into two groups [95]. Bid and Bim interact with and directly activate the multi BH domain pro-apoptotic proteins, Bax and Bak, whereas Bad and Bik function as “sensitizers” by binding the hydrophobic pocket of the anti-apoptotic members and freeing the pro-apoptotic multi BH domain proteins. On the other hand, the indirect activation model suggests that the BH3-only proteins only antagonize the anti-apoptotic proteins and prevent their neutralization of Bax and Bak (without the need for direct activation) [96]. In any events, it is clear that appropriate balance between pro- and anti-apoptotic proteins is required for tissue homeostasis. Deregulations of this balance have been implicated in several pathologies including cancer, autoimmune disease, degenerative disorders and others.

#### **1.5.4.4 Mechanism of mitochondrial outer membrane permeabilization**

MOMP is entirely controlled by the Bcl-2 family proteins. The multi-domain proteins Bax and Bak play a central role in the execution of this process. Although, mice lacking Bax or Bak developed normally, Bax/Bak double knock-out mice died peri-natally or present severe developmental defects [61]. Moreover, cells deficient in both Bax and Bak, but not cells lacking only one of these proteins were completely resistant to various apoptotic stimuli that induce MOMP [62]. This suggests that *in vivo*, Bax and Bak play redundant roles in regulating apoptosis. Over

the past ten years, the mechanism by which Bax or Bak regulate MOMP has been extensively studied and the following model has evolved: since structures of the Bcl-2 proteins show striking similarity to the pore-forming domain of colicins and diphtheria toxins it was suggested that these proteins may have the ability to form pores in the mitochondrial outer membranes [93]. In live cells, Bax and Bak are present as inactive monomers. Bax is a cytosolic protein whereas Bak resides at the surface of mitochondria and ER [97, 98]. In response to death signals, Bax and Bak are activated by the BH3-only proteins and undergo conformational changes that induce the exposure of their N-terminal domains. This results in the stable insertion and subsequent oligomerization of Bax and Bak in the mitochondrial outer membrane [99, 100]. These oligomers are thought to permeabilize the mitochondrial outer membrane resulting in the release of cytochrome *c* from the mitochondria [99, 100]. *In vitro* experiments using artificial reconstituted membranes suggested that activated Bax induces MOMP by forming a proteo-lipidic pore with the mitochondrial phospholipid, cardiolipin (CL) [101]. The importance of cardiolipin in this process is also controversial and will be discussed in *section 1.6*.

It is worth noting that another Bax and Bak independent mechanism has also been suggested to induce MOMP. This involves the opening of a high conductance pore, the permeability transition pore (PTP) located at the contact sites between the mitochondrial outer and inner membranes [102]. The topology of such a pore remains unclear but it assumes to be composed of several proteins including VDAC (Voltage Dependant Anion Channel), ANT (Nucleotide Adenylic Translocator) and cyclophilin D [103]. Opening of this pore results in the influx of ions and small molecules into the matrix leading to osmotic swelling of the matrix and the rupture of the mitochondrial outer membrane. However a growing body of evidence, using genetic models, suggests that the PTP is not involved in MOMP occurring during apoptosis but rather participates in necrotic cell death following calcium overload and ROS production [104, 105].

#### **1.5.4.5 Execution of mitochondrial apoptotic signals**

##### ***1.5.4.5.1 Cytochrome *c* release***

The release of cytochrome *c* from mitochondria was initially shown to induce the activation of caspase-3 [68]. Once released, cytosolic cytochrome *c* binds to Apaf-1,

a protein characterized by the presence of a caspase-recruitment domain CARD and a nucleotide binding domain [106]. Binding of dATP or ATP to the nucleotide binding domain of Apaf-1 results in the oligomerization of cytochrome *c*/Apaf-1 into a 1.4 MDa multimeric complex called the apoptosome [107]. Apaf-1 then recruits, via its CARD domain, the initiator pro-caspase-9, resulting in the clustering and activation of the enzyme [108]. Therefore, the apoptosome functions as an activating platform for pro-caspase-9. Activated caspase-9 is then able to cleave and activate caspase-3 and caspase-7, which, in turn, cleave their substrates, leading to the morphological features of apoptosis [109]. Determination of the structure of the apoptosome by cryo-electron microscopy revealed a wheel-shaped complex with seven-fold symmetry [110]. Results from knockout mice model have underscored the importance of the apoptosome pathway in apoptosis. Since cytochrome *c* is an essential protein for cellular respiration it has been difficult to evaluate the importance of this protein in developmental apoptosis [111]. This issue was resolved by generating a knockin mouse expressing a mutant of cytochrome *c* (KA mutant), which is still able to transfer electron but fails to activate Apaf-1 [112]. This mutant presented a similar phenotype to that seen in *Apaf-1* and *caspase-9* knockout mice [113-115]. These mutants displayed embryonic or peri-natal lethality due to severe defects in the central nervous system. MEFs generated from these mutants were equivalently resistant to apoptotic stimulations and failed to activate the caspase cascade.

#### ***1.5.4.5.2 Smac/DIABLO and Omi/HtrA2 release***

In some cases, cytochrome *c* release is not sufficient to initiate the caspase cascade. To avoid spontaneous caspases activation, which would have a catastrophic damaging effect, cells have evolved another check-point to control the activity of caspases. In the cells, activated-caspases are kept inactive by the Inhibitor of Apoptosis Proteins (IAPs). IAPs bind to mature caspases (caspases-3, 7, 9) via their BIR (Baculovirus IAP Repeat) domains and inhibit caspase activity [116]. Murine Smac and its human ortholog DIABLO are mitochondrial proteins of 25 KDa that are released from the mitochondria simultaneously with cytochrome *c* during apoptosis [74, 117]. Once in the cytosol, Smac/DIABLO lowers the threshold for caspase activation by neutralizing the inhibitory effect of the IAPs. In fact, Smac/DIABLO binds the BIR domains via its N-terminal region and thus competes with caspases for the interaction with the IAPs [118]. However, Smac-knockout mice were viable and

cells generated from these animals responded normally to wide variety of apoptotic-stimuli [119].

Omi/HtrA2 is a mitochondrial serine-protease of 49 KDa that lowers the threshold for caspase activation in a similar fashion to Smac/DIABLO [75]. The physiological relevance of this redundancy is still unclear.

#### ***1.5.4.5.3 AIF and EndoG release***

Apoptosis-inducing factor (AIF) is a 57 KDa flavoprotein located in the mitochondrial intermembrane space that shares homology with bacterial oxidoreductases [76]. After release from the mitochondria, AIF translocates to the nucleus where it induces chromatin condensation and DNA degradation in a caspase-independent manner [76]. Disruption of AIF in mice was embryonically lethal [120]. However, in contrast with the cytochrome *c* knockin, Apaf-1 and caspase-9 knockout mice, which were lethal due to defects in brain development, AIF knockout mice died during early embryogenesis [113-115, 120]. Moreover, embryonic stem cells lacking AIF remained sensitive to a wide variety of apoptotic stimuli, ruling out a general requirement for AIF in cell death [120]. Therefore, the lethality of AIF knockout mice is more likely to be caused by general developmental defects unrelated to apoptosis but due to the requirement of AIF for mitochondrial function, such as the formation of complex I in the respiratory chain [121].

Endonuclease G (EndoG) is a 30 KDa protein that resides in the mitochondrial inter membrane space where it is thought to be involved in the replication of mitochondrial DNA [122]. By analogy with AIF, EndoG translocates from the mitochondria to the nucleus during apoptosis and directly induces DNA degradation in a caspase-independent manner [77]. However, EndoG knockout mice were viable and indicated that EndoG is not required for apoptosis [123].

The identification of AIF and EndoG first suggested that mitochondria may execute apoptosis in a caspase-independent manner. However, as mentioned previously the involvement of these two proteins in apoptosis is still uncertain. AIF and EndoG are released from the mitochondria during apoptosis, but this is likely to occur long after a cell has committed to die, after caspases activation [80].

### **1.5.5 Bid and the type II death receptor signalling pathway**

As mentioned in *section 1.5.2.4*, DR-mediated apoptosis must be amplified by the mitochondrial pathway in type II cells. In this case, the connection between the extrinsic and intrinsic pathways is established by the BH3 interacting domain death agonist protein (Bid). Bid is a 22 KDa protein, which was identified as a BH3 only pro-apoptotic member of the Bcl-2 family [124]. In healthy cells, Bid predominantly resides in the cytosol. Following Fas-receptor activation, Bid is cleaved in its N-terminal region by activated caspase-8. The p15 truncated-Bid (tBid) rapidly translocates from the cytosol to the mitochondria and triggers cytochrome *c* release [125, 126]. tBid interacts with mitochondria at the contact sites between the inner and outer membranes via a specific binding to cardiolipin (CL) [127, 128]. The model of CL as a mitochondrial “docking” site for tBid will be discussed in *section 1.6.6.3*. Targeting of tBid to mitochondrial CL is independent of its BH3-domain and leads to mitochondrial dysfunction [129, 130]. Moreover, the interaction of tBid with CL results in changes in mitochondrial configuration characterized by the opening of the cristae to the intermembrane space [85, 131, 132]. These BH3-independent events may represent a prerequisite step to predispose mitochondria to MOMP. The cytochrome *c*-releasing activity of tBid-requires the presence of either Bax or Bak [62]. Through its BH3 domain tBid activates the oligomerization of the multi-domain proteins Bax and Bak and results in the permeabilization of the mitochondrial outer membrane to cytochrome *c* and other apoptogenic factors [99, 100].

The importance of this link between the extrinsic and the intrinsic pathways was demonstrated *in vivo* using Bid knockout mice [60]. These mice survived the injection of anti-Fas antibody whereas wild-type mice died from hepatic failure due to apoptosis. Hepatocytes lacking Bid were resistant to Fas-induced apoptosis and failed to release cytochrome *c* and to activate caspases (type II cells). However, thymocytes and MEFs from these mice were still sensitive to Fas-mediated apoptosis (type I cells).

## **1.5.6 Caspase family**

### **1.5.6.1 Definition and classification**

Caspases belong to a conserved family of proteases that use a cysteine residue as a catalytic nucleophile to cleave their substrates specifically after aspartic acid residues. In metazoans, caspases play an essential role in apoptosis and inflammation. The first member of the family, caspase-1, was discovered in humans in 1992 as an important regulator of inflammation and originally called interleukin-1 $\beta$  converting enzyme (ICE) [133, 134]. The role of caspases in apoptosis emerged several months later from genetic analysis in the nematode *C. elegans*. The team of Robert Horvitz generated *C. elegans* mutants in order to identify genes involved in developmental cell death. In 1993, they cloned the first cell death gene *ced3* and showed that it encodes a cysteine protease (CED3) related to the mammalian ICE [135]. Since then, a number of caspases have been cloned from mammals and other species. Twelve caspases have now been identified in human, ten in mouse, four in chicken, four in zebrafish, seven in *Drosophila melanogaster* and four in *C. elegans* [136]. Based on their function, structure and substrate specificity, human caspases are classified into three groups (**Figure 1-5**).

### Inflammatory caspases

Caspase-1, caspase-4, caspase-5 and caspase-12



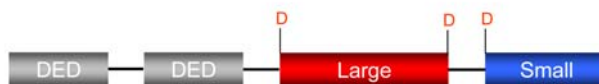
### Effector caspases

Caspase-3, caspase-6 and caspase-7



### Initiator caspases

Caspase-8 and caspase-10



Caspase-2 and caspase-9



#### Figure 1-5: Domain organization of human caspases.

Caspases have been grouped according to their function and sequence homology. The positions of aspartic acids (D) required for the maturation cleavage sites are shown in red. CARD, Caspase Recruitment Domain; DED, Death Effector Domain; Large and Small, the mature subunits of the fully active enzyme.

Group I or inflammatory caspases (caspase 1, 4, 5, 12) are characterized by the presence of a Caspase Recruitment Domain (CARD) at the N-terminus and they preferentially cleave their substrate after sequence XEHD where X is a hydrophobic residue [137]. Recently, caspase-12 has been shown to negatively regulate the inflammatory response by inhibiting the activity of caspase-1 [138, 139]. However, caspase-12 does not recognize the peptide XEHD and may specifically cleave itself at the ATAD site [140]. Group II, or effector caspases, (caspase 3, 6 and 7) recognize the tetrapeptide DEXD and are responsible for the cleavage of cellular components during apoptosis. Group III, or initiator caspases (caspases 2, 8, 9, 10) are characterized by the presence of protein-interacting domains in their N-terminus

(either CARD or DED) and they cleave specifically the sequence (I/L) EXD present in effector caspases and other substrates.

### 1.5.6.2 Caspase organization

In healthy cells, caspases are present in the cytosol as inactive precursors (also known as zymogen or pro-caspases). These precursors must undergo a maturation process in order to be activated. The structure of pro-caspases is highly conserved (**Figure 1-5**). Pro-caspases are composed of a pro-domain at the N-terminus and two C-terminal active subunits, one large (17-20 kDa) and one small (10-12 kDa). These different domains are separated by a linker peptide containing caspase cleavage sites that participate in the maturation process of the zymogen. Initiator caspases contain long pro-domains (>90 amino acids) with CARD or DED motifs (**Figure 1-5**). These motifs participate in interactions with other proteins and are essential for the transmission of the apoptotic signal. Conversely, effector caspases possess short pro-domains limited to 20-30 amino acids. During apoptosis, caspases undergo a hierarchical cascade of activation from the initiator to the effector caspases. Active caspases have a highly conserved, dimeric structure resulting from the association of two identical catalytic subunits. Each catalytic subunit contains one active site and is composed of one large and one small active domains. Upon maturation, pro-caspases are proteolytically processed at the cleavage site located between the large and the small subunits. In the past few years, the mechanism of caspase activation has been extensively investigated and debated. Considering that active caspases contain large and small domains derived from the zymogen, it has been assumed that all caspases are activated by proteolytic cleavage of their inter-subunit linker [141]. However, it is now well established that initiator and effector caspases are activated via two distinct processes.

### 1.5.6.3 Activation of the initiator caspases

Initiator caspases are the first to be activated during apoptosis, and they initiate the cascade of caspases that culminate in the degradation of essential cellular proteins by activating the executioner caspases. At first, initiator caspases were thought to be activated by induced proximity where the assembly of multiprotein complexes (PIDDosome for caspase-2, DISC for caspase-8, apoptosome for caspase-9) brings

together multiple identical pro-caspases leading to their autoprocessing. This model is supported by several observations, which demonstrated the cleavage of the active subunits during the formation of fully active initiator caspases [142]. Recently however, a growing body of evidence has led to the re-evaluation of this activation process, and a refined version of the proximity-induced model has been proposed [143-145]. Initiator caspase zymogens exist in the cytosol as latent monomers. After induction of apoptosis, the recruitment of these monomers to the activating complexes (such as DISC or apoptosome) effectively increases their local concentration allowing monomers to adopt a dimeric active conformation [143-145]. In this model, known as the proximity-induced dimerization, the dimerization provides essential active site rearrangements and thus is considered as a prerequisite for the activation of the initiator caspases. Proteolysis of the inter-subunit linkers is also required for the activation of the enzyme but it occurs after dimerization of the zymogen [143]. Whereas dimerization is sufficient to trigger self-processing of the initiator caspases, their auto-cleavage alters their substrate specificity and favours processing of the effector caspases [143, 146]. In other words, in the proximity-induced dimerization model, processing of an initiator caspase is not sufficient to induce its activation unless it is already in a dimeric configuration but it is required to drive forward the cascade of caspases. More recent works have re-investigated the activation process of initiator caspases [147, 148]. Contrary to the proximity-induced dimerization, these studies suggested that processing of caspase-8 is sufficient to drive activation of this caspase and that a dimerization platform is not a prerequisite for this process. The significance of the dimerization and cleavage of the initiator caspases is still debatable and need to be further clarified.

#### **1.5.6.4 Activation of the effector caspases**

In contrast to the initiator caspases that are monomeric as zymogens, the effector caspases are held in the cytosol as inactive dimers. Following apoptotic stimulation, effector pro-caspases are converted into catalytically active enzymes by cleavage in the linker region between their large and small active subunit. In most instances, this activating event is catalysed by active initiator caspases. The precise mechanism whereby effector caspases are activated after cleavage is still unclear. Analysis of the crystal structure of caspase-7 demonstrated that upon cleavage, the region of the active site of the enzyme undergoes conformational changes that render it accessible

to its substrates [149]. The active site is composed of four surface loops, L1 to L4, all from the same monomer and is stabilized by the L2' loop from the adjacent monomer. The catalytic cysteine is in the L2 loop. After cleavage, L2' is flipped by 180 degrees to unravel the catalytic site of L2. The high degree of similarity between the effector caspases strongly suggests that this mechanism of activation is conserved for caspase-3 and caspase-6.

Caspase-3 is the major effector caspase, which cleaves a plethora of cellular substrates during apoptosis [150]. Caspase-7 is highly similar to caspase-3 and it demonstrates similar substrate specificity [151]. Mice deficient in either caspase-3 or caspase-7 were viable on this genetic background whereas those that lacked both caspases had defects in heart development and died immediately after birth [152]. MEFs lacking both enzymes are resistant to intrinsic and extrinsic apoptotic stimuli, suggesting that caspase-3 and caspase-7 carry-out redundant, but essential functions during the execution of cell death. In stark contrast, caspase-6 presents a different substrate specificity and does not seem to be required for apoptosis [153].

### **1.5.6.5 Regulation of caspase-8 activity**

Caspase-8 was identified in 1996 as a component of the DISC. It is homologous to FADD and the ICE family and was originally named FLICE (FADD-Homologous ICE/CED3-like Protease) and MACH [154, 155]. In cells, procaspase-8 is expressed as two functional isoforms, caspase-8/a and 8/b (55 and 53 kDa, respectively) encoded by the same gene. Both zymogen are recruited to the DISC after Fas-activation [156]. Pro-caspase-8 is composed of a large prodomain containing a tandem of two DED domains and two active subunits, one large of 18 kDa and one small of 10 kDa (**Figure 1-5**).

Caspase-8 is the first caspase to be activated after DR stimulation. As mentioned above, caspase-8 activation is thought to follow the proximity induced-dimerization model. After Fas receptor engagement, cytosolic monomers of pro-caspase-8 are recruited via their DED to the DISC located at the plasma membrane. This clustering results in the dimerization of the zymogens which then acquire a limited capacity of enzymatic activity [144, 146]. In this context, dimerization favours an enzymatically competent conformation and promotes autoprocessing of the dimer [143]. *In vitro*,

dimerized procaspase-8 is capable of undergoing self cleavage between the p10 and p18 domains (intramolecular processing), as well as cleaving the neighbouring monomer (proteolysis in *trans*). However, judging from the crystal structure, it appears that the two catalytic subunits of the dimeric zymogen form a globular structure where the catalytic cysteines diametrically oppose each other making it difficult for one active site to cleave the other subunits [157]. Therefore, it is more likely that caspase-8 autoprocesses by intramolecular cleavage. In this scenario, formation of the dimeric zymogen is a prerequisite event for the autoprocessing of caspase-8 [146]. Upon dimerization, procaspase-8 is cleaved firstly between its two active subunits and secondly in the region linking the prodomain and the large active subunit to finally form the dimeric active enzyme. These two sequential cleavage events are required for the full activity of caspase-8. The inability of fully active caspase-8 to cleave procaspase-8 *in vitro* and the fact that only autoprocessed form of caspase-8 is capable of cleaving caspase-3 efficiently suggest that dimerized procaspase-8 and fully processed caspase-8 have different substrate specificity [146]. Moreover, the processed form of caspase-8 shows higher activity compared to the zymogen (called zymogenicity) [151]. Therefore, dimerization of caspase-8 zymogens represents the first activating event that confers sufficient activity for autoprocessing and for further activation.

Procaspace-8 is predominantly localized in the cytosol but was also recently shown to loosely associate with the mitochondrial outer membrane [158, 159]. After Fas-activation, mitochondria-associated procaspase-8 is cleaved to form an active dimer that moves to the cytosol and specifically targets its substrates, such as Bid and plectin [158, 159]. Since the signal is initiated at the cell surface, it is conceivable that a small amount of caspase-8, which is activated at the DISC, moves to the mitochondria and cleaves mitochondria-associated procaspase-8. In type II cells, the activation of caspase-8 is delayed and requires a mitochondrial step regulated by Bcl-2 and Bcl-x<sub>L</sub> [56]. Interestingly, it was found that Bcl-x<sub>L</sub> can block the activity of caspase-8 at the mitochondrial membrane by indirectly sequestering the enzyme at the mitochondrial outer membrane [159]. These data suggest that in type II cells, caspase-8 might be activated at the mitochondrial membrane. Details of the mechanisms of activation of caspase-8 at the mitochondrial membranes of type II cells await further investigation.

In addition to its crucial role in DR-mediated apoptosis, it appears recently that caspase-8 also participates in growth and development mechanisms, not only of lymphocytes, but of several other tissues. The inactive homologue of caspase-8, c-FLIP<sub>L</sub>, plays an important role in this process. In fact, c-FLIP<sub>L</sub> is able to dimerize and activate caspase-8, which in turn cleaves c-FLIP<sub>L</sub> and results in the recruitment of adaptor proteins that promote the activation of NF-κB and lead to cell proliferation [160].

## **1.6 *Cardiolipin in apoptosis***

Cardiolipin (CL) is a mitochondria-specific phospholipid which is known to be intimately linked with the mitochondrial bioenergetic machinery. Accumulating evidence now suggests that this unique lipid also takes active roles in several of the mitochondria-dependant steps of apoptosis [161].

### **1.6.1 *Cardiolipin synthesis***

The name “cardiolipin” alludes to the fact that it was first isolated from beef heart in 1942. CL or diphosphatidylglycerol can be distinguished from other glycerophospholipids by its dimeric structure containing four acyl chains per molecule and potentially having two negative charges (**Figure 1-6**).

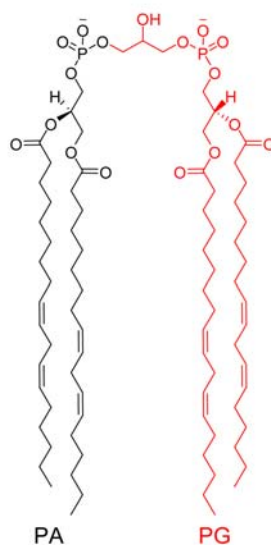


**Figure 1-6: Molecular structure of cardiolipin.**

Cardiolipin is a dimer of phosphatidyl glycerol (PG, in red) and phosphatidic acid (PA, in black). It contains four acyl chains, two phosphate groups and three glycerols. Under physiological pH, one of the phosphates is deprotonated, making CL a negatively charged phospholipid.

CL is exclusively localized to the membranes of bacteria and mitochondria providing more evidence for the endosymbiotic origin of the mitochondria. The biosynthetic pathway of CL has been well described in mammals [162, 163]. CL is synthesized *de novo* in a four step pathway catalyzed by four mitochondrial enzymes, yielding a CL archetype. The first three steps correspond to the phosphatidyl-glycerol pathway and pass through the generation of the common intermediates, phosphatidic acid (PA) and phosphatidyl-CMP. In the first step, CDP-diacylglycerol synthetase catalyses the activation of PA into CDP-diacylglycerol (CDP-DG). In a second reaction phosphatidyl-glycerol phosphate synthetase (PGS1) adds one molecule of glycerol-3-phosphate to the CDP-DG yielding a molecule of phosphatidyl-glycerol-3-phosphate (PGP). PGP is then rapidly dephosphorylated to form phosphatidyl-glycerol (PG) by PGP phosphatase. The final step is unique to CL synthesis and is catalyzed by CL synthase. During this reaction, PG condenses with a molecule of CDP-DG resulting in the generation of diphosphatidylglycerol or CL. The human CL synthase gene has recently been identified by its ability to restore the

CL profile of a CL synthase deficient yeast mutant [164, 165]. Each molecule of CL contains four acyl chains. Considering the variety of fatty acids, the number of potential combinations of the acyl chains is high, and indeed, the pattern of CL molecular species varies between organisms and even between tissues. Eukaryotic CL has a characteristic acyl chain pattern that is essentially restricted to C18 chains [166]. In human heart the predominant C18 fatty acid is linoleic acid (C<sub>18:2</sub>) so heart CL contains mostly C<sub>18:2</sub> acyl chains. However human lymphoblasts CL contain predominantly oleyl chains (C<sub>18:1</sub>) [167]. The significance of this specificity is still not understood. Interestingly, the enzymes involved in the pathway of CL synthesis exhibit no selectivity for a specific acyl chain length [168]. Therefore, once synthesized in mitochondria, a maturation step replacing the original acyl chains with specific C<sub>18</sub> unsaturated ones is required (**Figure 1-7**).

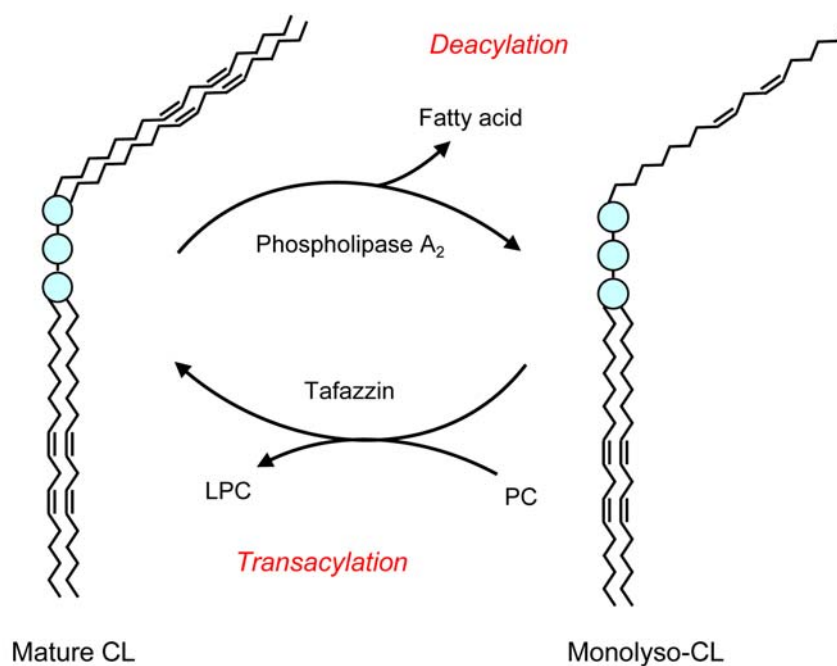


**Figure 1-7: Remodelling cycle of cardiolipin.**

The degree of unsaturation of CL acyl chains is constantly maintained by the cycle of two reactions. First, phospholipase A<sub>2</sub> hydrolyses one acyl chain of CL and generates a monolyso-CL (MLCL). Second, tafazzin catalyses the transfer of unsaturated acyl-chain from phosphatidyl-choline (PC) to MLCL. This results in the formation of mature CL with unsaturated acyl chains and lysophosphatidyl-choline (LPC).

The generation of mature CL requires a cycle of two reactions: the hydrolysis of one original acyl chain to generate a monolyso-CL (MLCL), now containing only three acyl groups, followed by the reacylation of MLCL with the specific acyl chain. Phospholipase A2 catalyzes the first step of acyl chain removal [169]. Reacylation of MLCL has been reported in rat and pig liver [170, 171]. This activity has recently been shown to be catalyzed by tafazzin, a mitochondrial enzyme whose mutations cause the Barth syndrome [172]. Tafazzin is a transacylase that catalyses the transfer of unsaturated acyl chains from phosphatidyl-choline (PC) to MLCL.

### **1.6.2 Barth syndrome**

Barth syndrome (BTHS, MIM#302060) is the first human disease discovered in which the primary cause is due to an alteration of CL metabolism [173, 174]. BTHS is clinically characterized by the triad cardioskeletal myopathy, neutropenia, and growth retardation. It has a high rate of mortality during infancy and early childhood due to cardiac arrest or overwhelming bacterial infections. 3-methylglutaconic aciduria is an important biochemical marker for the syndrome and is now recognized as a fourth major criterion for the diagnosis. Almost all children with BTHS have clinically significant heart failure and muscular hypotonia leading to general weakness and to delayed motor development. Cardioskeletal myopathy is due to mitochondrial dysfunction. Tissue biopsies from BTHS patients contained mitochondria with abnormal structure and diminished OXPHOS [173]. Neutropenia corresponds to a deficiency in circulating neutrophils. In BTHS, neutropenia is not due to an increase in apoptosis but rather from a maturation arrest at the premyelocyte stage of neutrophil development [173].

This genetic disorder is due to mutations in the *tafazzin* gene (TAZ) located in the Xq28.12 region in the human genome [175]. The *tafazzin* gene contains 11 exons and possesses two putative alternative translational initiation sites. The function of the second initiation site has not yet been defined. In humans, four different transcripts are produced due to alternative splicing of exons 5 to 7 which encode four protein variants ranging from 28.5 to 33.5 kDa [176, 177]. In tafazzin-deficient yeast, only the human variant lacking exon 5 was able to restore cardiolipin synthesis and to complement the retarded growth [178]. However, since exon 5 is only present in primate species, the function of the full length protein must be investigated in cells that normally include this exon. Moreover, identification of an exon 5 mutation in

BTBS patients strongly indicates that exon 5 is required for the activity of tafazzin in human [177]. Further investigation is required to understand the activities of the different tafazzin variants. To date, over 90 different pathogenic mutations have been reported and mapped in all 11 exons [177]. These include frameshift, non-sense, splice-site, and missense mutations and they result in either a complete loss of protein expression or in the expression of non-functional truncated tafazzin.

The first evidence that CL has a role in BTBS emerged in 2000 with the observations made by Barth and his colleagues that the total amount of CL as well as the rate of linoleyl chains incorporation into CL decreased in BTBS fibroblasts without detected changes in overall phospholipid synthesis [179]. Therefore, it was postulated that tafazzin is involved in the remodelling process of CL. Analyses of the CL profile from different tissues obtained from BTBS patients have revealed that the decrease in CL levels is associated with an increase in MLCL, further supporting this hypothesis [180, 181]. Recently, the enzymatic function of the full length isoform of *Drosophila melanogaster* tafazzin has been characterized. It is now described as a phospholipid transacylase that catalyzes the transfer of linoleyl chain from PC to MLCL [172].

### **1.6.3 Cardiolipin localization in mitochondria**

CL is specific to mitochondrial membranes but its precise localization within the different compartments of the organelle is still a subject of controversy. For many years, it was assumed that CL is exclusively associated with the mitochondrial inner membrane. CL appears to be more abundant in the inner leaflet than in the outer leaflet of the inner membrane, where they represent 18% and 6% of the total phospholipid composition, respectively [182]. More recently traces of CL have also been found in the mitochondrial outer membrane (~4%) and in the contact sites between the mitochondrial outer and inner membranes [183-185]. Through contact sites, CL may reach the mitochondrial outer membrane and the cytosolic face of the mitochondria. This notion is supported by the fact that the two major phospholipids present in contact sites, phosphatidyl-ethanolamine (PE) and CL (~25 % each) have the ability to adopt non bilayer hexagonal HII phase [186] (**Figure 1-8**). Such structures are known to contribute to the fusion of two membranes [187].

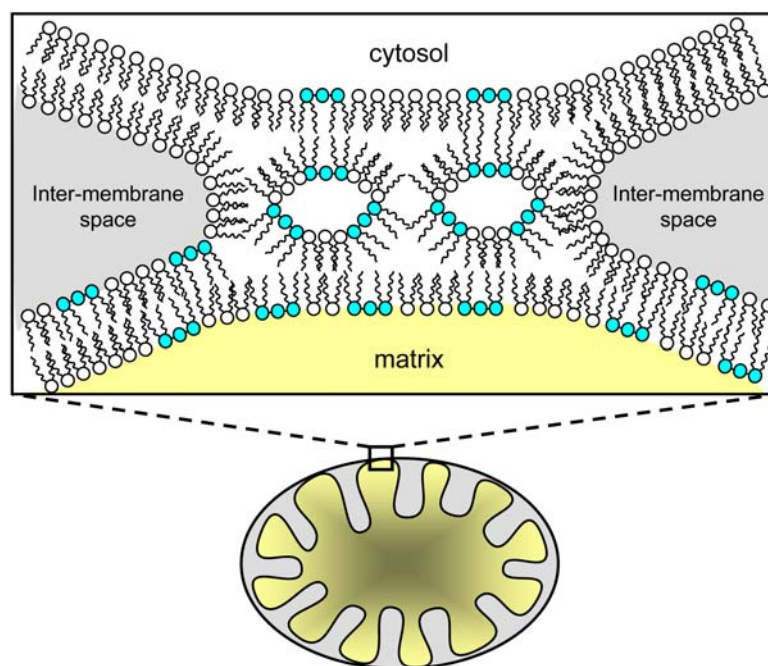


**Figure 1-8: Cardiolipin at the mitochondrial contact sites.**

The non-bilayer hexagonal structure of lipids was characterised *in vitro* and proposed to contribute to the structure of contact sites between the inner and outer membranes of mitochondria. Negatively charged phospholipids (such as CL) are more likely to adopt this structure which may fuse the mitochondrial membranes at the contact sites and redistribute cardiolipin on the cytosolic face of the mitochondria. CLs are highlighted in blue.

#### **1.6.4 The role of cardiolipin in bioenergetics**

The exclusive presence of CL in bioenergetic membranes suggests that it interacts with the electron transport chain complexes involved in OXPHOS. Indeed, CL is required for optimal activity of complex I (NADH dehydrogenase), complex II (Succinate dehydrogenase), complex IV (cytochrome c oxidase) and complex V (ATP synthase), four large complexes integrated in the inner mitochondrial membrane [188, 189]. Furthermore, complexes III, IV and V were shown to contain CL in their quaternary structure [188, 190, 191] and CL was observed within the 3D crystal structure of *Escherichia coli* succinate dehydrogenase, an orthologue of the mitochondrial respiratory complex II [192]. CL is also required by mitochondrial substrate carriers, including the ANT, acylcarnitine translocase and phosphate carrier [193-196]. It was therefore reasonable to predict that a deficiency in CL would result in alterations in cell respiration. The Chinese hamster ovary (CHO) cell line containing a temperature-sensitive (ts) mutant of PG synthase (CHO-PGS-S) has provided the first indication of the potential involvement of CL in cellular bioenergetics [197]. At the non-permissive temperature (40°C) these cells exhibit a

decrease in oxygen consumption and ATP production, accompanied by a compensatory increase in glycolysis [198]. However, since these cells have reduced levels of both PG and CL at 40°C, it is not possible to attribute these bioenergetic defects to CL alone. Other studies using the CL synthase deficient yeast mutant *crd1Δ* have provided more direct evidence for the requirement of CL for mitochondrial bioenergetics. Somewhat surprisingly, the *crd1Δ* mutant was able to grow, though not as efficiently as wild type yeast, on non-fermentable carbon sources, indicating that CL is not essential for OXPHOS in yeast [199]. However, several bioenergetic defects associated with a reduction of ANT activity, decreased mitochondrial membrane potential, and an overall decrease in OXPHOS, were observed in the *crd1Δ* mutant when grown under stress conditions [200-202]. Thus, CL appears to be required for sustaining mitochondrial inner membrane integrity, rendering it more resistant to unfavourable conditions such as high respiration rate, high temperature and hypotonic shock.

In mitochondria, only 15% of cytochrome *c* is free in the inter-membrane space [85, 203] while most of it is attached to the mitochondrial inner membrane via specific interactions with CL [204, 205]. Two types of interactions, hydrophobic and electrostatic, have been linked to two distinct CL binding sites on cytochrome *c*. Initially, these interactions were thought to play a role in the electron-shuttle activity of cytochrome *c* by keeping the molecule in the proximity of the respiratory chain [204]. More recently, CL-cytochrome *c* interactions were suggested to participate in the regulation of apoptosis.

### ***1.6.5 Cardiolipin maintains the structure of the mitochondrial inner membrane***

At 40°C, the mitochondria of CHO-PGS-S cells appear swollen and have disorganized cristae [198, 206]. However, as mentioned above, these alterations cannot be solely attributed to CL, since these cells lack both CL and PG. A more recent study of HeLa cells in which the expression of CL synthase was decreased by RNA interference (RNAi) indicated that CL is directly required for maintenance of mitochondrial structure [165]. This report, however, contrasts with the phenotype of the *crd1Δ* yeast mutants, which lack CL but maintain normal mitochondrial morphology [207]. The differences between CL synthase-deficient mammalian cells

and yeast may be due to the ability of PG to supplant the membrane-preserving function of CL in yeast.

### **1.6.6 *Cardiolipin in relation to apoptosis***

#### **1.6.6.1 Cardiolipin levels and oxidative stress**

Loss of CL is associated with diverse pathophysiological conditions such as ageing and ischemia/reperfusion processes [208, 209]. For example, the loss of CL during ischemia/reperfusion injury is followed by a decrease in OXPHOS which may contribute to myocyte death in the peri-infarct regions of the ischemic myocardium. The decline in mitochondrial respiratory functions causes the accumulation of reactive oxygen species (ROS). Under normal physiological conditions mitochondrial CL may protect cells from oxidative stress in part through the deacylation-reacylation cycle discussed above. However, CL is also a vulnerable target of ROS due to its unsaturated acyl chains and its close proximity to ROS generation sites. ROS cause the peroxidation of CL and a parallel decrease in the activities of complexes I and IV [210, 211]. Currently this seems to be very much a “chicken and egg” issue, and it is unclear whether ROS trigger the loss of CL or whether loss of CL triggers ROS generation. It is clear, however, that during many cell death processes ROS and loss of CL are closely linked in a cycle of CL peroxidation. Peroxidation of CL also occurs following a variety of apoptotic stimuli such as by nitric oxide, Fas receptor stimulation, NGF deprivation, staurosporine and actinomycin D treatments [212-214]. Interestingly, apoptosis via a pathway involving a decrease in CL synthesis was seen in neonatal rat cardiac myocytes and in breast cancer cells treated with saturated fatty acids, particularly palmitate [215, 216].

#### **1.6.6.2 Cardiolipin - cytochrome c interactions regulate cytochrome c release**

As mentioned above, the majority of cytochrome *c* is bound to the outer leaflet of the mitochondrial inner membrane. Cytochrome *c* has a net charge of +8 at physiological pH allowing it to bind membranes primarily through electrostatic interactions with the head groups of anionic phospholipids such CL [204, 205]. Cytochrome *c* has a

hydrophobic cavity which may account for hydrophobic interactions with the fatty acyl chains of CL [217]. Two CL binding sites on cytochrome *c* have been proposed; the A site which facilitates electrostatic interactions with the negative charges of CL and the C site which is involved in hydrophobic interactions with the fatty acyl chains of CL [204]. These sites are responsible for two different conformations of cytochrome *c* in the intermembrane space: a loosely bound conformation involving site A and a tightly bound conformation at site C that partially embeds the protein in the membrane [218]. Loosely bound cytochrome *c* participates in the transfer of electrons from complex III to complex IV, as well as in ROS scavenging [219, 220]. Tightly bound cytochrome *c* was proposed to possess peroxidase activity that utilizes hydrogen peroxide generated in the mitochondria to peroxidate CL [214].

For both types of CL binding it was proposed that cytochrome *c* release from mitochondria would first require the dissociation of its interactions with CL (**Figure 1-9**) [221, 222]. This is consistent with recent findings showing that in CL-deficient cells, a greater fraction of cytochrome *c* is free or loosely bound [165]. The fact that *in vitro*, cytochrome *c* has a lower affinity for peroxidized CL than CL, suggests that CL peroxidation may enable cytochrome *c* detachment from the inner membrane (**Figure 1.9**). Complete release of cytochrome *c* into the inter membrane space requires dissociation of both the hydrophobic and the electrostatic interactions between cytochrome *c* and CL [223]. The final release of cytochrome *c* from mitochondria requires additional steps in the process, consisting of the permeabilization of the outer membrane. Cristae remodelling was also shown to be required for cytochrome *c* re-distribution within the mitochondrial inter membrane space before its release [85] but whether the dissociation of CL-cytochrome *c* interactions is related to this process awaits further study. Still, the studies described above strongly indicate that CL and cytochrome *c* are physically associated and for some functions at least they are also interdependent.

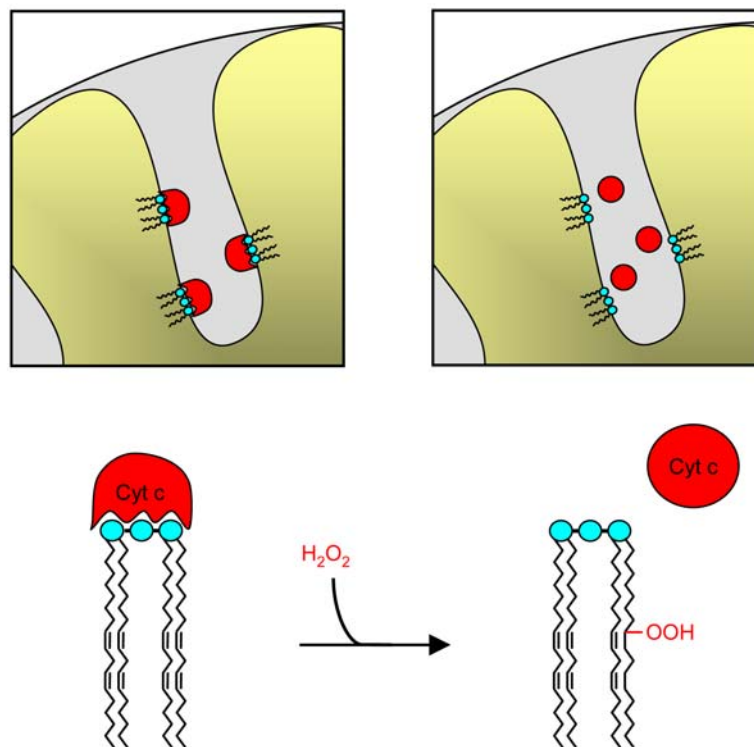


**Figure 1-9: Dissociation of cardiolipin-cytochrome c interaction during apoptosis.**

Cytochrome c (red) is attached to cardiolipin on the outer surface of the mitochondrial inner membrane and therefore, permeabilization of the mitochondrial outer membrane is not sufficient for cytochrome c release. The dissociation of cytochrome c from cardiolipin is a prerequisite step for outer membrane permeabilization and is triggered by cardiolipin peroxidation. Recently it was shown that cardiolipin peroxidation is catalyzed by the bound cytochrome c itself.

### 1.6.6.3 Cardiolipin: docking site for tBid

The first apoptosis-promoting role of CL emerged from biochemical studies of tBid interactions with mitochondrial lipids using liposomes and the CHO-PGS-S cell line [127]. Wang and co-workers showed that the pro-apoptotic protein tBid interacts exclusively with liposomes that contain at least physiological levels of CL and demonstrated that tBid co-localization with CHO-PGS-S mitochondria is CL-dependent. The CL-binding domain of tBid was mapped to helices 4-6 of the Bid protein [127]. Interestingly, helix 6 was later shown to be a part of a hairpin structure which is important for the lipid binding properties of tBid [224]. Subsequently, electron tomogram studies showed that tBid interacts with mitochondria specifically at the inner and outer membrane contact sites, which are rich in CL [128]. As discussed above, CL-rich membranes may adopt a non-bilayer hexagonal HII

configuration at the contact sites (**Figure 1-8**), enabling the access of CL to the cytosolic surface of mitochondria [185]. The model of CL as a mitochondrial “docking” site for tBid is supported by several studies (**Figure 1-10**). For example, *in vitro* assays using artificial membranes or isolated mitochondria showed that recombinant tBid can bind CL and MLCL [131, 132, 225-227]. Adding tBid to isolated mitochondria immediately inhibits ADP-stimulated respiration and oxidative phosphorylation, as a result of ANT inactivation [129, 130]. The function of tBid may be either BH3-domain-dependent or independent. The former induces oligomerization of the multi-BH domain pro-apoptotic Bcl-2 proteins Bax and Bak on the mitochondrial outer membrane, while a BH3-independent interaction of tBid with CL [227] could be responsible for cristae remodelling, [131] and for inhibition of OXPHOS [130]. Cristae remodelling and perturbations of mitochondrial bioenergetics take place simultaneously and are both independent of Bak. It is possible therefore that tBid acts by two sequential mechanisms: the first is BH3 domain independent, which involves CL, leading to structural and functional impairment, and the second is BH3 domain dependent, employing interactions with other pro-apoptotic Bcl-2 proteins, namely Bak and Bax, leading to mitochondrial outer membrane permeabilization. Thus, the interaction of tBid with CL may prime mitochondria for the action of Bax and Bak.

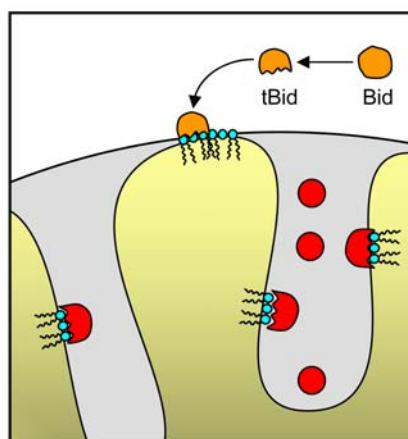


**Figure 1-10: Cardiolipin serves as a docking platform for the Bcl-2 proteins tBid.**

After cleavage, tBid translocates to the mitochondria via a specific interaction with CL (in blue) exposed to the surface of the mitochondrial contact sites. This leads to an unravelling of the pool of cytochrome c trapped in the mitochondrial cristae.

#### 1.6.6.4 Cardiolipin redistribution

Another feature of CL observed under apoptotic conditions is its redistribution within and between membranes. The exposure of CL on the outer leaflet of the mitochondrial inner membrane was observed after death receptor stimulation before mitochondria depolarization and PS exposure on the plasma membrane, and at the same time as ROS generation [228]. Peroxidation of CL may account for this redistribution by altering their molecular organization and favouring formation of a non-bilayer hexagonal structure [229]. This could increase exposure of CL on the contact sites of mitochondrial membranes and provide access for tBid. It is also suggested that Bid, which exhibits lipid transfer activity *in vitro*, relocates CL and MLCL to the plasma membrane of cells undergoing apoptosis [230, 231]. The mechanism and the significance of this relocation are still unclear. In addition, tBid may reorganize CL into micro-domains as was demonstrated in artificial lipid monolayers containing physiological amount of CL [130]. Considering the possible role of CL in maintaining mitochondrial structure, changes in CL organization may result in structural changes of the mitochondrial inner membrane which in turn may affect the activity of membrane-embedded proteins such as ANT. Therefore, it is conceivable that tBid affects the structure and function of mitochondria by binding to and redistributing mitochondrial CL within the mitochondrial inner membrane and/or within other cellular compartments.

#### 1.6.6.5 Cardiolipin and MOMP

CL has also been proposed to be required for the action of other pro-apoptotic Bcl 2 proteins [101]. To study individual functions of Bcl-2-family proteins Newmeyer and co-workers took an *in vitro* approach using liposomes and outer mitochondrial membrane vesicles. Their work has provided evidence that permeabilization of liposomes to dextran required both the presence of activated Bax and physiological levels of CL. Therefore, it was suggested that Bax may permeabilize the mitochondrial outer membrane by altering the local organization of CL without overall damage to the membrane itself (**Figure 1-11**). In contrast to this report, other studies using either the CL synthase deficient yeast *crd1Δ* or mitochondria from CL synthase knocked-down cells have shown that Bax does not require CL for the induction of cytochrome *c* release [129, 165, 232]. However, as discussed above, it is

possible that in yeast, PG, which accumulates in the absence of CL synthase, compensates for the loss of CL. It still awaits clarification whether CL or its PG precursor are needed, for Bax to release cytochrome *c* [233]. This is particularly interesting since hydrophobic and electrostatic interactions make a different contribution to the binding of cytochrome *c* to CL or PG [234].

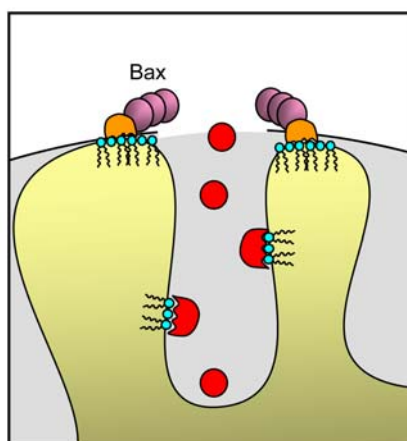


**Figure 1-11: Cardiolipin and permeabilization of the mitochondrial outer membrane.** Cardiolipin participates with tBid and Bax in the perforation of the mitochondrial outer membrane. The mechanism is still elusive.

#### 1.6.6.6 Cardiolipin-cytochrome *c* peroxidase activity

CL peroxidation appears to be an early event preceding the release of cytochrome *c* and caspase activation. The mechanism of CL peroxidation and its involvement in apoptosis has gained more attention recently [214, 235]. Kagan and colleagues showed that cytochrome *c* can interact with CL that contains two or more unsaturated acyl groups ( $C_{18:2}$  mostly) to form a hydrogen peroxide peroxidase capable of oxidizing CL to peroxi-CL (**Figure 1-9**). Using cytochrome *c*<sup>-/-</sup> mouse embryonic cells they provided the first evidence that cytochrome *c* is required for the peroxidation of CL. The CL-cytochrome *c* complex acts as a potent CL-specific oxygenase required for the release of pro-apoptotic factors such as cytochrome *c* and Smac/DIABLO. It is noteworthy that oxidized CL does not merely allow cytochrome *c* to detach from the mitochondrial inner membrane but rather has an active role in inducing apoptosis: when added to isolated mitochondria oxidized CL alone induces

cytochrome *c* and Smac/DIABLO release [214]. Importantly, the peroxidase activity of the CL-cytochrome *c* complex depends on unsaturated acyl chains on CL. Indeed, incubation of HL60 cells with the poly-unsaturated fatty acid docosahexaenoic acid (C<sub>22:6</sub>), enriches CL with C22:6 acyl chains, sensitizing the cells to staurosporine-induced apoptosis [214]. This promoted the notion that enriching CL with saturated acyl chains may protect from apoptosis. But although *in vitro*, saturated CL cannot stimulate CL-cytochrome *c* peroxidase activity [214], CL synthase in a cellular context does not incorporate saturated PG to form fully saturated CL [216]. Nevertheless, the results, together with the suggestion that oxidized CL may have a promoting effect on the pro-apoptotic activity of Bcl 2 proteins, point to the importance of CL acyl chain composition and suggest that manipulation of CL oxidation may present a good target for sensitising cells to apoptosis. This also raises the question whether Bcl-2 proteins can regulate CL-cytochrome *c* peroxidase activity.

## **1.7 Apoptosis: a target in cancer therapy**

Evading apoptosis is one of the six cardinal hallmarks of cancer [236]. Cancer cells have developed several strategies to evade programmed cell death by either negatively regulating death activators (e.g caspases) or overactivating apoptosis inhibitors (e.g Bcl-2). Over the past 15 years, advances in the knowledge of the molecular mechanisms of apoptosis provided numerous suitable targets for drug development and thus opened new therapeutic venues for the treatment of cancer. Reactivation of this endogenous pathway in tumour cells is the goal of many new anti-cancer strategies.

### **1.7.1 Targeting the TRAIL pathway**

As mentioned in *section 1.5.2.1*, the TNF-Related Apoptosis-Inducing Ligand receptors (TRAILR) belong to the TNF $\alpha$  family of receptors. To date, two types have been identified, TRAILR1 (DR4) and TRAILR2 (DR5). In analogy with Fas-receptor, activation of the TRAIL receptors induces the formation of the DISC, which ultimately leads to cell death. However, whereas Fas agonists have revealed severe toxicity in normal tissues [237], TRAIL seems to be a more promising candidate for cancer therapy, because it specifically kills tumour cells. Two strategies

have been developed by pharmaceutical companies to activate this endogenous pathway. They include the administration of either recombinant proteins, consisting of active fragment of the ligands, or agonistic antibodies that bind to TRAIL receptor and induce apoptosis [238]. In most cases, resistance of tumours to chemotherapy is due to defects in the intrinsic apoptotic pathway, as a result of mutations in the tumour suppressor p53 pathway, or due to the overexpression of the anti-apoptotic Bcl-2 proteins. However, TRAIL mediated apoptosis is independent of p53 and can bypass the “Bcl-2 checkpoint” by directly activating the caspases cascade independently of the mitochondrial pathway. To date, three TRAIL-targeting drugs are in clinical trial, with the most advanced candidate being in phase II (TRAIL R2 antibody; Human Genome Sciences, Inc.). However, the endogenous inhibitor of caspase-8, FLIPs, is overexpressed in a wide variety of tumours and may represent a barrier to the success of TRAIL-mediated therapy [48]. Inhibitors of FLIPs have been clinically tested and shown to restore the sensitivity of tumours to TRAIL antibodies [239]. Combination of these two targeted therapies may provide promising perspective for future anti-cancer therapies.

### **1.7.2 Targeting the IAPs**

Another strategy evolved by cancer cells to evade apoptosis is to inhibit the active caspases by overexpressing IAPs. Therefore, inhibiting IAPs in cancer cells have emerged as an attractive strategy for cancer therapy. IAPs sequester active caspases (caspases-3, 7, 9) via the presence of BIR domains (*section 1.5.4.5.2*). Two approaches to inhibit IAPs have been developed. The first one takes advantage of the properties of the endogenous IAPs inhibitors (Smac/DIABLO and Omi/HtrA2) and it implies small compounds that mimic these inhibitors [240]. All the compounds developed so far have not shown conclusive anti-cancer activity and thus remained in pre-clinical stages. An alternative strategy involves the screening of chemical libraries for compounds which displace caspases from IAPs [241]. Several compounds, which were identified by using pro-caspase-3 and XIAP have demonstrated promising single-agent activity in mice tumour xenografts without toxicity to normal tissues [241].

### **1.7.3 Targeting the *Bcl-2* family proteins**

Since altered expression and function of the *Bcl-2* family proteins have been reported in cancer, these proteins and their regulators have also emerged as attractive targets for cancer therapy. Overexpression of anti-apoptotic *Bcl-2* proteins is frequent in cancer and is associated with chemo-resistance. Two strategies have been developed to target these proteins. The first approach consists of sensitising cancer cells to chemotherapeutic treatment by reducing the expression of *Bcl-2* proteins. Modulators of steroid/retinoid family of nuclear receptors, such as tamoxifen, have been shown to suppress transcription of *Bcl-2* and may be promising chemosensitizers. DNA based drugs using antisense oligodeoxynucleotides targeting *Bcl-2* mRNAs have also shown encouraging clinical results. To date *Bcl-2* antisense is the only apoptosis-based therapy for cancer which is in phase III (Genasense; Genta, Inc) [242]. The second strategy is based on blocking the hydrophobic groove of the anti-apoptotic *Bcl-2* proteins that bind and neutralize the BH3-domain of the pro-apoptotic members. Several natural products that mimic the BH3 peptidyl structure have been identified. Gossypol (Ascenta Pharmaceutical, Inc., NCI) derived from cotton seed have shown efficacy against cancer and is now in phase II clinical trial. Other companies have designed synthetic chemical antagonists that bind the BH3-pocket of *Bcl-2*. Several synthetic BH3 mimetics are now in late preclinical and early clinical development. The pan-*Bcl-2* family inhibitor, GX15-07, developed by Gemin X Biotechnologies (Canada) has just advanced to a phase I clinical trial. Recently, using a structural based screening, Abbott Laboratories have identified a very promising BH3 mimetic, ABT-737 [243]. ABT-737 potently inhibits *Bcl-2*, *Bcl-X<sub>L</sub>* and *Bcl-w* and causes regression of established tumours in mice. This drug is now at early stages of clinical trials.

## **1.8 Aims**

As mentioned in *section 1.6*, CL was found to be involved in many of the mitochondria-dependent steps that lead to the release of apoptogenic factors from mitochondria. Despite this growing body of evidence implicating CL in apoptosis, the mechanism by which CL and its fatty acyl chain composition regulate mitochondrial apoptosis remains unresolved. This thesis is focused on the role of CL and its fatty acyl chains in regulating apoptosis.

## **CHAPTER 2 MATERIALS AND EXPERIMENTAL PROCEDURES**

## 2 Materials and experimental procedures

### 2.1 Materials

#### 2.1.1 General reagents

Unless listed, all reagents were purchased from Sigma. Materials for tissue culture were obtained from Becton Dickinson.

**Amersham:** ECL western-blotting detection kit

**Anachem:** Pure nitrocellulose transfer membrane 0.22 $\mu$ m

**Biorad:** agarose gel casters, agarose gel tanks, Mini-Protean III Ready Gel System for SDS-PAGE and Western-Blotting

**Dharmacon:** non targeting siRNA pool

**Fisher Scientific:** glycerol, glycin, KCl, KH<sub>2</sub>PO<sub>4</sub>, MgCl<sub>2</sub>, NaCl, Na<sub>2</sub>CO<sub>3</sub>, SDS, sucrose

**Finnzymes:** DyNamo SYBR Green 2-step qPCR Kit

**Invitrogen:** Lipofectamine 2000 transfection reagent, Novex mini-cell gel tank, NuPage 4-12% Bis-Tris gels, DH5 $\alpha$  competent cells, DMEM, RPMI, Hepes, L-glutamine, trypsin

**Melford:** Tris-Base Ultrapure

**Qiagen:** plasmid purification kits (mini and maxi), gel extraction kit, PCR Purification kit, RNA extraction kit

**Roche Applied Science:** Rapid DNA ligation kit, RNA PCR kit, restriction enzymes

**Stratagen:** QuikChange Site-Directed Mutagenesis Kit

**Severn Biotech Ltd:** 30% Acrylamide (19:1 bis-acrylamide)

### 2.1.2 Primers sequences

Name	Experiement	Sequence 5'-3'
cTAZHIII 5'	Cloning TAZ delta exon 5 cDNA into pEGFPN1 vector	CCCAAGCTTGGGTGGGGATGCCTCTGCAC
cTAZSalI 3'	Cloning TAZ delta exon 5 cDNA into pEGFPN1 vector	ACGCGTCGACGATCTCCCAGGCTGGAGGTGG
pEGFPN1 Forward	Sequencing pEGFPN1 vector	CGGAACTCAGATCTCGAGCTC
pEGFPN1 Reverse	Sequencing pEGFPN1 vector	TGAACTTGTGGCCGTTTTACGTCG
TazzEx7mut3 Forward	Site-directed mutagenesis in pcDNA <sub>3</sub> TAZHisTag	GCATATCTTCCCAGAAGGCAAGGTCAACATG AGTTCCGAATTCCTGCG
TazzEx7mut3 Reverse	Site-directed mutagenesis in pcDNA <sub>3</sub> TAZHisTag	CGCAGGAATTCGGAACTCATGTTGACCTTGC CTTCTGGGAAGATATGC
TAZ Forward	RT-PCR and qPCR	CCCAGAAGGGAAAGTGAACA
TAZ Reverse	RT-PCR and qPCR	GAGCTGCTCTGCCTGAGTCT
GAPDH Forward	RT-PCR and qPCR	TCCACCACCCTGTTGCTG
GAPDH Reverse	RT-PCR and qPCR	ACCACAGTCCATGCCATCAC
Actin Forward	RT-PCR and qPCR	TCCATCATGAAGTGTGACGT
Actin Reverse	RT-PCR and qPCR	TACTCCTGCTTGCTGATCCAC
T7	Sequencing pcDNA <sub>3</sub> TAZHisTag	TAATACGACTCACTATAGGG
SP6	Sequencing pcDNA <sub>3</sub> TAZHisTag	ATTTAGGTGACACTATAG
pSR5'	Sequencing pSUPERRetroGFPNeo	GGAAGCCTTGGCTTTTG
pSR3'	Sequencing pSUPERRetroGFPNeo	GATGACGTCAGCGTTTCG

**Table 1 Primer sequences**

### 2.1.3 Antiserum

Target	Supplier	Description	Dilution	Incubation time
Actin	Sigma	Mouse monoclonal	1:5000	1 hour
Bax	Upstate	Rabbit polyclonal	1:1000	overnight
Bak	Upstate	Rabbit polyclonal	1:1000	overnight
Bcl-2	BD Pharmingen	Mouse monoclonal	1:1000	overnight
Bcl-X <sub>L</sub>	Craig Thompson Lab	Rabbit polyclonal	1:1000	overnight
human Bid	Cell Signaling	Rabbit polyclonal	1:1000	overnight
mouse Bid	R&D	Goat polyclonal	1:1000	overnight
mouse Bid	Santa Cruz	Goat polyclonal	1:1000	overnight
Caspase-3	Cell Signaling	Rabbit monoclonal	1:1000	overnight
Caspase-8 (anti-DED)	BD Pharmingen	Mouse monoclonal	1:1000	overnight
Caspase-8 (anti-p18)	Cell Signaling	Mouse monoclonal	1:1000	overnight
Cytochrome c Clone 6H2.B4	BD Pharmingen	Mouse monoclonal Immunofluorescence	1:300	2 hours
Cytochrome c Clone 7H8.2C12	BD Pharmingen	Mouse monoclonal Western-blot	1:1000	overnight
Cytochrome c oxidase subunit IV	Molecular Probes	Mouse monoclonal	1:1000	overnight
Fas receptor Clone CH11	Upstate	Mouse immunoaffinity IgM Apoptosis induction	0.3 or 0.5 $\mu\text{g.ml}^{-1}$	depending on experiment
GFP	Sigma	Mouse monoclonal	1:1000	2 hours
NADH Dehydrogenase	Molecular Probes	Mouse monoclonal	1:1000	overnight
Succinate Dehydrogenase subunit B	Molecular Probes	Mouse monoclonal	4 $\mu\text{g.ml}^{-1}$	overnight
PARP	BD Pharmingen	Mouse monoclonal	1:1000	overnight
Smac-Diablo Clone 56	BD Pharmingen	Mouse monoclonal Western-blot	1:1000	overnight
Smac-Diablo Clone 7	BD Pharmingen	Mouse monoclonal Immunofluorescence	1:300	2 hours
Tafazzin	ABCAM	Goat polyclonal	1:1000	overnight

**Table 2 Primary antibodies list**

<b>Description</b>	<b>Supplier</b>	<b>Catalogue Number</b>	<b>Dilution</b>	<b>Incubation time</b>
Anti-mouse IgG, HRP-linked antibody	Cell Signaling	7076	1:5000	1 hour
Anti-rabbit IgG, HRP-linked antibody	Cell Signaling	7074	1:5000	1 hour
Anti-goat IgG, HRP-linked antibody	Chemicon International	AP106P	1:5000	1 hour

**Table 3 Secondary antibodies list**

### **2.1.4 RNA interference oligonucleotides sequences**

<b>Name</b>	<b>Gene targeted</b>	<b>Sequence sense</b>
siTaz	Human Tafazzin	GGGAAAGUGAACAUGAGUUTT
shTaz	Human Tafazzin	GATCCCCAAGGGAAAGTGAACATGAGTT TTCAAGAGAAACTCATGTTCACCTTCCCTT TTTTTA
siBid	Human Bid	GAAGACAUCAUCCGGAAUATT
siCaspase-8	Human Caspase-8	AAGGGUGAUGCUCUAUCAGAUTT

**Table 4 RNA interference targeting sequences**

## **2.2 Experimental procedures**

### **2.2.1 Plasmid constructs**

#### **2.2.1.1 Cloning tafazzin full-length and delta exon 5 cDNAs into pLpC retroviral vector**

Tafazzin full-length and delta exon 5 cDNAs were kindly provided by David Brooks of the University of Pennsylvania (USA). Both cDNAs were extracted from pCR2.1 vector by double digestion with the restriction enzymes EcoRV and Hind III (Roche) and sub-cloned into the retroviral expression vector pLpC (provided by Scott Lowe). pLpC was first digested with XhoI (Roche), blunted using the Klenow fragment (Cambio) and then digested with HindIII. pLpC contains element derived from

Moloney murine leukaemia virus and Moloney murine sarcoma virus and was designed for retroviral gene delivery. It provides sequences essential for the production of retroviruses: two long terminal repeats (LTR) located at the 5' and the 3' of the multiple cloning site and the packaging signal  $\Psi$ . However, it does not encode all the proteins required for the packaging of retroviral particles.

### **2.2.1.2 Cloning tafazzin delta exon 5 cDNA into pEGFPN1 vector**

Tafazzin delta exon 5 cDNA was generated by PCR using the cTAZHIII 5' and cTAZSall 3' primers (**Table 1**) containing HindIII and Sall restriction sites respectively, to allow cloning into the HindIII and Sall sites of the pEGFPN1 vector. Once the PCR product had been amplified, it was digested using the HindIII and Sall restriction enzymes to leave compatible ssDNA overhangs for ligation into the digested vector. Positive clones were sequenced using pEGFPN1 forward and reverse primers (**Table 1**) to confirm the correct formation of the fusion protein.

### **2.2.1.3 Cloning siRNA Taz duplex into pSUPERRetroGFPNeo**

To generate a short hairpin RNA (shRNA) encoding plasmid, a pair of complementary DNA oligonucleotides of 64 pb containing the siRNA Taz targeting sequence in both sense and anti-sense orientation (**Table 4**) were designed according to OligoEngine's instructions. The pSUPERRetroGFPNeo vector (OligoEngine, USA) was sequentially digested by BglII and HindIII. Then, the oligonucleotides were annealed and ligated with the BglII and HindIII sites of the linearized vector. DH5 $\alpha$  competent bacteria were transformed with the ligation product (see *Bacterial Transformation* below). Positive clones were sequenced using the pSR5' and pSR3' primers (**Table 1**). The tafazzin targeting shRNA encoding vector was called shTaz.

### **2.2.1.4 Site-directed mutagenesis in pcDNA<sub>3</sub>TAZHisTag**

The siRNA recognition sequence of pcDNA<sub>3</sub>TAZHisTag (provided by Frederick Vaz, Laboratory Genetic Metabolic Diseases of Amsterdam) has been mutated using a Mutagenic PCR kit from Stratagene according to the manufacturer's instructions.

The TazzEx7mut3 forward and reverse primers were used (**Table 1**). Briefly, the PCR program used was 95°C for 30 seconds, 52°C for 1 minute and 68°C for 8 minutes. The cycle was repeated 18 times. The silent mutations were generated at the third position of codons 182, 183 and 184 of *tafazzin* exon 7 in order to conserve the amino acids sequence while protecting the mutated-plasmid from siRNA-mediated degradation. After PCR, the parental plasmid was digested by DpnI for 2 hours at 37°C. DH5 $\alpha$  competent cells were transformed with the digestion product (see *Bacterial Transformation* below) and DNA harvested. In order to confirm the presence of the mutations, constructs were sequenced using specific primers of the T7 and Sp6 promoters of pcDNA<sub>3</sub> (**Table 1**).

### **2.2.2 Bacterial transformation**

50  $\mu$ l of DH5 $\alpha$  competent cells were incubated on ice and 4  $\mu$ l of plasmid DNA were added. Cells were left on ice for further 30 minutes and heat-shocked at 42°C for 40 seconds. 250  $\mu$ l of LB medium was added and cells were incubated at 37°C for 30 minutes. Cells were then plated onto agar plates containing the relevant antibiotic and left to grow overnight at 37°C. Colonies were picked from the plates and cultured overnight for DNA purification using Qiagen miniprep or maxiprep purification kits.

### **2.2.3 Tissue culture**

#### **2.2.3.1 Lymphoblastoid cell lines: DB037, DB015.2, DB105.2 and DB105.3**

The lymphoblastoid cell lines were generated from the blood of 2 unrelated patients with Barth Syndrome (DB105.2 and DB105.3) and 2 unrelated control-disease individuals (DB037, DB015.2). These were a gift from Richard I. Kelley of the Kennedy Krieger Institute (Baltimore, USA) and were immortalised by Epstein-Barr virus transformation. Cells were routinely cultured in RPMI 1640 complete medium (Invitrogen, UK) supplemented with 10% foetal calf serum (FCS, Harlan SERA-Lab, UK), 2 mM L-glutamine (Invitrogen, UK), penicillin (50 IU/ml) and streptomycin (50  $\mu$ g/ml) at 37°C under 5% CO<sub>2</sub> atmosphere. The serum was heat-inactivated at 56°C for 30 minutes prior to use. Lymphoblastoid cells were seeded at a density of 3.10<sup>5</sup> cells/ml and cultures were split at confluence.

### **2.2.3.2 HeLa cells**

The cervical carcinoma HeLa cell lines were cultured in DMEM medium (Invitrogen, UK) supplemented with 10% FCS (Harlan SERA-Lab, UK) and 2 mM L-glutamine (Invitrogen, UK). For routine culturing, cells were washed in phosphate-buffered saline (PBS, Beatson Institute Facilities), incubated with trypsin solution (0.25 g/100ml of PBS-EDTA, Invitrogen, UK) and then plated at a density that maintained exponential growth until needed.

### **2.2.3.3 BD RetroPack™ PT67 cells**

The PT67 Cell Line (BD Biosciences Clontech, UK) is derived from a mouse fibroblast (NIH 3T3) cell line and is designed to package retrovirus with a dualtropic envelope that recognizes receptors on mouse, rat, human, hamster, mink, cat, dog, and monkey cells. These cells were infected with a retroviral vector containing the Gag-Pol and Env sequences but are unable to produce viruses because of the absence of packaging signal  $\Psi$ . Upon transfection with a retroviral vector which provides the  $\Psi$  signal, these helper-defective packaging cells are capable of providing in trans the necessary proteins gag-pol and env required for the packaging, processing, reverse transcription and integration of the retroviruses into host genome. The PT67 cells were maintained in DMEM medium (Invitrogen, UK) supplemented with 10% FCS (Harlan SERA-Lab, UK) and 2 mM L-glutamine (Invitrogen, UK) and grown at 37°C under 5% CO<sub>2</sub> atmosphere. Once confluent, the cells were washed with PBS, incubated with trypsin solution and plated at a density that maintained exponential growth until needed.

### **2.2.3.4 Freezing and thawing cells**

To create frozen cell stocks, harvested cells were re-suspended in 90% FCS supplemented with 10% Dimethylsulphoxide (DMSO), and transferred to a cryo freezing container (Nalgen, USA) and frozen overnight at -80°C before being placed in the vapour phase of a liquid nitrogen cell tank. Cells were thawed rapidly at 37°C and added to warmed medium. Cells were then centrifuged at 500 x g for 5 minutes and re-suspended in warmed medium to remove the DMSO. Cells were regularly

tested for microplasma contamination by luciferase assay at the Beatson Institute of Cancer Research.

## **2.2.4 Transfection of cell lines**

### **2.2.4.1 HeLa cells**

HeLa Cells were transfected with Lipofectamine 2000 reagent (Invitrogen, UK) according to the manufacturer's protocol. Briefly, cells were seeded into 6 wells-plate ( $4 \cdot 10^5$  cells per wells) and grown overnight (until 80-90% confluency) in complete DMEM medium (C-DMEM) without antibiotics. The day of transfection, DNA and Lipofectamine 2000 were prepared separately in 250  $\mu$ l of serum free-DMEM and incubated for 5 minutes at room temperature. Diluted DNA was combined with the Lipofectamine 2000 and the mix was incubated for 20 minutes at room temperature. The transfection complexes were added dropwise to the cells and incubated for 4 hours at 37°C before replacing the medium with fresh C-DMEM. Cells were then grown for 48 hours before being assayed.

### **2.2.4.2 PT67 cells transfection and production of retroviruses**

Transfections of the dualtropic packaging cells with retroviral vectors were carried out using calcium phosphate co-precipitation method. PT67 cell lines were seeded into 10 cm plate and grown overnight to 80-90% confluency at the day of transfection. To prepare DNA for transfection, 15  $\mu$ g was diluted into 500  $\mu$ l of 2X HBS (50 mM HEPES, 250 mM NaCl, 1.5 mM NaHPO<sub>4</sub>, pH 7.12) and the mix was completed to 940  $\mu$ l with water. 60  $\mu$ l of 2 M CaCl<sub>2</sub> was added dropwise and the mix was then inverted vigorously for 3 to 15 seconds. The complex DNA/CaPO<sub>4</sub> was incubated 30 minutes at 37°C and added dropwise to the cells. The cells were incubated overnight at 37°C and the medium was replaced with a fresh C-DMEM. For the last 24 hours of virus production, packaging cells were grown at 32°C since the virus half-life is much lower at 37°C than at 32°C. After 10 hours at 32°C, the medium was replaced with 6 mL of RPMI medium supplemented with 20% FCS and 2 mM L-glutamine. The retroviruse-containing media were collected 14 hours latter and passed through a 0.45  $\mu$ m syringe-operated filter and freshly used to infect the targeted cell line.

### **2.2.5 Retroviruses infection of lymphoblastoid cell lines**

Lymphoblastoid cells ( $2.5 \times 10^6$ ) were resuspended in 5 mL of fresh retroviral supernatant and incubated at 32°C under 5% CO<sub>2</sub> atmosphere. To increase efficiency of the retroviral infection, 2.5 µg.ml<sup>-1</sup> of polybrene was added to the retroviral supernatant. After 12 hours incubation, the viral supernatant was removed and the lymphoblastoid cells were resuspended in 6 mL of fresh RPMI 1640 complete medium. Cells were then grown at 37°C. To control the retroviral infection, the cells were infected in parallel with a GFP-expressing retrovirus. The cells were then cultured for one week (until expression of the GFP was observed in the control) and the infected cells were selected in complete medium containing appropriate concentration of the selection antibiotic.

#### **2.2.5.1 DB037GFP and DB105.2GFP**

To establish lymphoblastoid DB037GFP and DB105.2GFP cell lines, DB037 and DB105.2 were infected with a retrovirus expressing pLpCGFP vector (gift from Kevin Ryan, Beatson Institute) and selected using 0.5 µg.ml<sup>-1</sup> puromycin.

#### **2.2.5.2 DB105.2TAZΔ5**

To establish lymphoblastoid DB105.2TazΔ5 cell lines, DB105.2 cells were infected with a retrovirus expressing pLpCTAZΔ5 vector and selected using 0.5 µg.ml<sup>-1</sup> puromycin.

### **2.2.6 Establishment of stable transfected HeLa cell lines**

Once transfected, cells were grown for 48 hours in a 6-wells plate. Then, cells were splitted 1:15 into 150 mm plates in complete medium containing the appropriate concentration of selection antibiotic. This medium was changed every week and the cells were grown until the formation of visible colonies (2-4 weeks). The antibiotic resistant clones were picked by trypsinization in plastic rings and seeded into one well of a 48-well plate containing 200 µl of complete medium with the selection drug.

### **2.2.6.1 HeLa shControl and shTaz**

To establish shControl and shTaz HeLa cell lines, HeLa cells were transfected as described previously with the vectors pSUPERGFPNeoScramble (a gift from Kevin Ryan, Beatson Institute) or pSUPERGFPNeoTAZ, respectively. Stable clones were selected in  $0.5 \text{ mg.ml}^{-1}$  G418.

### **2.2.6.2 HeLa Bcl-X<sub>L</sub>**

To generate HeLa Bcl-X<sub>L</sub>, HeLa cells were transfected with the pcDNA<sub>3</sub>Bcl-X<sub>L</sub> plasmid (a gift from Craig Thompson, University of Pennsylvania, USA). Stable clones were selected in  $0.5 \text{ mg.ml}^{-1}$  G418.

### **2.2.7 Preparation of cell lysates for protein analysis**

Incubated cells (treated or untreated) were washed twice in cold PBS and lysed in RIPA buffer [50 mM Tris-HCl (pH 7.4), 150 mM NaCl, 1 % Triton X100, 1% sodium deoxycholate, 0.1% SDS supplemented with protease inhibitors (SIGMA)]. Extracts were incubated for 20 minutes at 4°C and then centrifuged at 12,000 x g for 5 minutes at 4°C to remove cell debris. Supernatants were transferred to fresh tubes and the protein concentration was assessed in 96-well plates using the BCA Protein Assay kit (Pierce) according to the manufacturer's instructions. Dilution series of BSA from 0.08 to 2 mg/mL was used as standard. Ten µL of each protein extract (either undiluted and/or diluted 1:10) and each standard were added to 200 µL of the BCA assay reagent. The 96-well plate was incubated at 37°C for 30 minutes and light absorbance at 540 nm was analysed using a SpectraMax plus plate reader (Molecular Devices). A standard curve of absorbance versus protein concentration was then drawn and the protein concentration of each sample was determined accordingly.

### **2.2.8 Protein sample preparation**

Lysates were diluted to a final protein concentration of 2 mg/mL using lysis buffer and 2X sample buffer (5% v/v β-mercaptoethanol, 62.5 mM Tris-HCl, 2% w/v sodium dodecyl sulphate, 25% v/v glycerol, 0.01% w/v bromophenol blue) and boiled for 10 minutes. SDS-PAGE (sodium dodecyl sulphate polyacrylamide gel electrophoresis) was used to separate proteins and their size was determined by their

position on the gel with reference to molecular weight markers. The presence of a particular protein could then be determined by Western blot analysis (*see* 2.2.10). Loading was normally controlled by visualization of  $\beta$ -actin unless specified otherwise.

### **2.2.9 SDS-PAGE**

Cell lysates or mitochondrial extracts were resolved on SDS-PAGE. Denaturing polyacrylamide gels of 10, 12 or 15 % acrylamide (National Diagnostics) were cast using a mini-Protean gel caster (BioRad). Gels were poured into the caster, overlaid with butan-2-ol saturated water and allowed to set for 1 hour. Once set, water was removed and stacking gel (5% acrylamide, 125 mM Tris [pH 6.8], 1% SDS, 4 mM EDTA) was poured. Both reservoirs were then filled with 1x SDS-PAGE running buffer (250 mM Tris-Base, 192 mM glycine, 0.1% SDS). Protein samples (concentration dependent on protein to be visualised) were loaded and run through the stacking gel at 80 V before separating at 120 V.

### **2.2.10 Western blotting**

After electrophoresis, proteins were transferred from the gel to a nitrocellulose membrane (0.22  $\mu$ m, Anachem) using the wet transfer system (Biorad) in 1X SDS PAGE Blotting buffer (250 mM Tris-Base, 192 mM glycine, 0.01% SDS) in 20% methanol. The blotting device was placed in a tank filled with ice cold buffer and transfer was carried out at a current of 200 mA for 2 hours. The nitrocellulose membrane was blocked for non-specific interactions with 5% dried milk powder (Marvel) in PBS 0.05% Tween-20 at room temperature for 1 hour. The membrane was then incubated with the primary antibody (*see* **Table 2** for dilution and incubation time). Following, further 3 washes for 10 minutes in PBS; 0.05 % Tween-20, the appropriate peroxidase-conjugated secondary antibody was added to the membrane for 1 hour at room temperature (concentration specified in **Table 3**). Membranes were again washed three times for 10 minutes in PBS 0.05 % Tween-20 and finally visualised by using enhanced chemiluminescent reagents (Amersham) and exposure to Fuji X-Ray film. To reprobe the membrane with another primary antibody, antibodies were stripped by incubating the membrane for 15-45 minutes (depending on the antibody) at room temperature in stripping buffer (200 mM

glycine, 1% SDS, pH2.5). The membrane was then reblocked in 5% dried milk before being incubated with a new primary antibody.

### **2.2.11 RNA interference**

Twelve hours before transfection, HeLa cells were plated in 12 wells plate at a density of  $0.8 \times 10^5$  cells.ml<sup>-1</sup>. Cells were then transfected with 50 nM of siRNA using lipofectamine according to the manufacturer's instructions. Efficiency of silencing was generally validated by western-blot 48 hours post-transfection. The siRNA targeted sequences of siBid, siCaspase8, siTaz were designed and generated by MWG (UK). These sequences are shown in **Table 4**.

The targeting sequence of siTaz was used to generate a pair of complementary DNA oligonucleotides of 64 pb (**Table 4**). These oligonucleotides were annealed and cloned into the pSUPERRetroGFPNeo vector to generate a tafazzin-targeting shRNA vector (shTaz). HeLa cells were then stably transfected with shTaz as described previously. Clones were lysed and RNA and proteins were extracted. The efficiency of the gene silencing was finally analysed by quantitative PCR and western-blot. HeLa cells transfected with pSUPERGFPNeoScramble were used as controls (shControl).

### **2.2.12 RNA extraction**

Total cellular RNA was extracted from 10 cm plates of cells at 80% confluency using RNA-Bee reagent (TEL-Test, NC, Texas), in accordance with the manufacturer's instructions. Cells were lysed using 8 ml of RNA-Bee and incubate for 5 minutes to ensure complete dissociation of nucleoprotein complexes. Chloroform (0.8 ml) was then added and the homogenate was incubated for 5 minutes at 4°C and centrifuged at 12,000 x g for 15 minutes at 4°C. After centrifugation, the homogenate was separated into two phases: the lower blue phenol-chloroform phase and the colourless upper aqueous phase. RNA remained exclusively in the aqueous phase whereas DNA and proteins were in the interphase and organic phase. The upper phase was carefully transferred to a fresh tube and an equal volume of isopropanol was added to precipitate the RNA. The supernatant was then removed and the remaining RNA pellet was washed in 1 ml of 75% ethanol. The samples were vortexed briefly and centrifuged at 7,500 x g for 5 minutes at 4°C.

RNA pellets were dissolved in 30  $\mu\text{l}$  of diethylpyrocarbonate (DEPC)-treated  $\text{dH}_2\text{O}$ . RNA concentration was determined by UV spectrophotometry. The purity of the RNA extraction was assessed using the ratio of absorbance at 260 nm and 280 nm. When the final preparation is free of DNA or proteins, this ratio should be in the range of 1.8-2.0. RNA samples were stored at  $-70^\circ\text{C}$ .

### **2.2.13 Reverse Transcriptase - Polymerase Chain Reaction (RT-PCR)**

cDNAs were prepared by reverse transcription of RNA using the GeneAmp RNA PCR kit (Applied Biosystems, Roche) according to the manufacturer's instructions. Briefly, 1  $\mu\text{g}$  RNA was added to a master mix including 4  $\mu\text{l}$  of 25 mM  $\text{MgCl}_2$ , 2  $\mu\text{l}$  of 10 x PCR Buffer II (500 mM KCl, 100 mM Tris-HCl, pH 8.3), 8  $\mu\text{l}$  of 10 mM dNTPs, 20 U of RNase inhibitor, 50 U of MuLV Reverse Transcriptase, 1  $\mu\text{l}$  of 50  $\mu\text{M}$  Random Hexamers. The reaction mix was incubated for 10 minutes at room temperature and reverse transcription was carried out at  $42^\circ\text{C}$  for 15 minutes on Peltier Thermal Cycler (DNA Engine). The reaction was stopped by heating at  $99^\circ\text{C}$  for 5 minutes and cDNAs were then stored at  $-20^\circ\text{C}$ .

PCRs were carried out using the GeneAmp RNA PCR kit (Applied Biosystems, Roche) on a Peltier Thermal Cycler (DNA Engine). Ten  $\mu\text{l}$  of cDNAs was amplified in a final volume of 50  $\mu\text{l}$  containing 1 nM of each primer, 1.25 U of AmpliTaq DNA polymerase, 4  $\mu\text{l}$  of 10X PCR Buffer II and 2  $\mu\text{l}$  of 25 mM  $\text{MgCl}_2$ . The PCR reactions were carried out using the following program: Initial denaturation at  $95^\circ\text{C}$  for 2 minutes, 25 cycles of denaturation-annealing-elongation ( $95^\circ\text{C}$  for 2 minutes,  $60^\circ\text{C}$  for 1 minute) and a final elongation at  $72^\circ\text{C}$  for 7 minutes. Reaction products were resolved on 1% agarose gel containing  $0.1 \mu\text{g}\cdot\text{ml}^{-1}$  of ethidium bromide and cDNAs visualised using a UV transilluminator.

### **2.2.14 Quantitative Real Time Polymerase Chain Reaction (qRT-PCR)**

cDNA synthesis and qRT-PCR were carried out using the DyNAmo SYBR Green 2-step qRT-PCR Kit (Finnzymes). Total RNAs were first reverse transcribed into cDNAs using the MuLV Reverse Transcriptase. Briefly, 1  $\mu\text{g}$  RNA was added to a master mix including 10  $\mu\text{l}$  of RT buffer (including dNTPs mix and 10 mM  $\text{MgCl}_2$ ),

1  $\mu\text{l}$  of Random Hexamers (300 ng/ $\mu\text{l}$ ) and 2  $\mu\text{l}$  M-MuLV RNase H<sup>+</sup> reverse transcriptase. cDNA synthesis was performed using the following parameters: Primer Extension at 25°C for 10 minutes, cDNA synthesis at 37°C for 30 minutes, reaction termination at 85°C for 5 minutes.

qRT-PCR was carried out using 2  $\mu\text{l}$  of cDNAs, 10  $\mu\text{l}$  2X qPCR master mix, (containing modified hot start *Tbr* DNA polymerase, SYBR Green I, optimized PCR buffer, 5 mM MgCl<sub>2</sub> and dNTPs mix), and 0.5  $\mu\text{M}$  of designed primers for gene of interest. For each condition, GAPDH and actin primers were used as reference to standardise data. The PCR reaction was performed in 96 wells optical plate on a gradient Thermal Cycler (Chromo 4, DNA Engine) and analysed using the MJ Opticon Monitor Analysis Software version 3.1. The qPCR reactions were carried out using the following program: Initial denaturation at 95°C for 15 minutes, 44 cycles of denaturation-annealing-elongation (94°C for 10 seconds; 60°C for 30 seconds; 72°C for 30 seconds) followed by a final elongation step at 72°C for 10 minutes. The fluorescent signal was analysed at each cycle of amplification. To check the specificity of the amplified products a melting curve from 70°C to 95°C was performed at the end of the final extension.

### **2.2.15 Induction of cell death**

For cell death induction, cells were plated at the required density to be 80 % confluence on the day of the treatment. To induce apoptosis, cells were treated with the appropriate concentration of anti-Fas antibody (CH11 clone, Upstate, UK), mouse TNF $\alpha$  recombinant protein (Roche Applied Science, Germany) together with cycloheximide (Sigma) or with etoposide (Sigma) at 37°C for varying length of time as indicated for each experiments.

### **2.2.16 Assessment of cell death**

#### **2.2.16.1 Propidium Iodide staining**

Once treated with a cell death-inducing agent, HeLa cells were trypsinized and resuspended in their original medium containing the floating dead cells. After centrifugation, cells were resuspended in 500  $\mu\text{L}$  PBS containing 1  $\mu\text{g}\cdot\text{ml}^{-1}$  Propidium Iodide (Molecular Probes, Invitrogen, UK) and left at room temperature

for 10 minutes. Flow cytometric analyses were then performed using a FACScan (Becton Dickinson, San Jose, USA). The resulting fluorescence was captured via 585/42 nm band pass filter (FL-2) and analysed using the Cell Quest software (Becton Dickinson, San Jose, USA). In each experiments,  $10^4$  cells were analysed.

### **2.2.16.2 Annexin V/Propidium Iodide staining**

To analyse apoptosis induction in lymphoblastoid cells, cells were harvested as described previously. After centrifugation, 2  $\mu$ l of Annexin V-FITC (BD Biosciences, UK) was added to cells' pellet. Pellets were then resuspended in 500  $\mu$ l of binding buffer [10 mM HEPES/NaOH (pH 7.4), 140 mM NaCl, and 2.5 mM  $\text{CaCl}_2$ ] containing 1  $\mu\text{g}\cdot\text{ml}^{-1}$  Propidium Iodide (PI). Cells were incubated in the dark for 15 minutes at room temperature. Flow cytometric analyses were performed using the FACScan. Florescence was captured using the 530/30 nm band pass filter (FL-1) for Annexin V-FITC and 670 nm band pass (FL-3) for PI.

### **2.2.17 Mitochondrial membrane potential assay**

To monitor mitochondrial membrane potential, treated or untreated cells were harvested as described previously and incubated in 500  $\mu$ L of standart growth medium containing 50 nM of the mitochondrial potential probe Tetramethylrhodamine ethyl ester perchlorate (TMRE) (Molecular probes, Invitrogen). The cell suspension was allowed to equilibrate for 20 minutes at 37°C in the dark. Flow cytometry was performed with the FACScan using the 585/42 nm band pass filter (FL-2) to assess the mitochondrial membrane potential. In each experiments,  $10^4$  cells were analysed.

### **2.2.18 Monitoring of caspase activities**

Caspase-3 and caspase-8 activities were assessed using the caspase-3 and caspase-8 detection kits respectively, according to the manufacturer's instructions (Calbiochem, UK). Briefly, cells were harvested and resuspended in 300  $\mu$ l of complete medium. To monitor caspase activities, 1  $\mu$ l of cell permeable peptides, Red-DEVD-fmk (caspase-3) or Red-IETD-fmk (caspase-8), were added and the cells were incubated for 30 minutes at 37°C. Cells were washed in Wash Buffer (Calbiochem, UK) and resuspend in 500  $\mu$ l of Wash Buffer. Flow cytometric analyses

were performed using the FACScan. Fluorescence was captured using the 585/42 nm band pass filter (FL-2).

### **2.2.19 Transmission electron microscopy**

Cells ( $20 \times 10^6$ ) were harvested and resuspended in 1 mL of fixative solution [0.1 M Sodium cacodylate; 2% glutaraldehyde (EM grade), pH 7.4]. Cells were then centrifuged at 500 x g and 1 mL of fixative solution was added to cover the cell pellets. Samples were stored at 4°C and sent to the Electron Microscopy Unit of Cancer Research UK (London). The cell pellets were sectioned using a cryo-ultramicrotome and analysed by transmission electron microscopy (TEM). Analysis was carried out by Ken Blight.

### **2.2.20 Fluorescent microscopy**

#### **2.2.20.1 Tafazzin localization**

HeLa cells were seeded in 6 wells plate and transfected using lipofectamine with 100 ng of pEGFP<sub>TAZ</sub> or pEGFP<sub>N1</sub> (control). Twenty four hours after transfection, cells were incubated at 37 °C for 20 minutes in the presence of 50 nM of TMRE. After two washes in warm PBS, the cells were resuspended in warm complete medium and the fluorescence was captured under a Leica SP2 confocal microscope using TCS software.

#### **2.2.20.2 Immunocytochemistry**

HeLa cells were seeded on coverslips at  $2 \times 10^5$  cells.ml<sup>-1</sup> and treated with anti-Fas antibody to induce apoptosis. Twelve hours after treatment, cells were washed twice with PBS and fixed for 15 minutes at room temperature in 3.7% paraformaldehyde (PFA). After 3 washes in PBS, fixed cells were permeabilized for 5 minutes at room temperature using 0.2% Triton X-100 and non specific binding was blocked for 1 hour in 10 % FCS. Samples were stained using anti-cytochrome *c* antibody (BD Pharmingen, 566432) or anti-Smac/DIABLO antibody (BD Pharmingen, 612244) for 2 hours at room temperature and then washed 4 times for 4 minutes with PBS-0.025 % Tween 80. Samples were then incubated with anti-mouse IgG coupled with cyanine 3 (Jackson Immuno Research) for 1 hour at room temperature and washed

for 4 times for 4 minutes with PBS-0.025 % Tween 80. The coverslip were finally drained, mounted in medium containing DAPI (Vectashield, Vector Laboratories, USA) and sealed with nail varnish. Samples were analysed under a Leica SP2 confocal microscope using TCS software.

### **2.2.21 Preparation of mitochondrial fractions from anti-Fas antibody treated HeLa cells**

HeLa cells were plated into 10 cm plate to reach 80 % confluency at the day of the treatment. After activation of Fas-induced apoptosis, cells were harvested and resuspended in their original medium containing the detached dead cells. All of the following steps were performed at 4 °C. Cells were harvested as described previously and washed twice in cold PBS. Cells were then washed in cold Mitochondrial Isolation Buffer (MIB) [200 mM Mannitol, 70 mM Sucrose, 1 mM EGTA, 10 mM HEPES, 0.05% BSA; adjusted at pH 7.4]. Pellets were then resuspended in 1 ml of MIB and incubated at 4°C for 5 minutes. Cells were homogenized by 60 passes in a tight-fitting Dounce hand homogenizer. Mitochondrial fractions were then prepared by differential centrifugation of cell homogenates. The homogenates were separated by centrifugation at 750 x g for 5 minutes, yielding a mitochondria-rich supernatant and a nuclear and cell debris containing pellet. The mitochondria were finally pelleted by centrifugation 10,000 x g for 10 minutes and resuspended in a minimal volume of MIB. Mitochondrial protein concentration was assessed using the BCA Protein Assay kit (Pierce).

### **2.2.22 Isolation of mitochondria for *in vitro* assay**

For *in vitro* analysis, mitochondria were isolated from  $10^8$  HeLa cells or  $3.10^8$  lymphoblastoid cells. Cells were washed twice in cold PBS and once in cold MIB. Pellets were resuspended in 10 ml MIB and the cells were lysed by 20 strokes in a ¼” cylinder cell homogenizer (H&Y Enterprises, Redwood USA). Mitochondria were then isolated by differential centrifugation as described above.

### **2.2.23 Oxygen consumption monitoring**

Isolated mitochondria ( $0.5 \text{ mg protein.ml}^{-1}$  per assay) from lymphoblastoid cells were suspended in reaction buffer (125 mM KCl, 2.5 mM MgCl<sub>2</sub>, 5 mM HEPES, 1 mM KH<sub>2</sub>PO<sub>4</sub>, 0.2 mM EGTA and 0.5% BSA; pH 7.4). The mitochondrial respiration rate

(Vox) was monitored using a Clark-type electrode at 25°C (StrathKelvin). Mitochondrial electron transport chain was alimented with 10 mM succinate, an electron donor to complex II. To avoid the reflux of electrons from complex II to complex I, complex I was inhibited by the addition of 10 µM rotenone. The energy coupling of the succinate-oxidizing mitochondria was tested using 200 µM of ADP.

### **2.2.24 *In vitro* cytochrome *c* release assay**

Isolated mitochondria were resuspended at 0.5 mg.ml<sup>-1</sup> in the reaction buffer (125 mM KCl, 1 mM KH<sub>2</sub>PO<sub>4</sub>, 2.5 mM MgCl<sub>2</sub>, 0.2 mM EGTA, 5 mM HEPES, 0.1% BSA ; pH 7.4) containing protease inhibitor cocktail. Mitochondria were energized with 10 mM succinate and the reflux of electrons to complex I was inhibited by the addition of 10 µM rotenone. After 5 minutes incubation at room temperature (time for the mitochondria to establish their orthodox configuration), mitochondria were treated with the appropriate concentration of recombinant peptides or proteins and incubated at 37°C for 15 minutes. Mitochondria were collected by centrifugation at 10,000 g for 5 minutes. Supernatants and pellets were then analysed by SDS-PAGE and immunoblotting for the presence of cytochrome *c* or any indicated protein.

### **2.2.25 *In vitro* Bak oligomerization assay**

To assess the oligomerization of Bak on mitochondrial membranes, mitochondria were isolated and treated with appropriate concentration of recombinant peptides or proteins as described for the cytochrome *c* release assay. After centrifugation, supernatants were collected and mitochondrial pellets were cross-linked with the homobifunctional cross-linker, *Bis*-MaleimidoHexane (BMH) (Pierce) which conjugates sulfhydryl groups (-SH). For the cross-linking reaction, mitochondria were resuspended in reaction buffer and incubated for 30 minutes at room temperature in the presence of dimethylsulfoxide (DMSO) (vehicle control) or in 10 mM BMH. The mitochondria were then pelleted and resuspended in protein sample buffer containing DTT in order to quench the cross-linking reaction. Pellets were then analysed by SDS-PAGE on a 4-12% gradient gel (Nupage, Invitrogen) and immunoblotted for the presence of Bak.

### **2.2.26 Mitochondrial-caspase-8 oligomerization assay**

HeLa cells were plated in 10 cm plate to reach 80 % confluency on the day of treatment. After the activation of Fas-induced apoptosis for 12 hours, cells were harvested and resuspended in their original medium containing the detached dead cells. After two washes in PBS, cells were resuspended in cross-linking buffer (210 mM Mannitol, 70 mM Sucrose, 1 mM EGTA, 5 mM HEPES; pH 7.4) and permeabilized by using 0.05 % digitonin (Calbiochem). Ten mM BMH (or DMSO for vehicle control) was added and the cells were incubated for 30 minutes at room temperature. The cells were then homogenized by 10 passes in a tight-fitting Dounce hand homogenizer and mitochondrial fractions were prepared by differential centrifugation as described above. To quench the cross-linking reaction, mitochondrial pellets were resuspended in protein sample buffer containing DTT and finally analysed by SDS-PAGE in a 4-12% gradient gel (Nupage, Invitrogen) and immunoblotted for caspase-8.

### **2.2.27 Mitochondrial membranes insertion assay**

To analyse whether a protein was integrated into the mitochondrial membranes, isolated mitochondrial pellets were resuspended for 30 minutes at 4°C in an alkali buffer containing 0.1 M Na<sub>2</sub>CO<sub>3</sub>, (pH 11.5). At the end of the incubation, the mitochondrial membranes (Alkali-resistant fractions), containing the integrated proteins, were pelleted by ultracentrifugation at 100,000 x g for 30 minutes at 4°C. The supernatants (S100), alkali-sensitive fractions, containing the proteins which are loosely attached to the mitochondrial membranes were also collected. Alkali-resistant and sensitive fractions were then analysed by western blot. The efficiency of the alkali-extraction was controlled using two mitochondrial proteins, the NADH-deshydrogenase subunit-3 (a membrane integral protein) and the subunit-B of succinate deshydrogenase (loosely associated to the matrix side of the mitochondrial inner-membrane).

### **2.2.28 CL and MLCL analysis**

Lymphoblastoid or HeLa cells (20.10<sup>6</sup>) were harvested and washed twice in PBS. Cells pellets were placed in dry ice and sent to to the Laboratory of Genetic and Metabolic diseases at the University of Amsterdam. The extraction of lipids and CL

analysis were carried out by Riekelt Houtkooper. Cell pellets were sonicated for 20 seconds and phospholipids were extracted from the equivalent of 1 mg of protein of the homogenates as follows. After addition of 3 ml of 1:1 chloroform-methanol (v/v) the internal standards (tetramyristoyl-cardiolipin and dimyristoyl-phosphatidylglycerol) were added to the extraction. This mixture was shaken vigorously and placed on ice for 15 min, after which it was centrifuged at 1,000 x g for 10 min. The supernatant was transferred in a new tube, and the protein pellet was reextracted with 3 ml of 2:1 chloroform-methanol (v/v). The combined organic layers were evaporated under nitrogen at 45°C. The residue was dissolved in 150 µl of chloroform/methanol/water (50:45:5 v/v/v) containing 0.01% NH<sub>4</sub>OH, and 10 µl of this solution was injected into the HPLC MS system (Thermo Electron Corporation, Waltham, MA). The phospholipids were separated from interfering compounds by a linear gradient between solution B (chloroform-methanol, 97:3, v/v) and solution A (methanol-water, 85:15, v/v). Solution A and B contained 0.1 ml and 0.01 ml of 25% (v/v) aqueous ammonia per liter of eluent, respectively. The gradient (0.3 ml/min) was as follows: 0–10 min: 20% A to 100% A; 10–12 min, 100% A; 12–12.1 min: 100% A to 0% A; and 12.1–17 min, equilibration with 0% A. A splitter between the HPLC column and the mass spectrometer was used, and 75 µl/min eluent was introduced into the mass spectrometer. A TSQ Quantum AM (Thermo Electron Corporation) was used in the negative electrospray ionization mode. Nitrogen was used as nebulizing gas. The source collision-induced dissociation collision energy was set at 10 V. The spray voltage used was 3600 V, and the capillary temperature was 300°C. Mass spectra of CL and monolysocardiolipin MLCL molecular species were obtained by continuous scanning from m/z 400 to m/z 1000 with a scan time of 2 s. The spectra of CL and MLCL species were acquired during their corresponding retention time in the HPLC elution profile. The CL internal standard was set at 100% in each spectrum.

## **CHAPTER 3 ROLE OF CL IN APOPTOSIS**

## 3 Role of CL in apoptosis

### 3.1 Introduction

Over the past few years, CL has emerged as an important actor in many of the mitochondrial-dependant steps that lead to the release of apoptogenic factors [161]. Two initial studies implicated CL in the pro-apoptotic function of the Bcl-2 family proteins: first as “docking sites” for tBid on mitochondrial membranes [127, 128] and the second as a prerequisite for the activation of Bax and the permeabilization of the mitochondrial outer membrane [101]. CL was also described to have an anti-apoptotic function, anchoring cytochrome *c* associated with the mitochondrial inner membrane thus preventing its release in the intermembrane space [223]. In that model, complete release of cytochrome *c* requires an additional step to dissociate its interactions with CL. The peroxidation of the unsaturated acyl chains of CL may control this dissociation [222]. In fact, this event is catalyzed by cytochrome *c* and is required for the release of cytochrome *c* itself, and of other apoptogenic factors [214].

Despite this growing body of evidence implicating CL in apoptosis, the mechanism by which CL and its fatty acyl chain composition regulate mitochondrial pathways to apoptosis remains controversial. This discrepancy is mainly due to technical issues. As mentioned previously (*section 1.6*) most studies have been limited to *in vitro* use of artificial membrane systems or studies in yeast mutants. Recently, the human *CL synthase* gene was cloned and stably knocked down using shRNAs in the human epithelial carcinoma HeLa cell line [165]. Decreasing *CL synthase* expression in HeLa cells inhibited CL synthesis and manifested with a decrease in CL level and accumulation of its precursor PG. In this model, the acyl-chain composition of CL and MLCL was not modified indicating that CL synthesis does not affect its remodelling [165]. CL-deficiency leads to severe alterations in mitochondrial structure and to accelerated necrosis-like cell death likely due to an accumulation of free cytochrome *c* in the inter membrane space [165]. However, the residual levels of CL in cardiolipin-deficient cells were still able to sustain the activities of the respiratory chain complexes [165]. Therefore it is likely that reduction of the total pool of CL may render the cells more sensitive to bioenergetic insults and thus more sensitive to necrosis. To date, no mutation of *CL-synthase* has been identified in

human. Barth syndrome (BTHS) is the only human disease known to be mainly caused by a defect in CL metabolism [173, 174]. BTHS patients present mutations in the *tafazzin* gene encoding the CL transacylase involved in the remodelling cycle of CL [172]. Tafazzin catalyses the transfer of unsaturated acyl chain from PC to MLCL to generate mature CL. Unlike CL-synthase deficient cells that present a decrease in the total amount of CL, inactivation of tafazzin in BTHS cells results in a decrease in mature CL and an accumulation of saturated MLCL [180, 181]. This makes BTHS cells a unique model for studying the role of the acyl chain composition of CL in apoptosis. Mature CL strictly contains unsaturated fatty acyl chains, which are readily oxidizable targets. The evidence that oxidation of CL by cytochrome *c* is required for the release of apoptogenic factors underpinned the importance of the acyl chain composition of CL in apoptosis [214]. New strategies designed to manipulate the degree of saturation of CL acyl chains could represent a new mean of controlling the cell's fate and open new therapeutic window in anti-cancer treatment. In this context, CL remodelling, and tafazzin in particular, may constitute suitable targets to regulate apoptosis.

This chapter investigates the role of CL and its acyl-chain composition in apoptosis using two cellular models of tafazzin-deficient cells: BTHS-derived lymphoblastoid cells and HeLa-derived tafazzin-knockdown cell lines.

## **3.2 Results**

### **3.2.1 Characterisation of BTHS lymphoblastoid cells**

Lymphocytes were isolated from the blood of two unrelated BTHS patients (DB105.2 and DB105.3) and two unrelated disease-control individuals (DB037 and DB015.2). These cells were immortalised *ex-vivo* by Epstein-Barr virus infection to give rise to lymphoblastoid cell lines. BTHS cell lines have been provided and characterised previously by Richard I. Kelley [244]. BTHS patients carry mutations in the *tafazzin* gene that lead to the expression of inactive mutant forms of the protein. All patients were male and characterized by the triad, cardiomyopathy, neutropenia and 3-methylglutaconic aciduria. Lymphoblastoid cell samples from BTHS and control patients were prepared and sent to the Laboratory of Genetic and Metabolic diseases at the University of Amsterdam. The extraction of lipids and CL

analysis were carried out by Riekelt Houtkooper. Lipids were extracted and CL and MLCL were separated from non polar lipids and other phospholipids by High Performance Liquid Chromatography (HPLC) and analysed by mass spectrometer. **Figure 3-1A** represents the mass spectra of CL and MLCL molecular species isolated from cultured lymphoblastoid cells of a control (DB037) and a BTHS (DB105.2) patient. In each spectrum the levels of CL and MLCL molecular species are normalized to an exogenous CL internal standard ( $m/z$  619.5) set at 100 %. In control cells, five different clusters of CL molecular species are present. Each cluster contains CL with different acyl chain compositions. The difference of mass between clusters relates to the difference in acyl chains. Within the same cluster, peaks represent different degree of saturation of the fatty acyl chains; the higher  $m/z$  values the more saturated the acyl chains. In **Figure 3-1A**, CL clusters are numbered from 1 to 5. These clusters have been characterized previously [181]. In control cells, the most abundant CL molecular species were present in cluster 2 and 3 containing  $C_{16:1}$ ,  $C_{18:1}$  and  $C_{18:2}$  acyl chains. Cluster 4 contained  $C_{18:1}$  and  $C_{18:2}$  acyl chains only whereas cluster 5 corresponded to CL with  $C_{20:4}$ ,  $C_{18:2}$  and  $C_{18:1}$  acyl chains. In comparison to control cells, BTHS lymphoblastoid cells presented an overall reduction of CL molecular species with a dramatic decrease of cluster 3 (**Figure 3-1A**). In control and BTHS cells three clusters of MLCL fatty acyl chain species were observed. These MLCL clusters were strongly increased in BTHS cells, in particular cluster 2 containing MLCL with  $C_{18:1}$  and  $C_{16:0}$  acyl chains. Moreover, in BTHS cells each CL clusters moved to higher  $m/z$  values indicating an increasing in the degree of saturation of the acyl chains. In the mass spectra, the area of each CL ( $m/z$  655-745) and MLCL ( $m/z$  565-610) peaks were measured and normalized to the area of internal CL standard peaks and the quantity of protein. Summation of all these peak areas was used to quantify the total amount of CL and MLCL. Semi-quantitative analysis of total CL and MLCL levels in the DB037 control and two BTHS cells (DB105.2 and DB105.3) are represented in **figure 3-1.B**.

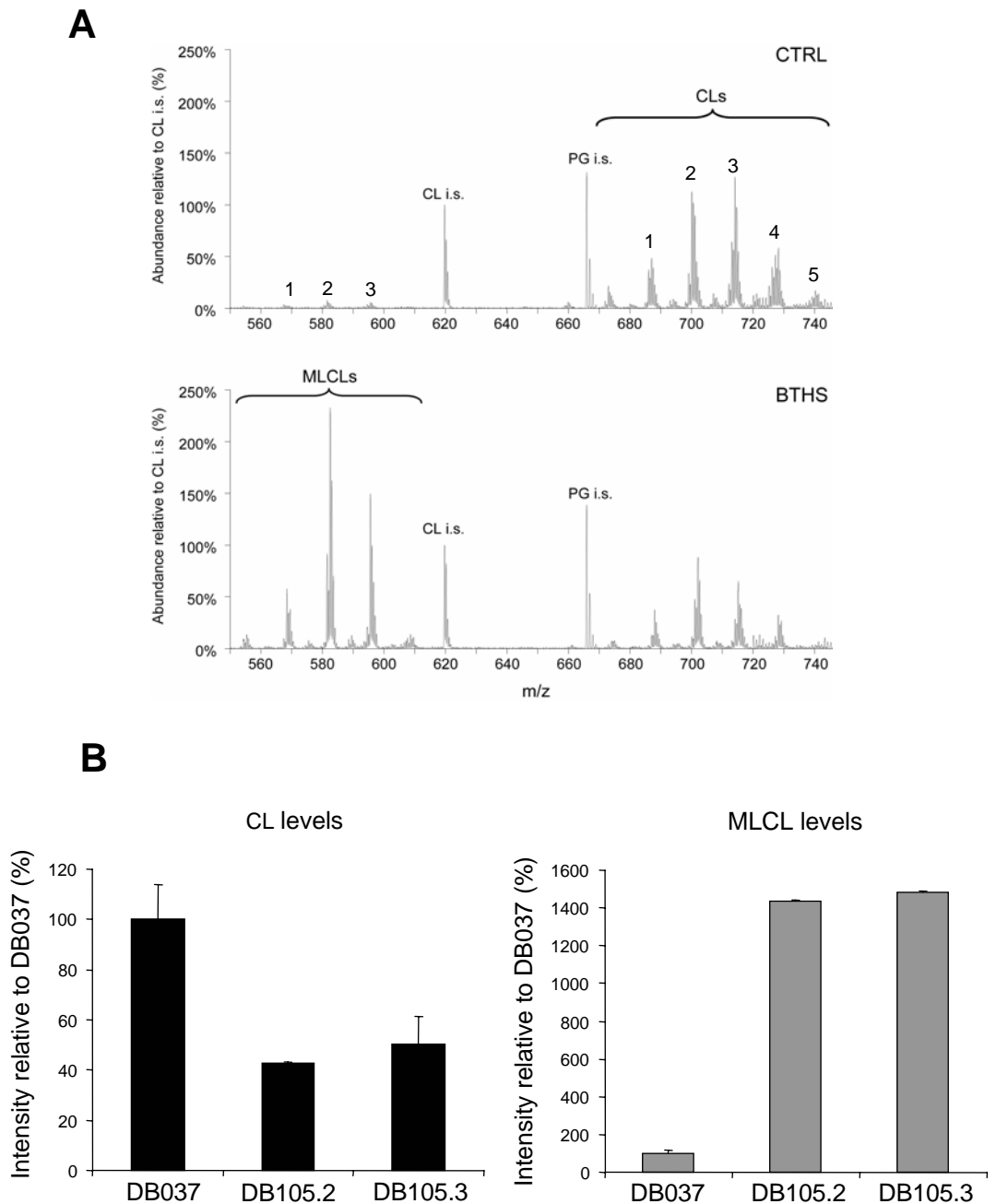


**Figure 3-1: Alteration of CL composition in Barth syndrome (BTHS) lymphoblastoid cells.**

(A) Representative mass spectra of MLCL and CL molecular species in control (DB037) and BTHS (DB105.2) cells. Cells were lysed and normalized for protein levels (1 mg) and lipids were extracted and analysed by mass spectrometry. CL i.s. and PG i.s. correspond to the CL and PG internal standards, respectively. (B) Semiquantitative representation of the levels of CL and MLCL in control (DB037) and two BTHS cells (DB105.2 and DB105.3). These values are averages  $\pm$  SD of duplicate samples for each cell lines.

Both BTHS cells, DB105.2 and DB105.3, exhibited a decrease in CL levels to 40 % and 50 % of the control. Additionally, in BTHS cells the level of MLCL was 14 times higher than in control cells. All together, these results show that BTHS lymphoblastoid cells display low level of mature CL and an accumulation of MLCL. This was also associated with a decrease in the degree of unsaturation of the acyl chains in CL. This is not surprising as *tafazzin* was shown to encode the CL transacylase catalysing the transfer of unsaturated acyl chains from PC to MLCL [172]. Therefore, BTHS lymphoblastoid cells represent a good model to investigate the role of CL and its acyl chain composition in apoptosis.

In CL synthase knockdown HeLa cells, mitochondria presented disorganised cristae indicated that CL is directly required for maintenance of mitochondrial inner membrane structure [165]. To address the role of CL remodelling in mitochondrial structure, two control and two BTHS lymphoblastoid cells were fixed and analysed by transmission electron microscopy. As shown in **figure 3-2**, in control cells (A-B, DB037 or DB015.2) mitochondria adopted an orthodox configuration characterized by relatively large matrix volume and by parallel and individualized tubular cristae, which often elongate through the entire body of the organelles (red arrow) [245]. In stark contrast, BTHS cells displayed abnormal mitochondrial morphology (**Figure 3-2C and D**). Mitochondria appeared swollen and presented complete disorganized cristae (red arrow). Cristae have lost their tubular shape and are interconnected to form honeycomb-like structures (**Figure 3-2C**, red arrow). Thus, these results suggest that CL remodelling is required for maintaining the structure of the mitochondrial inner membrane.

The different complexes of the electron transport chain reside in the mitochondrial inner membrane. Therefore, the effect of CL deprivation on OXPHOS was investigated in BTHS mitochondria. Mitochondria from control and BTHS cells were isolated and the ability of these mitochondria to oxidize succinate was monitored indirectly using an oxygen electrode. **Figure 3-3** represents the consumption of oxygen of control (A) and BTHS (B and C) mitochondria in the presence of succinate. Once added to the respiratory medium (containing  $\text{KH}_2\text{PO}_4$  and  $\text{MgCl}_2$ ), control mitochondria began to oxidize the endogenous succinate present in the

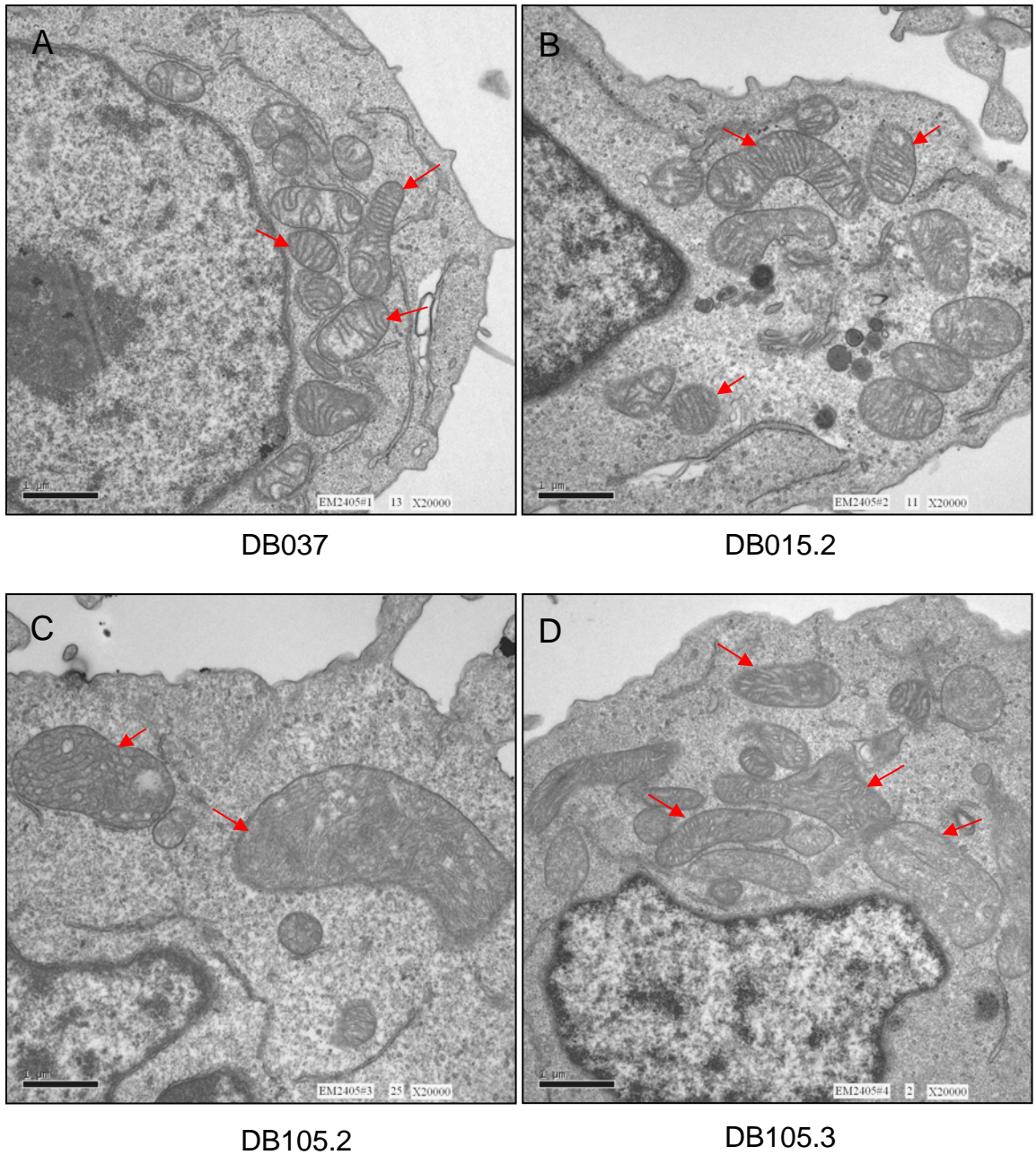


**Figure 3-2: Mitochondria from BTSH patients present an abnormal morphology.** (A and B) Electron micrographs of a cluster of normal mitochondria. (C and D) Electron micrographs of BTSH lymphoblastoid cells. These are representative of triplicate experiments for each cell lines. Red arrows point to the organization of the cristae in the different samples. Bars=1 µm.

matrix. Endogenous succinate was rapidly consumed by complex II and its oxidation resulted in a slight increase in oxygen consumption. This step was defined by Britton Chance as the respiratory state-1 [246] (**Figure 3-3A**). Upon addition of unlimited amount of exogenous succinate (10 mM), mitochondria generated and stabilized an electrochemical gradient of protons through the proton-pumping activity of the respiratory complexes III and IV. This resulted in a further increase in oxygen consumption (respiratory state-4). To challenge the coupling between the electron transport chain and ATP synthase, 200  $\mu$ M of ADP was added to the reaction. Under these conditions (respiratory state-3), the ATP synthase uses the gradient of protons generated as a driving force to phosphorylate ADP to ATP. In response to this influx of protons, the electron transport rate increases and thus more oxygen is consumed. As shown in **Figure 3.3A** the oxygen consumption stayed constant at state-3 after the first ADP addition indicating that ADP was added in excess. Finally, in order to test the activity of the electron transport chain independently of the ADP phosphorylation, carbonyl cyanide m-chloro phenyl hydrazone (CCCP) was added to the reaction. CCCP is a mitochondrial uncoupling agent that dissipates the electrochemical gradient of protons across the mitochondrial inner membrane and thus short-circuits the electron transport chain from the ATP synthase. This uncontrolled influx of protons activates the electron transport at its maximum rate and results in maximal respiration rate until anoxia is reached (32 min). The coupling of the electron transport chain to the ATP synthase characterized the quality of the mitochondria and can be evaluated by the respiratory control ratio value (RCR). RCR corresponds to the ratio of the respiration rate in state-3 to the respiration rate in state-4. In control lymphoblastoid cells the RCR was 2.25. The same experiment was performed on mitochondria isolated from BTHS cells (**Figure 3.3B and C**). BTHS mitochondria (DB105.2 and DB105.3) were able to oxidize succinate at state-4 with the same efficiency as control mitochondria. However, both had lost the ability to respond to ADP and to establish the respiratory state-3. As a result, BTHS mitochondria exhibited lower RCR: 1.08 and 1.3 for DB105.2 and DB105.3, respectively. This may be due to either a loss of coupling between the electron transport chain and the ATP synthase or to an inhibition of the phosphorylation machinery. The fact that CCCP was able to activate the oxygen consumption of BTHS mitochondria to a similar extent as in control mitochondria strongly suggests that the inhibition of the respiratory state-3 is due to an inhibition of the phosphorylation machinery. Altogether these data indicate that CL remodelling is

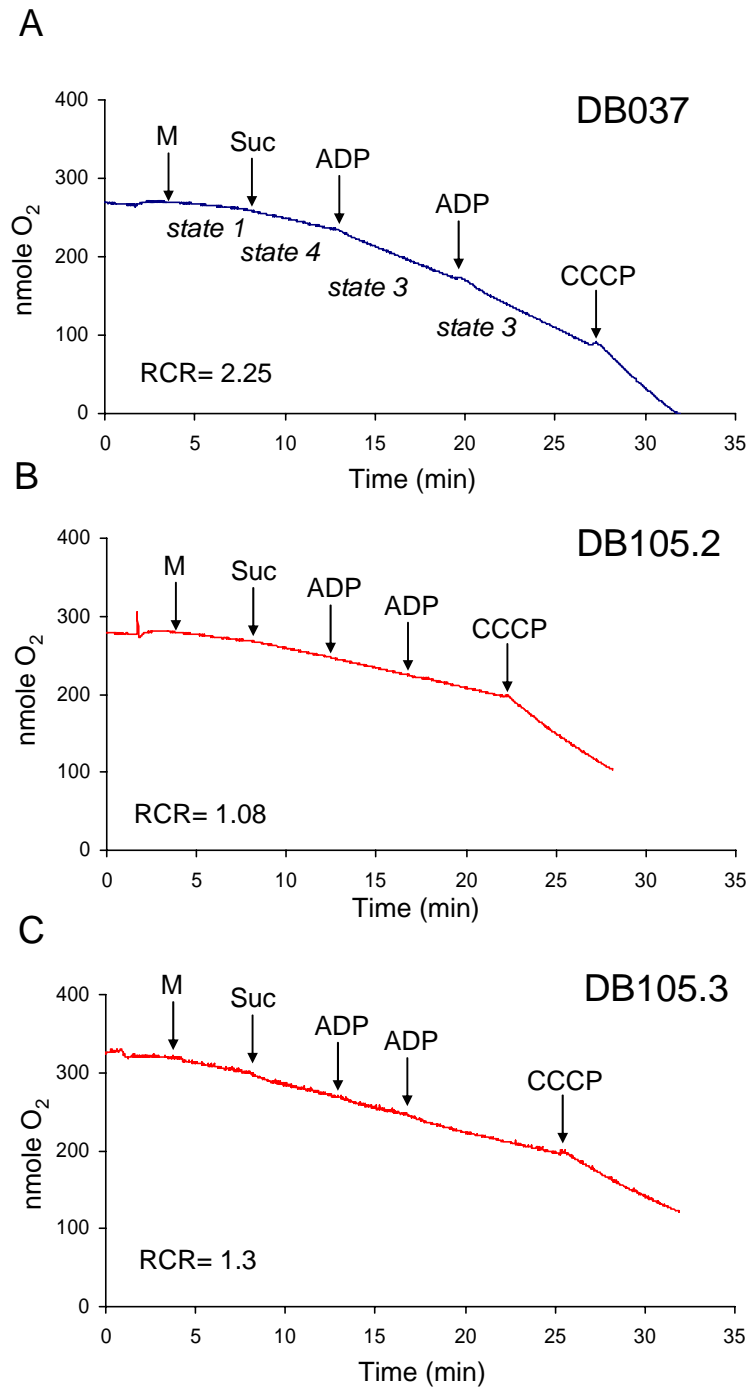


**Figure 3-3: Defective OXPHOS in BTHS mitochondria.**

(A) Oxygraph of control mitochondria oxidizing succinate. (B and C) Oxygraphs of BTHS mitochondria oxidizing succinate. Mitochondria (M) were incubated at 0.5 mg of protein/ml in reaction buffer and 10 mM of succinate (Suc) was added as oxidizable substrate. ADP was added to 0.2 mM and CCCP was added to 1  $\mu$ M. The value of the respiratory control ratio (RCR) is indicated for each cell lines. Each figure is a representative of 3 experiments.

required to sustain OXPHOS and to maintain mitochondrial structure.

In order to investigate the involvement of CL and its fatty acyl chain composition in apoptosis, the sensitivity of BTHS lymphoblastoid cells to extrinsic and intrinsic apoptotic stimuli was analyzed. The extrinsic pathway was challenged using anti-Fas antibody that mimics the Fas ligand and engages the Fas receptor at the plasma membrane to activate the cascade of caspases (see *section 1.5.2*). The intrinsic pathway was activated using the chemotherapeutic drug, etoposide (VP-16). Etoposide is a semi-synthetic compound derived from a toxin present in the mandrake root *Podophyllum*. It has been clinically used for more than 20 years to treat a wide spectrum of human cancers and remains one of the most prescribed anti-cancer drugs in the world. Etoposide targets and inhibits topoisomerase II, an enzyme that maintains the DNA topology. Topoisomerase II removes knots and tangles from the genome by generating transient double-stranded breaks in DNA. Etoposide stabilizes the topoisomerase II-cleaved DNA complex and thus kills cells through accumulation of DNA breaks. In fact, DNA damage activate p53 that triggers the intrinsic mitochondrial apoptotic pathway.

Lymphoblastoid cells from control and BTHS patients were treated with either anti-Fas antibody or etoposide and cell death was assessed by Annexin V/ Propidium iodide (PI) staining. The AnnexinV/PI assay allows the detection of phosphatidyl-serine (PS) externalization, characteristic of apoptosis, and the detection of the loss of plasma membrane integrity, a general feature of cell death. Phospholipids are asymmetrically distributed between the two leaflets of the plasma membrane. In healthy cells, phosphatidyl-choline (PC) and sphingomyelin (SM) predominantly reside in the outer leaflet whereas PS and phosphatidyl-ethanolamine (PE) are mainly located in the inner leaflet. Translocation of PS to the outer leaflet of the plasma membrane is an early event in apoptosis that occurs after caspase activation but before the loss of plasma membrane integrity *in vitro*. *In vivo*, exposure of PS to the extra-cellular surface serves a recognition signal for neighbouring cells to phagocytose the apoptotic cells in order to avoid the disruption of the plasma membrane and consequently an inflammatory reaction. Externalization of PS on the cell surface can be detected with Annexin V. Annexin V binds to the negatively charged phospholipids like PS in presence of  $\text{Ca}^{2+}$ . Therefore, after treatment, cells were resuspended in  $\text{Ca}^{2+}$  containing buffer. By conjugating FITC to Annexin V it is

possible to identify and quantify apoptotic cells by flow cytometry. PI binds to DNA by intercalating between the bases. PI is membrane impermeant and excluded from healthy cells. PI incorporates into DNA of cells that have lost their plasma membrane integrity. These have either undergone late apoptosis, a stage often referred to as secondary necrosis. Therefore, AnnexinV/PI double staining technique was used to distinguish between healthy cells (Annexin V negative / PI negative), early apoptotic cells (Annexin V positive / PI negative), late apoptotic or secondary necrotic cells (Annexin V positive / PI positive) and necrotic cells (Annexin V positive / PI positive).

Lymphoblastoid cells from control or BTHS patients were treated with  $0.5 \mu\text{g}\cdot\text{ml}^{-1}$  of anti-Fas antibody for 24 and 48 hours. **Figure 3.4A** shows two representative experiments of Annexin V/ PI assays on control (DB015.2) and BTHS (DB105.2) cells. At the beginning of the experiment (time 0), both control and BTHS cells were mostly detected at the lower left quadrant of the plot (double negative) indicative of viable cells (90 % and 92 % for control and BTHS cells, respectively). In both cell lines, there was a small population of cells in the upper right quadrant, corresponding to the basal level of cell death. This indicated that these cell lines were both in a good state before treatment. It is important to mention that basal cell death of untreated cells was always checked at each time point in order to rule out false interpretation of the effect of apoptotic stimulus (Data not shown). After 24 hours incubation with  $0.5 \mu\text{g}\cdot\text{ml}^{-1}$  of anti-Fas antibody, 5.26 % of control cells were detected at the early apoptotic quadrant (lower right) and 29.44 % at the late apoptotic quadrant (upper right). In contrast, at the same time, only 3.17 % of the BTHS cells became early apoptotic and only 11.54 % were at the late apoptotic stage. This difference was further amplified after 48 hours of treatment. In fact, only 57 % of the control cells were viable after 48 hours whereas almost 90 % of BTHS were still healthy. The percentages of Annexin V positive cells (early and late apoptosis) of three independent experiments are represented in **figure 3.4B** for the two control and two BTHS cell lines. Both control lymphoblastoid cell lines had similar behaviour upon anti-Fas antibody treatment with around 40 % of cells undergoing apoptosis after 48 hours (blue lines). On the other hand, BTHS were strongly resistant to anti-Fas antibody and only 8 % apoptosis was observed after two days of treatment (red lines).

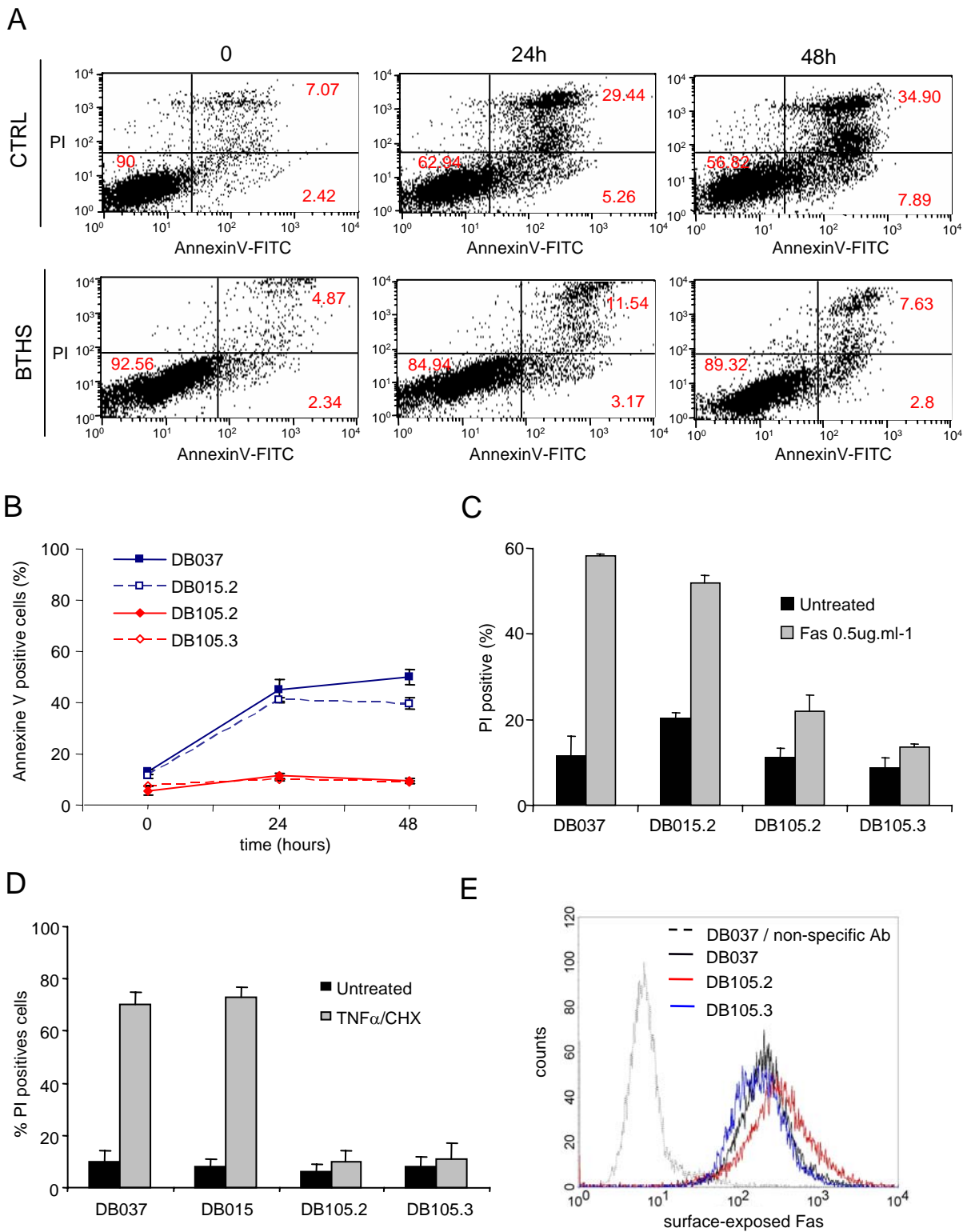


**Figure 3-4: BTHS cells are resistant to extrinsic apoptotic stimuli.**

(A) Dot plot of annexin V (green fluorescence @  $585 \pm 42$  nm) vs PI (red fluorescence @  $530 \pm 30$  nm) staining cells. Upper panels correspond to control DB015.2 cells and lower panels to the DB105.2 BTHS cells. These plots are representative of 6 experiments (B) Kinetics of apoptosis induced by anti-Fas antibody in control and BTHS cells. Control cells are represented in blue, BTHS in red. Error bars are standard errors of the mean of 6 independent experiments (C) Percentage of cell death induced by anti-Fas antibody after 48 hours incubation. (A-C) Cells were treated with a single dose of  $0.5 \mu\text{g.ml}^{-1}$  of anti-Fas antibody. (D) Percentage of cell death induced by recombinant  $\text{TNF}\alpha$  ( $20 \text{ ng.ml}^{-1}$ ) together with cycloheximide ( $\text{CHX}$ -  $20 \mu\text{g.ml}^{-1}$ ) after 24 hours incubation. (E) Control (DB037) and BTHS-derived (DB105.2 and DB105.3) cells were analysed by FACS, using anti-Fas antibody, for the levels of surface-exposed Fas receptor. Error bars are standard errors of the mean of 3 independent experiments.

The effect of anti-Fas antibody on the viability of control and BTHS lymphoblastoid cells was determined in an independent experiment by single PI staining (PI exclusion). **Figure 3.4C** represents the percentage of cell death (PI positive cells) after 48 hours in the presence of anti-Fas antibody. These results are consistent with data in **figure 3.4A and B** and provide more evidence that BTHS cells were protected from anti-Fas antibody induced apoptosis. Importantly, this resistance was not due to a decrease in levels of surface-exposed Fas on BTHS cells (**Figure 3.4E**). The same results were obtained when control and BTHS cells were treated with TNF $\alpha$  in the presence of cycloheximide, an inhibitor of protein translation. In the absence of protein synthesis, the anti-apoptotic pathway of TNFR1 mediated by NF $\kappa$ B is inhibited and TNF $\alpha$  activate extrinsic apoptosis. Like with anti-Fas antibody, BTHS lymphoblastoid cells were strongly resistant to TNF $\alpha$ -induced apoptosis (**Figure 3.4D**). Altogether these data suggest that the inactivation of tafazzin and consequently of CL remodelling confers resistance to the extrinsic pathway of apoptosis.

The same experiments were carried out using DNA-damage inducing agents that activate apoptosis through the intrinsic pathway. Lymphoblastoid cells from control and BTHS patients were treated with 5  $\mu$ M etoposide for 24 and 48 hours and cell death was assessed by Annexin V/ PI double staining. As shown in **figure 3.5A** even though the DB037 control cells exhibited a slightly lower sensitivity to etoposide, DB015.2 control and the two BTHS lymphoblastoid cells underwent apoptosis to the same extent and kinetics after treatment with etoposide. In fact, around 50 % of apoptosis was observed in these three cell lines after 48 hours. The measure of cell viability by PI exclusion further supported the data of **figure 3.5A**. **Figure 3.5B** shows the percentage of cell death (PI positive cells) of control and BTHS cells after treatment with 5  $\mu$ M etoposide for 48 hours. No differences of sensitivity were observed between the control and BTHS cells in response to etoposide; around 50 % of cell death was obtained after 48 hours treatment in the four cell lines. The same results were obtained using the DNA damage-inducing drug cisplatin (**Figure 3.5C**). To conclude, these results suggest that while inactivation of tafazzin does not affect the ability to undergo intrinsic apoptosis, it strongly protects cells from the extrinsic apoptotic pathway.

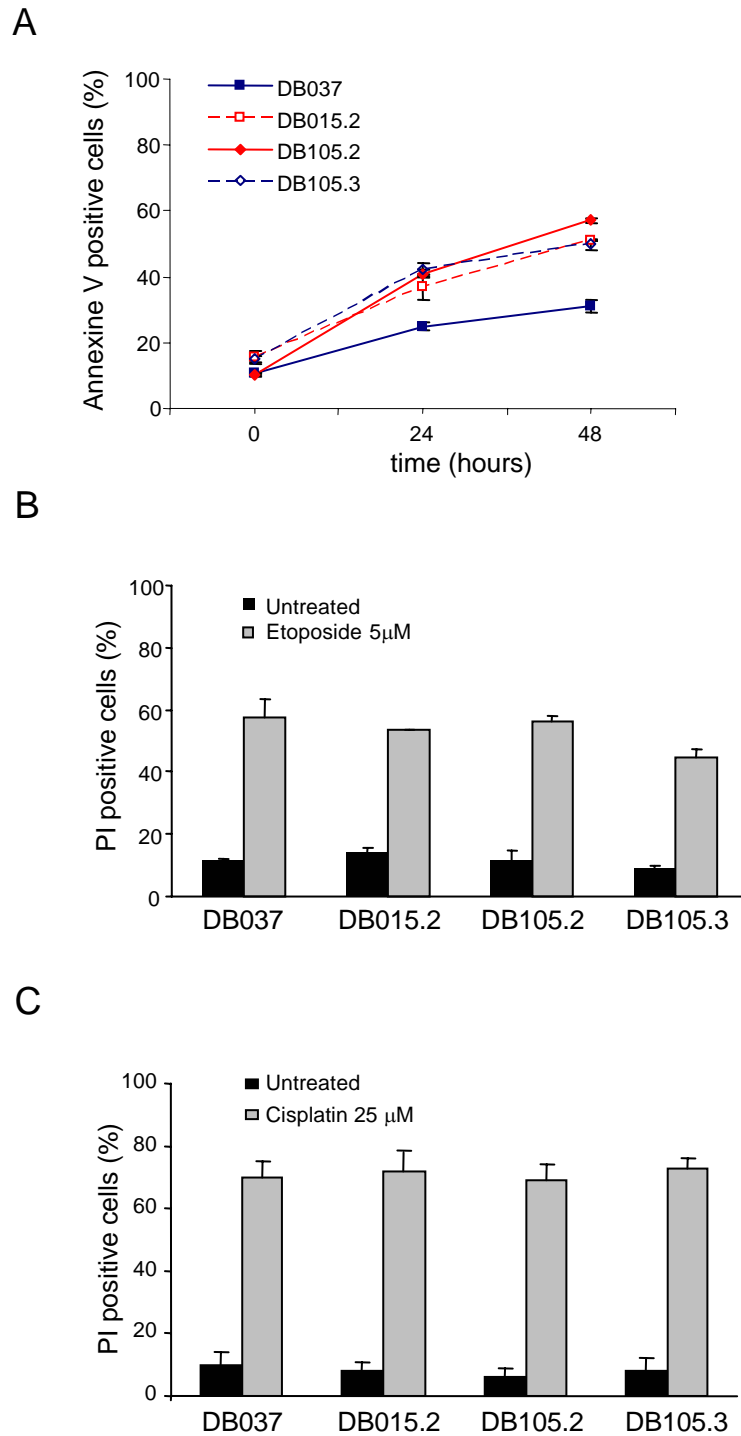


**Figure 3-5: BTHS cells are sensitive to intrinsic apoptotic stimuli.**

(A) Kinetics of apoptosis induced by etoposide in control and BTHS lymphoblastoid cells. Control cells (DB037 and DB015.2) are represented in blue, BTHS (DB105.2 and DB105.3) in red. Error bars are standard errors of the mean of 3 independent experiments (B) Percentage of cell death induced by etoposide after 48 hours incubation. (A and B) Cells were treated with a single dose of 5  $\mu$ M etoposide. (C) Percentage of cell death induced by cisplatin (25  $\mu$ M) after 48 hours incubation. Error bars are standard errors of the mean of 3 independent experiments.

### ***3.2.2 Knocking-down tafazzin decreases CL level and protects cells from extrinsic apoptosis.***

Since CL is a phospholipid specific of the mitochondrial membrane, it was reasonable to speculate that tafazzin inactivation and thus CL remodelling alteration inhibit the mitochondria-dependent step of the extrinsic apoptotic pathway (type II). However, lymphoblastoid cells were not an easy model to work with. These cells were difficult to grow and none of the methods of transfection tested (lipocarrier, Calcium Phosphate, electroporation) was successful. Therefore, in order to directly investigate the correlation between inactivation of tafazzin, alteration of CL metabolism and the resistance to extrinsic pathway it was important to generate a Barth syndrome-like model in a type II cell line. The cervical carcinoma HeLa cells are easy to grow, easily transfectable using common protocol and they also possess a individualized mitochondrial network making it a good cellular system for mitochondrial immunofluorescence analysis. First it was confirmed that HeLa cells behave as type II cells in response to Fas-receptor mediated apoptosis. In type II cells, the apoptotic signal initiated at the DR is relay to the mitochondria via the cleavage and activation of the BH3-only protein Bid. HeLa cells were transfected with incremental doses of short interfering RNA (siRNA) targeting the pro-apoptotic protein Bid and the efficiency of this oligonucleotide to reduce Bid expression was analysed by western-blot after 48 hours. As shown in **figure 3.6A**, 50 nM of siBid efficiently decreased the level of Bid in HeLa cells. This was due to a specific silencing of Bid expression since the non-targeting siRNA pool (scRNA) did not affect the level of Bid. 48 hours after transfection with 50 nM of each siRNA, HeLa cells were treated with  $0.3 \mu\text{g}\cdot\text{ml}^{-1}$  of anti-Fas antibody for 24 hours and cell viability was analysed by PI staining (**Figure 3.6B**). Depleting Bid in HeLa cells strongly inhibited Fas receptor-mediated cell death. In fact, 40 % of cells died in presence of scRNA whereas only 20 % of cell death was observed in HeLa siBid transfected cells. The Annexin V assay was originally developed to measure apoptosis in cells in suspension such as lymphocytes. This technique is not suitable for adherent cells such as HeLa cells. Detachment of adherent cells by trypsinization generally interferes with the binding of Annexin V to membrane PS, making apoptosis measurement a technical problem. Therefore, apoptosis was analysed by monitoring the activity of the effector caspases using the cell permeable substrate Red-DEVD-fmk. Caspase-3 is the major effector caspase that is activated in response to most of the apoptotic stimulations and cleaves a plethora of substrates after the DEVD motif.

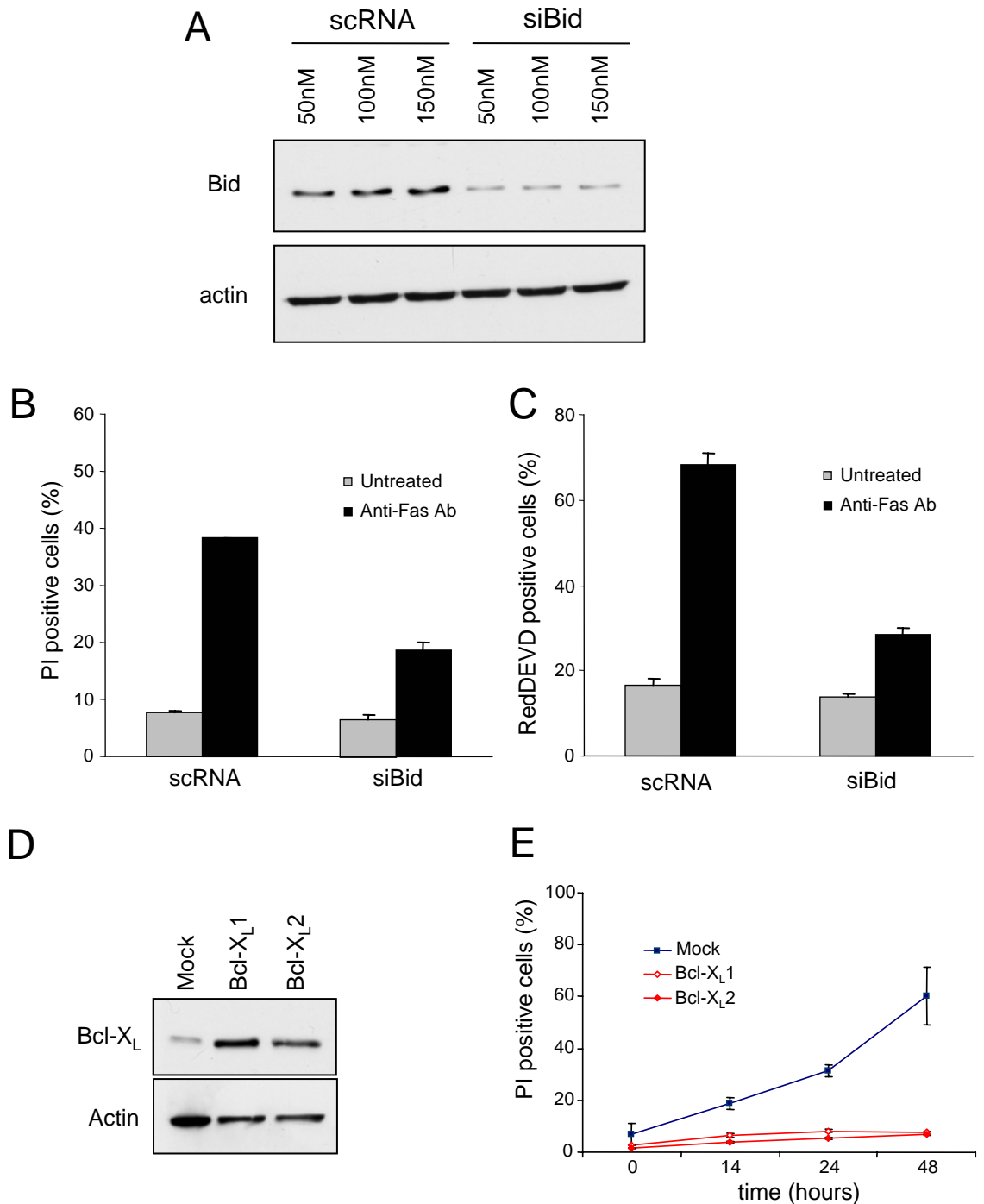


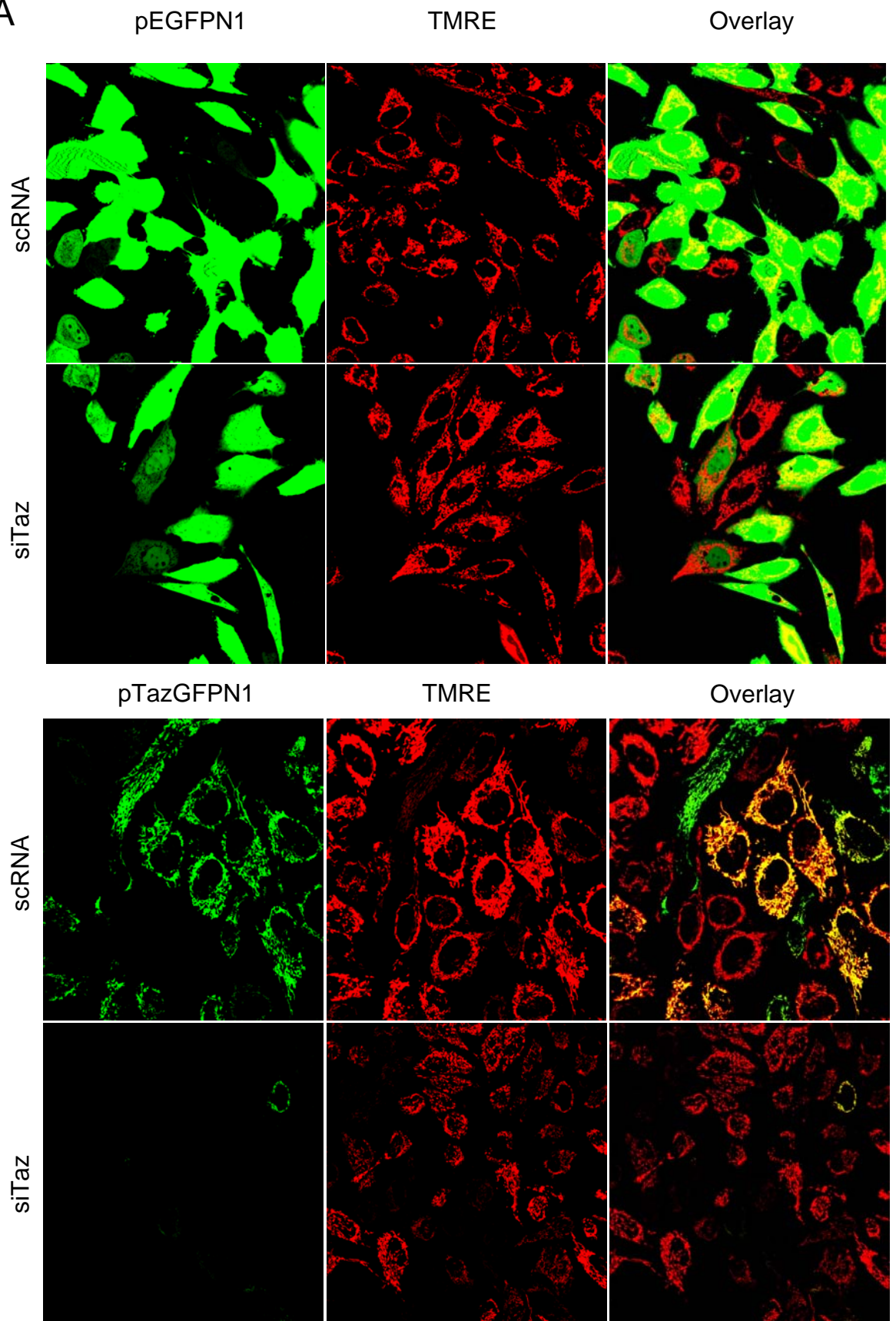
### Figure 3-6: HeLa cells display a type II response to Fas-induced apoptosis.

(A) Western-blot analysis of endogenous Bid in HeLa cells transfected with incremental doses of either non targeting (scRNA) or Bid-targeting siRNAs (siBid). (B-C) Involvement of Bid in Fas mediated-apoptosis. HeLa cells were transfected with 50 nM of scRNA or siBid for 48 hours and treated with 0.5  $\mu\text{g}\cdot\text{ml}^{-1}$  of anti-Fas antibody for 24 hours. (B) Cell death was analysed by PI exclusion. (C) Caspase-3 activation was monitored using Red-DEVD-fmk (D) Western-blot analysis of Bcl-X<sub>L</sub> expression in HeLa Bcl-X<sub>L</sub>-overexpressing stable clones (Bcl-X<sub>L</sub>1 and 2) as compared to the parental cell lines transfected with the empty vector (Mock). (E) Role of Bcl-X<sub>L</sub> in Fas-mediated apoptosis. Mock or Bcl-X<sub>L</sub> overexpressing HeLa cells were treated with 0.3  $\mu\text{g}\cdot\text{ml}^{-1}$  of anti-Fas antibody for 12, 24 and 48 hours. Cell death was analysed by PI exclusion. (A and D) Cell lysates were immunoblotted with the indicated antibody. Actin was used as loading control. (B, C and E) Error bars are standard errors of the mean of 3 independent experiments.

Once caspase-3 is activated Red-DEVD-fmk binds irreversibly to its active site and the cell become fluorescent. However, DEVD is not specific for caspase-3 and can be cleaved by high concentrations of other several caspases. According to the previous data, silencing Bid protected HeLa cells from Fas-induced apoptosis (**Figure 3.6C**). In fact, transfection of HeLa cells with siBid reduced apoptosis from 70 % to 30 %. These results indicate that Bid is required for Fas-induced apoptosis in HeLa cells and strongly suggest that HeLa are type II cells. It is worth noting that there was still a significant induction of apoptosis (30 %) in siBid-transfected HeLa cells. This may be a consequence of the inefficient Bid silencing with siBid. Indeed, as can be seen in **figure 3.6A**, siBid did not completely knockdown Bid in HeLa cells. In type II cells, but not type I cells, Fas receptor-mediated apoptosis requires a mitochondria-dependent step and is inhibited by Bcl-2 or Bcl-X<sub>L</sub> [56]. Therefore, to confirm that they are indeed type II cells HeLa cells were transfected with Bcl-X<sub>L</sub>, stable clones were selected and Bcl-X<sub>L</sub> expression was analysed by western-blot. **Figure 3-6D** shows Bcl-X<sub>L</sub> overexpression in two of these clones as compared to the endogenous level of Bcl-X<sub>L</sub> in the parental cells lines transfected with the empty vector (Mock). These cells were treated with 0.3 µg.ml<sup>-1</sup> of anti-Fas antibody for 14, 24 and 48 hours and cell death was assessed by PI exclusion. **Figure 3-6E** represents the kinetics of cell death in these two Bcl-X<sub>L</sub> overexpressing clones as compared to the mock transfected HeLa. Fas-induced apoptosis was completely inhibited by Bcl-X<sub>L</sub> overexpression in HeLa cells. These results together with the results presented in **figure 3-6B and C** demonstrate that HeLa cells are type II cells and require a mitochondrial amplification step to activate apoptosis in response to DR engagement. For these reasons, HeLa cells were chosen as cellular system to generate a model, similar to BTHS.

To knock down tafazzin in HeLa cells, siRNA targeting *tafazzin* were designed (siTaz). HeLa cells were transiently co-transfected with 100 ng of plasmid encoding tafazzin-GFP fusion protein and 50 nM of either a non-specific or *tafazzin*-targeting siRNAs. Twenty four hours after transfection, cells were incubated with 50 nM of TMRE to stain the mitochondrial network. TMRE is a fluorescent dye that accumulates in mitochondria in a mitochondrial membrane potential dependant manner. The efficient siRNAs were identified by their ability to decrease the expression of tafazzin-GFP. The level and localization of tafazzin-GFP were analysed by confocal microscopy (**Figure 3-7A**).

A



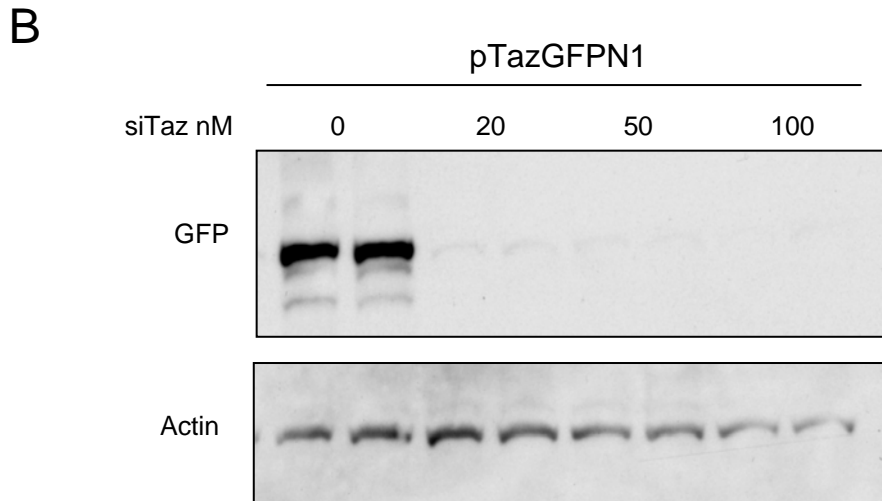


**Figure 3-7: Tafazzin localizes to the mitochondria and is efficiently ablated by a specific *tafazzin* siRNA.**

HeLa cells were transiently co-transfected with a plasmid encoding tafazzin-GFP fusion protein and either a non-specific (scRNA) or *tafazzin*-targeting siRNAs (siTaz). (A) Cells were analysed by confocal microscopy for the levels and localization of tafazzin-GFP 48 hours after transfection. TMRE was used to visualize the mitochondria. The specificity of siTaz was controlled by co-transfecting the oligonucleotides with pEGFPN1. These pictures are representative of triplicate experiments. (B) Western-blot analysis of tafazzin-GFP in HeLa cells co-transfected with pTazGFPN1 plasmid and incremental doses of siTAZ for 72 hours. Cell lysates were subjected to 12 % SDS-PAGE and immunoblotted with anti-GFP monoclonal antibody. Actin was used as loading control. Duplicates of each samples were ran.

When HeLa cells were transfected with 100 ng of parental plasmid pEGFPN1 in the presence of 50 nM of scRNA, cells displayed an overall green fluorescence. In contrast, tafazzin-GFP expressed as a punctuated pattern in the presence of scRNA. The green fluorescence perfectly overlaid with the TMRE fluorescence indicating that tafazzin localizes to the mitochondria. Interestingly, this result strongly suggests that the remodelling of CL takes place within the mitochondria. No tafazzin-GFP expression was observed when cells were co-transfected with 50 nM of siTaz. This knockdown was due to a specific silencing of *tafazzin* mRNA since siTaz did not modify the expression of GFP in pEGFPN1-transfected cells. The efficiency of siTaz was also verified by western-blot analysis 72 hours after transfection (**Figure 3-7B**). Altogether these results indicate that 50 nM of siTaz was able to efficiently reduce the expression of tafazzin and this silencing was maintained for at least 72 hours.

Next, HeLa cells were transfected with 50 nM of scRNA or siTaz and their sensitivity to Fas-mediated apoptosis was investigated. Two days after transfection cells were treated with anti-Fas antibody and the cell viability was analyzed by PI staining after 24 hours. Importantly, transient depletion of tafazzin in HeLa cells did not modify the sensitivity of these cells to Fas-induced apoptosis (**Figure 3-8B**). Even though tafazzin was efficiently knocked down by siTaz during the course of the treatment (**Figure 3-7B**), it is likely that due to their slow turnover, CL have not been changed 72 hours after transfection. In fact, lipid radio-labelling experiment has revealed that CL has the highest half life of all the mitochondrial phospholipids in rat liver and brain [247]. Thus, phospholipids were extracted from HeLa cells transiently transfected with scRNA or siTaz and the CL composition was analysed by HPLC-MS as described in *section 3.2.1*. The semiquantitative analysis of total CL level is shown in **figure 3-8A**. As expected, transient depletion of tafazzin using siTaz did not modify the level of CL. With this in mind, the generation of a stable tafazzin knockdown seemed the obvious approach to overcome this problem.

The 21mers targeting sequence of siTaz was used to generate a short hairpin RNA (shRNA) encoding plasmid (shTaz). Two complementary DNA oligonucleotides of 64 nucleotides containing the siRNA targeting sequence in both sense and antisense orientation were designed and cloned into the pSuperRetroGFPNeo vector to produce shTaz. A non-targeting shRNA plasmid, pSuperRetroGFPScramble (shControl), was used as control. HeLa cells were stably transfected with shTaz or

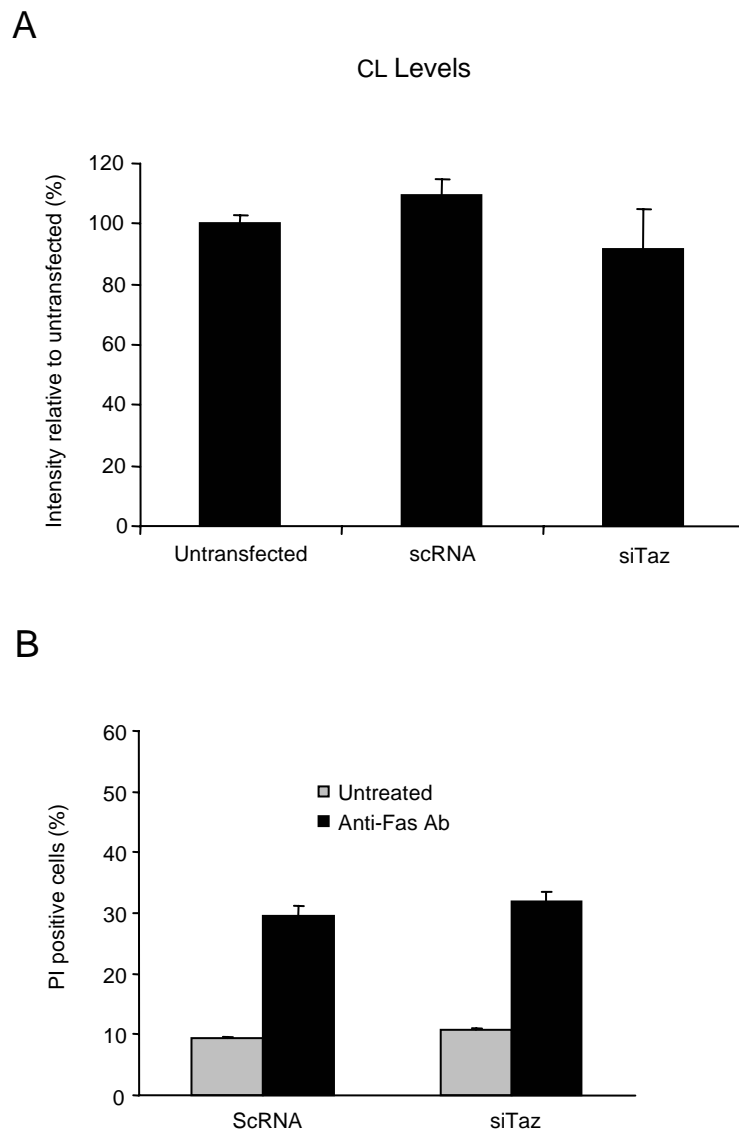


**Figure 3-8: Transient depletion of tafazzin using siTaz does not affect the level of CL and the sensitivity to Fas-mediated apoptosis.**

HeLa cells were transiently transfected for 48 hours with a non-specific (scRNA) or tafazzin-targeting siRNAs (siTaz) and analysed for their cardiolipin composition (A) or treated for 24 hours with  $0.5 \mu\text{g}\cdot\text{ml}^{-1}$  of anti-Fas antibody (B). (A). Semiquantitative representation of the levels of CL. (B). Cell death was analysed by PI exclusion. These values are averages  $\pm$  SD of triplicate samples for each condition.

shControl and 8 clones were isolated for each construct. Total RNA was extracted from these clones and cDNA was prepared by reverse transcriptase reaction. *Tafazzin* and *actin* cDNAs were specifically amplified by 30 cycles of PCR and the expression level of these cDNAs were analyzed on agarose gel and visualized by ethidium bromide staining. **Figure 3-9A** shows the expression of *tafazzin* in shTaz and shControl HeLa clones. As compared to the shControl clones, the level of *tafazzin* expression was reduced in 5 of the shTaz selected clones. Two clones for each construct were selected based on their relative *tafazzin* expression. These included clones 6 and 7 of shControl-transfected HeLa (called shControl1 and shControl2, respectively) and clones 7 and 8 for the shTaz transfected cells (called shTaz1 and shTaz2, respectively) (red tick). The detection of cDNAs products of a reverse-transcriptase PCR (RT-PCR) reaction on agarose gel does not allow accurate quantification since the ethidium bromide detection is rather insensitive and the PCR reaction may pass the exponential phase of amplification. In contrast, real time PCR (or Q-PCR) quantifies the level of cDNAs at each amplification cycle by monitoring the fluorescence of incorporation of SYBR green into the DNA. Q-PCR gives the expression level of target genes normalized to the level of reference genes under the same condition. In order to quantify the level of *tafazzin* expression in the selected HeLa clones, Q-PCR analysis were performed. **Figure 3-9B** shows the expression of *tafazzin* in shControl and shTaz HeLa clones relative to the level in parental untransfected HeLa cells. This expression was normalized using two housekeeping genes,  $\beta$  *actin* and *glyceraldehyde-3-phosphate dehydrogenase (GAPDH)* as reference. As compared to the parental cell line, no significant changes in *tafazzin* expression were observed in shControl HeLa clones. However, this expression was profoundly reduced when HeLa cells were stably transfected with shTaz. In fact, comparing to the parental cell lines *tafazzin* was down-regulated by 12 and 15 fold in the shTaz1 and shTaz2, respectively. Cell lysates were prepared from these different clones and the efficiency of shTaz to knockdown tafazzin protein was analysed by western-blot (**Figure 3-9C**). Both shTaz clones exhibited a significant reduction in endogenous tafazzin as compared to control cells.

Having shown that tafazzin was efficiently silenced in HeLa cells raised the question whether this would affect the CL composition in a similar pattern as in BTHS lymphoblastoid cells. Phospholipids were extracted from HeLa shControl and shTaz and the CL composition was analysed by HPLC-MS as described for the

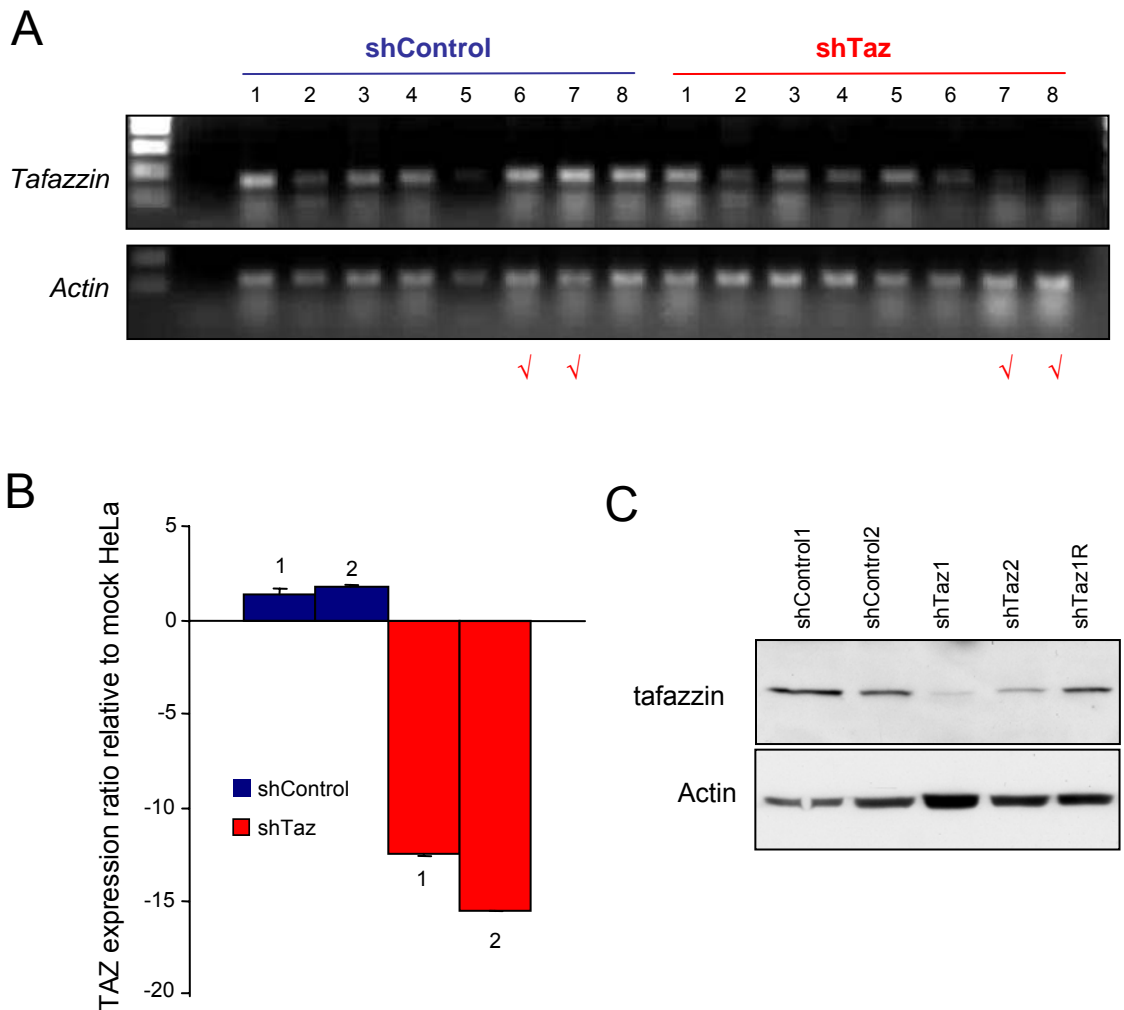


**Figure 3-9: Stably knockdown of tafazzin in HeLa cells using short hairpin RNA plasmid (shTaz).**

HeLa cells were stably transfected with a non-specific (shControl) or tafazzin-targeting shRNAs (shTaz) and clones were selected. (A) RT-PCR cDNA products of *tafazzin* and *actin* for shControl and shTaz clones (B) Real-time PCR analysis of *tafazzin* expression in shControl and shTaz HeLa clones relative to its expression in the parental untransfected HeLa cells. The reaction was normalized to the expression of *actin* and *GAPDH*. Error bars are standard errors of the mean of 3 independent experiments. The sequences of tafazzin, actin and GAPDH primers used for the PCR reactions are indicated in Table1 (section 2.1.2). (C) Western-blot analysis of endogenous tafazzin in shControl and shTaz HeLa clones. Actin was used as a loading control. Cell lysate from shTaz1R revertant clone was also analysed (last lane).

lymphoblastoid cells in *section 3.2.1*. **Figure 3-10A** represents the mass spectra of CL and MLCL molecular species in shControl1 (shControl) and shTaz1 (shTaz) clones. shControl HeLa presented four different clusters of CL molecular species with similar  $m/z$  values as in the lymphoblastoid cells. Like the BTHS cells, shTaz HeLa cells showed an overall reduction of CL molecular species as compared to shControl cells (**Figure 3-10A**). In shControl and shTaz cells three clusters of MLCL fatty acyl chain species were also present. The semiquantitative analysis of total CL and MLCL levels in shControl cells (shControl1 and shControl2) and shTaz cells (shTaz1 and shTaz2) is presented in **figure 3-10B**. In comparison with shControl cells, the level of CL was decreased by 24 % and 39 % in shTaz1 and shTaz2, respectively. As seen in lymphoblastoid cells, the level of MLCL was also increased in shTaz HeLa cells although to a lesser extent. These results show that HeLa shTaz cells display a similar CL pattern as BTHS cells characterized by a low level of mature CL and an accumulation of MLCL. These results indicate that tafazzin plays a crucial role in remodelling CL in HeLa cells. For these reasons, shTaz HeLa cells were used as a model to study the involvement of CL and its acyl chain composition in apoptosis.

In order to investigate the role of tafazzin and CL in apoptosis, the sensitivity of shTaz HeLa cells to extrinsic and intrinsic apoptotic stimulations was analyzed. shTaz HeLa cells were first treated with  $0.3 \mu\text{g}\cdot\text{ml}^{-1}$  anti-Fas antibody and the cell viability was monitored by PI exclusion after 14, 24 and 48 hours. **Figure 3-11A** shows the kinetics of cell death in shControl and shTaz HeLa cells. Like in BTHS lymphoblastoid cells, cell death was strongly inhibited in both shTaz HeLa clones as compared to shControl cells. In fact, only 25 % of shTaz cells died after 48 hours of treatment whereas more than 60 % of cell death was seen in both shControl cells. The extrinsic pathway was also challenged by the activation of  $\text{TNF}\alpha$ -mediated apoptosis pathway in the HeLa clones and the cell viability was analyzed by PI staining (**Figure 3-11B**). When HeLa cells were treated with  $1 \text{ ng}\cdot\text{ml}^{-1}$  of recombinant  $\text{TNF}\alpha$  protein in combination with  $1 \mu\text{g}\cdot\text{mL}^{-1}$  of cycloheximide for 24 hours, 80 % and 42 % of cell death was induced in shControl1 and shControl2, respectively. In stark contrast, shTaz HeLa clones were strongly protected from  $\text{TNF}\alpha$ -mediated apoptosis and only 12 % and 8 % of cell death was detected in the shTaz1 and shTaz2, respectively. Altogether, these data suggest that inactivation of

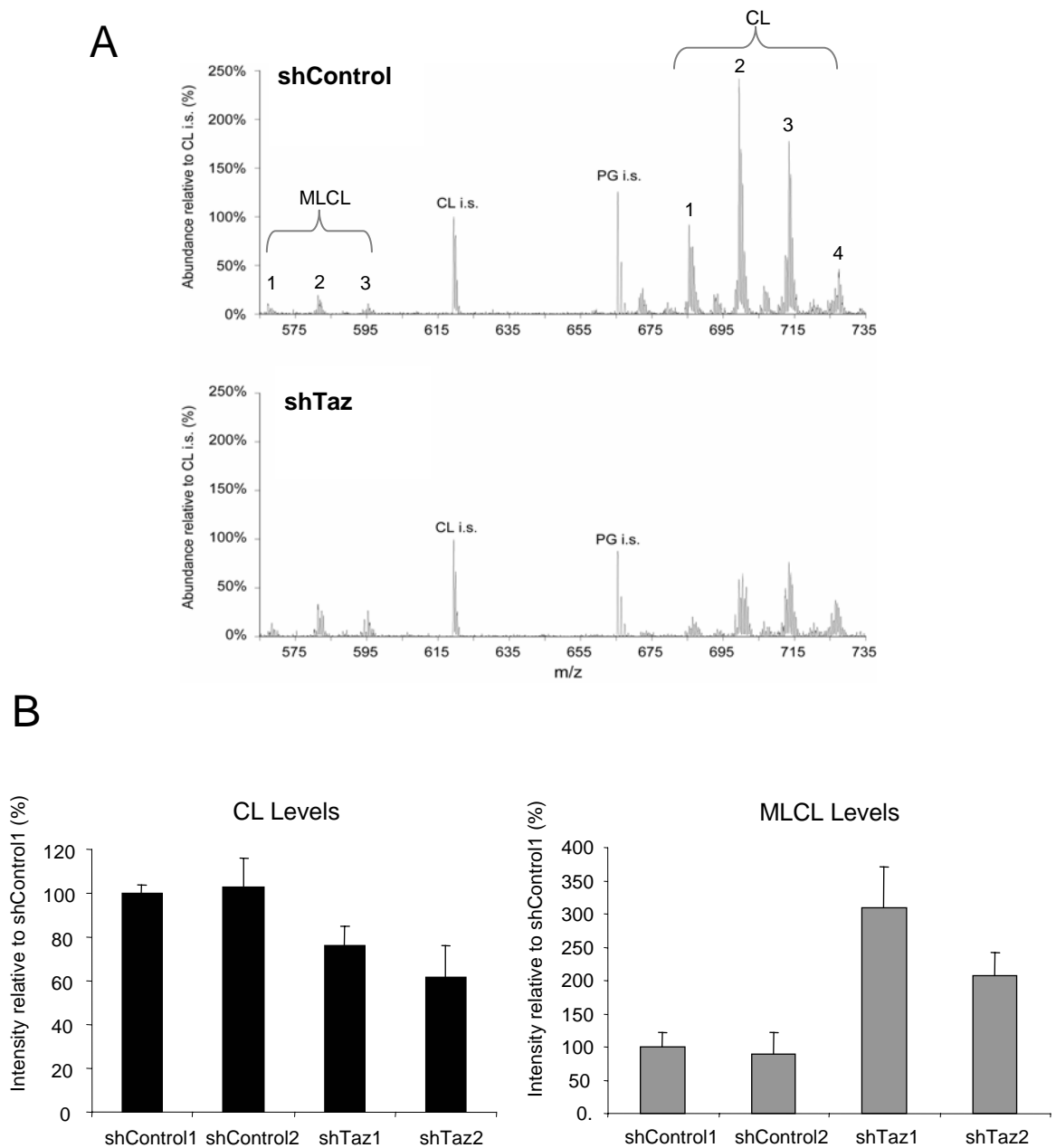


**Figure 3-10: Barth-syndrome like model in HeLa cells.**

HeLa cells were stably transfected with a non-specific (shControl) or Tafazzin-targeting shRNAs (shTAZ) and analysed for their cardiolipin composition. (A) Representative mass spectra of MLCL and CL molecular species in shControl (shControl1) and shTaz (shTaz1) cells. The same amount of protein (1 mg) was extracted for each sample. CL i.s and PG i.s correspond respectively to the CL and PG internal standards. (B) Semiquantitative representation of the levels of CL and MLCL in two shControl cells (shControl1 and shControl2) and two shTaz cells (shTaz1 and shTaz2). These values are averages  $\pm$  SD of triplicate samples for each cell lines.

tafazzin and consequently of CL remodelling, confers resistance to the extrinsic pathway of apoptosis.

Finally, the sensitivity of shControl and shTaz HeLa cells to intrinsic stimulation was tested using etoposide (**Figure 3-11C**). HeLa cells were more resistant to etoposide than lymphoblastoid cells. No cells death was induced when HeLa were treated using 5, 10 or 20  $\mu\text{M}$  of etoposide for 48 hours (Data not shown) and only 35 % of shControl died after 24 hours in presence of 60  $\mu\text{M}$  etoposide. Surprisingly, only 10 % of cells death was observed in shTaz HeLa cells under the same conditions indicating that these cells were also protected from etoposide-induced apoptosis.

Taken together, these results show that tafazzin inactivation in BTHS or HeLa cells lead to an inhibition of CL maturation and confer resistance to the extrinsic apoptotic pathway. Although these data established a correlation between CL remodelling and apoptosis, the role play by CL and its acyl chain pattern in apoptosis needed to be further investigated.

### **3.2.3 Full-length tafazzin is required for CL remodelling and Fas-induced apoptosis.**

Having shown that inactivating tafazzin altered CL maturation and extrinsic apoptosis in BTHS and HeLa shTaz cells raised the question whether introducing active tafazzin back to these cells could reverse their CL composition and restore their sensitivity to extrinsic apoptosis stimulations. As mentioned in *section 1.6.2*, four splice variants of tafazzin are expressed in human [176, 177]. The functionality of these different variants has been investigated by complementation analysis in tafazzin-deficient yeast  $\Delta\text{taz}$  [178]. This yeast mutant strain presents a similar CL profile to BTHS cells with a decrease in CL and accumulation of MLCL levels. Only the human variant lacking exon 5 ( tafazzin $\Delta 5$ ) was able to completely restore the CL composition of  $\Delta\text{taz}$  yeast suggesting that tafazzin $\Delta 5$  was the only functional splice variant in human [178]. Based on these results, this variant was re-introduced by retroviral-infection in BTHS lymphoblastoid cells. Retroviruses are an efficient way of stably delivering genes into mammalian cells. Unlike adenovirus-mediated delivery, retroviruses integrate into the host genome and thus allow a long term expression of target genes. To optimize the conditions of infection, a retroviral construct encoding GFP (pLpC-GFP) was transfected into packaging cells

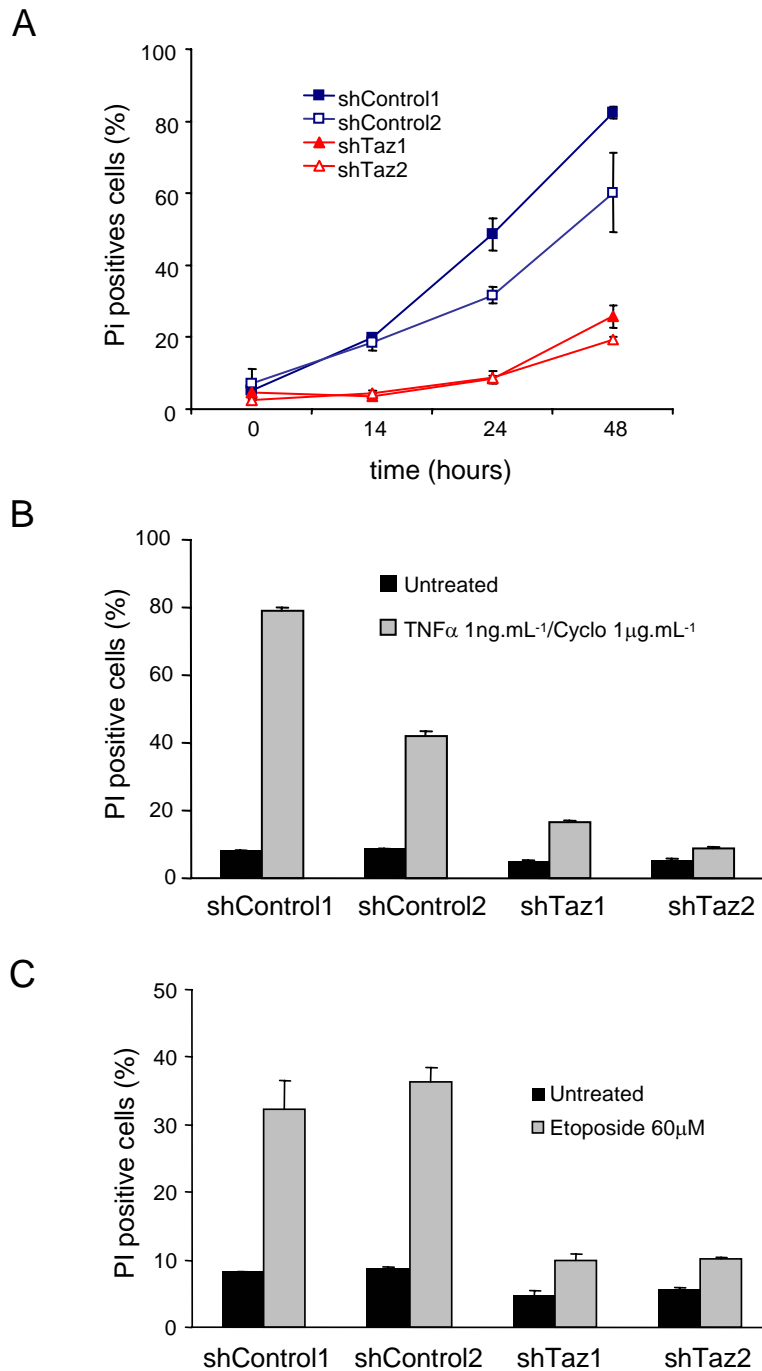


**Figure 3-11: Tafazzin-deficient HeLa cells are resistant to apoptosis.**

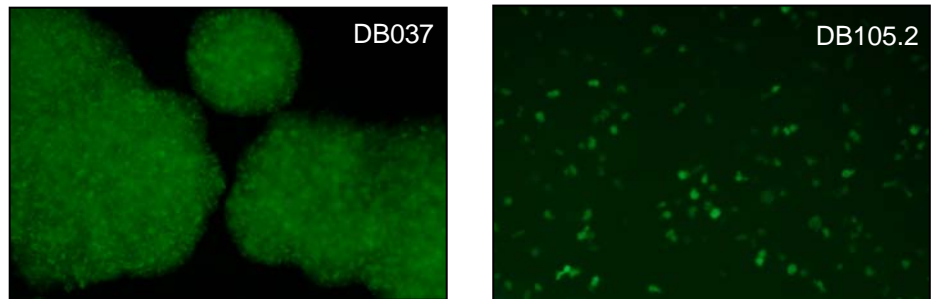
(A) Kinetics of cell death induced by anti-Fas antibody in shControl (blue) and shTaz (red) clones. Cells were treated with a single dose of  $0.3 \mu\text{g.ml}^{-1}$  of anti-Fas antibody and cell death was analysed by PI exclusion. (B) Percentage of cell death induced by recombinant TNF $\alpha$  in shControl and shTaz HeLa cells. Cells were treated for 48 hours with  $1 \text{ ng.ml}^{-1}$  of recombinant TNF $\alpha$  in the presence of  $1 \mu\text{g.ml}^{-1}$  of cycloheximide. (C) Etoposide-induced cell death in shControl and shTaz HeLa cells. Cells were treated for 24 hours with  $60 \mu\text{M}$  of etoposide. Error bars are standard errors of the mean of 3 independent experiments.

(see section 1.2.4.2). The produced retroviruses were collected and used to infect the lymphoblastoid control cells DB037. After two days, the cells were transferred into selective medium. The efficiency of selection was monitored under fluorescent microscope (**Figure 3-12A**, left panel). Three weeks after selection, a high GFP expression was observed in DB037 control. Once the infection method has been optimized, the DB105.2 BTHS cells were infected with retroviruses encoding tafazzin $\Delta$ 5. To control the efficiency of infection, the same cells were infected in parallel with GFP-expressing retroviruses. Like the control cells, most of the DB105.2 cells were green after three weeks of selection (**Figure 3-12A**, right panel). It is worth noting that while the control lymphoblastoid cells DB037 clumped in culture, BTHS DB105.2 cells grew as individualized cells. The expression of tafazzin was quantified by Q-PCR in DB105.2 cells infected with either GFP or tafazzin $\Delta$ 5 expressing retroviruses (**Figure 3-12B**).

Phospholipids were extracted from these cells lines and their CL composition was analyzed by HPLC-MS. The semi-quantitative analysis of total CL and MLCL levels in DB105.2GFP and DB105.2tafazzin $\Delta$ 5 are shown in **figure 3-13A**, in comparison to those levels in DB037 control and in DB105.2 parental cells. No significance difference in CL or MLCL levels was observed between the DB105.2GFP and the parental cell lines DB105.2. Surprisingly, introducing tafazzin $\Delta$ 5 into DB105.2 did not significantly affect the CL level, while the MLCL level was completely reduced to its normal level. Since CL level was still low in DB105.2tafazzin $\Delta$ 5 cells (45 % of the control) it was investigated whether reversion of the MLCL to its normal level would be sufficient to restore the sensitivity of these cells to the extrinsic apoptotic pathway. To address this issue, DB105.2GFP and DB105.2tafazzin $\Delta$ 5 were treated with anti-Fas antibody for 24 hours and cell death was analysed by PI staining. The experiment was also carried out in control DB037 and the parental cell line DB105.2. As shown in **figure 3-13B**, the over-expression of tafazzin $\Delta$ 5 in DB105.2 did not restore sensitivity to Fas-mediated apoptosis. In fact, only 10 % of DB105.2tafazzin $\Delta$ 5 cells died in response to anti-Fas antibody whereas more than 45 % of cell death was induced under the same conditions in DB037 control cells.

In parallel, the full-length tafazzin variant was introduced into HeLa tafazzin-deficient cells (shTaz1). To overcome the effect of shTaz on tafazzin expression, a siRNA resistant vector expressing human full length tafazzin was generated.

A



pLpC-GFP retroviral infection

B

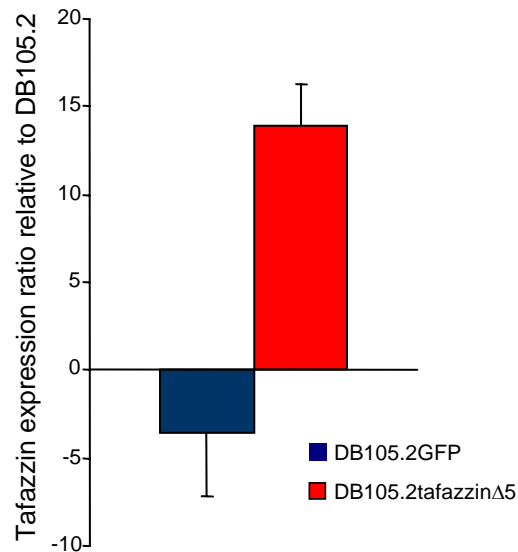


### Figure 3-12: Retroviral infection of lymphoblastoid cells.

(A) Expression of GFP in lymphoblastoid cells. Control (DB037) and BTHS (DB105.2) cells were infected using a retroviral vector expressing GFP (pLpC GFP). Three weeks after selection the cells were observed under a fluorescent microscope (B) Real-time PCR analysis of *tafazzin* expression in DB105.2GFP and DB105.2tafazzin $\Delta$ 5 relative to its expression in the parental DB105.2 cell line. This was normalized to the expression of *actin* and *GAPDH*. Error bars are standard errors of the mean of 3 independent experiments. The sequences of tafazzin, actin and GAPDH primers used for the PCR reactions are indicated in Table1 (section 2.1.2).

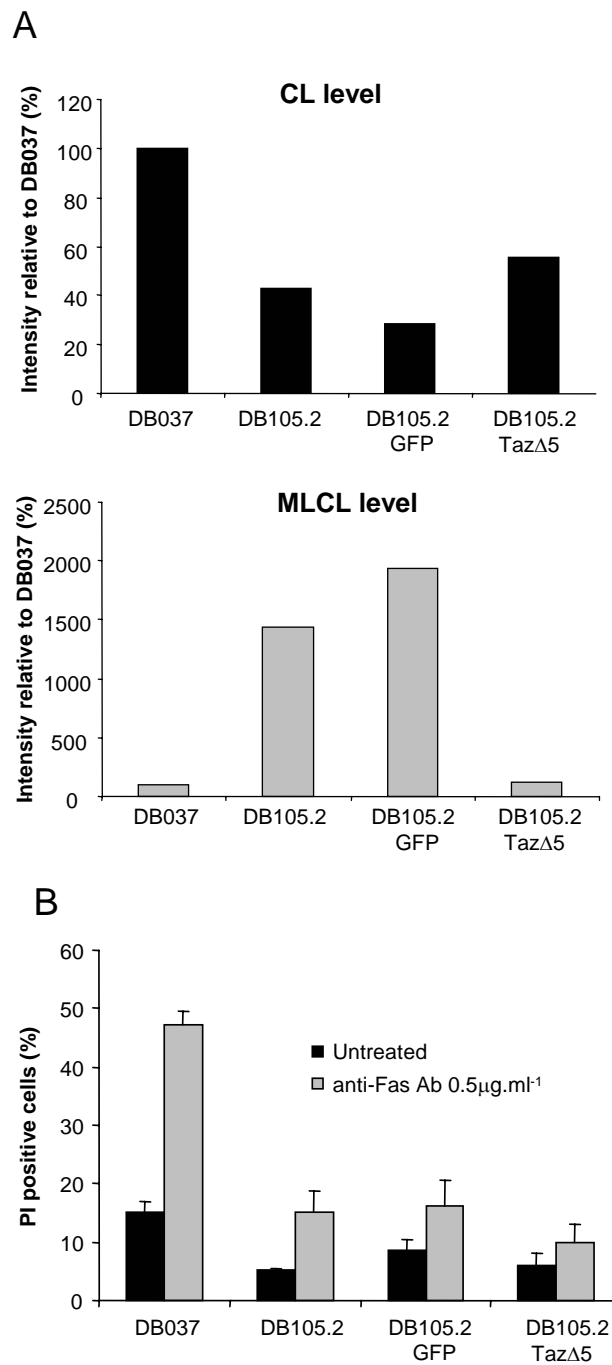


**Figure 3-13: Tafazzin  $\Delta$ 5 does not restore the CL composition and the sensitivity of BTHS cells to Fas-mediated apoptosis.**

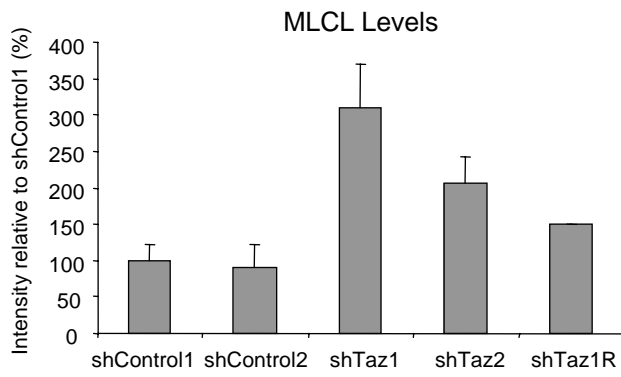
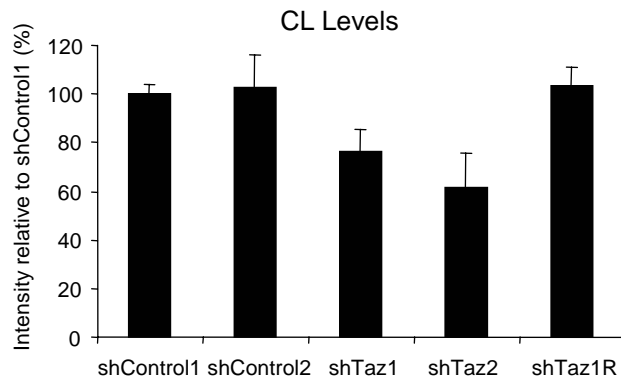
(A). Semiquantitative analysis of the levels of CL and MLCL in control (DB037), BTHS (DB105.2), DB105.2GFP and DB105.2tafazzin $\Delta$ 5 (DB105.2Taz $\Delta$ 5). (B). Fas-induced cell death in DB105.2tafazzin $\Delta$ 5. Control (DB037), BTHS (DB105.2), DB105.2GFP and DB105.2tafazzin $\Delta$ 5 were treated for 24 hours with 0.5  $\mu$ g.ml<sup>-1</sup> of anti-Fas antibody and cell death was analysed by PI staining. Error bars are standard errors of the mean of 3 independent experiments.

Three silent mutations were introduced within the siTaz targeted sequence of tafazzin to avoid the recognition of *tafazzin* mRNA by the siRNA and therefore protect it from degradation. shTaz1 HeLa cells were stably transfected with this siRNA-resistant vector and tafazzin expression was analyzed by western blot. As shown in **figure 3-9C**, expressing the siRNA resistant vector into shTaz1 restored the expression of tafazzin to a similar level than shControl cells. To investigate whether re-expressing tafazzin into shTaz1HeLa cells restored a normal cardiolipin profile, CL and MLCL levels were quantified in the revertant shTaz1R cell line (**Figure 3-14 A**). In shTaz1R, CL rose to a similar level as control cells and the MLCL level was profoundly reduced as compared to the parental cell line (shTaz1). Contrary to tafazzin $\Delta$ 5, which only restored the level of MLCL in BTHS cells, expression of the full-length variant reversed both CL and MLCL levels to the normal level in HeLa tafazzin-deficient cells. This data strongly suggest that full length tafazzin is the only functional variant of tafazzin in human. The transduction of full-length tafazzin into BTHS lymphoblastoid cells was also attempted but unfortunately it was unsuccessful.

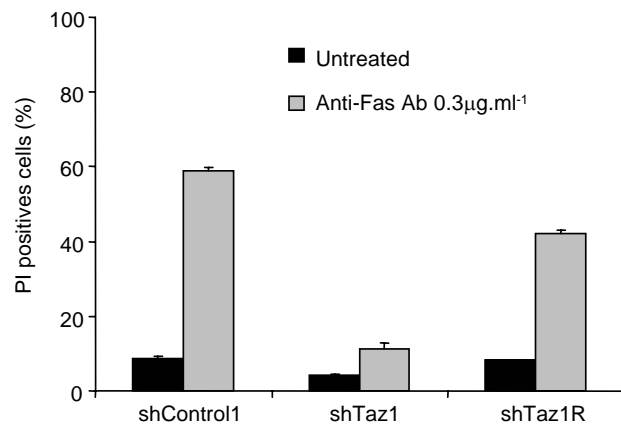
To check whether the restoration of CL profile also restored sensitivity to Fas-mediated apoptosis, shControl1, the revertant shTaz1R and its parental cell lines shTaz1 were treated with anti-Fas antibody for 24 hours and analysed by PI staining (**Figure 3-14B**). Consistent with the previous results (**Figure 3-11A**), tafazzin-deficient shTaz1 cells were strongly resistant to Fas-mediated apoptosis as compared to shControl1. Importantly, the revertant shTaz1R cells showed a 4 fold increase in their sensitivity to Fas-mediated apoptosis as compared to the parental cell lines (shTaz1). In fact, more than 40 % of shTaz1R cells died after Fas-treatment whereas only 10 % of cell death was induced in shTaz1.

In response to a wide variety of apoptotic stimulations, executioner caspases such as caspase-3 cleaves the Poly-ADP Ribose Polymerase (PARP) at the DEVD motif into a 85 kDa and a 25 kDa fragment [248, 249]. Therefore, PARP cleavage was used as a marker to detect apoptosis in the different HeLa clones (shControls, shTaz and shTaz1R) after treatment with anti-Fas antibody (**Figure 3-14C**). Fas-activation induced PARP cleavage in both shControl cells. This cleavage was strongly inhibited in both shTaz. Consistent with the previous data, more PARP cleavage was observed in the revertant shTaz1R cells as compared to the parental cell lines. In fact, the level of cleaved form in the revertant was comparable to those levels in control cells.

A



B



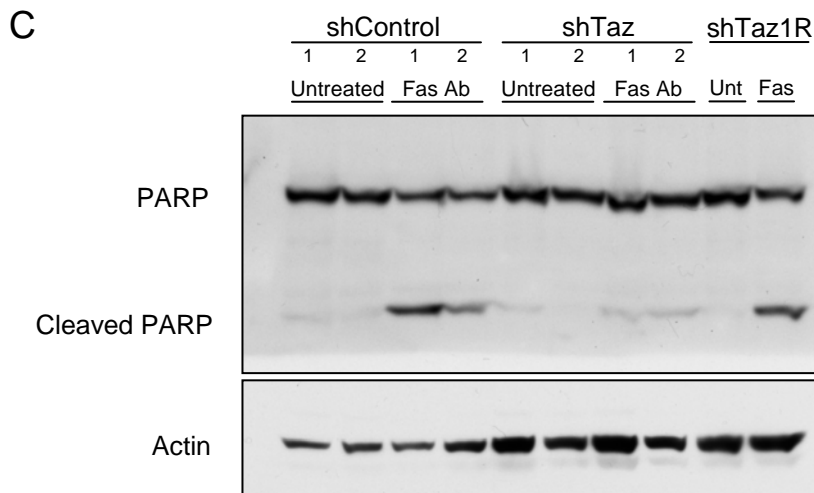


**Figure 3-14: Full length tafazzin restores the CL composition and sensitises HeLa tafazzin-deficient cells to Fas-mediated apoptosis.**

(A). Semiquantitative representation of the levels of CL and MLCL in two shControl cells (shControl1 and shControl2), two shTaz cells (shTaz1 and shTaz2) and in shTaz1 revertant (shTaz1R). These values are averages  $\pm$  SD of triplicate samples for each cell lines. (B). Fas-induced cell death in shTaz1 revertant. shControl1, shTaz1 and shTaz1 revertant cell lines were treated for 24 hours with  $0.3 \mu\text{g.ml}^{-1}$  of anti-Fas antibody. Error bars are standard errors of the mean of 3 independent experiments. (C). Western-blot analysis of PARP cleavage in shControl, shTaz and shTaz1R. HeLa cells were treated for 14 hours with  $0.3 \mu\text{g.ml}^{-1}$  of anti-Fas antibody. Actin was used as loading control.

Hence, expressing the full length variant of tafazzin in tafazzin-deficient cells sensitized the cells to Fas-mediated apoptosis. This indicates that the resistance to apoptosis observed in tafazzin knockdowned HeLa cells was not due to an unspecific-targeting of the shTaz construct.

All together, these data provide the first evidence that tafazzin and thus mature CL can influence the extrinsic-apoptotic pathway.

### **3.3 Discussion**

To shed more light on the role of CL in apoptosis, two experimental approaches have been used. The first was the use of BTHS lymphoblastoid cells that are defective in CL maturation due to an inactive mutant form of tafazzin. The second strategy was the generation of a Barth-syndrome-like model by knocking-down *tafazzin* in HeLa cell lines.

In the first experimental approach, immortalized lymphoblastoid cells generated from BTHS and control patients were analysed for their CL composition. These analyses were performed at Ronald Wanders' Laboratory (AMC, Amsterdam), which developed an accurate method to quantify CL and MLCL using HPLC-ESI-tandem-MS [181, 250]. As expected, BTHS cells exhibited a reduced level of CL and a profound accumulation of its degradation intermediate MLCL. These two features were associated with a reduction of the unsaturation degree of CL acyl chains. CL deficiency has been reported in a wide variety of BTHS tissues including fibroblasts, lymphoblasts, myocardium, skeletal muscle and platelets [179, 180, 250-252]. This defect was not due to a decrease in CL biosynthesis but due to an inhibition in CL remodelling [179]. Decrease of the degree of unsaturation of the CL acyl chains was also reported in several BTHS tissues [181]. In BTHS heart for example, tetralinoleyl-CL (C<sub>18:2</sub>)<sub>4</sub> was completely absent whereas the levels of saturated CL molecular species were increased. Only few studies have shown an accumulation of MLCL in BTHS tissues. This may account for a lack of detection due to technical and experimental limitations. Elevated levels of MLCL were found in muscle, heart, lymphocytes, and in fibroblasts generated from BTHS patients [181, 253].

To date, diagnosis of BTHS is based on molecular screening of platelets or fibroblasts for *tafazzin* mutations. However, more than 90 different pathogenic mutations have been described making it a time consuming approach. Detection of 3-methylglutaconic aciduria has also been used as biochemical marker to diagnose BTHS, but elevations of 3-methyl glutaconic acid has been observed in other mitochondrial disorders [253]. Elevated level of MLCL was recently shown to be a specific hallmark of BTHS. Measurement of the MLCL/CL ratio in fibroblasts has been proposed as a simpler and more sensitive diagnostic test for BTHS [253].

In his seminal report in 1983, Barth observed the presence of abnormal mitochondria in tissue biopsies from BTHS patients [173]. In cardiac biopsy, mitochondria appeared enlarged with disorganized cristae [254]. The same mitochondrial alterations were observed in BTHS lymphoblastoid cells. In these cells, mitochondrial cristae have lost their tubular and individualized shape and appeared interconnected. These observations are supported by a recent electron microscopy tomography study on mitochondria from BTHS lymphoblasts [255]. 3-D reconstruction of these mitochondria showed that their cristae contact to each other forming an enclosed and continuous cavities with multiple branches. These mitochondrial inner membrane connections would account for the honeycomb appearance of the mitochondria observed in BTHS cells (**Figure 3-2C**).

Since CL is mostly located in the mitochondrial inner membrane (see *section 1.6.3*), these results suggest that inhibition of CL remodelling due to tafazzin inactivation is responsible for the alteration of cristae organization. This hypothesis is supported by the phenotype of tafazzin-deficient *Drosophila* [256]. In these flies, mutations of *tafazzin* generated a BTHS phenotype, with the characteristic features: CL deficiency, alterations of mitochondrial configuration namely cristae disorganization, and motor weakness. The role of CL in mitochondrial structure has also emerged from studies of other cellular models. Mitochondria of CHO-PGS-S cells lacking PG and CL appeared swollen and have disorganized cristae [198, 206]. More recently, mitochondrial cristae reorganization has also been observed in the CL-synthase knockdown HeLa cells [165]. Inhibiting CL synthesis in these cells decreased the total level of CL without affecting its molecular species composition. Therefore, it is likely that mature CL are required to maintain the mitochondrial inner membrane configuration. In CL-synthase and tafazzin-deficient yeast models, CL have been

shown to be required for the stabilization and the organization of the respiratory complexes III and IV into supercomplexes [257-259]. Deficiency of CL may predispose the mitochondrial inner membrane to protein aggregation and thus may lead to cristae membrane adhesions observed in BTHS mitochondria. Clearly, further studies are required to define the exact mechanism by which CL maintains the structure of the mitochondrial inner membrane.

The discussed above alterations in mitochondrial morphology due to CL deficiency are also associated with an impaired OXPHOS capacity. Mitochondria isolated from BTHS cells were able to oxidize succinate at the same rate than the control but have lost their ability to respond to ADP and to establish the respiratory state-3. No change in the respiration rate of uncoupled BTHS-derived mitochondria was observed suggesting that the respiratory state-3 inhibition was due to an alteration of the phosphorylation machinery. This machinery includes the ANT, the mitochondrial phosphate carrier and the ATP synthase, three mitochondrial enzymes that require CL for their optimal activities [191, 193, 195]. Thus, it is conceivable that in BTHS mitochondria the CL deficiency is not sufficient to inhibit the activity of the respiratory complexes but it results in the inhibition of the phosphorylation machinery. To summarize, these findings strongly suggest that tafazzin and thus CL remodelling are required to sustain OXPHOS and to maintain mitochondrial structure.

Analysis of the sensitivity of BTHS cells to apoptotic stimulations revealed that these cells were protected from the DR-inducing extrinsic apoptotic pathways (Fas and TNF) but were still able to undergo apoptosis in response to intrinsic stimulations such as DNA damage-inducing drugs (etoposide and cisplatin). This raised the question whether tafazzin inactivation rendered the BTHS cells resistant to extrinsic apoptosis. Silencing *tafazzin* using siRNA oligonucleotides seemed the obvious approach to address this issue. Since tafazzin is a mitochondrial enzyme involved in the acylation of CL, it was assumed that tafazzin inactivation would inhibit extrinsic apoptosis at the mitochondrial level and thus would only protect type II cells from Fas-mediated apoptosis. Therefore, the type II HeLa cells were chosen as a cell model for the siRNA approach. Transient knockdown of tafazzin in HeLa cells did not affect the CL composition and the sensitivity of these cells to anti-Fas antibody mediated apoptosis. To surmount this problem, tafazzin has been stably silenced

using a short-hairpin RNA expressing plasmid. To date, this is the first tafazzin-deficient model generated in human cells. These cells displayed a reduced level of CL and an accumulation of MLCL making them a good BTHS-like model. Moreover, ectopic expression of full length tafazzin to level equivalent to the endogenous levels (**Figure 3-9C**) in tafazzin-deficient HeLa cells, using a siRNA resistant vector, reversed the CL and MLCL pattern. These data provide the first evidence that full length tafazzin is required for the remodelling of CL in human cells.

Like the BTHS cells, tafazzin-deficient-HeLa cells were protected from the extrinsic apoptotic pathway. Importantly, the sensitivity of these cells to anti-Fas antibody was restored by expressing full length tafazzin. Taken together, these data strongly indicate that tafazzin and thus mature CL are required for efficient Fas-mediated apoptosis in type II cells. These findings contrast with those obtained in CL-synthase deficient HeLa cells where CL deficiency was associated with an increase in Fas and TNF mediated cell death [165]. However, it is difficult to compare CL-synthase deficient and tafazzin-deficient HeLa cells. First, different biochemical reactions are affected in both models: CL synthesis and CL remodelling. Whereas inhibition of CL synthesis reduce CL and MLCL without discriminating between their molecular species, inhibition of CL remodelling alters its fatty acyl composition and leads to a deficiency in unsaturated mature CL. Second, CL synthase deficiency was associated with an increasing in PG which may substitute, to some extent, for CL [165]. However, under stress conditions, such as apoptotic stimulations, the lack of total CL would result in bioenergetic alterations that would predispose the cells to necrosis. In fact, CL-synthase knockdown cells appeared necrotic when stimulated with anti-Fas antibody [165].

In contrast to BTHS cells, tafazzin-deficient HeLa cells were also resistant to etoposide-induced apoptosis. This may account for the fact that HeLa cells present an innate resistance to DNA damage-induced apoptosis. While 40 % of lymphoblastoid cells died after 24 hours of treatment with 5  $\mu\text{M}$  of etoposide, 60  $\mu\text{M}$  of drug was required to kill a similar proportion of HeLa cells. HeLa cells contain integrated human papilloma virus (HPV) 18 DNA sequence in their genome encoding the HPV proteins E6 and E7 [260, 261]. The viral protein E6 promotes the degradation of p53 [262]. Because p53 is degraded by E6 in HeLa cells, these cells are likely to be

resistant to p53-mediated apoptosis and thus to DNA damage-inducing agents. Therefore, it is conceivable that when treated with high concentration of etoposide, HeLa cells undergo apoptosis through a p53-independent pathway that require tafazzin. It will be interesting to study whether this cell death is now dependant on extrinsic signals via an autocrine loop.

Interestingly, while full length tafazzin restored the CL and MLCL composition in tafazzin-deficient HeLa cells, the variant lacking exon-5 only restored low MLCL levels in BTHS cells. In stark contrast, only the  $\Delta$ exon5 and not the full length variant of human tafazzin was able to restore the CL profile in tafazzin-deficient yeast model [178]. This may be due to the absence of exon 5 in yeast tafazzin. In fact, exon 5 was only found in primate species [177, 178]. These results, together with the recent discovery of BTHS patients with mutations in exon 5, strongly support the idea that full length tafazzin represents the only functional variant in human. More studies are needed to further understand the role of these two tafazzin variants in human. This has never been investigated in human before mainly due to the lack of a suitable experimental model. Tafazzin-deficient HeLa cells may represent a novel model to address this issue.

Moreover, only full length tafazzin was able to restore the sensitivity of tafazzin-deficient cells to Fas-mediated apoptosis. No reversion in sensitivity was observed when just MLCL was restored to normal level by tafazzin $\Delta$ 5, suggesting that decrease of CL level and not accumulation of MLCL confer resistance to Fas-mediated apoptosis. It would be interesting to investigate whether the full length tafazzin is able to restore the CL level and the sensitivity to Fas-mediated apoptosis in BTHS cells. Unfortunately, BTHS cells were only infected with retroviruses expressing the exon 5-deficient variant.

To conclude, this chapter showed for the first time that tafazzin and thus mature CL are required for extrinsic apoptotic pathways in type II cells. It also underpins the importance of the acyl chain composition of CL in apoptosis. This raised the question how alterations of CL remodelling make cells resistant to the extrinsic apoptotic pathways without affecting their sensitivity to intrinsic apoptosis. The mechanism by which tafazzin inactivation confer resistance to Fas-mediated apoptosis will be discussed in the next chapter.

**CHAPTER 4 MECHANISM OF APOPTOSIS  
RESISTANCE IN TFAZZIN-DEFICIENT  
CELLS**

## **4 Mechanism of apoptosis resistance in tafazzin-deficient cells**

### **4.1 Introduction**

The previous chapter demonstrated that tafazzin deficiency confers resistance to the extrinsic apoptotic pathway in type II cells. It does not however address any of the molecular mechanisms involved in this resistance. Since tafazzin catalyses the remodelling of CL in mitochondria, it was logical to speculate that inhibition of CL maturation would block the transduction of the apoptotic signal at the mitochondria. As mentioned previously, CL has been previously implicated in several mitochondrial steps leading to the release of apoptogenic factors from the mitochondria. These steps include the transmission of the apoptotic signal to the mitochondria by the Bcl-2 family of proteins and the execution of the mitochondrial outer membrane permeabilization [101, 127, 128]. The results described in the previous chapter, together with recent observation showing that CL peroxidation is required for the release of apoptogenic factors from the mitochondria suggest that the acyl chain composition of CL is playing an important role in apoptosis [214]. However, the mechanism by which these acyl chains participate in apoptosis has not been shown. In order to understand the role of unsaturated mature CL in apoptosis, this chapter explores the molecular mechanisms by which tafazzin inactivation protects cells from the extrinsic apoptotic pathway.

### **4.2 Results**

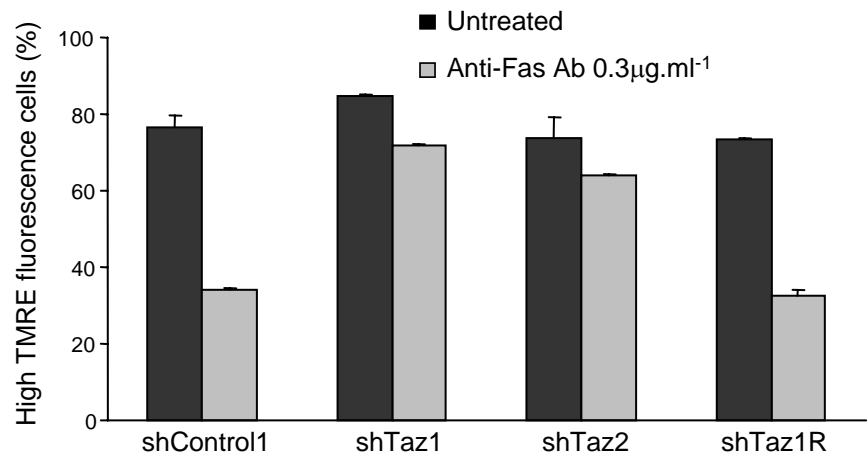
#### **4.2.1 Inhibition of mitochondrial apoptosis in tafazzin-deficient cells**

As mentioned in *section 1.5.5.4*, caspase-3 is one of the key effector caspases in apoptosis, responsible for the cleavage of many essential cellular proteins such as PARP. In response to apoptotic stimuli, initiator caspases are activated and drive forward the caspase cascade by directly activating the effector caspases. Upon cleavage, caspase-3 zymogens adopt an active dimeric conformation composed of two subunits, a large subunit of 17 kDa and a small subunit of 12 kDa [249].



Caspase-3 activation was analysed by western-blot in control and tafazzin-deficient HeLa cells after treatment with anti-Fas antibody for 14 hours (**Figure 4-1A**). The antibody used was raised against the p17 subunit and detects the pro-caspase-3 (32 kDa). As expected, anti-Fas antibody activated caspase-3 in shControl cells as judged by the formation of three cleaved products of caspase-3 at around 20 kDa in size. These products result from the cleavage of three different sites in the pro-domain of caspase-3. No cleavage was observed when cells were pre-incubated with 20  $\mu$ M of DEVD-fmk prior to treatment, indicating that DEVD-fmk efficiently inhibited caspase-3 activation. As compared to the control, caspase-3 activation was strongly inhibited in shTaz2 HeLa cells. Similar results were obtained when caspase-3 activity was analysed by the cleavage of its substrate, PARP. As shown in **Figure 3-14C**, PARP cleavage was strongly reduced in tafazzin-deficient cells. In order to confirm and quantify the inhibition of caspase activation in shTaz cells, caspase activity was directly monitored using the cell permeable substrate Red-DEVD-fmk. Red-DEVD-fmk irreversibly binds to activated caspases and labelled the cells with a red fluorescence that can be detected by FACS. shControl and shTaz cells were treated with anti-Fas antibody for 8 hours and caspase-3 activity was assessed (**Figure 4-1B**). Consistent with the western-blot analysis, caspase-3 activity was strongly reduced in both tafazzin-deficient clones as compared to the two control clones. Altogether, these results show that inactivation of tafazzin in HeLa cells inhibits Fas-mediated caspase-3 activation. As mentioned in *section 1.5.3.3*, cells undergoing apoptosis are characterized by an early dissipation of their mitochondrial membrane potential ( $\Delta\psi_m$ ).  $\Delta\psi_m$  can be measured by flow cytometry using TMRE, a mitochondria-specific cationic lipophilic fluorescent dye. TMRE is cell permeable and accumulates in the mitochondria matrix in a  $\Delta\psi_m$  dependant manner. Therefore, a loss of  $\Delta\psi_m$  is detected by a decrease of the fluorescence intensity. HeLa cells were treated with anti-Fas antibody for 24 hours and mitochondrial membrane potential was assessed by TMRE staining. **Figure 4-2A** represents the percentage of cells with high TMRE fluorescence (High  $\Delta\psi_m$ ) before and after Fas-receptor activation. After anti-Fas antibody treatment, more than 50 % of the shControl1 cells have lost their  $\Delta\psi_m$  whereas only 10 % of the tafazzin-deficient cells exhibited a low  $\Delta\psi_m$  under the same condition. Interestingly, expressing full-length tafazzin in these cells restored their ability to undergo mitochondrial membrane depolarization to a level comparable to shControl cells. These data indicate that tafazzin and thus mature CL are required for Fas-induced mitochondrial depolarization.

A



B

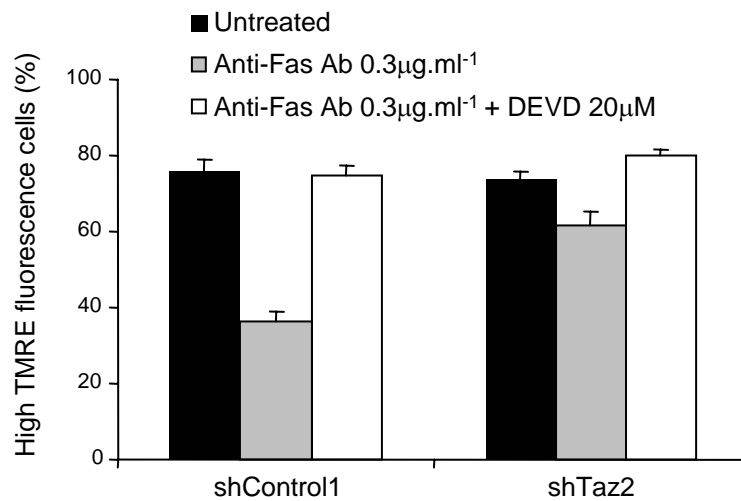


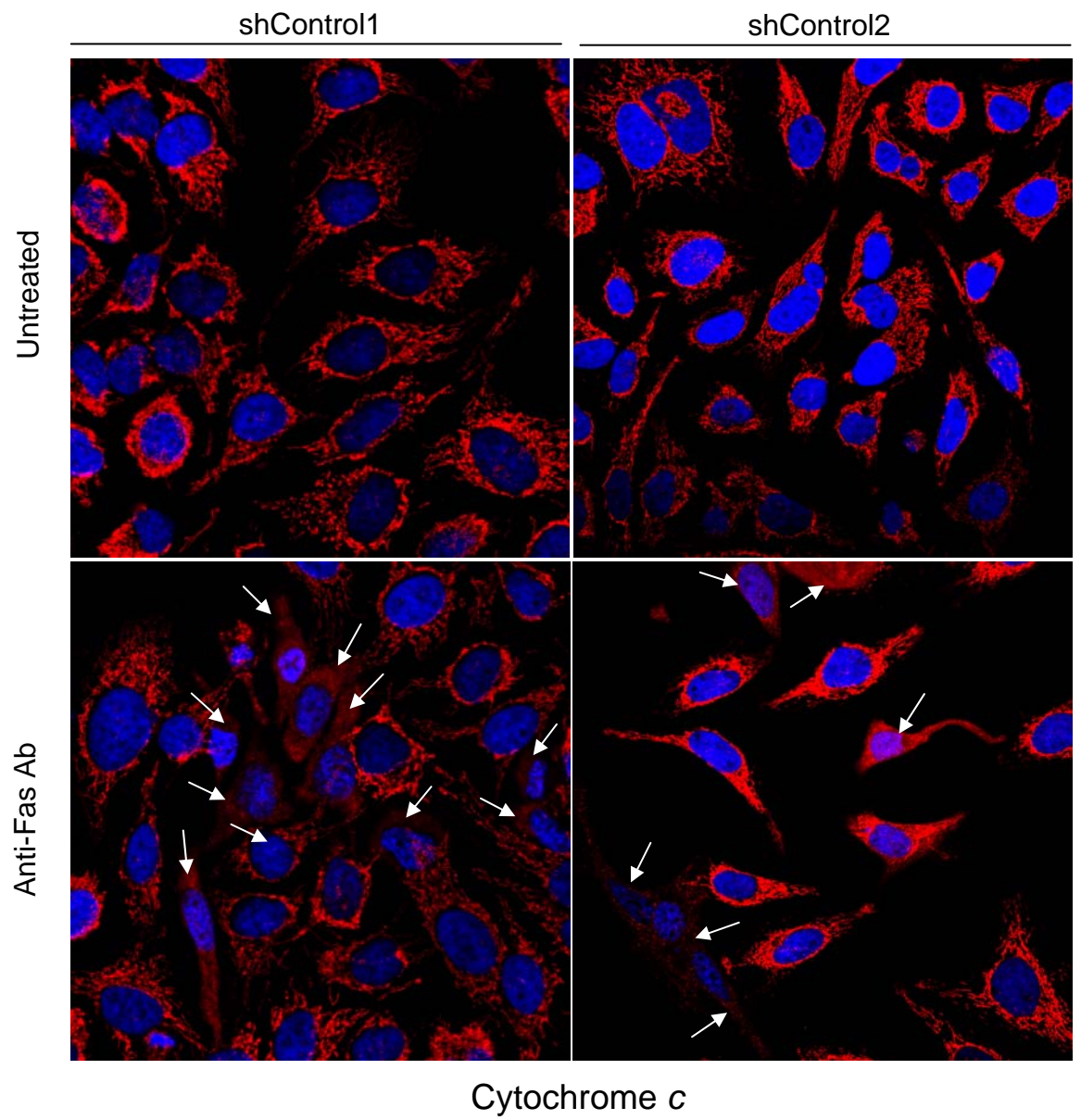
**Figure 4-2: Inhibition of mitochondrial membrane depolarization in tafazzin-deficient HeLa cells.**

(A) HeLa shControl, shTaz and shTaz1R were treated with 0.3 µg.ml<sup>-1</sup> of anti-Fas antibody for 24 hours. Cells were then stained with 50 nM of TMRE and the fluorescence was quantified by flow cytometry. (B) Effect of DEVD on mitochondrial membrane depolarization. ShControl1 and shTaz2 cells were incubated in the presence or absence of 20 µM of DEVD and treated as in (A). Error bars are standard errors of the mean of 3 independent experiments.

This raised the question whether the loss of  $\Delta\psi_m$  induced by Fas receptor activation occurred upstream or downstream of the mitochondrial outer membrane permeabilization. In order to address this issue, caspases were inhibited using 20  $\mu\text{M}$  of DEVD (**Figure 4-1A**). Incubation with DEVD completely protected shControl1 cells from mitochondrial depolarization (**Figure 4-2B**). This indicates that the loss of  $\Delta\psi_m$  observed after anti-Fas antibody treatment is dependent on caspase activation. In type II cells, such as HeLa cells, caspase-3 activation requires the release of apoptogenic factors from the mitochondria [56]. In this context, caspase-3 is activated by caspase-9 following cytochrome *c* release and apoptosome formation (*section 1.5.3.7.1*). This suggests that loss of  $\Delta\psi_m$  occurs downstream of the mitochondrial outer membrane permeabilization.

Since caspase-3 was inactivated in tafazzin-deficient cells, the ability of these cells to induce mitochondrial outer membrane permeabilization (MOMP) was investigated. Following MOMP, release of apoptogenic factors occurs in a hierarchical manner. First, cytochrome *c*, Smac/DIABLO and EndoG are released to the cytosol and activate the caspases cascade. Once activated, effector caspases (such as caspase-3) target the mitochondria and then further amplify the release of apoptogenic factors [80]. In response to intrinsic stimulations, cytochrome *c* and Smac/DIABLO are released in a caspase independent-manner [80, 81]. However, in type II cells transduction of the extrinsic apoptotic signal from Fas receptor to the mitochondria required the activation of caspase-8 at the DISC (*section 1.5.4*). To avoid the amplifying effect of caspase-3 on mitochondrial permeabilization, caspase-3 was inhibited with 20  $\mu\text{M}$  DEVD (**Figure 4-1A**). Under these conditions, tafazzin-deficient HeLa cells were treated with anti-Fas antibody for 14 hours and cytochrome *c* and Smac/DIABLO releases were analysed by immunostaining. As can be seen in **figure 4-3A and B**, under untreated conditions cytochrome *c* was distributed in a punctated pattern within the cytosol of shControl and shTaz cells. This pattern is characteristic of a mitochondrial staining (**Figure 1-7**). When shControl cells were treated with anti-Fas antibody, several cells in each microscopic field lost their mitochondrial punctated pattern and displayed a diffused cytoplasmic distribution of cytochrome *c*, indicative of cytochrome *c* release from mitochondria (**Figure 4-3A**, white arrows). No diffused pattern was observed when tafazzin-deficient HeLa cells were treated with anti-Fas antibody (**figure 4-3B**).

A



B

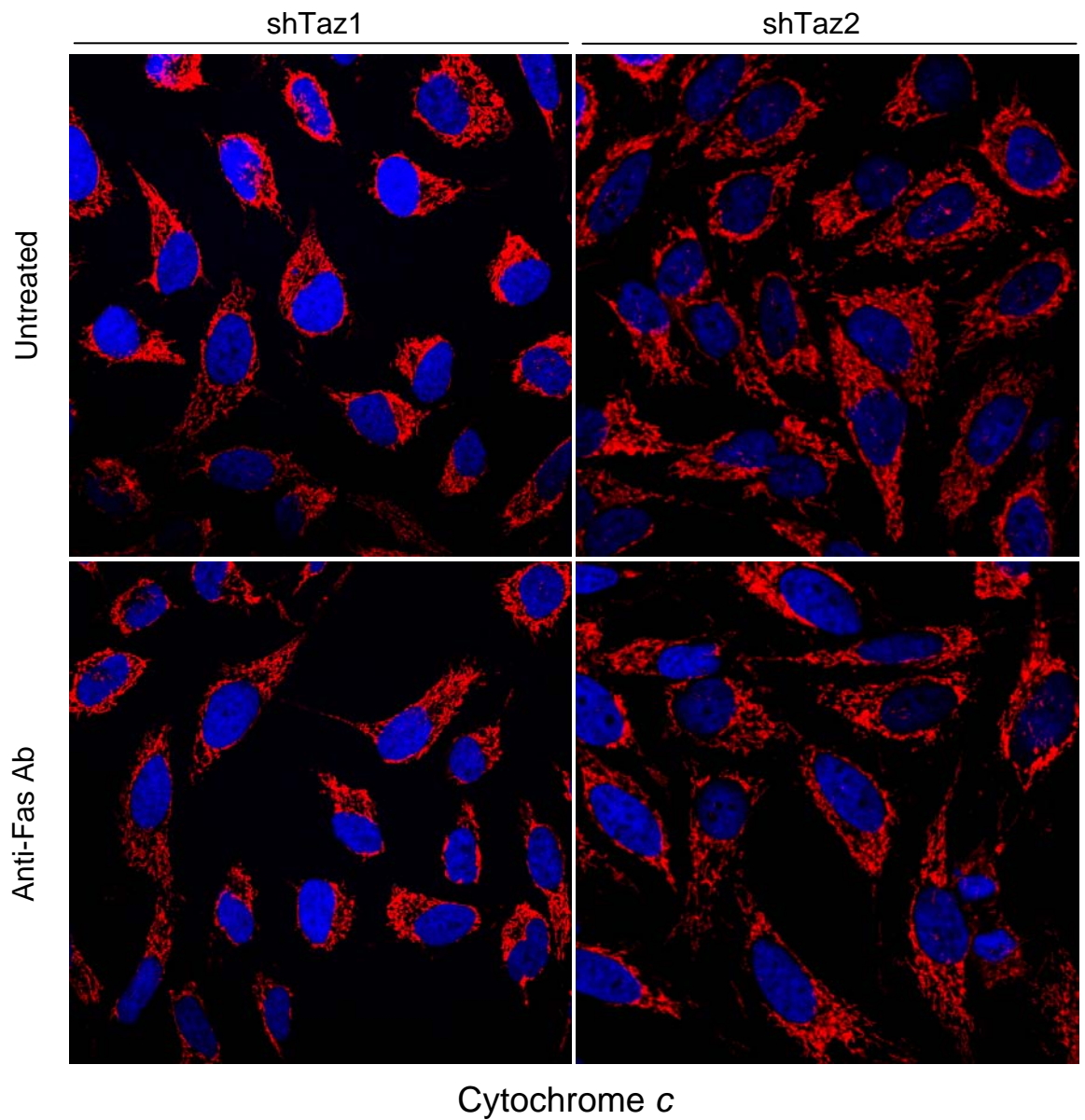


**Figure 4-3: Inhibition of cytochrome c release in Tafazzin-deficient HeLa cells.**

(A). Confocal microscopy analysis of cytochrome c immunostaining in shControl cells. (B) Confocal microscopy analysis of cytochrome c immunostaining in shTaz HeLa cells. HeLa shControl and shTaz were incubated with 20  $\mu\text{M}$  of DEVD and then treated with 0.3  $\mu\text{g}\cdot\text{ml}^{-1}$  anti-Fas antibody for 14 hours. Cells were fixed, permeabilized and stained using anti-cytochrome c antibody (red). DAPI (blue) was used to stain the nuclei. Each picture is a representative of all the microscopic field observed under each condition.

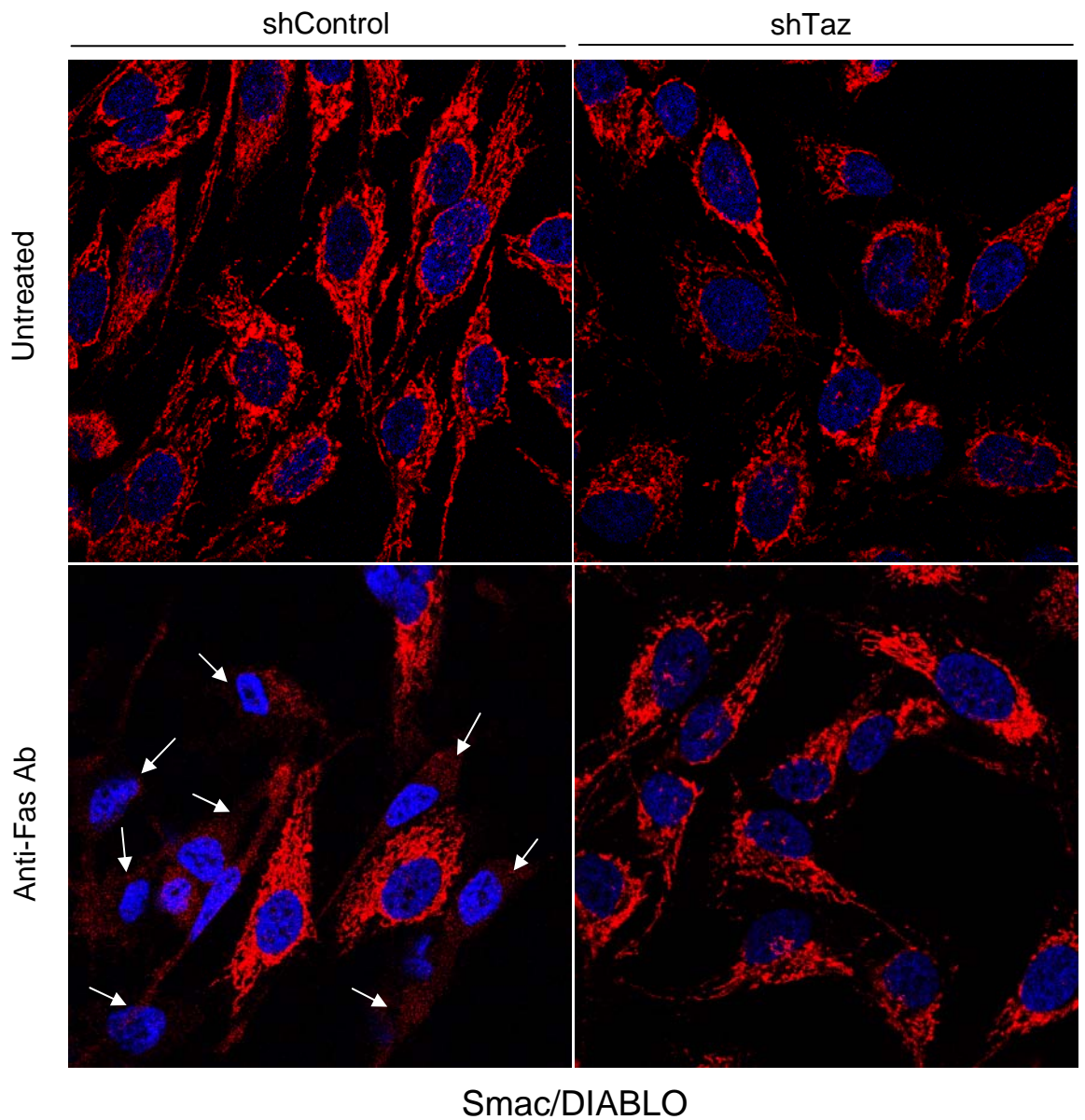


**Figure 4-4: Inhibition of Smac/DIABLO release in tafazzin-deficient HeLa cells.**

Confocal microscopy analysis of Smac/DIABLO immunostaining in shControl and shTaz HeLa cells. HeLa shControl and shTaz were incubated with 20  $\mu\text{M}$  of DEVD and then treated with 0.3  $\mu\text{g}\cdot\text{ml}^{-1}$  anti-Fas antibody for 14 hours. Cells were fixed, permeabilized and stained using anti-Smac/DIABLO antibody (red). DAPI (blue) was used to stain the nuclei. Each picture is a representative of all the microscopic fields observed under each condition.

Similar results were observed when cells were stained for Smac/DIABLO (**Figure 4-4**). Fas-induced Smac/DIABLO release was observed in shControl cells whereas no diffused pattern was observed in shTaz cells under the same conditions. These findings indicate that Fas mediated cytochrome *c* and Smac/DIABLO releases are inhibited in tafazzin-deficient cells. Therefore, it appeared that the block in the apoptotic cascade in tafazzin-deficient cells is due to either defects in the process of the release of apoptogenic factors from the mitochondria or due to alterations in upstream steps.

#### **4.2.2 Tafazzin-deficient mitochondria are able to release cytochrome *c* in vitro**

It was previously suggested that CL is required for Bax-mediated permeabilization of the mitochondrial outer membrane [101]. The observation that cytochrome *c* and Smac/DIABLO release were inhibited in tafazzin-deficient cells raised the question whether the inhibition of apoptosis in these cells was due to alterations in the mechanism of MOMP. To address this issue, mitochondria were isolated from tafazzin-deficient cells and their ability to release cytochrome *c* was tested *in vitro* using a synthetic peptide derived from the BH3 domain of Bid (Bid BH3). BidBH3 was shown to induce cytochrome *c* release through the activation of Bax and Bak oligomerization [95, 96]. To maintain the electron transport chain functional during the experiment, isolated mitochondria from control and BTHS cells were incubated in the presence of succinate and rotenone (*section 1.2.1*). These mitochondria were then treated for 15 minutes with incremental doses of BidBH3 peptide (from 1 to 100  $\mu$ M) and the presence of cytochrome *c* in the buffer was analysed by western-blot (**Figure 4-5**). The amount of cytochrome *c* present in the buffer of untreated mitochondria (first lane) is an indication of the quality of the mitochondrial preparation. In fact, mitochondria in good shape retain cytochrome *c* in their intermembrane space. To determine the maximal amount of cytochrome *c* available for release, mitochondria were lysed using a detergent (Triton, last lane). In the absence of treatment, only small amounts of total cytochrome *c* were detected in the buffer of control and BTHS mitochondria, indicating that mitochondria preparations were of good quality. As expected, BidBH3 peptide induced cytochrome *c* release in a dose-dependant manner. No cytochrome *c* was released when mitochondria from control cells (DB037) were treated with 1  $\mu$ M of BidBH3 (second lane). Cytochrome *c* releasing activity was initiated when 5  $\mu$ M of BidBH3 (third lane) was used and the

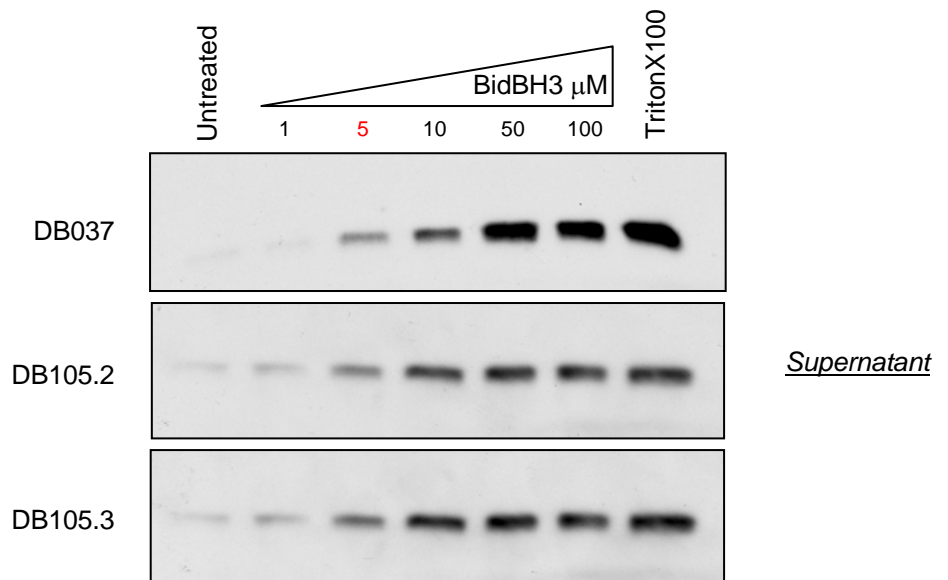


**Figure 4-5: BTHS mitochondria are capable of releasing cytochrome c in response to BidBH3 peptide.**

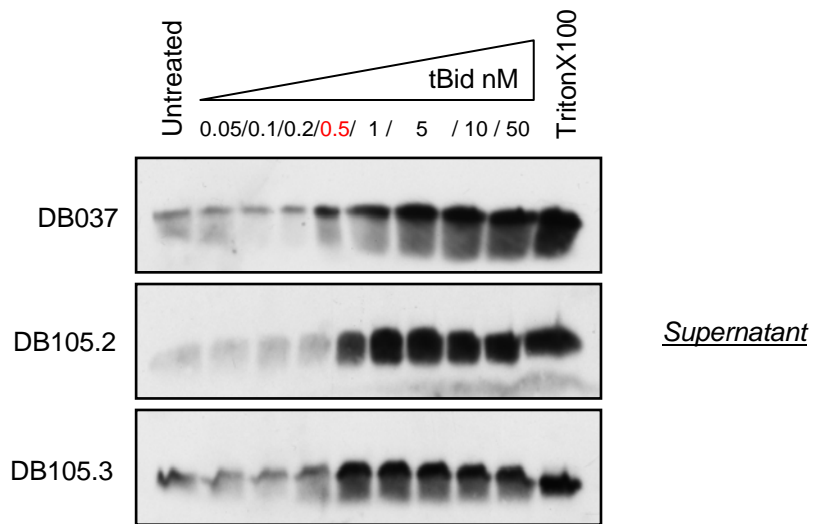
Mitochondria were isolated from control (DB037) and BTHS lymphoblastoid cells (DB105.2 and DB105.3) and incubated in the presence of 10 mM of succinate and 1  $\mu$ M rotenone. Mitochondria were treated with incremental doses of BidBH3 peptide for 15 minutes at 37°C and then centrifuged at 10,000 x g for 5 minutes. The supernatants were collected and immunoblotted with anti-cytochrome c antibody.

release was further increased with increasing amount of the peptide. In fact, 50  $\mu\text{M}$  of peptide was sufficient to completely release cytochrome *c* from control mitochondria. Interestingly, BidBH3 peptide was as efficient in releasing cytochrome *c* in BTHS mitochondria as it was in control mitochondria. Initial and maximal cytochrome *c* release from BTHS mitochondria was observed at BidBH3 peptide concentration of 5  $\mu\text{M}$  and 50  $\mu\text{M}$ , respectively. These results indicate that even though BTHS cells are protected from the extrinsic apoptotic pathway, their mitochondria are capable of undergoing MOMP, suggesting that the block in apoptosis in BTHS cells occurs upstream of this event.

#### **4.2.3 tBid interacts with and releases cytochrome *c* from tafazzin-deficient mitochondria**

As mentioned in *section 1.6.6.3*, the first demonstration that CL plays a role in apoptosis was when it was shown to provide a “docking” site for tBid at the contact sites between the inner and the outer mitochondrial membranes [127, 128]. In type II cells, Bid is essential for the transduction of the apoptotic signal from the DR to the mitochondria (*section 1.5.4*). Following Fas receptor activation, Bid is cleaved into its active form tBid by caspase-8. Then, tBid translocates to the mitochondria and release cytochrome *c* through Bax/Bak activation [99, 100, 125, 126]. Several studies have shown that interaction of tBid with CL does not involve its BH3 domain but a CL binding domain that become exposed after caspase-8 cleavage [127, 131, 132, 263]. Therefore, the ability of tBid to translocate to and to induce cytochrome *c* release from tafazzin-deficient mitochondria was tested. Under similar conditions to the previous experiment, mitochondria were isolated from control and BTHS cells and incubated for 15 minutes in the presence of increasing amounts of recombinant tBid. The release of cytochrome *c* to the buffer was then analysed by western-blot (**Figure 4-6.A**). Surprisingly, tBid released cytochrome *c* with the same efficiency in BTHS mitochondria and in control mitochondria. In both mitochondria, no cytochrome *c* release was detected with 0.2 nM tBid and the maximum release was observed using 0.5 nM tBid. Previously, tBid was shown to require either Bax or Bak to induce cytochrome *c* release [62]. In fact, via its BH3 domain tBid induces the oligomerization of the proteins Bax and Bak on the mitochondrial membrane and leads to the permeabilization of the outer membrane [99, 100]. Since Bax is mainly in the cytosol and Bak normally resides in the mitochondrial outer membrane, the

A



B

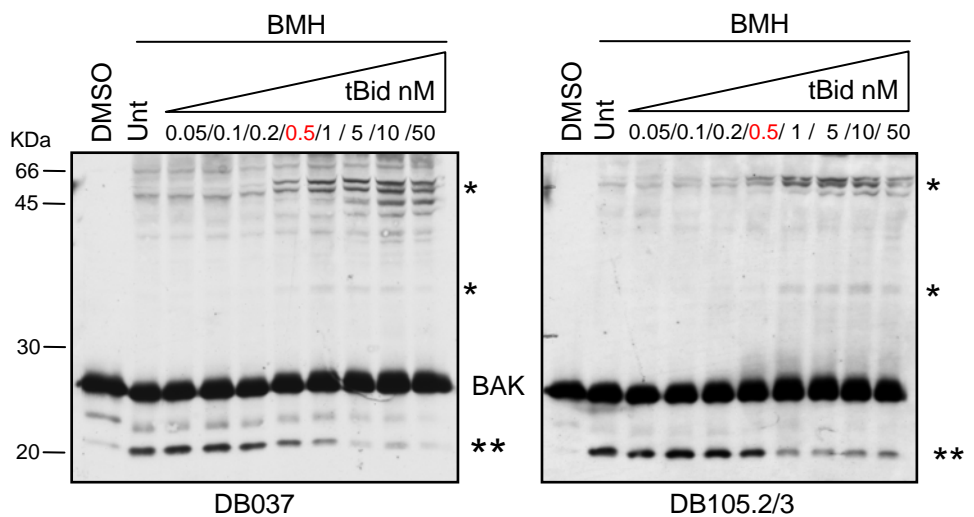


**Figure 4-6: tBid induces Bak oligomerization and cytochrome c release in BTHS mitochondria.**

Mitochondria were isolated from control or BTHS cells and incubated in the presence of 10 mM succinate and 1  $\mu$ M rotenone. Mitochondria were treated with incremental doses of tBid for 15 minutes at 37°C and then centrifuged at 10,000 x g for 5 minutes. The supernatant and mitochondrial pellets were collected. Supernatant were immunoblotted with anti-cytochrome c antibody (A). Mitochondrial pellets were resuspended in 10 mM of DMSO or 10 mM of BMH and immunoblotted with anti-Bak antibody. Only DB037 and DB105.2 are shown in (B) but similar results were obtained in mitochondria isolated from DB105.3 cells. \* and \*\* indicate the inter and intra cross-linked forms of Bak, respectively.

ability of tBid to induce Bak oligomerization in BTHS mitochondria was investigated. After tBid treatment, mitochondrial membranes were collected and incubated with the cross-linker, *Bis*-MaleimidoHexane (BMH) [100]. BMH is a homobifunctional maleimide that is able to covalently cross-link sulfhydryl groups (-SH) and therefore to stabilize the Bak oligomers in the mitochondrial membrane. The oligomerization of Bak was then visualized by western-blot analysis (**Figure 4-6B**). In the absence of cross-linker (first lane) Bak monomer was detected as a single band that migrated at around 27-kDa (Control or BTHS). BMH cross-linking was characterized by the appearance of a faster mobility band of around 21 kDa (\*\*), which corresponds to an intramolecular cross-linked Bak monomer. As for cytochrome *c* release, Bak oligomerization was initiated with 0.5 nM tBid. In the presence of BMH, addition of tBid to control mitochondria (DB037) shifted Bak into two higher molecular weight complexes at around 38 kDa and 55 kDa (\*). At the same time, the faster mobility species of Bak (21 kDa) decreased. These changes were further evident when increasing amounts of tBid were used. In accordance with the cytochrome *c* releasing experiments, tBid induced Bak oligomerization with the same efficiency in mitochondria from control or BTHS cells.

In order to confirm these controversial results, the same *in vitro* experiments were carried out in mitochondria isolated from tafazzin-deficient HeLa cells. Mitochondria isolated from shControl1 and shTaz2 HeLa cells were incubated for 15 minutes with increasing amount of recombinant tBid and the release of cytochrome *c* and Smac/DIABLO was analysed by western-blot (**Figure 4-7A**). Consistent with the previous data, tBid released cytochrome *c* and Smac/DIABLO in a dose dependant manner with the same efficiency in shControl1 and shTaz2 mitochondria. In fact, 0.1 nM of tBid was sufficient to initiate the release of cytochrome *c* and Smac/DIABLO and complete release of these proteins were obtained using 0.25 nM tBid. In this experiment the mitochondrial fractions were also collected and analysed by western-blot for the presence of cytochrome *c*. The mitochondrial complex I was used as a loading control. In agreement with the analysis of the supernatants, the amount of cytochrome *c* in the mitochondrial pellets was reduced with the same kinetics in shControl1 and shTaz2 cells. To determine whether mature CL were required for the binding of tBid to the mitochondria, mitochondrial pellets were also analysed for the presence of tBid. Due to limitation in detectability of tBid antibody used, no bands

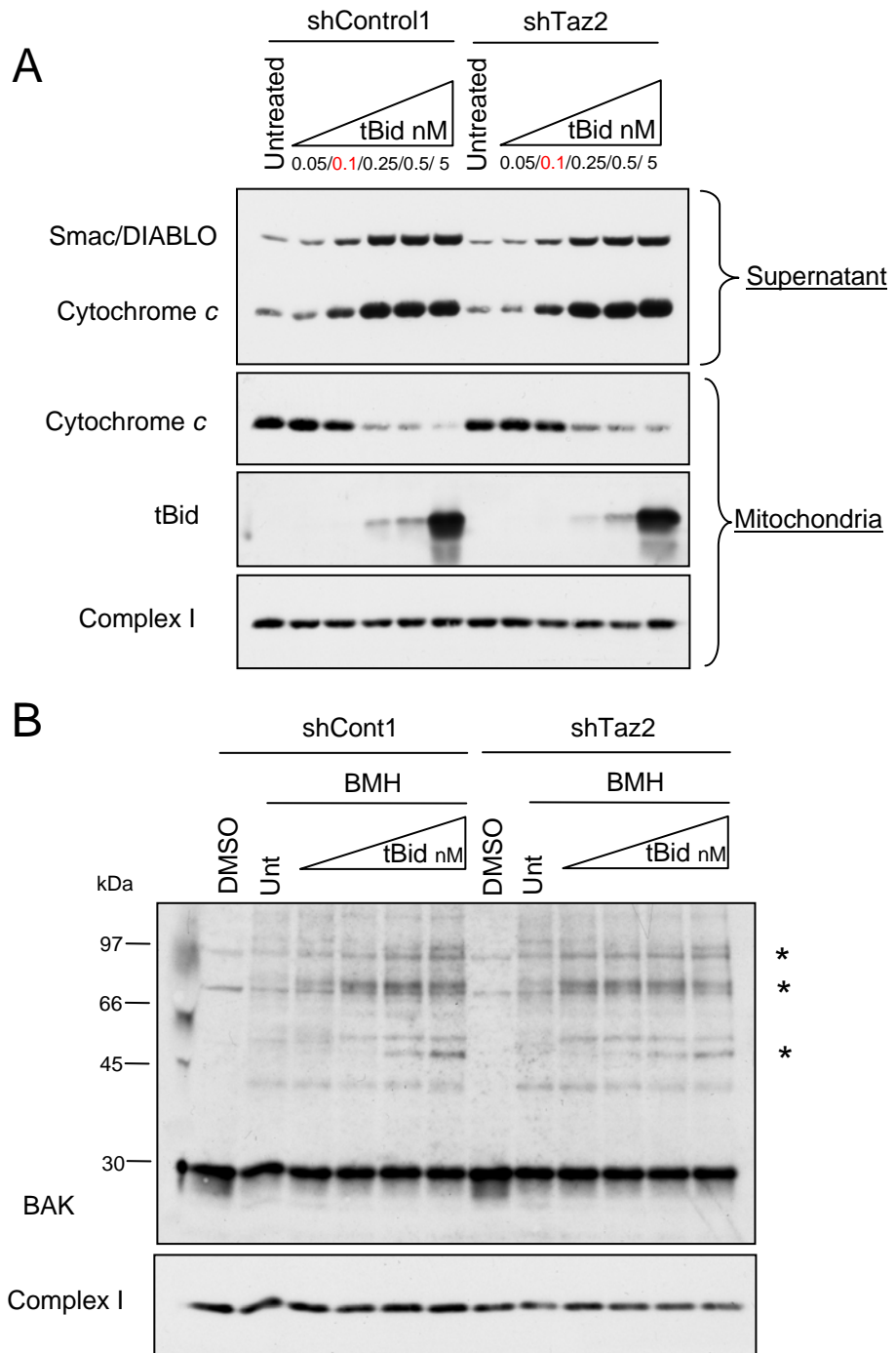


**Figure 4-7: tBid interacts with mitochondria and induces Bak-oligomerization and subsequent cytochrome c release in tafazzin-deficient mitochondria.**

(A) tBid interacts with mitochondria and release cytochrome c and Smac/DIABLO from tafazzin-deficient mitochondria (shTaz2). Mitochondria were isolated from control (shControl1) or shTaz2 cells and incubated in the presence of 10 mM succinate and 1  $\mu$ M rotenone. Mitochondria were treated with incremental doses of tBid for 15 minutes at 37°C and then centrifuged at 10,000 x g for 5 minutes. The supernatant and mitochondrial pellets were collected and immunoblotted with the indicated antibody. (B) tBid induces Bak-oligomerization in tafazzin-deficient mitochondria (shTaz2). Mitochondrial pellets were resuspended in DMSO or 10 mM BMH and immunoblotted with anti-Bak antibody. Complex I was used as a loading control of mitochondrial fractions.

were detected at tBid concentration lower than 0.25 nM. Importantly, at tBid concentration higher than 0.25 nM, tBid was detected at the same extent in mitochondria from tafazzin-deficient and control HeLa cells. The ability of tBid to induce Bak-oligomerization in mitochondria from tafazzin-deficient HeLa cells was also investigated by cross-linking the mitochondrial pellet (**Figure 4-7B**). In the presence of BMH, tBid shifted Bak into three higher order multimers around 50 kDa, 75 kDa and 96 kDa (\*). The sizes of these complexes are consistent with that of dimeric, trimeric and tetrameric form of Bak. Like in mitochondria from lymphoblastoid cells, Bak oligomerization after tBid treatment was as efficient in mitochondria from tafazzin-deficient HeLa cells (shTaz2) as it was in mitochondria from shControl cells. Altogether, these results show that the inactivation of tafazzin and consequently the decrease of mature CL do not affect the ability of tBid to interact with mitochondria, to induce Bak-oligomerization and subsequently to release apoptogenic factors from the mitochondria. These results also indicate that the apoptotic block in tafazzin-deficient cells lies upstream to tBid activity.

#### ***4.2.4 Inhibition of caspase-8 activity in tafazzin-deficient cells***

Next, the cleavage of Bid by caspase-8 was assessed in tafazzin-deficient cells. To achieve this goal, lymphoblastoid cells from BTHS and control patients were incubated with anti-Fas antibody for 24 hours and cell lysates were analysed by western-blot for the presence of Bid (**Figure 4-8A**). As seen under untreated conditions, Bid full length was expressed at the same level in control and BTHS cells. After Fas-activation this level was decreased in both control cells (DB037 and DB015.2). Unfortunately, the cleaved product, tBid was below detection level in this experiment. Surprisingly, when BTHS cells were treated with anti-Fas antibody, no change in full-length Bid level was observed. Bid cleavage was also analysed in tafazzin-deficient HeLa cells (**Figure 4-8B**). Expression of full-length Bid was similar in shControl1 and shTaz2 cells. As expected, the level of full-length Bid was reduced in shControl1 after Fas-treatment. However, like in BTHS cells, no reduction in the full-length Bid was detected in shTaz1. Therefore, these results indicate that the processing of Bid is inhibited in tafazzin-deficient cells. Since Bid is cleaved by caspase-8 following Fas activation in type II cells, it was assumed that the inhibition of apoptosis in tafazzin-deficient cells occurred at the level of caspase-8 activity.

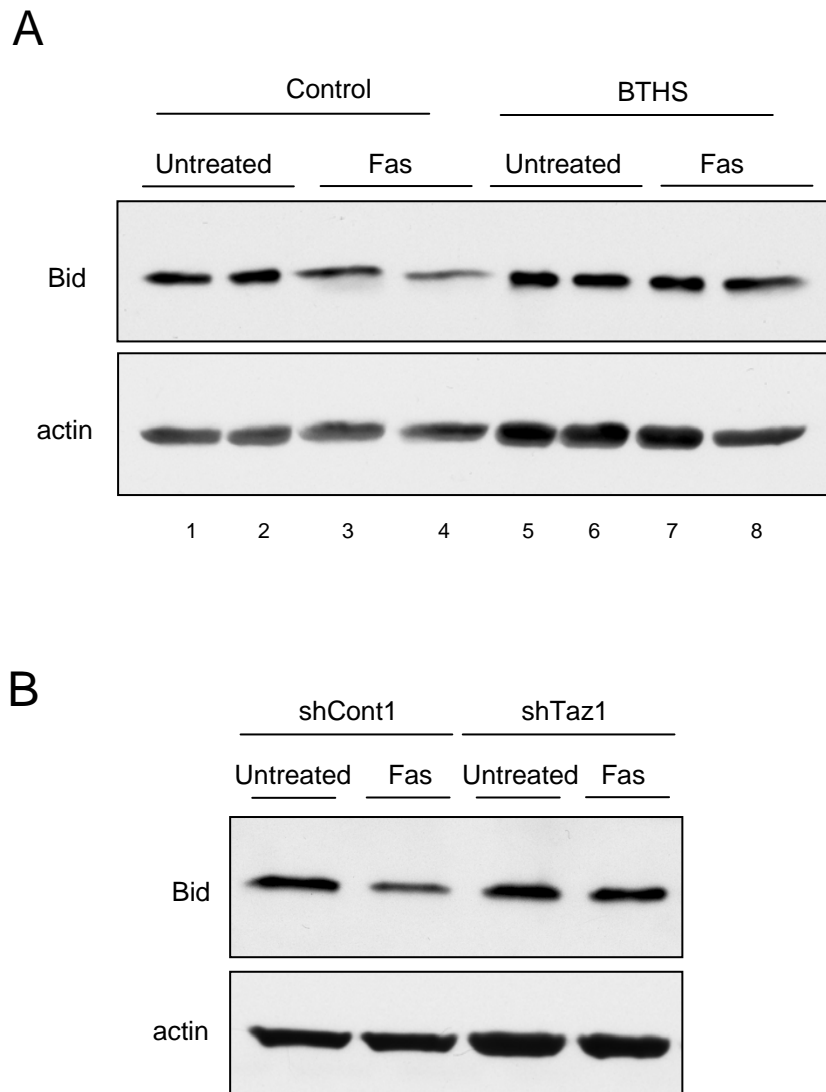
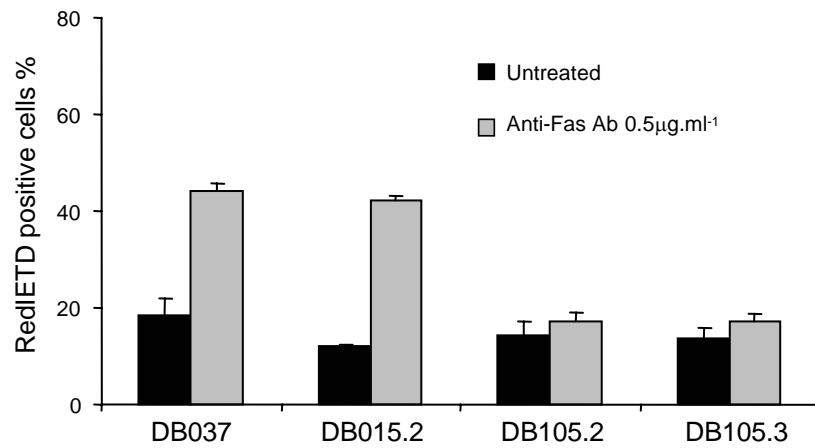


**Figure 4-8: Inhibition of Bid cleavage in tafazzin-deficient cells.**

(A) Bid cleavage in control and BTHS lymphoblastoid cells. Control (DB037-lanes 1, 3; DB015.2-lanes 2, 4) and BTHS (DB105.2-lanes 5, 7; DB105.3-lanes 6, 8) cells were incubated for 24 hours with  $0.5 \mu\text{g}\cdot\text{ml}^{-1}$  of anti-Fas antibody and cells lysates were immunoblotted with anti-Bid antibody. (B) Bid cleavage in shControl1 and shTaz1 HeLa cells. HeLa shControl1 and shTaz2 were incubated for 14 hours with  $0.3 \mu\text{g}\cdot\text{ml}^{-1}$  of anti-Fas antibody and cells lysates were immunoblotted with anti-Bid antibody. (A-B) Actin was used as loading control. Each blot is representative of 3 independent experiments.

To directly test this assumption, caspase-8 activation was monitored in tafazzin-deficient cells using a caspase-8 activity detection kit (Calbiochem). This assay utilizes the specific cleavage sequence of caspase-8, IETD, conjugated to sulforhodamine (Red-IETD-fmk) as a fluorescent marker. Red-IETD-fmk is a cell permeable and non-toxic compound that irreversibly binds to active caspase-8 in cells. The fluorescence label allows the detection of caspase-8 activation directly by flow cytometry. Lymphoblastoid cells from control and BTHS patients were incubated for 24 hours with anti-Fas antibody and caspase-8 activity was assessed (**Figure 4-9A**). In response to Fas treatment, caspase-8 was activated in around 40 % of the control cells (DB037 and DB015.2). However, this activation was strongly reduced in both BTHS cell lines. Next, shControl1 and shTaz HeLa cells were treated with anti-Fas antibody for 8 hours and caspase-8 activation was analysed (**Figure 4-9B**). After Fas-activation, more than 70 % of shControl1 cells activated caspase-8. Like in BTHS cells, this activation was significantly diminished in both shTaz cells. In fact, less than 30 % of shTaz cells displayed caspase-8 activity. As described in *section 1.5.5.5*, dimerization of caspase-8 zymogen at the DISC is a prerequisite event for the autoprocessing of caspase-8 into its fully active form [143, 144, 146]. Upon dimerization, pro-caspase-8 is first cleaved between its two active subunits to generate the p43 and p10 products. Then, cleavage of the p43 between the DED prodomain and the p18 subunit produce the dimeric active form p18/p10. Therefore, caspase-8 autocleavage was analysed by western-blot in tafazzin-deficient cells (**Figure 4-10**). Two anti-caspase-8 antibodies were used to detect the different cleavage products of caspase-8: an antibody raised against the large active subunit p18 to recognize the p43 and the p18 subunits and the anti-DED antibody to detect the procaspase-8 (p55), the p43 and the cleaved DED domain (p26). As expected, Fas activation induced the cleavage of procaspase-8 (p55) into p43, p26 and p18 in both lymphoblastoid control cells (**Figure 4-10A**). The amounts of these cleaved products were all reduced in BTHS cells in particular the p43 and the active cleaved form p18. Auto-processing of caspase-8 was also assessed in tafazzin-deficient HeLa cells. When shControl1 were treated with anti-Fas antibody, procaspase-8 was cleaved into p43, p26 and p18 (**Figure 4-10B**). Like in BTHS cells, these cleaved forms were strongly diminished in shTaz2 cells. These data together with the results of **figures 4-8** and **4-9** strongly indicate that tafazzin and thus mature CL are required for the activation of caspase-8 after Fas-engagement in type II cells.

A



B

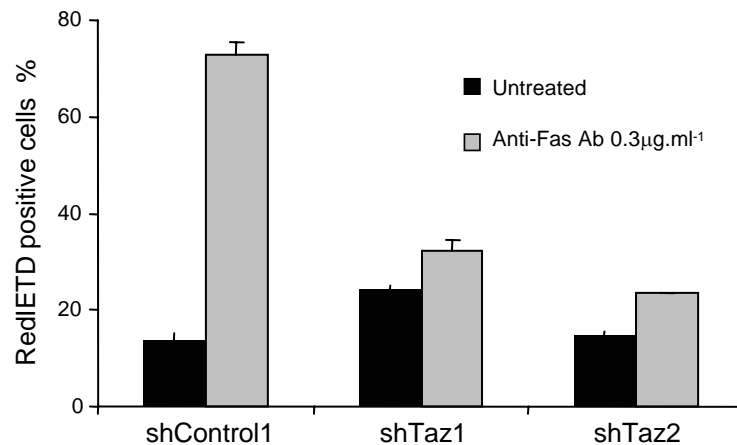


**Figure 4-9: Inhibition of caspase-8 activity in tafazzin-deficient cells.**

(A) Control (DB037 and DB015.2) and BTHS (DB105.2 and DB105.3) lymphoblastoid cells were incubated for 24 hours with 0.5 µg.ml<sup>-1</sup> of anti-Fas antibody and then labelled using the cell permeable caspase-8 substrate Red-IETD-fmk. Red-labelled cells were quantified by flow cytometry. (B) shControl1, shTaz1 and shTaz2 HeLa clones were incubated for 8 hours with 0.3 µg.ml<sup>-1</sup> anti-Fas antibody and then labelled using the cell permeable caspase-8 substrate Red-IETD-fmk. Red-labelled cells were quantified by flow cytometry. Error bars are standard errors of the mean of 3 independent experiments.

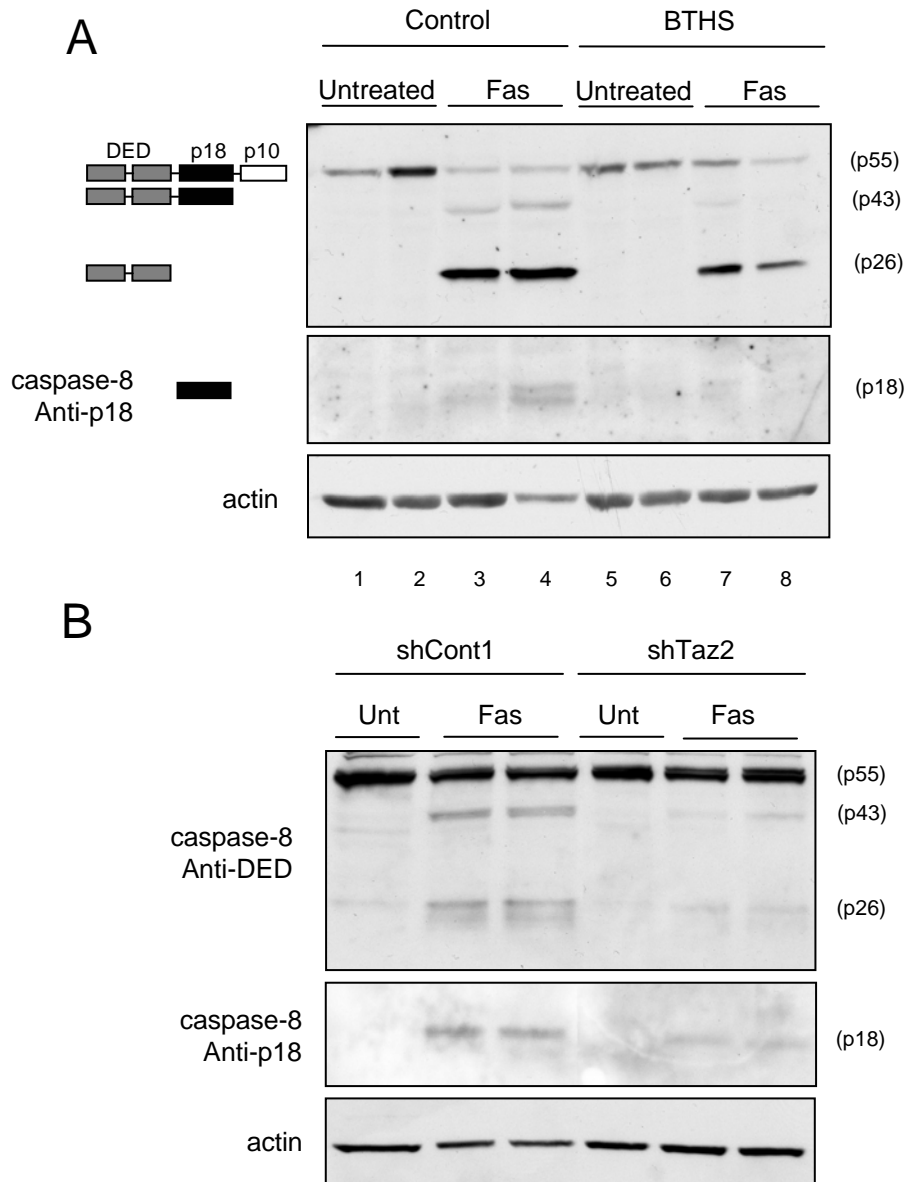


**Figure 4-10: Inhibition of caspase-8 cleavage in tafazzin-deficient cells.**

(A) Caspase-8 cleavage in BTHS lymphoblastoid cells. Control (DB037-lanes 1, 3; DB015.2-lanes 2, 4) and BTHS (DB105.2-lanes 5, 7; DB105.3-lanes 6, 8) cells were incubated for 24 hours with  $0.5 \mu\text{g}\cdot\text{ml}^{-1}$  anti-Fas antibody and cells lysates were immunoblotted with anti-caspase-8 antibodies (anti-DED, upper panel and anti-p18, middle panel). (B) Caspase-8 cleavage in tafazzin-deficient HeLa cells. shControl1 and shTaz2 HeLa cells were incubated for 14 hours with  $0.3 \mu\text{g}\cdot\text{ml}^{-1}$  of anti-Fas antibody and cells lysates were immunoblotted with anti-caspase-8 antibodies (anti-DED, upper panel and anti-p18, middle panel). (A-B) Actin was used as loading control. Each blot is representative of 3 independent experiments.

These results further suggest that the inhibition of the apoptotic cascade in tafazzin-deficient cells occurs at the level of caspase-8 activation.

#### ***4.2.5 Mitochondrial caspase-8 translocation is inhibited in tafazzin-deficient cells***

Procaspase-8 was previously shown to interact with the mitochondria under physiological conditions and active caspase-8 was also found to associate with the mitochondrial outer membrane during apoptosis [158, 159, 264, 265]. Since caspase-8 activity was affected by the inactivation of tafazzin it was tempting to speculate that mature CL were required for the activation of caspase-8 on the mitochondria. To address this, the processing of caspase-8 was analyzed on the mitochondria of control and tafazzin-deficient cells. shControl1 and shTaz2 HeLa cells were treated with anti-Fas antibody for 14 hours and cytosolic- or mitochondria-enriched fractions were isolated by differential centrifugations. These fractions were then analysed by western-blot for caspase-8 using the anti-p18 antibody. Because of experimental limitations, it was impossible to normalize these two fractions based on their cellular volume ratio. In **figure 4-11**, the mitochondria-enriched fraction is ten times higher than cytosolic fraction. The quality of the cell fractionation was controlled using an antibody against the subunit 4 of the respiratory complex IV (COXIV) localized in the mitochondrial inner membrane and an antibody recognizing the cytosolic protein actin. As shown in **figure 4-11**, COXIV was detected only in the mitochondria-enriched fractions whereas actin was mainly present in the cytosol. The small traces of actin detected in the mitochondrial fraction may account for the interactions of mitochondria with actin cytoskeleton [266]. Under physiological conditions (untreated), procaspase-8 (p55) was detected in the cytosol and the mitochondria of shControl1 and shTaz2 cells. No difference in procaspase-8 expression was detected between these two cell lines. Activation of Fas in shControl1 cells induced the cleavage of cytosolic and mitochondria-associated procaspase-8 into the p43 and p18 products. As compared to control cells, no difference in caspase-8 cleavage was observed in the cytosolic fraction of Fas-treated shTaz2 cells. However, mitochondria from these cells showed a significant reduction in the levels of p43 and p18 cleaved products. These results show that the processing of caspase-8 in the mitochondria requires tafazzin and indicate that mature CL might be involved in the activation of caspase-8 on the mitochondrial membrane. This suggests that either cytosolic pro-caspase-8 undergoes an initial step of autocleavage at the DISC (the

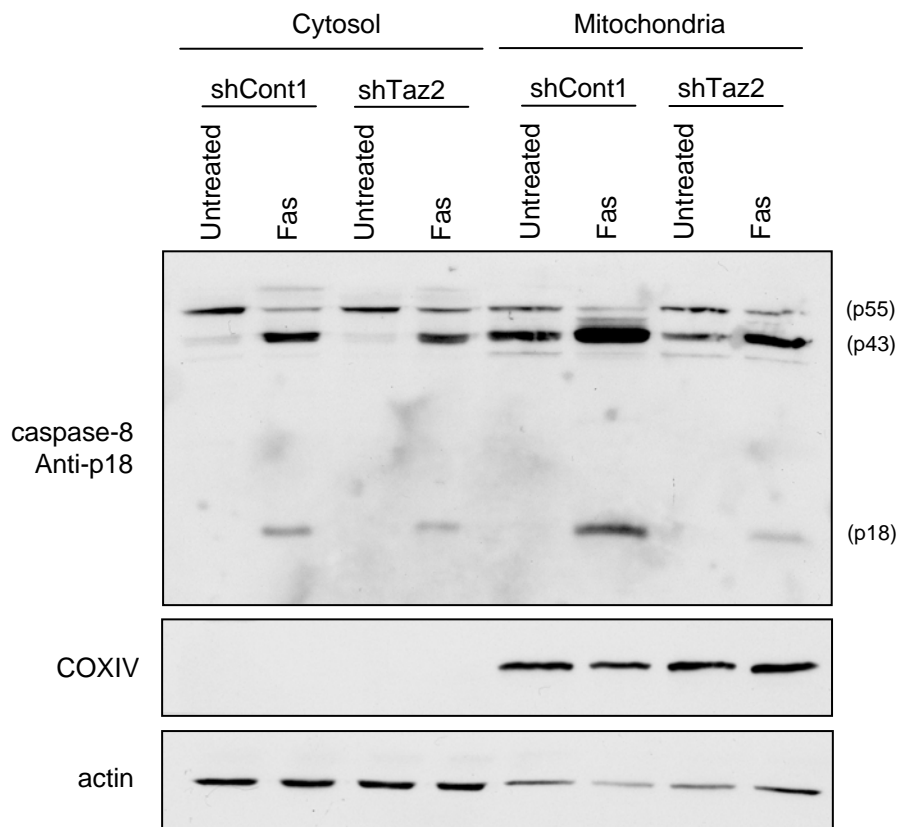


**Figure 4-11: Tafazzin is required for the autoprocessing of caspase-8 on the mitochondria.**

shControl1 and shTaz2 cells were incubated for 14 hours with  $0.3 \mu\text{g}\cdot\text{ml}^{-1}$  anti-Fas antibody and fractionated to cytosolic- and mitochondria-enriched fractions. For each fraction,  $100 \mu\text{g}$  of proteins were resolved on acrylamide gel and immunoblotted with anti-caspase-8 antibody (anti-p18 subunit). Subunit 4 of complex IV (COXIV) and actin were used as loading controls for mitochondria and cytosolic fractions, respectively. This blot is representative of 3 independent experiments .

removal of its C-terminus p10 domain) before translocating to the mitochondria or mitochondrial pro-caspase-8 autoprocesses at the mitochondria following an apoptotic signal and acquires enhanced activity.

To determine whether procaspase-8 and its cleavage products were integrated into or loosely attached to the mitochondrial membranes, mitochondrial-enriched fractions from untreated or Fas treated shControl1 cells were washed with an alkali carbonate buffer. This technique removes soluble and peripheral membrane proteins and separates them from membrane integral proteins. After 30 minutes, mitochondrial membrane proteins were collected by centrifugation at 100,000 g (Alkali-resistant fraction) and the loosely attached proteins were released in the supernatant (Alkali-sensitive fraction). These two fractions were then analysed by western-blot for the presence of caspase-8. Bak and the respiratory complex I were used as markers of the mitochondrial outer and inner membranes, respectively. The efficiency of the alkali extraction was controlled by the dissociation of the subunit B of the respiratory complex II (SDHB), which is loosely associated to the matrix side of the mitochondrial inner membrane. In untreated or Fas-treated mitochondria, SDHB was released by alkali wash whereas Bak and complex I were only detected in the alkali-resistant fraction (**Figure 4-12**). In untreated mitochondria, procaspase-8 was extracted by alkali treatment indicating that under normal conditions procaspase-8 is loosely attached to the mitochondrial outer membrane. The sensitivity of procaspase-8 to alkali treatment was not affected by Fas activation, indicating that procaspase-8 is only loosely attached to the mitochondrial outer membrane. In contrast to procaspase-8, the cleaved products of caspase-8, especially p43 and p18, were resistant to the extraction. However, significant amounts of the p26 product, which is the non active DED domain of the enzyme, was also released into the supernatant after alkali extraction, suggesting that unlike the active domains of processed caspase-8, the DED is not fully inserted into the mitochondrial membranes. These results suggest that once the first cleavage of pro-caspase-8 occurs at the DISC, p43 product translocates and integrates into the mitochondrial membranes through its exposed p18 subunit.

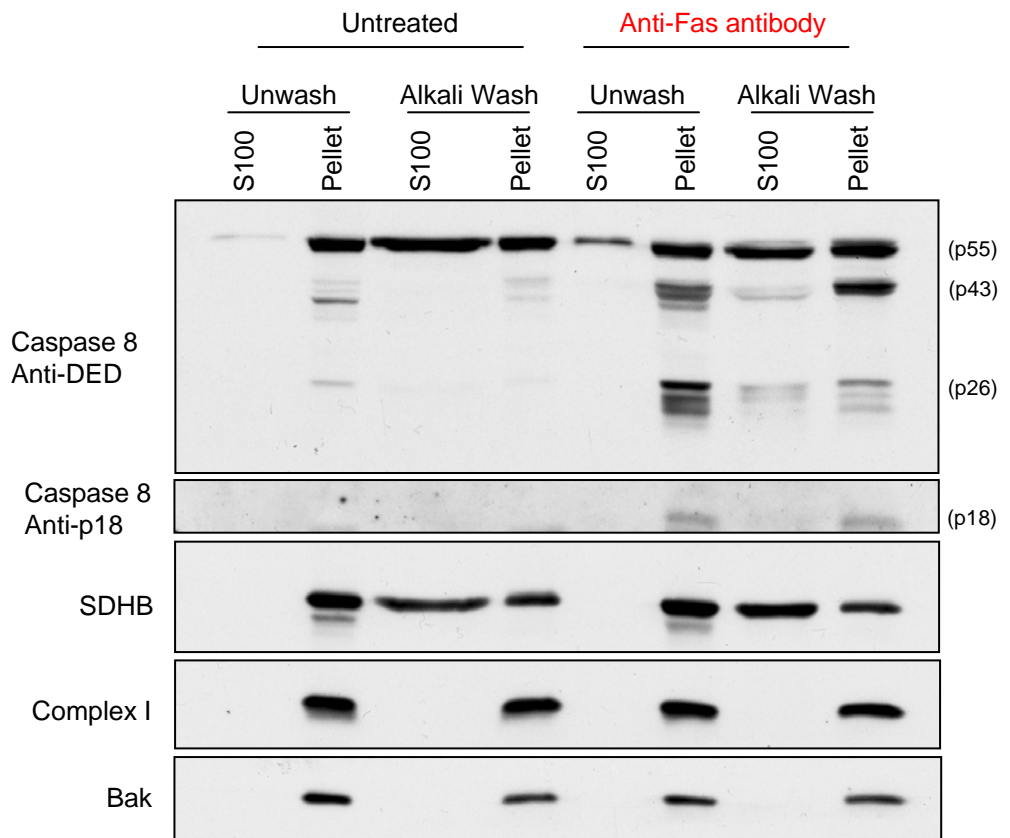


**Figure 4-12: The p18 and p43 subunits of caspase-8 integrate into the mitochondrial membranes after Fas activation.**

shControl1 cells were either untreated or treated for 14 hours with  $0.3 \mu\text{g}\cdot\text{ml}^{-1}$  anti-Fas antibody. Mitochondria-enriched fractions were isolated and resuspended for 30 minutes at  $4^\circ\text{C}$  in respiration buffer (unwash) or in alkali medium (Alkali wash) containing  $0.1 \text{ M Na}_2\text{CO}_3$ , pH11.5. Mitochondrial membranes were then pelleted by ultracentrifugation and the supernatants (S100 fraction) and pellets were collected. For each fraction,  $100 \mu\text{g}$  of proteins were resolved on acrylamide gel and immunoblotted with anti-caspase-8 antibodies (antiDED and anti-p18 subunits). The efficiency of the alkali-extraction was controlled using three mitochondrial proteins: Bak (mitochondrial outer-membrane protein) complex I (mitochondrial inner-membrane protein) and subunit-B of the succinate dehydrogenase (SDHB, loosely associated to the matrix side of the mitochondrial inner-membrane). This blot is representative of 3 independent experiments.

#### **4.2.6 Mitochondrial caspase-8 translocation is an early apoptotic event independent of Bid**

Following Fas-activation, caspase-8 cleaves the BH3-only protein Bid into tBid, which rapidly translocates from the cytosol to the mitochondria [125, 126]. Since the cleavage of Bid was inhibited in tafazzin-deficient cells it was assumed that tBid may be involved in the targeting of caspase-8 to the mitochondria. To directly address this issue, Bid was knocked down in shControl1 cells using siBid as previously described (*section 3.2.2*). Two days after transfection, cells were treated with anti-Fas antibody for 14 hours and mitochondria-enriched fractions were isolated. These fractions were then analysed by western-blot for the presence of caspase-8. As shown in **figure 4-13**, siBid efficiency reduced the level of full-length Bid in the cytosolic and mitochondrial fractions. In the presence of untargeting control siRNA and anti-Fas antibody, cleavage of Bid was detected in the cytosol and mitochondria. Interestingly, depleting Bid did not affect the ability of caspase-8 cleaved products (p43 and p18) to translocate to the mitochondria.

### **4.3 Discussion**

The results presented in the previous chapter showed that tafazzin is required for efficient Fas-mediated apoptosis in type II cells and highlighted the importance of the acyl chain composition of CL in this pathway. This chapter focused on understanding the mechanism by which mature CL participates in extrinsic apoptosis by using two models of tafazzin-deficient cells, BTHS-derived lymphoblastoid cells and tafazzin-knockdown HeLa cell lines.

To understand the role of mature CL in extrinsic apoptosis, the known steps in this process were investigated in tafazzin-knockdown cells after activating Fas signalling. First, analysis of caspase-3 activity, which in type II cells requires cytochrome *c* release from mitochondria and the formation of apoptosome, showed a marked decrease in caspase-3 activity in tafazzin-deficient cells. This indicates that the block in the apoptotic pathway in tafazzin-deficient cells was either due to an inhibition of apoptosome formation or to defects in upstream steps.

Even though CL have been previously reported to participate in many of the mitochondrial-dependent steps that lead to the release of apoptogenic factors, the

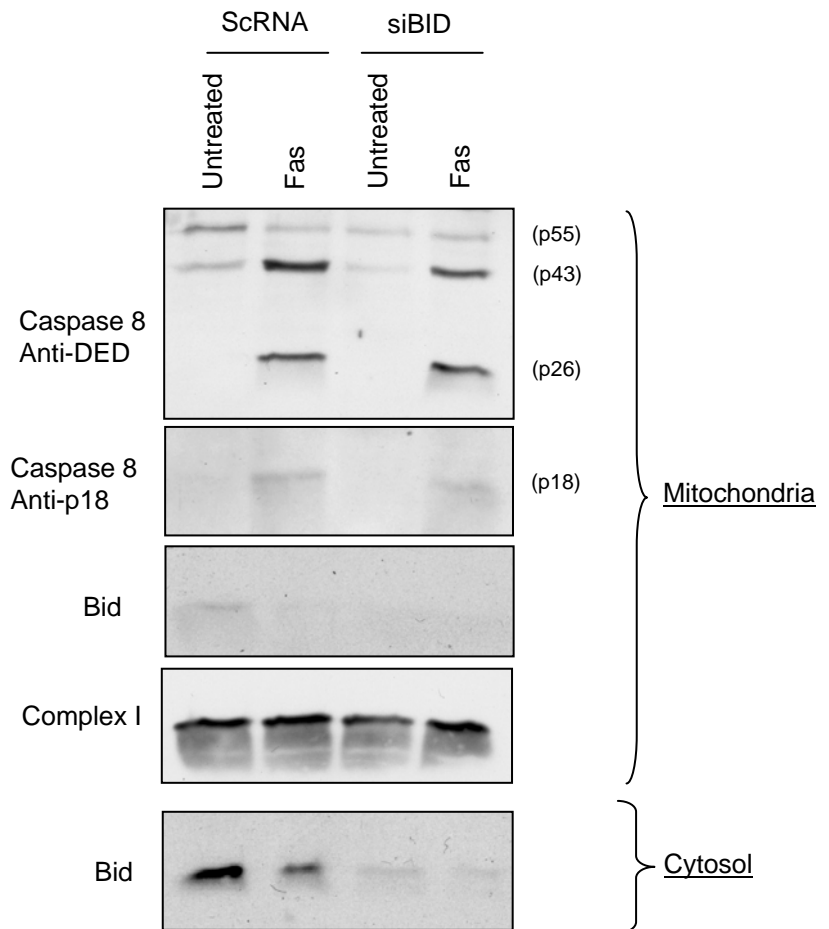


**Figure 4-13: Mitochondrial caspase-8 translocation is independent of Bid.**

shControl1 cells were transfected with 50 nM of scRNA or siBid for 48 hours and incubated with  $0.3 \mu\text{g}\cdot\text{ml}^{-1}$  anti-Fas antibody for 14 hours. Mitochondrial and cytosolic fractions were isolated by differential centrifugations and immunoblotted with the indicated antibody. Complex I was used as a loading control for mitochondrial fraction. This blot is representative of 3 independent experiments.

exact mechanism played by CL and its fatty acyl composition in this process still awaits further investigation [161]. Therefore, the role of mature CL in the release of apoptogenic factors was investigated. Fas-activation failed to release cytochrome *c* and Smac/DIABLO from mitochondria in tafazzin-deficient HeLa cells. This was not due to alterations in MOMP mechanisms since isolated mitochondria from these cells were still able to release cytochrome *c* in response to BidBH3 peptide. Moreover, the ability of tBid to induce Bak-oligomerization and cytochrome *c* release was not affected in tafazzin-deficient mitochondria. Interestingly, tBid was 100 times more efficient in releasing cytochrome *c* than BidBH3 peptide thus supporting the model that the cytochrome *c* releasing activity of tBid required BH3 independent events [85, 130]. Taken together, these results indicate that mature CL is not required for the permeabilization of the mitochondrial outer membrane by the multi-BH domain protein Bax and Bak. This is consistent with previous results obtained using CL-synthase deficient mitochondria from yeast and HeLa cells, which showed that Bax does not require CL to release cytochrome *c* [129, 165, 232].

Next, the model of CL as a mitochondrial “docking” site for tBid was investigated in mitochondria from BTHS and tafazzin-knockdown HeLa cells. tBid interacted with the same efficiency with control and tafazzin-deficient mitochondria. This may account for the ability of MLCL, which accumulates in tafazzin-deficient cells to compensate the function of CL. Indeed, tBid was previously found to bind to MLCL in artificial membranes [226, 227]. Therefore, it is likely that in tafazzin-deficient mitochondria, MLCL support the association of tBid with the mitochondrial outer membrane.

Given that neither MOMP nor interaction and apoptotic function of tBid on mitochondria were affected in tafazzin-deficient cells, further investigation of the impaired apoptotic process focused on the pathway connecting Fas response to the mitochondria. Upon Fas activation in lymphoblastoid cells or HeLa control cells, caspase-8 was activated and induced the cleavage of Bid into its active form tBid. Surprisingly, these two events were strongly inhibited in BTHS and tafazzin-deficient HeLa cells. This was also associated with the inhibition of the autoprocessing of caspase-8 into p43 and p18 cleaved products. These results demonstrate for the first time that tafazzin plays a crucial role in the activation of caspase-8 in response to Fas activation in type II cells, and underscore the

importance of mature CL in this process. This unexpected observation raised the question how a mitochondrial specific lipid affects the activity of caspase-8. Because pro- and active caspase-8 were previously shown to associate with the mitochondria [158, 159, 264, 265], it was investigated whether mature CL were involved in the activation of caspase-8 on the mitochondria. Under normal conditions, procaspase-8 was found associated with the cytosolic and mitochondria-enriched fractions in control HeLa cells. After Fas-activation, autoprocessing of procaspase-8 into p43, p26 and p18 cleaved products was detected in both fractions. Procaspase-8 and p26 were loosely attached to the mitochondria (alkali-sensitive fraction) whereas p43 and p18 cleaved forms were inserted into the mitochondrial membranes (alkali-resistant fraction). Therefore, upon Fas activation, p43 cleaved product translocates and integrates into the mitochondrial membranes through its p18-exposed subunit. The translocation of p43 caspase-8 to the mitochondria was significantly reduced in tafazzin-deficient cells. The fact, that procaspase-8 was cleaved in the cytosolic fraction of tafazzin-deficient cells after Fas engagement, together with the lack of caspase-8 activation in BTHS and tafazzin-knockdown cells strongly indicate that activation of caspase-8 in type II cells mainly occurs at the mitochondria and requires mature CL. This is consistent with the seminal description of the type I and type II Fas-signalling pathways. In type II cells, DISC formation is strongly reduced and activation of caspase-8 is delayed and requires a mitochondrial step [56]. The observation that caspase-8 activation was inhibited by overexpressing Bcl-2 and Bcl-X<sub>L</sub> raised the questions whether caspase-8 was activated downstream to the mitochondria or at the mitochondrial membrane [56]. It was previously shown that Bcl-X<sub>L</sub>, with the help of the protein BAR (bifunctional apoptosis regulator), sequesters active caspase-8 at the mitochondrial outer membrane [159]. Altogether these data provide strong evidence that in type II cells, caspase-8 is activated in a two step process. First, after Fas activation a small amount of procaspase-8 is activated at the DISC to produce the p43 cleaved products. Then, p43 translocates to the mitochondria in a CL dependant manner and enhances the full activation of procaspase-8 at the mitochondrial membrane. The delay in caspase-8 activation in type II cells may account for the time required for p43 caspase-8 to relay the signal from the cell surface to the mitochondria. However, these results did not exclude the possibility that other partners may be involved in the activation of caspase-8 at the mitochondrial membranes. Recently, the FLICE-associated huge protein (FLASH) was shown to translocate from the nucleus to the mitochondria in response to Fas

activation, where it interacts with mitochondrial-associated caspase-8 [267]. Whether FLASH participates or not in the regulation of caspase-8 activation on the mitochondria awaits further investigation. Furthermore, the BH3 only protein Bid was not required for the translocation of p43 to the mitochondria in HeLa cells indicating that activation of caspase-8 on mitochondria is an early event that precedes the processing of Bid.

In summary, this chapter demonstrated that the inhibition of the extrinsic apoptotic pathway in tafazzin-deficient cells takes place at the level of caspase-8 activation. Cells deficient in caspase-8 are resistant to Fas and TNF $\alpha$ -mediated apoptosis but are still sensitive to death induced by intrinsic stimulations such as etoposide [53]. Inactivation of caspase-8 is consistent with the results obtained in the previous chapter where it was shown that BTHS cells were protected from extrinsic apoptosis but were still able to undergo apoptosis in response to DNA damage. In contrast, tafazzin-deficient HeLa cells were protected from apoptosis induced by high dose of etoposide. However, as mentioned previously, etoposide activates the p53 apoptotic pathway, which is impaired in HeLa cells. It is possible that in this context, HeLa cells undergo apoptosis through a p53-independent pathway which involves a tafazzin-dependent step. Moreover, etoposide-induced apoptosis was found to require caspase-8 in several p53-deficient cells such as Jurkat and breast cancer cells [264, 268]. Taken together, these results suggest that etoposide induce apoptosis via two signalling pathways, a p53 dependant pathway and a caspase-8 dependant pathway. It is likely that inhibition of both pathways in tafazzin-deficient HeLa cells conferred resistance to etoposide-induced apoptosis.

It was shown here for the first time that mature CL are required for the interaction and in turn the activation of caspase-8 on the mitochondrial membrane in type II cells. It is still to be determined whether other proteins, such as FLASH, participate with mature CL in the activation of caspase-8 on the mitochondrial membranes. However, the exact mechanism by which mature CL specifically recruits caspase-8 p43 to the mitochondria remains unclear. Nevertheless, caspase-8 is likely to interact with mitochondria at the contact site between the mitochondrial inner and outer membranes, where CL is exposed to the cytosolic face of the mitochondria (**Figure 1-7**). As mentioned in *section 1.6.6.1*, the unsaturated acyl chains of CL are peroxidized by ROS following a wide variety of apoptotic stimulations [212-214].

A decrease of the unsaturation degree of CL may protect CL from peroxidation. Therefore, it is likely that in BTHS and tafazzin-deficient HeLa cells the reduction of unsaturated mature CL may decrease its sensitivity to peroxidation. One can speculate that peroxidized CL may be the recognition signal of caspase-8 on the surface of mitochondria. Clearly, further study is required to identify the mechanism of interaction between CL and caspase-8 and to elucidate whether peroxidation plays a role in this process.

**CHAPTER 5 ACTIVATION OF CASPASE-8 AT  
THE MITOCHONDRIAL MEMBRANE: THE  
ACTIVATING PLATFORM MODEL**

## **5 Activation of caspase-8 at the mitochondrial membrane: the activating platform model**

### **5.1 Introduction**

The previous chapter showed that mature CL are required for the activation of caspase-8 on the mitochondrial membranes in type II cells. Even though the activation of caspase-8 on the mitochondria has already been proposed, the exact mechanism by which this initiator caspase become activated at the mitochondrial membranes remains elusive [158, 159, 264, 265, 267]. As discussed in *section 1.5.5.3*, activation of initiator caspases requires the recruitment of the zymogens to activating platform (PIDDosome for caspase-2, DISC for caspase-8, apoptosome for caspase-9) that promotes the dimerization of the pro-caspases and in turn, leads to their autoprocessing into active forms [143-145]. The results from chapter 4 demonstrated that targeting the p43 caspase-8 cleaved product to mature CL is required for the full activation of caspase-8 in type II cells and suggested that mature CL provides an activating platform for procaspase-8 at the mitochondria. One question remained is what are the consequences of activating caspase-8 on the mitochondria. Stegh *et al* proposed a model in which active caspase-8 translocates from the mitochondria to the cytosol to target the cleavage of plectin, a cross-linking protein of cytoskeletal filaments [158]. However, whether mitochondrial active caspase-8 can directly induce MOMP has not been investigated yet.

The aim of the results discussed in this chapter was to understand the mechanisms governing the activation of caspase-8 on the mitochondrial membranes, and to analyse the effects of this activation on the mitochondria-dependant steps of apoptosis.

## **5.2 Results**

### **5.2.1 Caspase-8 oligomerizes on mitochondrial-membranes following Fas activation**

Previous studies have demonstrated that initiator caspases are activated upon dimerization on activating platforms. Therefore, it was of interest to examine whether caspase-8 could oligomerize on mitochondrial membranes following Fas activation. shControl1 HeLa cells were treated with anti-Fas antibody for 14 hours, and mitochondria were incubated in the presence of BMH to stabilize caspase-8 oligomers in the mitochondrial membrane. The oligomerization of caspase-8 was then visualized by western-blot analysis (**Figure 5-1**). In the presence of DMSO, procaspase-8 was detected as a single band that migrated at around 55-kDa. As expected, only the p43 and p26 cleaved products were detected using the anti-DED antibody after Fas-activation. Following BMH cross-linking, a slightly faster mobility band for procaspase-8 was observed (asterisks). This probably corresponds to an intramolecular cross-linked form of procaspase-8. It is noteworthy that after Fas activation, BMH shifted the first cleaved form of caspase-8 (p43) (which disappeared) into higher molecular weight complexes at around 50 kDa, 80 kDa (major species\*), 120 kDa, 160 kDa and 200 kDa (minor species\*). The 50 kDa is likely to be the heteromer of p43 and the active subunit p10. However, the estimated sizes of the other caspase-8 cross-linked complexes are consistent with homo-oligomerization of p43 into dimer, trimer, tetramer and pentamer, respectively. These oligomers were not detected using the anti-p18 antibody. It is possible that oligomerization of caspase-8 hides the epitope recognized by the anti-p18 antibody. Therefore, these results provide the first evidence that p43 caspase-8 oligomerizes in the mitochondrial membranes in response to Fas activation and further suggest that mitochondria provide an activating platform for caspase-8.

### **5.2.2 Active caspase-8 induces cytochrome c release in a CL dependant manner**

Next it was investigated whether mitochondrial active caspase-8 could initiate the mitochondrial step of apoptosis. To address this, mitochondria were isolated from HeLa cells and incubated with increasing amounts of recombinant active caspase-8 (p18/p10 heteromer). Then, the ability of the active heteromer to translocate to the

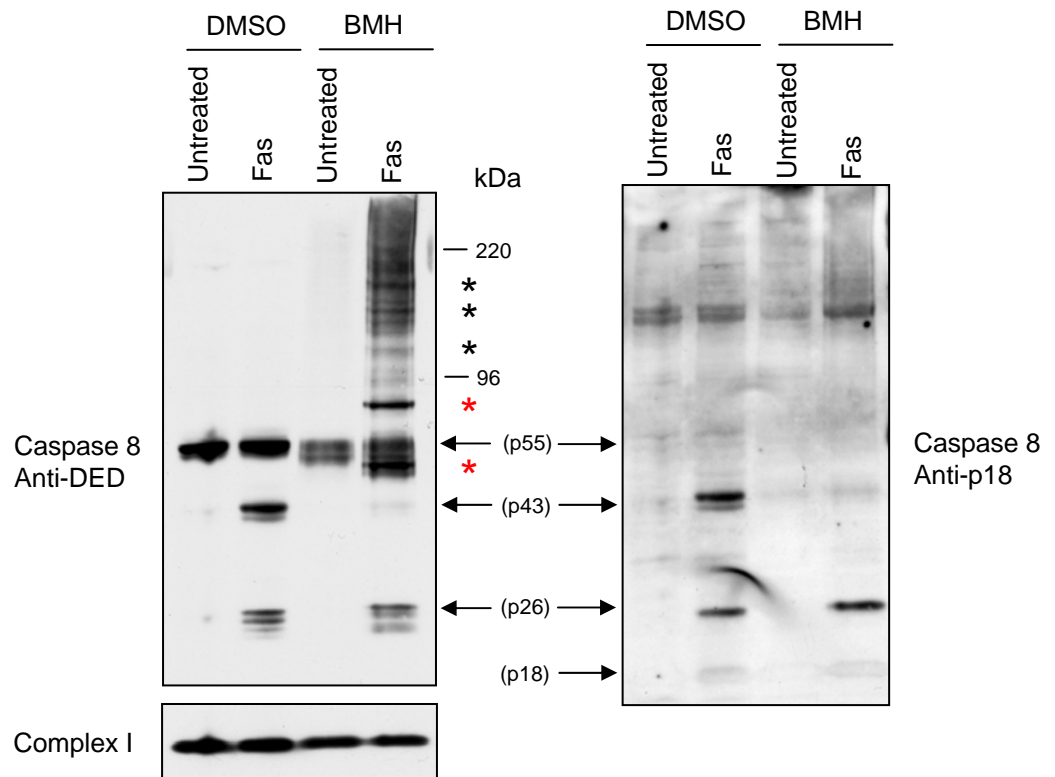


**Figure 5-1: Caspase-8 oligomerizes in the mitochondrial membranes in response to Fas-activation.** shControl1 cells were treated with  $0.3 \mu\text{g}\cdot\text{ml}^{-1}$  anti-Fas antibody for 14 hours and mitochondrial fractions were isolated by differential centrifugations. Mitochondrial fractions were resuspended in buffer containing either DMSO or 10 mM of BMH for 30 minutes. Mitochondrial pellets were then collected and immunoblotted with anti-DED caspase-8 antibody (left). The blot was then stripped and re probed with the anti-p18 caspase-8 antibody (right). Complex I was used as a loading control for mitochondrial fraction. This blot is representative of 3 independent experiments.

mitochondria and to release cytochrome *c* was assessed by western-blot (**Figure 5-2A**). Active caspase-8 interacted with shControl1 mitochondria and induced cytochrome *c* release in a dose dependant manner. In fact, 100 ng of recombinant caspase-8 initiated the releasing of cytochrome *c* from these mitochondria and almost all the cytochrome *c* was released with 500 ng. Importantly, active caspase-8 had the same affinity to tafazzin-deficient mitochondria. However, active caspase-8 was less efficient in releasing cytochrome *c* from shTaz2 mitochondria. In these mitochondria, cytochrome *c* release was initiated when 200 ng of active caspase-8 was used and 500 ng had comparable activity to 200 ng in shControl1 mitochondria. These results indicate that active caspase-8 requires tafazzin, thus mature CL, to release cytochrome *c* from isolated mitochondria. Although the early processed form of caspase-8 (p43) requires CL to interact with and to be processed on the mitochondrial membrane (**Figure 4-11**), the fully active caspase-8 (p18/p10) had the same affinity for control and tafazzin-deficient mitochondria (**Figure 5-2A**). These results suggest that mature CL is essential either for the activity of fully processed caspase-8 on mitochondrial membranes or for the availability of its substrates on the mitochondrial membranes.

To investigate whether the lack of mature CL affect the activity of recombinant caspase-8 on mitochondrial membranes, the oligomerization of active caspase-8 was analysed in tafazzin-deficient mitochondria. Isolated mitochondria from shControl1 and shTaz2 were treated with increasing amount of recombinant active caspase-8 and incubated in the presence of BMH to stabilize the caspase-8 oligomers in the mitochondrial membrane. The oligomerization of caspase-8 was then visualized by western-blot analysis using the anti-p18 antibody (**Figure 5-2B**). In the presence of BMH, active caspase-8 oligomerized into higher molecular weight complexes in shControl1 mitochondria. The major specie (\*\*\*) at around 28 kDa likely corresponds to the active heteromer p18/p10. The size of the other crosslinked complexes (~36 kDa, 38 kDa, 45 kDa and 55 kDa) is consistent with that of multimers of p18 either alone, or together with p10. Interestingly, active recombinant caspase-8 efficiently oligomerized on tafazzin-deficient mitochondria suggesting that mature CL were not require to sustain the activity of active caspase-8 on mitochondrial membrane.



### **5.2.3 Caspase-8 induced cytochrome *c* release is regulated by the Bcl-2 family proteins**

In order to investigate whether active caspase-8 induced cytochrome *c* through Bax/Bak activation, the ability of recombinant active caspase-8 to induce mitochondrial Bak oligomerization was analysed. Under the same conditions as in the previous experiment (**Figure 5-2**), mitochondria from shControl1 and shTaz2 were treated with increasing doses of active recombinant caspase-8 and the membranes were crosslinked using BMH (**Figure 5-3A**). In both mitochondria, BMH induced the appearance of the faster mobility form of Bak at around 21 kDa (\*\*). In shControl1, active caspase-8 induced Bak oligomerization in a dose dependant manner. Active-caspase-8 shifted the faster mobility form of Bak into a higher molecular weight complexe at around 38 kDa (\*) correlating to a dimeric form of Bak (**Figure 4-6B**). Interestingly, the formation of these higher order complexes was considerably reduced in shTaz2 mitochondria and the level of the faster mobility species of Bak was not decreased (**Figure 5-3A**).

Next, the ability of the anti-apoptotic protein Bcl-X<sub>L</sub> to regulate caspase-8-induced cytochrome *c* release was tested. Mitochondria were isolated from shControl1 and Bcl-X<sub>L</sub>1 cells and incubated with 200 ng of active recombinant p18/p10. Consistent with previous results, active caspase-8 interacted and released cytochrome *c* from shControl1 mitochondria (**Figure 5-3B**). However, even though active caspase-8 interacted with mitochondria overexpressing Bcl-X<sub>L</sub>, it failed to release cytochrome *c* from these mitochondria. Taken together, these results indicate that caspase-8 induced-cytochrome *c* release is tightly regulated by the Bcl-2 family proteins.

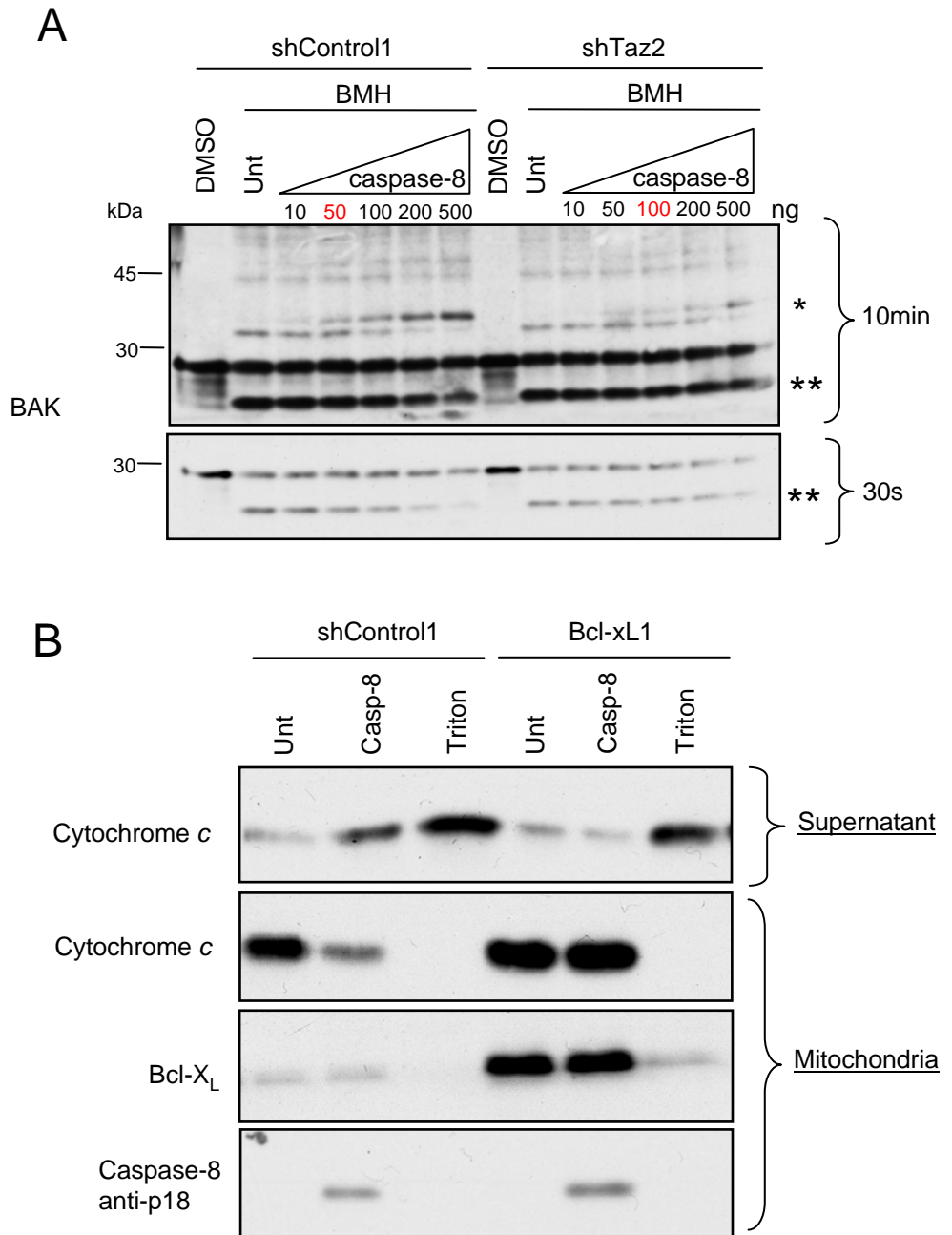


**Figure 5-3: Caspase-8 induced-cytochrome c release is regulated by the Bcl-2 family proteins.**

(A) Active caspase-8 induces Bak-oligomerization in a CL-dependant manner. Mitochondria were isolated from shControl1 or shTaz2 cells and incubated in the presence of 10 mM succinate and 1  $\mu$ M rotenone. Mitochondria were treated with increasing amount of recombinant active caspase-8 p18/p10 for 15 minutes at 37°C. Mitochondrial pellets were resuspended in DMSO or 10 mM BMH and immunoblotted with anti-Bak antibody. A low (30 seconds) and a high (10 minutes) exposure of the same blot are shown. (B) Bcl-X<sub>L</sub> inhibits caspase-8-induced cytochrome c release. Isolated mitochondria from shControl1 or Bcl-X<sub>L</sub>1 cells were incubated in the presence of 200 ng recombinant caspase-8. The supernatant and mitochondrial pellets were collected and immunoblotted with the indicated antibody. These blots are representative of 3 independent experiments.

#### ***5.2.4 Active caspase-8 induced cytochrome c release through the cleavage of mitochondrial-associated Bid***

Since caspase-8 cytochrome *c* releasing activity was dependant on Bak and completely blocked by Bcl-X<sub>L</sub>, it was tested whether the BH3 only protein Bid, specific substrate of caspase-8, may be involved in this process. To directly address this issue, Bid was depleted from shControl1 cells using siBid. Two days after transfection, mitochondria were isolated and treated with recombinant active caspase-8 to induce cytochrome *c* release (**Figure 5-4**). When mitochondria isolated from scRNA transfected cells were incubated with active caspase-8, cytochrome *c* was efficiently released. At the same time, mitochondrial-associated Bid was cleaved into tBid. Importantly, depleting mitochondrial Bid did not affect the interaction of active caspase-8 with the mitochondria but significantly reduced its ability to release cytochrome *c* (**Figure 5-4**). These results indicate that caspase-8-induced cytochrome *c* release activity requires the presence of full-length Bid on the mitochondria and the cleavage of mitochondrial associated Bid into tBid.

#### ***5.2.5 CL is required for the physiological association of full-length Bid with the mitochondria***

Having shown that active caspase-8 cleaves mitochondrial-associated Bid to induce cytochrome *c* release, it was investigated whether the full-length Bid protein was present on tafazzin deficient mitochondria and available to caspase-8. As can be seen in **figure 5-5A**, the levels of the full-length Bid were dramatically reduced in mitochondria isolated from tafazzin-deficient cells as compared to control mitochondria. It is therefore likely that the lack of Bid on shTaz2 mitochondria decreases the mitochondrial formation of tBid and subsequently inhibits cytochrome *c* release after treatment with active caspase-8.

To compare the appearance of tBid on mitochondria from control and tafazzin-deficient cells, isolated mitochondria were incubated with incremental doses of active caspase-8 and then subjected to an alkali wash to extract the loosely associated proteins (**Figure 5-5B**). Consistent with the previous results, recombinant active caspase-8 inserted with the same efficiency into shControl1 and shTaz2 mitochondria. However, following incubation of mitochondria with increasing amounts of recombinant caspase-8, a corresponding rise in membrane-inserted tBid

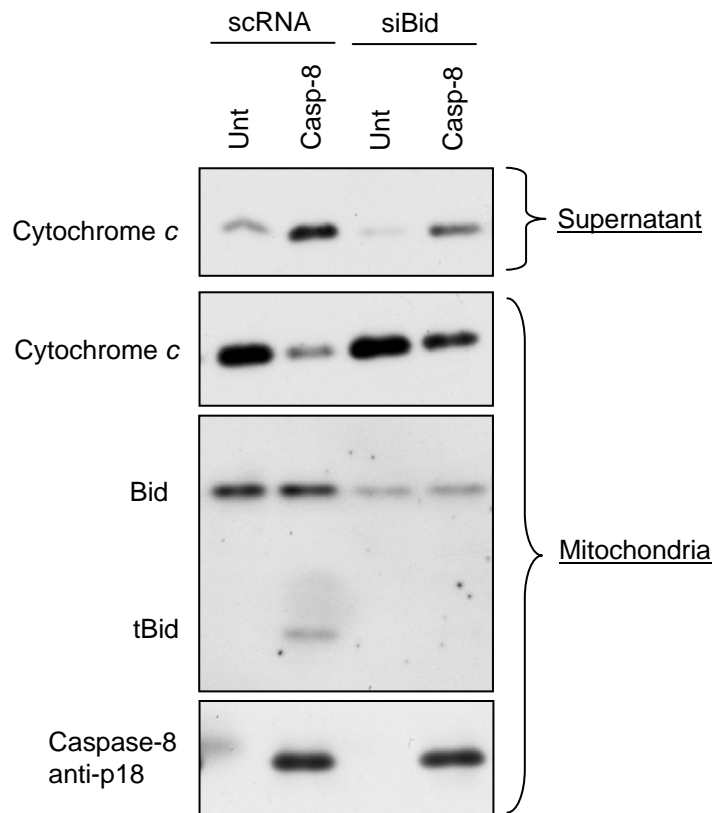


**Figure 5-4: Caspase-8 cleaves mitochondrial-associated Bid and induces cytochrome c release.**

shControl1 cells were transfected with 50 nM of scRNA or siBid for 48 hours. Mitochondria isolated from scRNA or siBid transfected cells were incubated in the presence of 10 mM succinate and 1  $\mu$ M rotenone and treated with 200 ng of recombinant active caspase-8 p18/p10 for 15 minutes at 37°C. The supernatant and mitochondrial pellets were collected and immunoblotted with the indicated antibody. These blots are representative of 3 independent experiments.

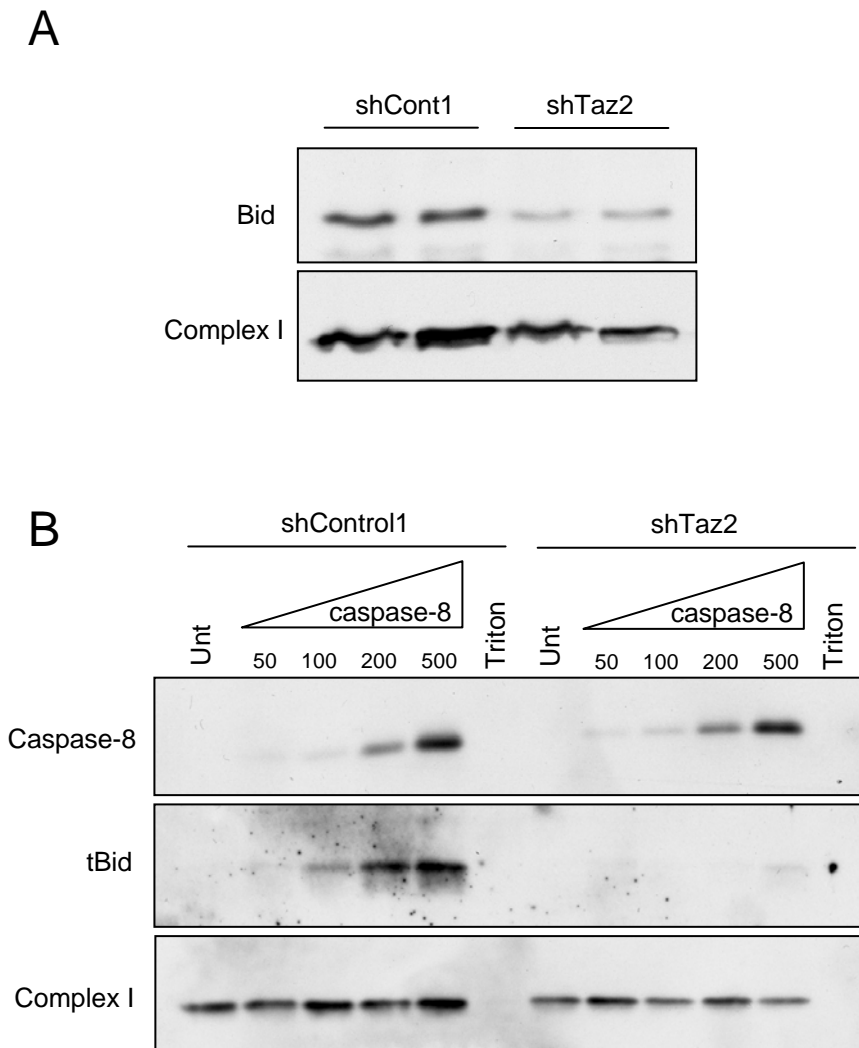


**Figure 5-5: CL is required for the physiological association of full-length Bid with the mitochondria and for presenting Bid to active caspase-8.**

(A) Tafazzin deficient mitochondria lack full-length Bid. The levels of endogenous full-length Bid protein on untreated mitochondria, isolated from shControl1 or tafazzin-knockdown (shTaz2) HeLa cells were analysed by western blot. (B) Active caspase-8 inserts into mitochondrial membranes and cleaves mitochondrial-associated Bid into tBid. Mitochondria were isolated from shControl1 and shTaz2 cells and incubated in the presence of 10 mM succinate and 1  $\mu$ M rotenone and treated with increasing amount of recombinant active caspase-8 p18/p10 for 15 minutes at 37°C. The mitochondrial pellets were then washed in alkali buffer and analysed by western-blot for caspase-8 insertion into mitochondrial membranes and for tBid formation. (A-B) Subunit 6 of complex I was used as mitochondrial loading control. These blots are representative of 3 independent experiments.

was seen in control but not in tafazzin-deficient mitochondria. Altogether, these results demonstrate that caspase-8 cleaves Bid on the mitochondrial membrane and that the lack of Bid on tafazzin-deficient mitochondria prevents caspase-8-mediated cytochrome *c* release. These results further indicate that mature CL is essential for the physiological association of full-length Bid with the mitochondria and it plays a crucial role in presenting Bid to active caspase-8.

### **5.3 Discussion**

The previous chapter provides the first evidence that CL are essential for the activation of caspase-8 on the mitochondrial membranes in type II cells. It did not however address any of the mechanisms by which this initiator caspase acquires full activity on the mitochondrial membranes. This chapter focused on understanding the mechanism by which caspase-8 is activated on the mitochondrial membranes and the effect of this activation on the mitochondrial step of apoptosis.

In stark contrast to effector caspases that are directly activated upon cleavage by the initiator caspases, activation of the initiator caspases requires the recruitment and subsequent dimerization of the zymogens on activating platform. Such triggering complexes include the DISC for caspase-8 and 10 [41], the apoptosome for caspase-9 [107], the PIDDosome for caspase-2 [269] and the inflammasome for caspase 1 and 5 [270]. Activation of caspase-8 on the mitochondria has been reported before [158, 159, 264, 265, 267]. However, none of these studies have unravelled the mechanism by which this activation takes place. Here, it is shown for the first time that in response to Fas activation, the p43 caspase-8 cleaved product oligomerizes in the mitochondrial membranes. It is likely that by analogy to the DISC, oligomerization of caspase-8 at the mitochondria involves homophilic interaction through their DEDs. This is supported by the observation that active caspase-8 was unable to process its own precursor *in vitro* [146]. Whether or not the oligomerization of caspase-8 on the mitochondrial membranes involves protein adaptor, such as FADD in the DISC, awaits more investigations.

These findings, together with the results of the previous chapter, suggest that in response to Fas activation, the p43 caspase-8 product generated at the DISC moves and inserts to the mitochondrial membranes where it oligomerizes and subsequently

further processes into its fully active form p18/p10. It remains unclear whether only DISC-generated p43 translocates and oligomerizes on mitochondria, or whether p43 oligomerizes with mitochondria-associated procaspase-8. Since DISC formation is reduced in type II cells [56], it is likely that the small amount of p43 caspase-8 produced at the DISC moves to the mitochondria and oligomerizes with mitochondrial-associated pro-caspase-8 to enhance its activation.

The significance of the cleavage events for the activation of initiator caspases is still a matter of debate. Dimerization of procaspase-8 was reported to be sufficient for the acquisition of the catalytic activity [144]. In contrast, another model states that auto-processing is a prerequisite event for the activation of procaspase-8 [143, 146]. In this scenario, the cleavage of the dimerized procaspase-8 leads to a change in its substrate specificity and enable the enzyme to recognize and activate the effector caspases [143, 146]. The results of this chapter further support the importance of procaspase-8 cleavages for the full activation of the enzyme. Therefore, it is conceivable that oligomerization of p43 caspase-8 on the mitochondria represents a prerequisite event that brings two identical catalytic units together and provides enzymatically competent conformation for the autoprocessing of the active dimer on the mitochondrial membranes.

Once it was demonstrated that caspase-8 translocated to and activated in the mitochondrial membranes in response to Fas activation in type II cells, further emphasis was given to explore the role of active caspase-8 in the mitochondrial phase of apoptosis. *In vitro*, active recombinant caspase-8, p18/p10, inserted into mitochondrial membranes and released cytochrome *c* from mitochondria. Caspase-8-induced cytochrome *c* releasing activity was dependent on Bak oligomerization and was completely blocked by Bcl-X<sub>L</sub>. Therefore, it was tested whether caspase-8-induced cytochrome *c* release was dependent on the BH3 only protein Bid. Depletion of Bid on the mitochondria by RNA interference showed that caspase-8-induced cytochrome *c* releasing activity requires the cleavage of mitochondrial associated Bid into tBid. In the seminal study that identified Bid as a substrate of caspase-8, active caspase-8 was shown to require cytosolic Bid in order to release cytochrome *c* *in vitro* [126]. Here, it was shown that caspase-8-induced cytochrome *c* release activity does not require a cytosolic factor. Indeed, active caspase-8 inserts into the mitochondria and cleaves mitochondrial associated Bid into tBid that integrates into

the mitochondrial membrane and subsequently releases cytochrome *c*. The reason for this discrepancy is likely to be the amount of caspase-8 used in both studies. In fact, Luo *et al.* did not detect any cytochrome *c* release by incubating mitochondria with 20 ng of recombinant active caspase-8, which is 5 times lower than the amount required for initiating the release of cytochrome *c* in this study (**Figure 5-2**).

Importantly, although active caspase-8 was able to interact with and efficiently insert into tafazzin-deficient mitochondria, it was less efficient in releasing cytochrome *c* from these mitochondria. However, the basal level of full-length Bid was dramatically reduced in tafazzin-deficient mitochondria and hence less available for caspase-8 cleavage. Indeed, following incubation of mitochondria with increasing amounts of recombinant caspase-8, a corresponding rise in membrane-inserted tBid was seen in control, but not in tafazzin-deficient mitochondria. Taken together, these results provide the first evidence that tafazzin is required for the physiological association of full-length Bid with the mitochondria. Even though Bid was first described as a cytosolic protein [124-126], a growing body of evidences suggest that Bid binds to the surface of mitochondria [230, 271, 272]. Additionally, these results indicate that mature CL promotes the association of Bid to the surface of the mitochondria and that MLCL, which accumulate in tafazzin-deficient mitochondria are not able to compensate for CL in this function. This was surprising since tBid was shown to efficiently translocate to tafazzin-deficient mitochondria (*Chapter 4*). This may be due to different type of interactions between Bid or its truncated form with the mitochondria. In fact, while Bid is loosely associated with the surface of the mitochondria, tBid inserts into the mitochondrial membranes. The three-dimensional structure of Bid presents an overall similarity to that of Bax and Bcl-X<sub>L</sub> [263, 273]. However, Bid lacks the hydrophobic C terminal domain responsible for the insertion of Bax and Bcl-X<sub>L</sub> into the mitochondria (**Figure 1-4**). Bid is composed of eight  $\alpha$ -helices, of which  $\alpha$ 3 contains the BH3 domain, and two hydrophobic helices (H6 and H7) are buried at the centre of the molecule. Upon caspase-8 cleavage, these hydrophobic helices become exposed to the surface and the net charge of the molecule increased [263]. This may provide the targeting of tBid to the mitochondrial CL [224, 274]. However, whether this specific binding involved hydrophobic and/ or electrostatic interactions remains to be defined. Clearly, more investigations are required to characterize the mechanism by which Bid and tBid interact with CL.

To summarize, this chapter shows that CL enables the association of full length Bid with the mitochondrial membranes under normal physiological conditions. Thus, Bid is directly available for active caspase-8 on the mitochondrial surface and is cleaved into tBid, which in turn inserts into the mitochondrial membranes and induces cytochrome *c* release. Therefore, by tethering full-length Bid on mitochondria and by providing an activation site for caspase-8 following Fas signalling, CL brings together both the enzyme and its substrate and provides a platform from which to launch the mitochondrial phase of apoptosis. Thus, in type II cells CL is required both for grasping and activating the less or pre-active forms of caspase-8 on the mitochondria and for holding and presenting its substrate Bid.

## **CHAPTER 6 GENERAL DISCUSSION AND SUMMARY**

## 6 General discussion and summary

One of the hallmarks of cancer cells is their acquired resistance to apoptosis [236]. Most of the signals that elicit apoptosis converge on the mitochondria to induce MOMP and commit cells to death [31, 32]. The fact that MOMP represents a point of no return in the apoptotic pathway has prompted efforts to develop agents capable of triggering it in cancer cells. MOMP is a complex event involving the coordinated effort between numerous Bcl-2 family proteins.

In addition to this complex protein machinery, CL has emerged as a participant in many of the mitochondrial-dependent steps that lead to MOMP [161]. However, until recently, investigation of the role of CL and its fatty acyl chain composition in apoptosis has been limited by the lack of cellular model. Following the cloning of human CL synthase, the role of CL in apoptosis was further studied in a mammalian cell model in which CL synthase was knocked down [165]. Inhibition of CL synthesis decreased the total level of CL without affecting its acyl chain composition and resulted in the accumulation of its precursor PG. These CL-deficient cells, however, displayed accelerated necrosis-like cell death likely due to severe bioenergetic alterations [165].

In this work, the role of CL and its acyl chain composition in apoptosis was investigated using novel cell models of BTHS patient-derived cells and tafazzin-knocked down HeLa cells containing reduced amounts of unsaturated mature CL and an accumulation of MLCL. In both cellular models, inactivation of tafazzin conferred resistance to the extrinsic pathway of apoptosis. This resistance was directly due to the inhibition of CL remodelling. Indeed, when tafazzin was transiently knocked down in HeLa cells, neither the CL pattern nor the sensitivity of these cells to Fas-mediated apoptosis was altered. These results, together with the fact that rescuing the level of mature CL in tafazzin-deficient cells sensitized the cells to extrinsic apoptosis demonstrate that mature CL are required for efficient Fas-mediated apoptosis in type II cells.

Further investigation of the impaired apoptotic pathway in tafazzin-deficient cells revealed that the major block was in caspase-8 activation. In this study, mature CL was identified as a crucial component of a mitochondrial platform required for

caspase-8 translocation, oligomerization and activation following Fas signalling in type II cells. Additionally, it is shown here that mature CL provides the physiological association of full-length Bid with the mitochondria. Therefore, by normally presenting Bid on the mitochondria and by providing an activation site for caspase-8 after Fas activation, CL brings both the enzyme and its substrate together and provides a platform from which to initiate the mitochondrial phase of apoptosis. This newly identified activating platform, we termed “mitosome”, is likely to be localized at the contact site between the mitochondrial inner and outer membranes, where CL is exposed to the surface of the mitochondria.

Altogether, these data suggest a model in which the p43/p10 caspase-8 cleaved product relays the apoptotic signal from the plasma membrane to the mitochondria in type II cells (**Figure 6-1**). In response to Fas receptor engagement, a small amount of procaspase-8 is activated at the DISC and produces the p43 products. Then, the p43/p10 caspase-8 translocates and inserts into CL-enriched mitochondrial membrane domains, where it further oligomerizes and subsequently autoprocesses into its fully active form p18/p10. Next, active caspase-8 directly cleaves Bid associated with these CL-enriched mitochondrial domains into tBid, which in turn inserts into the mitochondrial membrane and induces cytochrome *c* release. This work provides strong evidence that in type II cells, caspase-8 is activated in a two steps process, first at the DISC where it generates the p43/p10 form and second on the mitochondria where it acquires its full activity. The reason of such a complex regulation of caspase-8 activation was likely evolved to minimize the chances of accidental activation in healthy cells. However, while caspase-8 has been shown to require mature CL to be activated on the mitochondrial membranes, it is unclear whether this activation is direct, or whether other partners such as FLASH [267] participates in the activation of caspase-8 on mitochondria. It is also possible that Bcl-xL and BAR which have been shown to sequester active caspase-8 on the mitochondrial membranes take part in the “mitosome” [159]. Therefore, it will be interesting and important to perform mass spectrometry analysis of immunoprecipitated mitochondrial caspase-8 complexes to identify other components of this mitochondrial platform.

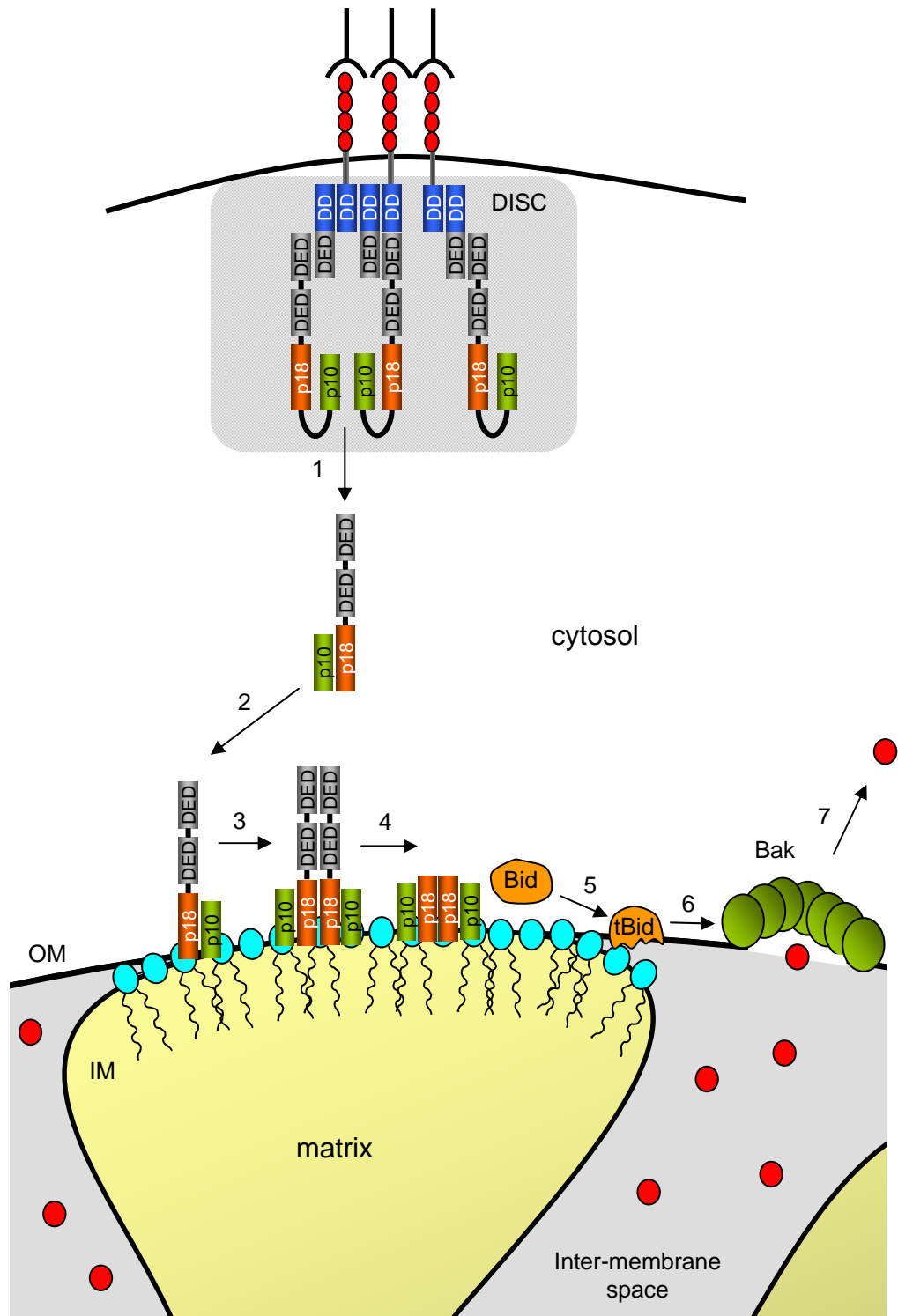


**Figure 6-1: The “mitosome” model in type II cells.**

1. In response to Fas receptor activation, a small amount of procaspase-8 is activated at the DISC and generates the p43/p10 product. 2. The p43/p10 caspase-8 translocates and inserts via its exposed p18 subunit into CL-enriched mitochondrial membrane domains. 3. This results in the clustering and subsequent oligomerization of p43/p10 in the mitochondrial membranes. 4. Mitochondrial caspase-8 oligomerization provides enzymatically competent conformation for the autoprocessing of p43/p10 into the active heterodimer p18/p10. 5. CL also provides the association of Bid with the mitochondria. Thus, Bid is directly available for active caspase-8 on the mitochondrial surface and is cleaved into tBid, which in turn, inserts to the mitochondria and induces Bak oligomerization (6.) and subsequent cytochrome c release (7.).

Decrease of *tafazzin* expression has been previously reported in B-cell lymphoma and breast carcinoma [275, 276]. These findings suggest that tafazzin may represent a new tumour suppressor. To date, BTHS has not been correlated with cancers. However, since BTHS has a high rate of mortality during infancy and early childhood it is possible that improving the life expectancy of BTHS patients would increase their predisposition to cancers. The characteristic symptoms of BTHS include cardiomyopathy, skeletal myopathy, neutropenia and growth retardation [173, 174]. BTHS children usually die early from cardiac failure or septicaemia. No sign of apoptosis resistance has been associated with the BTHS phenotype. Most of the neutropenic disorders have been attributed to an increased of neutrophil apoptosis. However, in the case of BTHS, this deficiency has been ascribed to an alteration in the development of neutrophils [173]. In addition to these four cardinal features, BTHS is often characterized by noncompaction of the left ventricular myocardium due to prominent trabeculations [277]. Interestingly, the same defects in heart development were observed in mice-deficient in caspase-8 [53]. Therefore, it is possible that the developmental abnormalities associated with BTHS have evolved at least partially from the inactivation of caspase-8.

Recently, *caspase-8* has been defined as a metastasis suppressor gene in neuroblastoma cells [278]. Stupack *et al* reported that caspase-8 does not impact on primary tumours growth but prevents the spread of invasive neuroblastoma cells by promoting cell death at tumour margins. In this context, caspase-8 mediated-apoptosis is independent on DR and controls by other cell surface receptors known as integrins, which bind to components of the extracellular matrix. This process, called integrin-mediated death (IMD), occurs when cells are present in an inappropriate extracellular matrix and results in the recruitment and thus activation of caspase-8 by clusters of unligated integrins at the plasma membrane [279]. Thus, loss of caspase-8 in neuroblastoma overcomes IMD and facilitates the survival and invasion of the cells into surrounding tissues. However, the molecular mechanisms that link cell surface adhesion and the intracellular apoptotic machinery are unknown. It will be therefore of considerable interest to investigate whether mitochondria in general and mature CL in particular are required for activating caspase-8 in response to IMD, and whether CL levels are altered during advanced tumour development.

To conclude, the work presented in this thesis provides some new insight into the mechanism by which CL regulates apoptosis with the discovery that mature CL participates in a new mitochondrial-associated platform, called the “mitosome”, required for the activation of caspase-8 in type II cells.

## **APPENDIX I**

# Cardiolipin: Setting the beat of apoptosis

François Gonzalvez · Eyal Gottlieb

Published online: 6 February 2007  
© Springer Science + Business Media, LLC 2007

**Abstract** Cardiolipin (CL) is a mitochondria-specific phospholipid which is known to be intimately linked with the mitochondrial bioenergetic machinery. Accumulating evidence now suggests that this unique lipid also has active roles in several of the mitochondria-dependant steps of apoptosis. CL is closely associated with cytochrome *c* at the outer leaflet of the mitochondrial inner membrane. This interaction makes the process of cytochrome *c* release from mitochondria more complex than previously assumed, requiring more than pore formation in the mitochondrial outer membrane. While CL peroxidation could be crucial for enabling cytochrome *c* dissociation from the mitochondrial inner membrane, cytochrome *c* itself catalyzes CL peroxidation. Moreover, peroxy-CL directly activates the release of cytochrome *c* and other apoptogenic factors from the mitochondria. CL is also directly involved in mitochondrial outer membrane permeabilization by enabling docking and activation of pro-apoptotic Bcl-2 proteins. It appears therefore that CL has multiple roles in apoptosis and that CL metabolism contributes to the complexity of the apoptotic process.

**Keywords** Mitochondria · Apoptosis · Cardiolipin

## Background

It has long been known that mitochondria are the ATP generating powerhouse of the cell and the site of other key metabolic pathways involving fatty acid, amino acid and steroid metabolism. However, in the early 1990s it became

clear that in addition to these critical life-supporting roles, mitochondria play a central part in the execution of apoptotic cell death.

The involvement of mitochondria in apoptosis first came into focus with the discoveries that most pro-apoptotic stimuli induce an early release of mitochondrial proteins, which activates the cellular apoptotic program and disrupts mitochondrial bioenergetics [1, 2]. These mitochondrial proteins, known as apoptogenic factors, include cytochrome *c*, smac/diablo, HtrA2/Omi, AIF and endonuclease G, of which cytochrome *c* has been the most intensively studied. Cytochrome *c* is normally involved in the ATP generation pathway in mitochondria, transferring electrons from the cytochrome bc1 complex (complex III) to cytochrome oxidase (complex IV). But once released into the cytosol, cytochrome *c* induces a cytochrome *c*/dATP/Apaf-1/pro-caspase-9 complex termed the apoptosome [3]. The apoptosome activates caspase-3, resulting in the degradation of many cellular components. Cells deficient in cytochrome *c*, Apaf-1, caspase-9 or caspase-3 have impaired apoptosis in response to intrinsic mitochondria-dependent signals, underpinning the importance of these components [4–7].

In response to apoptotic signals coming from the cytosol, mitochondria-dependent apoptosis requires permeabilization of the mitochondrial outer membrane. Mitochondrial membrane permeabilization is tightly regulated by proteins of the Bcl-2 family and is often considered the point of no return in the apoptotic signalling cascade, leading to several events such as DNA degradation in the nucleus and exposure of phosphatidylserine (PS) on the outer leaflet of the plasma membrane [8, 9].

PS was the first lipid identified to have a role in apoptosis regulation, when it was shown that exposure of PS on the surface of apoptotic lymphocytes forms a recognition site for phagocytosis by macrophages [10]. The sphingolipid

F. Gonzalvez · E. Gottlieb (✉)  
Cancer Research UK, The Beatson Institute for Cancer Research,  
Glasgow, G61 1BD, United Kingdom  
e-mail: e.gottlieb@beatson.gla.ac.uk

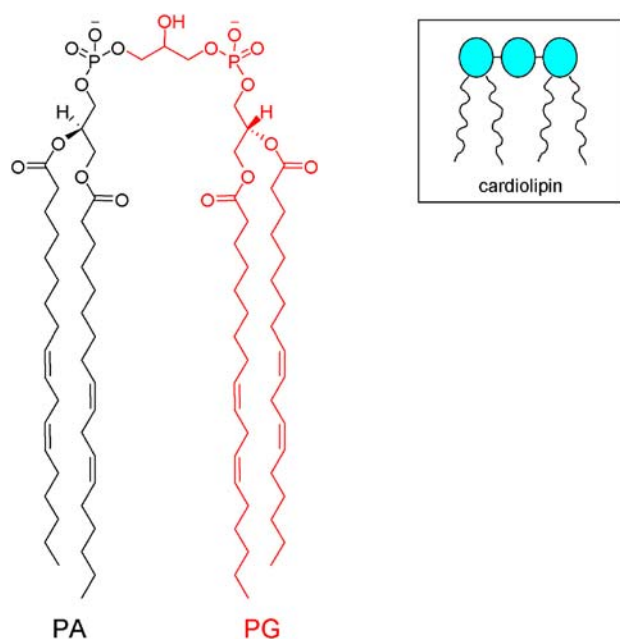


**Fig. 1** Molecular (left) and schematic (inset) structure of cardiolipin. Cardiolipin is a dimer of phosphatidylglycerol (PG) and phosphatidic acid (PA). It comprises four acyl chains, two phosphate groups and three glycerols (schematically represented by blue circles). Under physiological pH one of the phosphate groups is de-protonated, making cardiolipin a negatively-charged phospholipid

ceramide has attracted much attention in recent years. Cellular ceramide levels increase in response to a wide variety of apoptotic stimuli (e.g.  $\text{TNF}\alpha$ , Fas ligand,  $\text{IFN}\gamma$ , staurosporine and etoposide) preceding the mitochondrial steps of apoptosis [11]. Although the mechanism of ceramide-mediated apoptosis is still a matter of debate, a growing body of evidence supports a direct effect of ceramide on mitochondria resulting in alterations in bioenergetics, generation of reactive oxygen species and permeabilization of the mitochondrial outer membrane [11].

Another class of lipids termed cardiolipin (CL) has attracted new interest in the field of cell death. CL is a glycerol-based phospholipid (Fig. 1) most of which is found in the mitochondrial inner membrane. Several independent studies suggest that CL has either survival- or death-supporting roles in cells. This review summarizes recent data and discusses the complex and controversial role of CL in apoptosis.

## Cardiolipin physiology

### Cardiolipin synthesis

The name “cardiolipin” alludes to the fact that it was first isolated from bovine heart. CL or diphosphatidylglycerol, whose dimeric structure distinguishes it from other glycerophospholipids, has the glycerol-phosphate and two acyl groups of each monomer bound together through a single

glycerol head. This results in four acyl chains, three glycerols and two phosphate groups per molecule (Fig. 1). CL is detected exclusively in bioenergetic membranes such as those of bacteria and mitochondria, thus providing more evidence for the endosymbiotic origin of mitochondria. The biosynthetic pathway of CL in mammals has been well described [12, 13]. Briefly, CL is synthesized *de novo* in a four step pathway catalyzed by four mitochondrial enzymes, yielding a CL archetype. The first three steps correspond to the phosphatidylglycerol (PG) pathway and pass through the generation of the common intermediates, phosphatidic acid (PA), cytidine-5'-diphosphate-diacylglycerol (CDP-DG) and phosphatidylcytidine-monophosphate (CMP). The final step is unique to CL synthesis and is catalyzed by CL synthase. In this reaction, a molecule of PG condenses with a molecule of the intermediate CDP-DG to yield diphosphatidylglycerol or CL. The human CL synthase gene has recently been identified by its ability to restore a CL profile to the CL synthase deficient yeast mutant *crd1*  $\Delta$  [14]. Considering the variety of fatty acids, the number of potential combinations of the acyl chains is high, and indeed, the pattern of CL molecular species varies between organisms and even between tissues. Eukaryotic CL has a characteristic acyl chain pattern which is restricted to 18 carbons [15]. In human heart the predominant  $\text{C}_{18}$  fatty acid is linoleic acid ( $\text{C}_{18:2}$ ) so heart CL contains mostly  $\text{C}_{18:2}$  acyl chains. However human lymphoblast CL contains predominantly oleyl chains ( $\text{C}_{18:1}$ ) [16]. The significance of this specificity is still not understood. Interestingly, the enzymes involved in the pathway of CL synthesis exhibit no selectivity for a specific acyl chain length [17]. Therefore, once synthesized in mitochondria, a maturation step replacing the original acyl chains with specific  $\text{C}_{18}$  unsaturated ones is required.

The generation of mature CL requires a cycle of two reactions: the hydrolysis of one original acyl chain to generate a monolyso-CL (MLCL), now containing only three acyl groups, followed by the reacylation of MLCL with a specific  $\text{C}_{18}$  acyl chain. Phospholipase A2 catalyzes the first step of acyl chain removal [18]. However, the enzyme catalyzing MLCL-acyltransferase activity has not been identified [18, 19].

Barth syndrome (OMIM # 302060) is the only human genetic disorder discovered where alterations of CL metabolism are a primary cause of disease [20, 21]. This X-linked genetic disorder is due to mutations in the *tafazzin* gene (*TAZ*) located on region Xq28 [22]. Analyses of the CL profile of different tissues obtained from Barth syndrome patients revealed a decrease in CL and an increase in MLCL and sequence alignments of *TAZ* showed homology with the glycerolipid acyltransferase family [23–25]. While these data suggest *TAZ* encodes the mitochondrial MLCL acyltransferase, the biochemical function of Tafazzin has not been fully characterized.

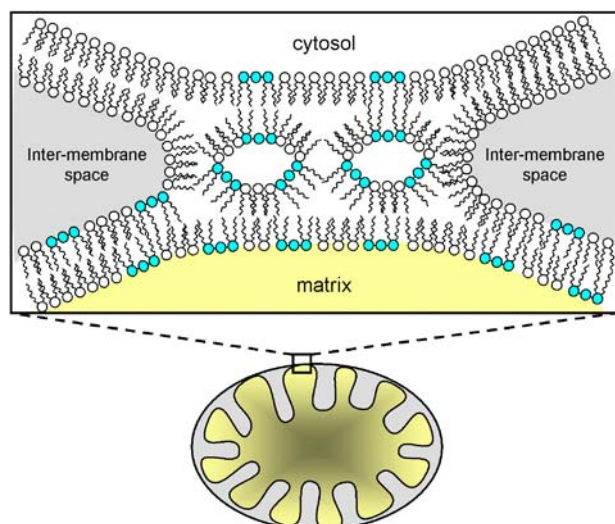


**Fig. 2** The non-bilayer hexagonal structure of lipids was characterised *in vitro* and proposed to contribute to the structure of contact sites between the inner and outer membranes of mitochondria. Negatively-charged phospholipids (such as cardiolipin) are more likely to adopt this structure which may fuse the mitochondrial membranes at the contact sites and redistribute cardiolipin on the cytosolic face of the mitochondria

#### Cardiolipin localization in mitochondria

CL is specific to mitochondrial membranes but its precise location within the different compartments of the organelle is still the subject of controversy. For many years CL was assumed to be associated exclusively with the mitochondrial inner membrane where, as measured in bovine heart mitochondria, it represents ~25% of the total phospholipids [26]. More recently CL has also been identified in the mitochondrial outer membrane (~4%) and especially at the contact sites connecting the outer membrane with the inner one [27–29]. Through the contact sites, CL may reach the mitochondrial outer membrane and the cytosolic face of the mitochondria. This notion is supported by the fact that the two major phospholipids present in contact sites, phosphatidylethanolamine (PE) and CL (~25% each) have the ability to adopt a non-bilayer hexagonal  $H_{II}$  phase *in vitro* (Fig. 2) [30]. Such structures can contribute to the fusion of two membranes [31].

#### The role of cardiolipin in bioenergetics

The exclusive presence of CL in bioenergetic membranes suggests that it interacts with the electron transport chain complexes involved in oxidative phosphorylation. Indeed, CL is required for optimal activity of complex I (NADH:ubiquinone oxidoreductase), complex III (ubiquinone:cytochrome *c* oxidoreductase), complex IV (cytochrome *c* oxidase) and complex V (ATP synthase), four large complexes integrated in the inner mitochondrial

membrane [32, 33]. Further, complexes III, IV and V were shown to contain CL in their quaternary structure [32, 34, 35] and CL was observed within the 3D crystal structure of *Escherichia Coli* succinate dehydrogenase, an ortholog of the mitochondrial respiratory complex II (succinate:ubiquinone oxidoreductase) [36]. CL is also required by mitochondrial substrate carriers, including the adenine nucleotide translocator (ANT), acylcarnitine translocase and phosphate carrier [37–40]. It was reasonable to predict therefore that a deficiency in CL would result in alterations in cell respiration. A Chinese hamster ovary (CHO) cell line containing a temperature-sensitive (*ts*) mutant of PG synthase (CHO-PGS-S) has provided the first indication of the potential involvement of CL in cellular bioenergetics [41]. At the non-permissive temperature (40°C) these cells exhibit a decrease in oxygen consumption and ATP production, accompanied by a compensatory increase in glycolysis [42]. However, since these cells have reduced levels of both PG and CL at 40°C, it is not possible to attribute these bioenergetic defects to CL alone. Other studies using the CL synthase deficient yeast mutant *crd1*Δ, have provided more direct evidence for the requirement of CL for mitochondrial bioenergetics. Somewhat surprisingly, the *crd1*Δ mutant could grow, though not as efficiently as wild type yeast, on non-fermentable carbon sources, indicating that CL is not essential for oxidative phosphorylation [43]. However, several bioenergetic defects, associated with a reduction of ANT activity, reduced mitochondrial membrane potential and an overall decrease in oxidative phosphorylation, were observed in the *crd1*Δ mutant when grown under stress conditions [44–46]. Thus, CL appears to be required for sustained mitochondrial inner membrane integrity and function.

Cytochrome *c* is an essential hemoprotein which functions as a mobile electron carrier between complex III and complex IV. Only 15% of cytochrome *c* is free in the inter-membrane space [47, 48] while most of it is attached to the mitochondrial inner membrane via specific interactions with CL [49, 50]. Two types of interactions, hydrophobic and electrostatic, have been linked to two distinct CL binding sites on cytochrome *c*. Initially, these interactions were thought to play a role in the electron-shuttling activity of cytochrome *c* by keeping the molecule in the proximity of the respiratory chain [50]. More recently, CL-cytochrome *c* interactions were suggested to participate in the regulation of apoptosis (see below).

#### Cardiolipin maintains the structure of the mitochondrial inner membrane

The mitochondria of CHO-PGS-S cells appear swollen and have disorganized cristae [42, 51]. However, as mentioned above, these alterations cannot be solely attributed to CL since these cells lack both CL and PG. A more recent study

of HeLa cells in which the expression of CL synthase was decreased by RNA interference (RNAi) indicated that CL is directly required for maintenance of mitochondrial structure [52]. This report, however, contrasts with the phenotype of the *crd1*  $\Delta$  yeast mutants, which lack CL but maintain normal mitochondrial morphology [53]. The differences between CL synthase-deficient mammalian cells and yeast may be due the ability of PG to supplant the membrane-preserving function of CL in yeast.

### Cardiolipin in relation to apoptosis

#### Cardiolipin levels and oxidative stress

Loss of CL is associated with diverse pathophysiological conditions such as ageing and ischemia/reperfusion processes [54, 55]. For example, the loss of CL during ischemia/reperfusion is followed by a decrease in oxidative phosphorylation which may contribute to myocyte death in the peri-infarct regions of the ischemic myocardium. The decline in mitochondrial respiratory functions the accumulation of reactive oxygen species (ROS). Under normal physiological conditions mitochondrial CL may protect cells from oxidative stress in part through the deacylation-reacylation cycle discussed above. However, CL is also a vulnerable target of ROS due to its unsaturated acyl chains and its close proximity to ROS generation sites. ROS cause the peroxidation of CL and a parallel decrease in the activities of complexes I and IV [56, 57]. Currently this seems to be very much a “chicken and egg” issue, and it is unclear whether ROS trigger the loss of CL or whether loss of CL triggers ROS generation. It is clear, however, that during many cell death processes ROS and loss of CL are closely linked in a cycle of CL peroxidation. Peroxidation of CL also occurs following a variety of apoptotic stimuli such as nitric oxide, Fas receptor stimulation, NGF deprivation, staurosporine and actinomycin D [58–60]. Interestingly, apoptosis via a pathway involving a decrease in CL synthesis was seen in neonatal rat cardiac myocytes and in breast cancer cells treated with saturated fatty acids, particularly palmitate [61, 62].

#### Cardiolipin—Cytochrome *c* interactions regulate cytochrome *c* release

As mentioned above, the majority of cytochrome *c* is bound to the outer leaflet of the mitochondrial inner membrane. Cytochrome *c* has a net charge of +8 at physiological pH allowing it to bind membranes primarily through electrostatic interactions with the head groups of anionic phospholipids such CL [49, 50]. Cytochrome *c* has a hydrophobic cavity which may account for hydrophobic interactions with the

fatty acyl chains of CL [63]. Two CL binding sites on cytochrome *c* have been proposed; the A-site which facilitates electrostatic interactions with the negative charges of CL and the C-site which is involved in hydrophobic interactions with the fatty acyl chain of CL [50]. These sites are responsible for two different conformations of cytochrome *c* in the inter-membrane space: a loosely bound conformation involving site A and a tightly bound conformation at site C that partially embeds the protein in the membrane [64]. Loosely bound cytochrome *c* participates in the transfer of electrons from complex III to complex IV, as well as in ROS scavenging [65, 66]. Tightly bound cytochrome *c* was proposed to possess peroxidase activity that utilizes hydrogen peroxide generated in the mitochondria to peroxidate CL (see below) [58].

For both types of CL binding it was proposed that cytochrome *c* release from mitochondria would first require the dissociation of its interactions with CL (Fig. 3) [67, 68]. This is consistent with recent findings showing that in CL-deficient cells, a greater fraction of cytochrome *c* is free or loosely bound [52]. The fact that, *in vitro*, cytochrome *c* has a lower affinity for peroxidized CL than CL, suggests that CL peroxidation may enable cytochrome *c* detachment from the inner membrane (Fig. 3). Complete release of cytochrome *c* into the inter-membrane space requires dissociation of both the hydrophobic and the electrostatic interactions between cytochrome *c* and CL [69]. The final release of cytochrome *c* from mitochondria requires additional steps in the process, consisting of the permeabilization of the outer membrane. Cristae remodelling was also shown to be required for cytochrome *c* re-distribution within the mitochondrial inter-membrane space before its release [70] but whether the dissociation of CL–cytochrome *c* interactions is related to this process awaits further studies. Still, the studies described above strongly indicate that CL and cytochrome *c* are physically associated and for some functions at least they are also interdependent.

#### Cardiolipin: Docking site for tBid

Bid is a pro-apoptotic protein of the diverse Bcl-2 family, possessing sequence homology only within the conserved Bcl-2 Homology 3 (BH3) domain [71]. Bid has attracted increasing interest since it was identified to be a substrate of caspase-8 in response to activation of death receptors such as Fas. During apoptosis, N-terminal cleavage of Bid by caspase-8 produces p15 tBid, the active form which rapidly targets mitochondria and triggers cytochrome *c* release [72, 73]. One important target of tBid on the mitochondrial outer membrane is Bax, a multi-BH domain pro-apoptotic Bcl-2 protein which interacts with the BH3 domain of tBid [74]. In fact, tBid binding to the first  $\alpha$  helix of Bax was shown to be crucial for the pro-apoptotic activity of tBid [74].

**Fig. 3** Cytochrome *c* (red) is attached to cardiolipin on the outer surface of the mitochondrial inner membrane and therefore, permeabilization of the mitochondrial outer membrane is not sufficient for cytochrome *c* release. The dissociation of cytochrome *c* from cardiolipin is a required step prior to outer membrane permeabilization and is triggered by cardiolipin peroxidation. Recently it was shown that cardiolipin peroxidation is catalyzed by the bound cytochrome *c* itself [58]

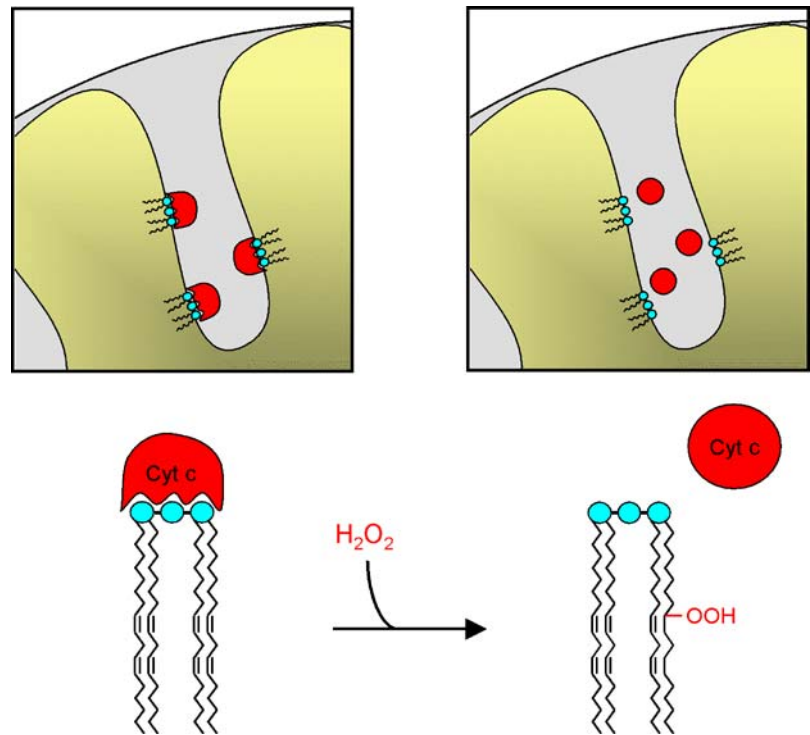
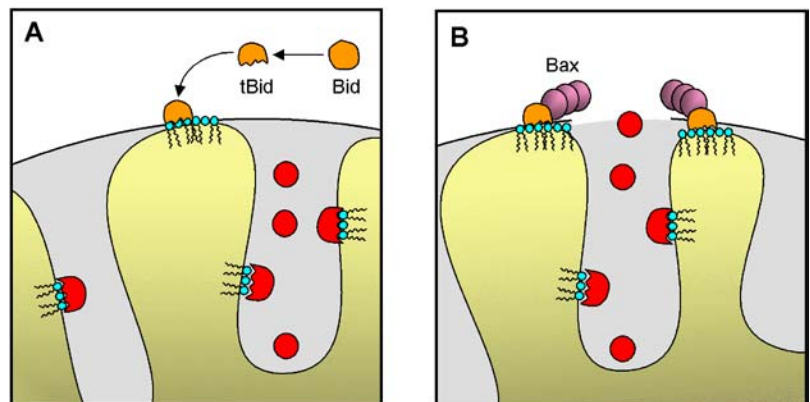


**Fig. 4** Cardiolipin executes apoptosis-supporting roles at the mitochondrial outer membrane. (A) Cardiolipin serves as a docking platform for the pro-apoptotic Bcl-2 protein tBid, particularly at contact sites of the inner and outer membranes. (B) Cardiolipin assists the perforation of the mitochondrial outer membrane by tBid and Bax. The mechanism is still elusive



The first apoptosis-promoting role of CL emerged from biochemical studies of tBid interactions with mitochondrial lipids using liposomes and the CHO-PGS-S cell line [75]. Wang and co-workers showed that the pro-apoptotic protein tBid interacts exclusively with liposomes that contain at least physiological levels of CL and demonstrated that tBid co-localization with CHO-PGS-S mitochondria is CL-dependent. The CL-binding domain of tBid was mapped to helices 4–6 of the Bid protein [75]. Interestingly, helix 6 was later shown to be a part of a hairpin structure which is important for the lipid binding properties of tBid [76]. Subsequently, electron tomogram studies showed that tBid interacts with mitochondria specifically at the inner and outer membrane contact sites, which are rich in CL (Fig. 4(A))

[77]. As discussed above, CL-rich membranes may adopt a non-bilayer hexagonal  $H_{II}$  configuration at the contact sites (Fig. 2), enabling access of CL to the cytosolic surface of mitochondria [27]. The model of CL as a mitochondrial “docking” site for tBid is supported by several studies. For example, *in vitro* assays using artificial membranes or isolated mitochondria showed that recombinant tBid can bind CL and MLCL [78–83]. Adding tBid to isolated mitochondria immediately inhibits ADP-stimulated respiration and oxidative phosphorylation, as a result of ANT inactivation [84, 85]. The function of tBid may be either BH3-domain-dependent or independent. The former induces oligomerization of the multi-BH domain pro-apoptotic Bcl-2 proteins Bax and Bak on the mitochondrial outer membrane,

while a BH3-independent interaction of tBid with CL [82] could be responsible for cristae remodelling, [80] and for inhibition of oxidative phosphorylation [85]. Cristae remodelling and perturbations of mitochondrial bioenergetics take place simultaneously and are both independent of Bak. It is possible therefore that tBid acts by two sequential mechanisms: the first is BH3 domain independent, which involves CL, leading to structural and functional impairment, and the second is BH3 domain dependent, employing interactions with other pro-apoptotic Bcl-2 proteins, namely Bak and Bax, leading to mitochondrial outer membrane permeabilization. Thus, the interaction of tBid with CL may prime mitochondria for the action of Bax and Bak.

#### Cardiolipin redistribution

Another feature of CL observed under apoptotic conditions is its redistribution within and between membranes. The exposure of CL on the outer leaflet of the mitochondrial inner membrane was observed after death receptor stimulation before mitochondria depolarization and PS exposure on the plasma membrane, and at the same time as ROS generation [86]. Peroxidation of CL may account for their redistribution by altering their molecular organization and favouring formation of a non-bilayer hexagonal structure [87]. This could increase exposure of CL on the contact sites of mitochondrial membranes and provide access for tBid. It is also suggested that Bid, which exhibits lipid transfer activity *in vitro*, relocates CL and MLCL to the plasma membrane of cells undergoing apoptosis [88, 89]. The mechanism and the significance of this relocation are still unclear. In addition, tBid may reorganize CL into micro-domains as was demonstrated in artificial lipid monolayers containing physiological amount of CL [85]. Considering the possible role of CL in maintaining mitochondrial structure, changes in CL organization may result in structural changes of the mitochondrial inner membrane which in turn may affect the activity of membrane-embedded proteins such as ANT. Therefore, it is conceivable that tBid affects the structure and function of mitochondria by binding to and redistributing mitochondrial CL within the mitochondrial inner membrane and/or within other cellular compartments.

#### Cardiolipin and permeabilization of the mitochondrial outer membrane

CL was also proposed to be required for the action of other pro-apoptotic Bcl-2 proteins [90]. To study individual functions of Bcl-2-family proteins Newmeyer and co-workers took an *in vitro* approach using liposomes and outer mitochondrial membrane vesicles. Their work has provided evidence that permeabilization of liposomes to dextran required both the presence of activated Bax and physiological levels

of CL. Therefore, it was suggested that Bax may permeabilize the mitochondrial outer membrane by altering the local organization of CL without overall damage to the membrane itself (Fig. 4(B)). In contrast to this report, other studies using either the CL synthase deficient yeast *crd1*  $\Delta$ , or mitochondria from CL synthase knocked-down cells have shown that Bax does not require CL for the induction of cytochrome *c* release [52, 84, 91]. However, as discussed above, it is possible that in yeast, PG, which accumulates in the absence of CL synthase, compensates for the loss of CL. It still awaits clarification whether CL or its PG precursor are needed, for Bax to release cytochrome *c* [92]. This is particularly interesting since hydrophobic and electrostatic interactions make a different contribution to the binding of cytochrome *c* to CL or PG [93].

#### Cardiolipin-cytochrome *c* peroxidase activity

CL peroxidation appears to be an early event preceding the release of cytochrome *c* and caspase activation. The mechanism of CL peroxidation and its involvement in apoptosis has gained more attention recently [58, 94]. Kagan and colleagues showed that cytochrome *c* can interact with CL that contains two or more unsaturated acyl groups ( $C_{18:2}$  mostly) to form a hydrogen peroxide peroxidase capable of oxidizing CL to peroxi-CL (Fig. 3). Using cytochrome *c*<sup>-/-</sup> mouse embryonic cells they provided the first evidence that cytochrome *c* is required for the peroxidation of CL. CL-cytochrome *c* complex acts as a potent CL-specific oxygenase required for the release of pro-apoptotic factors such as cytochrome *c* and smac/diablo. It is noteworthy that oxidized CL does not merely allow cytochrome *c* to detach from the mitochondrial inner membrane but rather has an active role in inducing apoptosis: when added to isolated mitochondria, oxidized CL alone induces cytochrome *c* and smac/diablo release [58]. Importantly, the peroxidase activity of the CL-cytochrome *c* complex depends on unsaturated acyl chains on CL. Indeed, incubation of HL60 cells with the poly-unsaturated fatty acid docosahexaenoic acid ( $C_{22:6}$ ), enriches CL with  $C_{22:6}$  acyl chains, sensitizing the cells to staurosporine-induced apoptosis [58]. This promoted the notion that enriching CL with saturated acyl chains may protect from apoptosis. But although *in vitro*, saturated CL cannot stimulate CL-cytochrome *c* peroxidase activity [58], CL synthase in a cellular context does not incorporate saturated PG to form fully saturated CL [62]. Nevertheless, the results, together with the suggestion that oxidized CL may have a promoting effect on the pro-apoptotic activity of Bcl-2 proteins, point to the importance of CL acyl chain composition and suggest that manipulation of CL oxidation may present a good target for sensitising cells to apoptosis. This also raises the question whether Bcl-2 proteins can regulate CL-cytochrome *c* peroxidase activity.

## Conclusions and perspectives

Since their characterization in 1942 research has yielded increasing knowledge of the structure, localization and biosynthetic pathway of CL. Due to its specific location in the mitochondrial membranes, CL has long been viewed through its interactions with mitochondrial proteins: because it is required for the optimal activity of most of the respiratory chain complexes and of several mitochondrial substrate carriers, CL is crucial for efficient oxidative phosphorylation and for correct function and structure of the mitochondrial inner membrane.

In addition to its role in maintaining mitochondrial integrity, it is now clear that CL participates in the mitochondrial apoptotic pathway. CL is turning out to be involved in many of the mitochondrial-dependent steps that lead to the release of apoptogenic factors. These steps include interactions with Bcl-2 proteins, cytochrome *c* association with and dissociation from the mitochondrial inner membrane, alteration of the structure of the mitochondrial inner membrane and permeabilization of the outer one. Moreover, this review emphasized that CL undergoes both reorganisation and modification within the mitochondrial membranes. Degradation of CL into MLCL and transition of CL to the mitochondrial outer membrane (and potentially to the plasma membrane) appear to be early events in apoptosis. Peroxidation of the acyl chains of CL also plays a crucial role in its apoptotic functions. In fact, this event is catalyzed by cytochrome *c* and is required for the release of cytochrome *c* itself, and of other apoptogenic factors, from mitochondria.

By way of analogy with sphingomyelin in the plasma membrane, it is conceivable that CL participates in the formation of signalling platforms in the mitochondrial membranes. The arrival of an apoptotic stimulus at the mitochondrial surface may result in the redistribution of CL into microdomains and in further amplification of the apoptotic signal. This reorganization of CL could lead to the remodelling of the mitochondrial cristae and to the loss of mitochondrial functions observed during apoptosis. However, the presence of CL domains in mitochondria, their structure and the effect of peroxidation on their organization are not well understood.

This review also highlighted the importance of CL acyl chain composition. CL strictly contains unsaturated fatty acyl chains, which are readily oxidizable targets. Manipulating the degree of saturation of the CL acyl chains may represent a new means of controlling the cell's fate. New strategies designed to pharmacologically manipulate the oxidation sensitivity of CL may help control cell death and open new prospects for the treatment of pathologies with diminished or excessive apoptosis. The recent surge of research into CL will hopefully provide better understanding both of acyl chain remodelling and of the role of CL in apoptosis in the near future.

## References

- Danial NN, Korsmeyer SJ (2004) Cell death: critical control points. *Cell* 116:205–219
- Newmeyer DD, Ferguson-Miller S (2003) Mitochondria: releasing power for life and unleashing the machineries of death. *Cell* 112:481–490
- Wang X (2001) The expanding role of mitochondria in apoptosis. *Genes Dev* 15:2922–2933
- Kuida K, Haydar TF, Kuan CK et al (1998) Reduced apoptosis and cytochrome *c*-mediated caspase activation in mice lacking caspase 9. *Cell* 94:325–337
- Kuida K, Zheng TS, Na S et al (1996) Decreased apoptosis in the brain and premature lethality in CPP32-deficient mice. *Nature* 384:368–372
- Li K, Li Y, Shelton JM et al (2000) Cytochrome *c* deficiency causes embryonic lethality and attenuates stress-induced apoptosis. *Cell* 101:389–399
- Yoshida H, Kong YY, Yoshida R et al (1998) Apaf1 is required for mitochondrial pathways of apoptosis and brain development. *Cell* 94:739–750
- Garrido C, Galluzzi L, Brunet M et al (2006) Mechanisms of cytochrome *c* release from mitochondria. *Cell Death Differ* 13:1423–1433
- van Loo G, Saelens X, van Gurp M et al (2002) The role of mitochondrial factors in apoptosis: a Russian roulette with more than one bullet. *Cell Death Differ* 9:1031–1042
- Fadok VA, Voelker DR, Campbell PA et al (1992) Exposure of phosphatidylserine on the surface of apoptotic lymphocytes triggers specific recognition and removal by macrophages. *J Immunol* 148:2207–2216
- Siskind LJ (2005) Mitochondrial ceramide and the induction of apoptosis. *J Bioenerg Biomembr* 37:143–153
- Hauff KD, Hatch GM (2006) Cardiolipin metabolism and Barth Syndrome. *Prog Lipid Res* 45:91–101
- Schlame M, Rua D, Greenberg ML (2000) The biosynthesis and functional role of cardiolipin. *Prog Lipid Res* 39:257–288
- Houtkooper RH, Akbari H, van Lenthe H et al (2006) Identification and characterization of human cardiolipin synthase. *FEBS Lett* 580:3059–3064
- Hoch FL (1992) Cardiolipins and biomembrane function. *Biochim Biophys Acta* 1113:71–133
- Schlame M, Ren M, Xu Y, Greenberg ML, Haller I (2005) Molecular symmetry in mitochondrial cardiolipins. *Chem Phys Lipids* 138:38–49
- Rustow B, Schlame M, Rabe H, Reichmann G, Kunze D (1989) Species pattern of phosphatidic acid, diacylglycerol, CDP-diacylglycerol and phosphatidylglycerol synthesized de novo in rat liver mitochondria. *Biochim Biophys Acta* 1002:261–263
- Schlame M, Rustow B (1990) Lysocardiolipin formation and reacylation in isolated rat liver mitochondria. *Biochem J* 272:589–595
- Xu Y, Kelley RI, Blanck TJ, Schlame M (2003) Remodeling of cardiolipin by phospholipid transacylation. *J Biol Chem* 278:51380–51385
- Barth PG, Scholte HR, Berden JA et al (1983) An X-linked mitochondrial disease affecting cardiac muscle, skeletal muscle and neutrophil leucocytes. *J Neurol Sci* 62:327–355
- Kelley RI, Cheatham JP, Clark BJ et al (1991) X-linked dilated cardiomyopathy with neutropenia, growth retardation, and 3-methylglutaconic aciduria. *J Pediatr* 119:738–747
- Bione S, D'Adamo P, Maestrini E et al (1996) A novel X-linked gene, G4.5, is responsible for Barth syndrome. *Nat Genet* 12:385–389
- Neuwald AF (1997) Barth syndrome may be due to an acyltransferase deficiency. *Curr Biol* 7:R465–R466

24. Schlame M, Kelley RI, Feigenbaum A et al (2003) Phospholipid abnormalities in children with Barth syndrome. *J Am Coll Cardiol* 42:1994–1999
25. Valianpour F, Mitsakos V, Schlemmer D et al (2005) Monolysocardiolipins accumulate in Barth syndrome but do not lead to enhanced apoptosis. *J Lipid Res* 46:1182–1195
26. Krebs JJ, Hauser H, Carafoli E (1979) Asymmetric distribution of phospholipids in the inner membrane of beef heart mitochondria. *J Biol Chem* 254:5308–5316
27. Ardail D, Privat JP, Egret-Charlier M et al (1990) Mitochondrial contact sites. Lipid composition and dynamics. *J Biol Chem* 265:18797–18802
28. de Kroon AI, Dolis D, Mayer A, Lill R, de Kruijff B (1997) Phospholipid composition of highly purified mitochondrial outer membranes of rat liver and *Neurospora crassa*. Is cardiolipin present in the mitochondrial outer membrane? *Biochim Biophys Acta* 1325:108–116
29. Hovius R, Lambrechts H, Nicolay K, de Kruijff B (1990) Improved methods to isolate and subfractionate rat liver mitochondria. Lipid composition of the inner and outer membrane. *Biochim Biophys Acta* 1021:217–226
30. Cullis PR, Verkleij AJ, Ververgaert PH (1978) Polymorphic phase behaviour of cardiolipin as detected by <sup>31</sup>P NMR and freeze-fracture techniques. Effects of calcium, dibucaine and chlorpromazine. *Biochim Biophys Acta* 513:11–20
31. Van Venetie R, Verkleij AJ (1982) Possible role of non-bilayer lipids in the structure of mitochondria. A freeze-fracture electron microscopy study. *Biochim Biophys Acta* 692:397–405
32. Eble KS, Coleman WB, Hantgan RR, Cunningham CC (1990) Tightly associated cardiolipin in the bovine heart mitochondrial ATP synthase as analyzed by <sup>31</sup>P nuclear magnetic resonance spectroscopy. *J Biol Chem* 265:19434–19440
33. Fry M, Green DE (1981) Cardiolipin requirement for electron transfer in complex I and III of the mitochondrial respiratory chain. *J Biol Chem* 256:1874–1880
34. Sedlak E, Panda M, Dale MP, Weintraub ST, Robinson NC (2006) Photolabeling of cardiolipin binding subunits within bovine heart cytochrome *c* oxidase. *Biochemistry* 45:746–754
35. Yue WH, Zou YP, Yu L, Yu CA (1991) Crystallization of mitochondrial ubiquinol-cytochrome *c* reductase. *Biochemistry* 30:2303–2306
36. Yankovskaya V, Horsefield R, Tornroth S et al (2003) Architecture of succinate dehydrogenase and reactive oxygen species generation. *Science* 299:700–704
37. Bisaccia F, Palmieri F (1984) Specific elution from hydroxylapatite of the mitochondrial phosphate carrier by cardiolipin. *Biochim Biophys Acta* 766:386–394
38. Hoffmann B, Stockl A, Schlame M, Beyer K, Klingenberg M (1994) The reconstituted ADP/ATP carrier activity has an absolute requirement for cardiolipin as shown in cysteine mutants. *J Biol Chem* 269:1940–1944
39. Nalecz KA, Bolli R, Wojtczak L, Azzi A (1986) The monocarboxylate carrier from bovine heart mitochondria: partial purification and its substrate-transporting properties in a reconstituted system. *Biochim Biophys Acta* 851:29–37
40. Noel H, Pande SV (1986) An essential requirement of cardiolipin for mitochondrial carnitine acylcarnitine translocase activity. Lipid requirement of carnitine acylcarnitine translocase. *Eur J Biochem* 155:99–102
41. Ohtsuka T, Nishijima M, Akamatsu Y (1993) A somatic cell mutant defective in phosphatidylglycerophosphate synthase, with impaired phosphatidylglycerol and cardiolipin biosynthesis. *J Biol Chem* 268:22908–22913
42. Ohtsuka T, Nishijima M, Suzuki K, Akamatsu Y (1993) Mitochondrial dysfunction of a cultured Chinese hamster ovary cell mutant deficient in cardiolipin. *J Biol Chem* 268:22914–22919
43. Jiang F, Rizavi HS, Greenberg ML (1997) Cardiolipin is not essential for the growth of *Saccharomyces cerevisiae* on fermentable or non-fermentable carbon sources. *Mol Microbiol* 26:481–491
44. Jiang F, Ryan MT, Schlame M et al (2000) Absence of cardiolipin in the *crd1* null mutant results in decreased mitochondrial membrane potential and reduced mitochondrial function. *J Biol Chem* 275:22387–22394
45. Koshkin V, Greenberg ML (2000) Oxidative phosphorylation in cardiolipin-lacking yeast mitochondria. *Biochem J* 347(Pt 3):687–691
46. Koshkin V, Greenberg ML (2002) Cardiolipin prevents rate-dependent uncoupling and provides osmotic stability in yeast mitochondria. *Biochem J* 364:317–322
47. Bernardi P, Azzone GF (1981) Cytochrome *c* as an electron shuttle between the outer and inner mitochondrial membranes. *J Biol Chem* 256:7187–7192
48. Scorrano L, Ashiya M, Buttle K et al (2002) A distinct pathway remodels mitochondrial cristae and mobilizes cytochrome *c* during apoptosis. *Dev Cell* 2:55–67
49. Nicholls P (1974) Cytochrome *c* binding to enzymes and membranes. *Biochim Biophys Acta* 346:261–310
50. Rytomaa M, Mustonen P, Kinnunen PK (1992) Reversible, nonionic, and pH-dependent association of cytochrome *c* with cardiolipin-phosphatidylcholine liposomes. *J Biol Chem* 267:22243–22248
51. Kawasaki K, Kuge O, Chang SC et al (1999) Isolation of a chinese hamster ovary (CHO) cDNA encoding phosphatidylglycerophosphate (PGP) synthase, expression of which corrects the mitochondrial abnormalities of a PGP synthase-defective mutant of CHO-K1 cells. *J Biol Chem* 274:1828–1834
52. Choi SY, Gonzalez F, Jenkins GM et al (2006) Cardiolipin deficiency releases cytochrome *c* from the inner mitochondrial membrane and accelerates stimuli-elicited apoptosis. *Cell Death Differ* advance online publication, doi:10.1038/sj.cdd.4402020
53. Chang SC, Heacock PN, Mileyskova E, Voelker DR, Dowhan W (1998) Isolation and characterization of the gene (*CLS1*) encoding cardiolipin synthase in *Saccharomyces cerevisiae*. *J Biol Chem* 273:14933–14941
54. Paradies G, Petrosillo G, Pistolese M et al (1999) Lipid peroxidation and alterations to oxidative metabolism in mitochondria isolated from rat heart subjected to ischemia and reperfusion. *Free Radic Biol Med* 27:42–50
55. Paradies G, Ruggiero FM, Petrosillo G, Quagliariello E (1997) Age-dependent decline in the cytochrome *c* oxidase activity in rat heart mitochondria: role of cardiolipin. *FEBS Lett* 406:136–138
56. Paradies G, Petrosillo G, Pistolese M, Ruggiero FM (2000) The effect of reactive oxygen species generated from the mitochondrial electron transport chain on the cytochrome *c* oxidase activity and on the cardiolipin content in bovine heart submitochondrial particles. *FEBS Lett* 466:323–326
57. Paradies G, Petrosillo G, Pistolese M, Ruggiero FM (2002) Reactive oxygen species affect mitochondrial electron transport complex I activity through oxidative cardiolipin damage. *Gene* 286:135–141
58. Kagan VE, Tyurin VA, Jiang J et al (2005) Cytochrome *c* acts as a cardiolipin oxygenase required for release of proapoptotic factors. *Nat Chem Biol* 1:223–232
59. Kirkland RA, Adibhatla RM, Hatcher JF, Franklin JL (2002) Loss of cardiolipin and mitochondria during programmed neuronal death: evidence of a role for lipid peroxidation and autophagy. *Neuroscience* 115:587–602
60. Ushmorov A, Ratter F, Lehmann V et al (1999) Nitric-oxide-induced apoptosis in human leukemic lines requires mitochondrial lipid degradation and cytochrome *c* release. *Blood* 93:2342–2352

61. Hardy S, El-Assaad W, Przybytkowski E et al (2003) Saturated fatty acid-induced apoptosis in MDA-MB-231 breast cancer cells. A role for cardiolipin. *J Biol Chem* 278:31861–31870
62. Ostrand DB, Sparagna GC, Amoscato AA, McMillin JB, Dowhan W (2001) Decreased cardiolipin synthesis corresponds with cytochrome *c* release in palmitate-induced cardiomyocyte apoptosis. *J Biol Chem* 276:38061–38067
63. Rytomaa M, Kinnunen PK (1995) Reversibility of the binding of cytochrome *c* to liposomes. Implications for lipid-protein interactions. *J Biol Chem* 270:3197–3202
64. Gorbenko GP (1999) Structure of cytochrome *c* complexes with phospholipids as revealed by resonance energy transfer. *Biochim Biophys Acta* 1420:1–13
65. Cortese JD, Voglino AL, Hackenbrock CR (1995) Persistence of cytochrome *c* binding to membranes at physiological mitochondrial intermembrane space ionic strength. *Biochim Biophys Acta* 1228:216–228
66. Pereverzev MO, Vygodina TV, Konstantinov AA, Skulachev VP (2003) Cytochrome *c*, an ideal antioxidant. *Biochem Soc Trans* 31:1312–1315
67. Nomura K, Imai H, Koumura T, Kobayashi T, Nakagawa Y (2000) Mitochondrial phospholipid hydroperoxide glutathione peroxidase inhibits the release of cytochrome *c* from mitochondria by suppressing the peroxidation of cardiolipin in hypoglycaemia-induced apoptosis. *Biochem J* 351:183–193
68. Shidoji Y, Hayashi K, Komura S, Ohishi N, Yagi K (1999) Loss of molecular interaction between cytochrome *c* and cardiolipin due to lipid peroxidation. *Biochem Biophys Res Commun* 264:343–347
69. Ott M, Robertson JD, Gogvadze V, Zhivotovsky B, Orrenius S (2002) Cytochrome *c* release from mitochondria proceeds by a two-step process. *Proc Natl Acad Sci USA* 99:1259–1263
70. Gottlieb E (2006) OPA1 and PARL keep a lid on apoptosis. *Cell* 126:27–29
71. Adams JM, Cory S (1998) The Bcl-2 protein family: arbiters of cell survival. *Science* 281:1322–1326
72. Li H, Zhu H, Xu CJ, Yuan J (1998) Cleavage of BID by caspase 8 mediates the mitochondrial damage in the Fas pathway of apoptosis. *Cell* 94:491–501
73. Luo X, Budihardjo I, Zou H, Slaughter C, Wang X (1998) Bid, a bcl-2 interacting protein, mediates cytochrome *c* release from mitochondria in response to activation of cell surface receptors. *Cell* 94:481–490.
74. Cartron PF, Gallenne T, Bougras G et al (2004) The first alpha helix of Bax plays a necessary role in its ligand-induced activation by the BH3-only proteins Bid and PUMA. *Mol Cell* 16:807–818
75. Lutter M, Fang M, Luo X et al (2000) Cardiolipin provides specificity for targeting of tBid to mitochondria. *Nat Cell Biol* 2:754–761
76. Garcia-Saez AJ, Mingarro I, Perez-Paya E, Salgado J (2004) Membrane-insertion fragments of Bcl-xL, Bax, and Bid. *Biochemistry* 43:10930–10943
77. Lutter M, Perkins GA, Wang X (2001) The pro-apoptotic Bcl-2 family member tBid localizes to mitochondrial contact sites. *BMC Cell Biol* 2:22
78. Epand RF, Martinou JC, Fornallaz-Mulhauser M, Hughes DW, Epand RM (2002) The apoptotic protein tBid promotes leakage by altering membrane curvature. *J Biol Chem* 277:32632–32639
79. Esposti MD, Cristea IM, Gaskell SJ, Nakao Y, Dive C (2003) Proapoptotic bid binds to monolysocardiolipin, a new molecular connection between mitochondrial membranes and cell death. *Cell Death Differ* 10:1300–1309
80. Kim TH, Zhao Y, Ding WX et al (2004) Bid-cardiolipin interaction at mitochondrial contact site contributes to mitochondrial cristae reorganization and cytochrome *c* release. *Mol Biol Cell* 15:3061–3072
81. Liu J, Durrant D, Yang HS et al (2005) The interaction between tBid and cardiolipin or monolysocardiolipin. *Biochem Biophys Res Commun* 330:865–870
82. Liu J, Weiss A, Durrant D, Chi NW, Lee RM (2004) The cardiolipin-binding domain of Bid affects mitochondrial respiration and enhances cytochrome *c* release. *Apoptosis* 9:533–541
83. Zha J, Weiler S, Oh KJ, Wei MC, Korsmeyer SJ (2000) Post-translational N-myristoylation of BID as a molecular switch for targeting mitochondria and apoptosis. *Science* 290:1761–1765
84. Gonzalez F, Bessoule JJ, Rocchiccioli F, Manon S, Petit PX (2005) Role of cardiolipin on tBid and tBid/Bax synergistic effects on yeast mitochondria. *Cell Death Differ* 12:659–667
85. Gonzalez F, Pariselli F, Dupaigne P et al (2005) tBid interaction with cardiolipin primarily orchestrates mitochondrial dysfunctions and subsequently activates Bax and Bak. *Cell Death Differ* 12:614–626
86. Garcia Fernandez M, Troiano L, Moretti L et al (2002) Early changes in intramitochondrial cardiolipin distribution during apoptosis. *Cell Growth Differ* 13:449–455
87. Aguilar L, Ortega-Pierres G, Campos B et al (1999) Phospholipid membranes form specific nonbilayer molecular arrangements that are antigenic. *J Biol Chem* 274:25193–25196
88. Esposti MD, Erler JT, Hickman JA, Dive C (2001) Bid, a widely expressed proapoptotic protein of the Bcl-2 family, displays lipid transfer activity. *Mol Cell Biol* 21:7268–7276
89. Sorice M, Circella A, Cristea IM et al (2004) Cardiolipin and its metabolites move from mitochondria to other cellular membranes during death receptor-mediated apoptosis. *Cell Death Differ* 11:1133–1145
90. Kuwana T, Mackey MR, Perkins G et al (2002) Bid, bax, and lipids cooperate to form supramolecular openings in the outer mitochondrial membrane. *Cell* 111:331–342
91. Iverson SL, Enoksson M, Gogvadze V, Ott M, Orrenius S (2004) Cardiolipin is not required for Bax-mediated cytochrome *c* release from yeast mitochondria. *J Biol Chem* 279:1100–1107
92. Polcic P, Su X, Fowlkes J et al (2005) Cardiolipin and phosphatidylglycerol are not required for the in vivo action of Bcl-2 family proteins. *Cell Death Differ* 12:310–312
93. Rytomaa M, Kinnunen PK (1994) Evidence for two distinct acidic phospholipid-binding sites in cytochrome *c*. *J Biol Chem* 269:1770–1774
94. Kagan VE, Tyurina YY, Bayir H et al (2006) The “pro-apoptotic genes” get out of mitochondria: oxidative lipidomics and redox activity of cytochrome *c*/cardiolipin complexes. *Chem Biol Interact* 163:15–28

## REFERENCES

1. Vogt, C., *Untersuchungen über die Entwicklungsgeschichte der Geburtshelerkroete*. (Alytes obstetricians), Solothurn: Jent und Gassman, 1842: p. pp 130.
2. Lockshin, R.A. and C.M. Williams, *Programmed cell death. V. Cytolytic enzymes in relation to the breakdown of the intersegmental muscles of silkmoths*. J Insect Physiol, 1965. **11**(7): p. 831-44.
3. Kerr, J.F.R., A.H. Wyllie, and A.R. Currie, *Apoptosis: a basic biological phenomenon with wide-ranging implications in tissue kinetics*. Br. J. Cancer, 1972. **26**: p. 239-257.
4. Glucksmann, A., *Cell deaths in normal vertebrate ontogeny*. Biol. Rev, 1951. **26**: p. 59-86.
5. Kroemer, G., et al., *Classification of cell death: recommendations of the Nomenclature Committee on Cell Death*. Cell Death Differ, 2005. **12 Suppl 2**: p. 1463-7.
6. Golstein, P. and G. Kroemer, *Cell death by necrosis: towards a molecular definition*. Trends Biochem Sci, 2007. **32**(1): p. 37-43.
7. Barkla, D.H. and P.R. Gibson, *The fate of epithelial cells in the human large intestine*. Pathology, 1999. **31**(3): p. 230-8.
8. Roach, H.I. and N.M. Clarke, *Physiological cell death of chondrocytes in vivo is not confined to apoptosis. New observations on the mammalian growth plate*. J Bone Joint Surg Br, 2000. **82**(4): p. 601-13.
9. Chautan, M., et al., *Interdigital cell death can occur through a necrotic and caspase-independent pathway*. Curr Biol, 1999. **9**(17): p. 967-70.
10. Edinger, A.L. and C.B. Thompson, *Death by design: apoptosis, necrosis and autophagy*. Curr Opin Cell Biol, 2004. **16**(6): p. 663-9.
11. Levine, B. and D.J. Klionsky, *Development by self-digestion: molecular mechanisms and biological functions of autophagy*. Dev Cell, 2004. **6**(4): p. 463-77.
12. Reggiori, F. and D.J. Klionsky, *Autophagy in the eukaryotic cell*. Eukaryot Cell, 2002. **1**(1): p. 11-21.
13. Klionsky, D.J. and S.D. Emr, *Autophagy as a regulated pathway of cellular degradation*. Science, 2000. **290**(5497): p. 1717-21.
14. Juhasz, G., et al., *The Drosophila homolog of Aut1 is essential for autophagy and development*. FEBS Lett, 2003. **543**(1-3): p. 154-8.
15. Melendez, A., et al., *Autophagy genes are essential for dauer development and life-span extension in C. elegans*. Science, 2003. **301**(5638): p. 1387-91.
16. Yue, Z., et al., *Beclin 1, an autophagy gene essential for early embryonic development, is a haploinsufficient tumor suppressor*. Proc Natl Acad Sci U S A, 2003. **100**(25): p. 15077-82.
17. Yu, L., et al., *Regulation of an ATG7-beclin 1 program of autophagic cell death by caspase-8*. Science, 2004. **304**(5676): p. 1500-2.
18. Shimizu, S., et al., *Role of Bcl-2 family proteins in a non-apoptotic programmed cell death dependent on autophagy genes*. Nat Cell Biol, 2004. **6**(12): p. 1221-8.
19. Meier, P., A. Finch, and G. Evan, *Apoptosis in development*. Nature, 2000. **407**(6805): p. 796-801.
20. Vaux, D.L. and S.J. Korsmeyer, *Cell death in development*. Cell, 1999. **96**(2): p. 245-54.
21. Opferman, J.T. and S.J. Korsmeyer, *Apoptosis in the development and maintenance of the immune system*. Nat Immunol, 2003. **4**(5): p. 410-5.

22. Fadeel, B., S. Orrenius, and B. Zhivotovsky, *Apoptosis in human disease: a new skin for the old ceremony?* Biochem Biophys Res Commun, 1999. **266**(3): p. 699-717.
23. Tsujimoto, Y., et al., *Cloning of the chromosome breakpoint of neoplastic B cells with the t(14;18) chromosome translocation.* Science, 1984. **226**(4678): p. 1097-9.
24. Tsujimoto, Y., et al., *Involvement of the bcl-2 gene in human follicular lymphoma.* Science, 1985. **228**(4706): p. 1440-3.
25. Vaux, D.L., S. Cory, and J.M. Adams, *Bcl-2 gene promotes haemopoietic cell survival and cooperates with c-myc to immortalize pre-B cells.* Nature, 1988. **335**(6189): p. 440-2.
26. McDonnell, T.J., et al., *bcl-2-immunoglobulin transgenic mice demonstrate extended B cell survival and follicular lymphoproliferation.* Cell, 1989. **57**(1): p. 79-88.
27. Hockenbery, D., et al., *Bcl-2 is an inner mitochondrial membrane protein that blocks programmed cell death.* Nature, 1990. **348**(6299): p. 334-6.
28. Yonish-Rouach, E., et al., *Wild-type p53 induces apoptosis of myeloid leukaemic cells that is inhibited by interleukin-6.* Nature, 1991. **352**(6333): p. 345-7.
29. Wallace-Brodeur, R.R. and S.W. Lowe, *Clinical implications of p53 mutations.* Cell Mol Life Sci, 1999. **55**(1): p. 64-75.
30. Carr, A.M., M.H. Green, and A.R. Lehmann, *Checkpoint policing by p53.* Nature, 1992. **359**(6395): p. 486-7.
31. Kroemer, G., B. Dalaporta, and M. Resche-Rigon, *The mitochondria death/life regulator in apoptosis and necrosis.* Annu. Rev. Physiol., 1998. **60**: p. 619-642.
32. Green, D.R. and J.C. Reed, *Mitochondria and apoptosis.* Science, 1998. **281**(5381): p. 1309-12.
33. Peter, M.E., et al., *The death receptors.* Results Probl Cell Differ, 1999. **23**: p. 25-63.
34. Peter, M.E. and P.H. Krammer, *The CD95(APO-1/Fas) DISC and beyond.* Cell Death Differ, 2003. **10**(1): p. 26-35.
35. Peter, M.E. and P.H. Krammer, *Mechanisms of CD95 (APO-1/Fas)-mediated apoptosis.* Curr Opin Immunol, 1998. **10**(5): p. 545-51.
36. Lavrik, I., A. Golks, and P.H. Krammer, *Death receptor signaling.* J Cell Sci, 2005. **118**(Pt 2): p. 265-7.
37. Chen, G. and D.V. Goeddel, *TNF-R1 signaling: a beautiful pathway.* Science, 2002. **296**(5573): p. 1634-5.
38. Walczak, H. and P.H. Krammer, *The CD95 (APO-1/Fas) and the TRAIL (APO-2L) apoptosis systems.* Exp Cell Res, 2000. **256**(1): p. 58-66.
39. Trauth, B.C., et al., *Monoclonal antibody-mediated tumor regression by induction of apoptosis.* Science, 1989. **245**(4915): p. 301-5.
40. Dhein, J., et al., *Induction of apoptosis by monoclonal antibody anti-APO-1 class switch variants is dependent on cross-linking of APO-1 cell surface antigens.* J Immunol, 1992. **149**(10): p. 3166-73.
41. Kischkel, F.C., et al., *Cytotoxicity-dependent APO-1 (Fas/CD95)-associated proteins form a death-inducing signaling complex (DISC) with the receptor.* Embo J, 1995. **14**(22): p. 5579-88.
42. Kischkel, F.C., et al., *Death receptor recruitment of endogenous caspase-10 and apoptosis initiation in the absence of caspase-8.* J Biol Chem, 2001. **276**(49): p. 46639-46.
43. Sprick, M.R., et al., *Caspase-10 is recruited to and activated at the native TRAIL and CD95 death-inducing signalling complexes in a FADD-dependent manner but can not functionally substitute caspase-8.* Embo J, 2002. **21**(17): p. 4520-30.
44. Wang, J., et al., *Caspase-10 is an initiator caspase in death receptor signaling.* Proc Natl Acad Sci U S A, 2001. **98**(24): p. 13884-8.

45. Milhas, D., et al., *Caspase-10 triggers Bid cleavage and caspase cascade activation in FasL-induced apoptosis*. J Biol Chem, 2005. **280**(20): p. 19836-42.
46. Zhu, S., et al., *Genetic alterations in caspase-10 may be causative or protective in autoimmune lymphoproliferative syndrome*. Hum Genet, 2006. **119**(3): p. 284-94.
47. Park, W.S., et al., *Inactivating mutations of the caspase-10 gene in gastric cancer*. Oncogene, 2002. **21**(18): p. 2919-25.
48. Thome, M. and J. Tschopp, *Regulation of lymphocyte proliferation and death by FLIP*. Nat Rev Immunol, 2001. **1**(1): p. 50-8.
49. Kimura, M. and A. Matsuzawa, *Autoimmunity in mice bearing lprcg: a novel mutant gene*. Int Rev Immunol, 1994. **11**(3): p. 193-210.
50. Adachi, M., et al., *Enhanced and accelerated lymphoproliferation in Fas-null mice*. Proc Natl Acad Sci U S A, 1996. **93**(5): p. 2131-6.
51. Rieux-Laucat, F., et al., *Mutations in Fas associated with human lymphoproliferative syndrome and autoimmunity*. Science, 1995. **268**(5215): p. 1347-9.
52. Yeh, W.C., et al., *FADD: essential for embryo development and signaling from some, but not all, inducers of apoptosis*. Science, 1998. **279**(5358): p. 1954-8.
53. Varfolomeev, E.E., et al., *Targeted disruption of the mouse Caspase 8 gene ablates cell death induction by the TNF receptors, Fas/Apo1, and DR3 and is lethal prenatally*. Immunity, 1998. **9**(2): p. 267-76.
54. Chun, H.J., et al., *Pleiotropic defects in lymphocyte activation caused by caspase-8 mutations lead to human immunodeficiency*. Nature, 2002. **419**(6905): p. 395-9.
55. Kang, T.B., et al., *Caspase-8 serves both apoptotic and nonapoptotic roles*. J Immunol, 2004. **173**(5): p. 2976-84.
56. Scaffidi, C., et al., *Two CD95 (APO-1/Fas) signaling pathways*. Embo J, 1998. **17**(6): p. 1675-87.
57. Schmitz, I., et al., *Differences between CD95 type I and II cells detected with the CD95 ligand*. Cell Death Differ, 1999. **6**(9): p. 821-2.
58. Lacronique, V., et al., *Bcl-2 protects from lethal hepatic apoptosis induced by an anti-Fas antibody in mice*. Nat Med, 1996. **2**(1): p. 80-6.
59. Strasser, A., et al., *Bcl-2 and Fas/APO-1 regulate distinct pathways to lymphocyte apoptosis*. Embo J, 1995. **14**(24): p. 6136-47.
60. Yin, X.M., et al., *Bid-deficient mice are resistant to Fas-induced hepatocellular apoptosis*. Nature, 1999. **400**(6747): p. 886-91.
61. Lindsten, T., et al., *The combined functions of proapoptotic Bcl-2 family members bak and bax are essential for normal development of multiple tissues*. Mol Cell, 2000. **6**(6): p. 1389-99.
62. Wei, M.C., et al., *Proapoptotic BAX and BAK: a requisite gateway to mitochondrial dysfunction and death*. Science, 2001. **292**(5517): p. 727-30.
63. Schneider, T.J., et al., *Bcl-x protects primary B cells against Fas-mediated apoptosis*. J Immunol, 1997. **159**(10): p. 4834-9.
64. Algeciras-Schimmich, A., et al., *Two CD95 tumor classes with different sensitivities to antitumor drugs*. Proc Natl Acad Sci U S A, 2003. **100**(20): p. 11445-50.
65. Newmeyer, D.D., D.M. Farschon, and J.C. Reed, *Cell-free apoptosis in Xenopus egg extracts: inhibition by Bcl-2 and requirement for an organelle fraction enriched in mitochondria*. Cell, 1994. **79**(2): p. 353-64.
66. Zamzami, N., et al., *Reduction in mitochondrial potential constitutes an early irreversible step of programmed lymphocyte death in vivo*. J Exp Med, 1995. **181**(5): p. 1661-72.
67. Zamzami, N., et al., *Sequential reduction of mitochondrial transmembrane potential and generation of reactive oxygen species in early programmed cell death*. J Exp Med, 1995. **182**(2): p. 367-77.
68. Liu, X., et al., *Induction of apoptotic program in cell-free extracts: requirement for dATP and cytochrome c*. Cell, 1996. **86**(1): p. 147-57.

69. Margulis, L., *Archaeal-eubacterial mergers in the origin of Eukarya: phylogenetic classification of life*. Proc Natl Acad Sci U S A, 1996. **93**(3): p. 1071-6.
70. Mitchell, P., *Coupling of phosphorylation to electron and hydrogen transfer by a chemi-osmotic type of mechanism*. Nature, 1961. **191**: p. 144-8.
71. Martin, S.J., et al., *Cell-free reconstitution of Fas-, UV radiation- and ceramide-induced apoptosis*. Embo J, 1995. **14**(21): p. 5191-200.
72. Kluck, R.M., et al., *The release of cytochrome c from mitochondria: a primary site for Bcl-2 regulation of apoptosis*. Science, 1997. **275**(5303): p. 1132-6.
73. Green, D.R. and G. Kroemer, *The pathophysiology of mitochondrial cell death*. Science, 2004. **305**(5684): p. 626-9.
74. Du, C., et al., *Smac, a mitochondrial protein that promotes cytochrome c-dependent caspase activation by eliminating IAP inhibition*. Cell, 2000. **102**(1): p. 33-42.
75. Suzuki, Y., et al., *A serine protease, HtrA2, is released from the mitochondria and interacts with XIAP, inducing cell death*. Mol Cell, 2001. **8**(3): p. 613-21.
76. Susin, S.A., et al., *Molecular characterization of mitochondrial apoptosis-inducing factor*. Nature, 1999. **397**(6718): p. 441-6.
77. Li, L.Y., X. Luo, and X. Wang, *Endonuclease G is an apoptotic DNase when released from mitochondria*. Nature, 2001. **412**(6842): p. 95-9.
78. Wang, X., *The expanding role of mitochondria in apoptosis*. Genes Dev, 2001. **15**(22): p. 2922-33.
79. Green, D.R. and G.P. Amarante-Mendes, *The point of no return: mitochondria, caspases, and the commitment to cell death*. Results Probl Cell Differ, 1998. **24**: p. 45-61.
80. Arnoult, D., et al., *Mitochondrial release of AIF and EndoG requires caspase activation downstream of Bax/Bak-mediated permeabilization*. Embo J, 2003. **22**(17): p. 4385-99.
81. Goldstein, J.C., et al., *The coordinate release of cytochrome c during apoptosis is rapid, complete and kinetically invariant*. Nat Cell Biol, 2000. **2**(3): p. 156-62.
82. Bossy-Wetzel, E., D.D. Newmeyer, and D.R. Green, *Mitochondrial cytochrome c release in apoptosis occurs upstream of DEVD-specific caspase activation and independently of mitochondrial transmembrane depolarization*. Embo J, 1998. **17**(1): p. 37-49.
83. Ricci, J.E., R.A. Gottlieb, and D.R. Green, *Caspase-mediated loss of mitochondrial function and generation of reactive oxygen species during apoptosis*. J Cell Biol, 2003. **160**(1): p. 65-75.
84. Ricci, J.E., et al., *Disruption of mitochondrial function during apoptosis is mediated by caspase cleavage of the p75 subunit of complex I of the electron transport chain*. Cell, 2004. **117**(6): p. 773-86.
85. Scorrano, L., et al., *A distinct pathway remodels mitochondrial cristae and mobilizes cytochrome c during apoptosis*. Dev Cell, 2002. **2**(1): p. 55-67.
86. Frezza, C., et al., *OPA1 controls apoptotic cristae remodeling independently from mitochondrial fusion*. Cell, 2006. **126**(1): p. 177-89.
87. Cipolat, S., et al., *Mitochondrial rhomboid PARL regulates cytochrome c release during apoptosis via OPA1-dependent cristae remodeling*. Cell, 2006. **126**(1): p. 163-75.
88. Gottlieb, E., et al., *Mitochondrial membrane potential regulates matrix configuration and cytochrome c release during apoptosis*. Cell Death Differ, 2003. **10**(6): p. 709-17.
89. Karbowski, M. and R.J. Youle, *Dynamics of mitochondrial morphology in healthy cells and during apoptosis*. Cell Death Differ, 2003. **10**(8): p. 870-80.
90. Cory, S. and J.M. Adams, *The Bcl2 family: regulators of the cellular life-or-death switch*. Nat Rev Cancer, 2002. **2**(9): p. 647-56.

91. Petros, A.M., E.T. Olejniczak, and S.W. Fesik, *Structural biology of the Bcl-2 family of proteins*. Biochim Biophys Acta, 2004. **1644**(2-3): p. 83-94.
92. Petros, A.M., et al., *Solution structure of the antiapoptotic protein bcl-2*. Proc Natl Acad Sci U S A, 2001. **98**(6): p. 3012-7.
93. Muchmore, S.W., et al., *X-ray and NMR structure of human Bcl-xL, an inhibitor of programmed cell death*. Nature, 1996. **381**(6580): p. 335-41.
94. Adams, J.M. and S. Cory, *The Bcl-2 protein family: arbiters of cell survival*. Science, 1998. **281**(5381): p. 1322-6.
95. Letai, A., et al., *Distinct BH3 domains either sensitize or activate mitochondrial apoptosis, serving as prototype cancer therapeutics*. Cancer Cell, 2002. **2**(3): p. 183-92.
96. Chen, L., et al., *Differential targeting of prosurvival Bcl-2 proteins by their BH3-only ligands allows complementary apoptotic function*. Mol Cell, 2005. **17**(3): p. 393-403.
97. Hsu, Y.T., K.G. Wolter, and R.J. Youle, *Cytosol-to-membrane redistribution of Bax and Bcl-X(L) during apoptosis*. Proc Natl Acad Sci U S A, 1997. **94**(8): p. 3668-72.
98. Griffiths, G.J., et al., *Cell damage-induced conformational changes of the pro-apoptotic protein Bak in vivo precede the onset of apoptosis*. J Cell Biol, 1999. **144**(5): p. 903-14.
99. Eskes, R., et al., *Bid induces the oligomerization and insertion of Bax into the outer mitochondrial membrane*. Mol Cell Biol, 2000. **20**(3): p. 929-35.
100. Wei, M.C., et al., *tBID, a membrane-targeted death ligand, oligomerizes BAK to release cytochrome c*. Genes Dev, 2000. **14**(16): p. 2060-71.
101. Kuwana, T., et al., *Bid, bax, and lipids cooperate to form supramolecular openings in the outer mitochondrial membrane*. Cell, 2002. **111**(3): p. 331-42.
102. Marchetti, P., et al., *Mitochondrial permeability transition is a central coordinating event of apoptosis*. J Exp Med, 1996. **184**(3): p. 1155-60.
103. Crompton, M., S. Virji, and J.M. Ward, *Cyclophilin-D binds strongly to complexes of the voltage-dependent anion channel and the adenine nucleotide translocase to form the permeability transition pore*. Eur J Biochem, 1998. **258**(2): p. 729-35.
104. Nakagawa, T., et al., *Cyclophilin D-dependent mitochondrial permeability transition regulates some necrotic but not apoptotic cell death*. Nature, 2005. **434**(7033): p. 652-8.
105. Kokoszka, J.E., et al., *The ADP/ATP translocator is not essential for the mitochondrial permeability transition pore*. Nature, 2004. **427**(6973): p. 461-5.
106. Zou, H., et al., *Apaf-1, a human protein homologous to C. elegans CED-4, participates in cytochrome c-dependent activation of caspase-3*. Cell, 1997. **90**(3): p. 405-13.
107. Zou, H., et al., *An APAF-1-cytochrome c multimeric complex is a functional apoptosome that activates procaspase-9*. J Biol Chem, 1999. **274**(17): p. 11549-56.
108. Li, P., et al., *Cytochrome c and dATP-dependent formation of Apaf-1/caspase-9 complex initiates an apoptotic protease cascade*. Cell, 1997. **91**(4): p. 479-89.
109. Rodriguez, J. and Y. Lazebnik, *Caspase-9 and APAF-1 form an active holoenzyme*. Genes Dev, 1999. **13**(24): p. 3179-84.
110. Acehan, D., et al., *Three-dimensional structure of the apoptosome: implications for assembly, procaspase-9 binding, and activation*. Mol Cell, 2002. **9**(2): p. 423-32.
111. Li, K., et al., *Cytochrome c deficiency causes embryonic lethality and attenuates stress-induced apoptosis*. Cell, 2000. **101**(4): p. 389-99.
112. Hao, Z., et al., *Specific ablation of the apoptotic functions of cytochrome C reveals a differential requirement for cytochrome C and Apaf-1 in apoptosis*. Cell, 2005. **121**(4): p. 579-91.
113. Cecconi, F., et al., *Apaf1 (CED-4 homolog) regulates programmed cell death in mammalian development*. Cell, 1998. **94**(6): p. 727-37.

114. Yoshida, H., et al., *Apaf1 is required for mitochondrial pathways of apoptosis and brain development*. Cell, 1998. **94**(6): p. 739-50.
115. Kuida, K., et al., *Reduced apoptosis and cytochrome c-mediated caspase activation in mice lacking caspase 9*. Cell, 1998. **94**(3): p. 325-37.
116. Deveraux, Q.L., et al., *IAPs block apoptotic events induced by caspase-8 and cytochrome c by direct inhibition of distinct caspases*. Embo J, 1998. **17**(8): p. 2215-23.
117. Verhagen, A.M., et al., *Identification of DIABLO, a mammalian protein that promotes apoptosis by binding to and antagonizing IAP proteins*. Cell, 2000. **102**(1): p. 43-53.
118. Srinivasula, S.M., et al., *A conserved XIAP-interaction motif in caspase-9 and Smac/DIABLO regulates caspase activity and apoptosis*. Nature, 2001. **410**(6824): p. 112-6.
119. Okada, H., et al., *Generation and characterization of Smac/DIABLO-deficient mice*. Mol Cell Biol, 2002. **22**(10): p. 3509-17.
120. Joza, N., et al., *Essential role of the mitochondrial apoptosis-inducing factor in programmed cell death*. Nature, 2001. **410**(6828): p. 549-54.
121. Vahsen, N., et al., *AIF deficiency compromises oxidative phosphorylation*. Embo J, 2004. **23**(23): p. 4679-89.
122. Ohsato, T., et al., *Mammalian mitochondrial endonuclease G. Digestion of R-loops and localization in intermembrane space*. Eur J Biochem, 2002. **269**(23): p. 5765-70.
123. Irvine, R.A., et al., *Generation and characterization of endonuclease G null mice*. Mol Cell Biol, 2005. **25**(1): p. 294-302.
124. Wang, K., et al., *BID: a novel BH3 domain-only death agonist*. Genes Dev, 1996. **10**(22): p. 2859-69.
125. Li, H., et al., *Cleavage of BID by caspase 8 mediates the mitochondrial damage in the Fas pathway of apoptosis*. Cell, 1998. **94**(4): p. 491-501.
126. Luo, X., et al., *Bid, a Bcl2 interacting protein, mediates cytochrome c release from mitochondria in response to activation of cell surface death receptors*. Cell, 1998. **94**(4): p. 481-90.
127. Lutter, M., et al., *Cardiolipin provides specificity for targeting of tBid to mitochondria*. Nat Cell Biol, 2000. **2**(10): p. 754-761.
128. Lutter, M., G.A. Perkins, and X. Wang, *The pro-apoptotic Bcl-2 family member tBid localizes to mitochondrial contact sites*. BMC Cell Biol, 2001. **2**(1): p. 22.
129. Gonzalvez, F., et al., *Role of cardiolipin on tBid and tBid/Bax synergistic effects on yeast mitochondria*. Cell Death Differ, 2005. **12**(6): p. 659-667.
130. Gonzalvez, F., et al., *tBid interaction with cardiolipin primarily orchestrates mitochondrial dysfunctions and subsequently activates Bax and Bak*. Cell Death Differ, 2005. **12**(6): p. 614-26.
131. Kim, T.H., et al., *Bid-cardiolipin interaction at mitochondrial contact site contributes to mitochondrial cristae reorganization and cytochrome C release*. Mol Biol Cell, 2004. **15**(7): p. 3061-72.
132. Liu, J., et al., *The cardiolipin-binding domain of Bid affects mitochondrial respiration and enhances cytochrome c release*. Apoptosis, 2004. **9**(5): p. 533-41.
133. Thornberry, N.A., et al., *A novel heterodimeric cysteine protease is required for interleukin-1 beta processing in monocytes*. Nature, 1992. **356**(6372): p. 768-74.
134. Cerretti, D.P., et al., *Molecular cloning of the interleukin-1 beta converting enzyme*. Science, 1992. **256**(5053): p. 97-100.
135. Yuan, J., et al., *The C. elegans cell death gene ced-3 encodes a protein similar to mammalian interleukin-1 beta-converting enzyme*. Cell, 1993. **75**(4): p. 641-52.
136. Lamkanfi, M., et al., *Alice in caspase land. A phylogenetic analysis of caspases from worm to man*. Cell Death Differ, 2002. **9**(4): p. 358-61.

137. Thornberry, N.A., et al., *A combinatorial approach defines specificities of members of the caspase family and granzyme B. Functional relationships established for key mediators of apoptosis.* J Biol Chem, 1997. **272**(29): p. 17907-11.
138. Saleh, M., et al., *Enhanced bacterial clearance and sepsis resistance in caspase-12-deficient mice.* Nature, 2006. **440**(7087): p. 1064-8.
139. Saleh, M., et al., *Differential modulation of endotoxin responsiveness by human caspase-12 polymorphisms.* Nature, 2004. **429**(6987): p. 75-9.
140. Scott, A.M. and M. Saleh, *The inflammatory caspases: guardians against infections and sepsis.* Cell Death Differ, 2007. **14**(1): p. 23-31.
141. Shi, Y., *Mechanisms of caspase activation and inhibition during apoptosis.* Mol Cell, 2002. **9**(3): p. 459-70.
142. Salvesen, G.S. and V.M. Dixit, *Caspase activation: the induced-proximity model.* Proc Natl Acad Sci U S A, 1999. **96**(20): p. 10964-7.
143. Chen, M., et al., *Activation of initiator caspases through a stable dimeric intermediate.* J Biol Chem, 2002. **277**(52): p. 50761-7.
144. Boatright, K.M., et al., *A unified model for apical caspase activation.* Mol Cell, 2003. **11**(2): p. 529-41.
145. Donepudi, M., et al., *Insights into the regulatory mechanism for caspase-8 activation.* Mol Cell, 2003. **11**(2): p. 543-9.
146. Chang, D.W., et al., *Interdimer processing mechanism of procaspase-8 activation.* Embo J, 2003. **22**(16): p. 4132-42.
147. Murphy, B.M., E.M. Creagh, and S.J. Martin, *Interchain proteolysis, in the absence of a dimerization stimulus, can initiate apoptosis-associated caspase-8 activation.* J Biol Chem, 2004. **279**(35): p. 36916-22.
148. Sohn, D., K. Schulze-Osthoff, and R.U. Janicke, *Caspase-8 can be activated by interchain proteolysis without receptor-triggered dimerization during drug-induced apoptosis.* J Biol Chem, 2005. **280**(7): p. 5267-73.
149. Chai, J., et al., *Crystal structure of a procaspase-7 zymogen: mechanisms of activation and substrate binding.* Cell, 2001. **107**(3): p. 399-407.
150. Porter, A.G. and R.U. Janicke, *Emerging roles of caspase-3 in apoptosis.* Cell Death Differ, 1999. **6**(2): p. 99-104.
151. Fuentes-Prior, P. and G.S. Salvesen, *The protein structures that shape caspase activity, specificity, activation and inhibition.* Biochem J, 2004. **384**(Pt 2): p. 201-32.
152. Lakhani, S.A., et al., *Caspases 3 and 7: key mediators of mitochondrial events of apoptosis.* Science, 2006. **311**(5762): p. 847-51.
153. Loegering, D.A., et al., *Evaluation of the role of caspase-6 in anticancer drug-induced apoptosis.* Cell Death Differ, 2006. **13**(2): p. 346-7.
154. Muzio, M., et al., *FLICE, a novel FADD-homologous ICE/CED-3-like protease, is recruited to the CD95 (Fas/APO-1) death-inducing signaling complex.* Cell, 1996. **85**(6): p. 817-27.
155. Boldin, M.P., et al., *Involvement of MACH, a novel MORT1/FADD-interacting protease, in Fas/APO-1- and TNF receptor-induced cell death.* Cell, 1996. **85**(6): p. 803-15.
156. Scaffidi, C., et al., *FLICE is predominantly expressed as two functionally active isoforms, caspase-8/a and caspase-8/b.* J Biol Chem, 1997. **272**(43): p. 26953-8.
157. Blanchard, H., et al., *Caspase-8 specificity probed at subsite S(4): crystal structure of the caspase-8-Z-DEVD-cho complex.* J Mol Biol, 2000. **302**(1): p. 9-16.
158. Stegh, A.H., et al., *Identification of the cytolinker plectin as a major early in vivo substrate for caspase 8 during CD95- and tumor necrosis factor receptor-mediated apoptosis.* Mol Cell Biol, 2000. **20**(15): p. 5665-79.
159. Stegh, A.H., et al., *Inactivation of caspase-8 on mitochondria of Bcl-xL-expressing MCF7-Fas cells: role for the bifunctional apoptosis regulator protein.* J Biol Chem, 2002. **277**(6): p. 4351-60.

160. Krueger, A., et al., *Cellular FLICE-inhibitory protein splice variants inhibit different steps of caspase-8 activation at the CD95 death-inducing signaling complex*. J Biol Chem, 2001. **276**(23): p. 20633-40.
161. Gonzalvez, F. and E. Gottlieb, *Cardiolipin: Setting the beat of apoptosis*. Apoptosis, 2007.
162. Schlame, M., D. Rua, and M.L. Greenberg, *The biosynthesis and functional role of cardiolipin*. Prog Lipid Res, 2000. **39**(3): p. 257-88.
163. Hauff, K.D. and G.M. Hatch, *Cardiolipin metabolism and Barth Syndrome*. Prog Lipid Res, 2006. **45**(2): p. 91-101.
164. Houtkooper, R.H., et al., *Identification and characterization of human cardiolipin synthase*. FEBS Lett, 2006. **580**(13): p. 3059-64.
165. Choi, S.Y., et al., *Cardiolipin deficiency releases cytochrome c from the inner mitochondrial membrane and accelerates stimuli-elicited apoptosis*. Cell Death Differ, 2007. **14**(3): p. 597-606.
166. Hoch, F.L., *Cardiolipins and biomembrane function*. Biochim Biophys Acta, 1992. **1113**(1): p. 71-133.
167. Schlame, M., et al., *Molecular symmetry in mitochondrial cardiolipins*. Chem Phys Lipids, 2005. **138**(1-2): p. 38-49.
168. Rustow, B., et al., *Species pattern of phosphatidic acid, diacylglycerol, CDP-diacylglycerol and phosphatidylglycerol synthesized de novo in rat liver mitochondria*. Biochim Biophys Acta, 1989. **1002**(2): p. 261-3.
169. Hostetler, K.Y., B.D. Zenner, and H.P. Morris, *Altered subcellular and submitochondrial localization of CTP:phosphatidate cytidyltransferase in the Morris 7777 hepatoma*. J Lipid Res, 1978. **19**(5): p. 553-60.
170. Schlame, M., et al., *Intramembraneous hydrogenation of mitochondrial lipids reduces the substrate availability, but not the enzyme activity of endogenous phospholipase A. The role of polyunsaturated phospholipid species*. Biochim Biophys Acta, 1990. **1045**(1): p. 1-8.
171. Xu, Y., et al., *Remodeling of cardiolipin by phospholipid transacylation*. J Biol Chem, 2003. **278**(51): p. 51380-5.
172. Xu, Y., et al., *The enzymatic function of tafazzin*. J Biol Chem, 2006. **281**(51): p. 39217-24.
173. Barth, P.G., et al., *An X-linked mitochondrial disease affecting cardiac muscle, skeletal muscle and neutrophil leucocytes*. J Neurol Sci, 1983. **62**(1-3): p. 327-55.
174. Kelley, R.I., et al., *X-linked dilated cardiomyopathy with neutropenia, growth retardation, and 3-methylglutaconic aciduria*. J Pediatr, 1991. **119**(5): p. 738-47.
175. Bione, S., et al., *A novel X-linked gene, G4.5, is responsible for Barth syndrome*. Nat Genet, 1996. **12**(4): p. 385-9.
176. Lu, B., et al., *Complex expression pattern of the Barth syndrome gene product tafazzin in human cell lines and murine tissues*. Biochem Cell Biol, 2004. **82**(5): p. 569-76.
177. Gonzalez, I.L., *Barth syndrome: TAZ gene mutations, mRNAs, and evolution*. Am J Med Genet A, 2005. **134**(4): p. 409-14.
178. Vaz, F.M., et al., *Only one splice variant of the human TAZ gene encodes a functional protein with a role in cardiolipin metabolism*. J Biol Chem, 2003. **278**(44): p. 43089-94.
179. Vreken, P., et al., *Defective remodeling of cardiolipin and phosphatidylglycerol in Barth syndrome*. Biochem Biophys Res Commun, 2000. **279**(2): p. 378-82.
180. Schlame, M., et al., *Phospholipid abnormalities in children with Barth syndrome*. J Am Coll Cardiol, 2003. **42**(11): p. 1994-9.
181. Valianpour, F., et al., *Monolysocardiolipins accumulate in Barth syndrome but do not lead to enhanced apoptosis*. J Lipid Res, 2005. **46**(6): p. 1182-95.

182. Krebs, J.J., H. Hauser, and E. Carafoli, *Asymmetric distribution of phospholipids in the inner membrane of beef heart mitochondria*. J Biol Chem, 1979. **254**(12): p. 5308-16.
183. Hovius, R., et al., *Improved methods to isolate and subfractionate rat liver mitochondria. Lipid composition of the inner and outer membrane*. Biochim Biophys Acta, 1990. **1021**(2): p. 217-26.
184. de Kroon, A.I., et al., *Phospholipid composition of highly purified mitochondrial outer membranes of rat liver and Neurospora crassa. Is cardiolipin present in the mitochondrial outer membrane?* Biochim Biophys Acta, 1997. **1325**(1): p. 108-16.
185. Ardail, D., et al., *Mitochondrial contact sites. Lipid composition and dynamics*. J Biol Chem, 1990. **265**(31): p. 18797-802.
186. Cullis, P.R., A.J. Verkleij, and P.H. Ververgaert, *Polymorphic phase behaviour of cardiolipin as detected by 31P NMR and freeze-fracture techniques. Effects of calcium, dibucaine and chlorpromazine*. Biochim Biophys Acta, 1978. **513**(1): p. 11-20.
187. Van Venetie, R. and A.J. Verkleij, *Possible role of non-bilayer lipids in the structure of mitochondria. A freeze-fracture electron microscopy study*. Biochim Biophys Acta, 1982. **692**(3): p. 397-405.
188. Fry, M. and D.E. Green, *Cardiolipin requirement for electron transfer in complex I and III of the mitochondrial respiratory chain*. J Biol Chem, 1981. **256**(4): p. 1874-80.
189. Eble, K.S., et al., *Tightly associated cardiolipin in the bovine heart mitochondrial ATP synthase as analyzed by 31P nuclear magnetic resonance spectroscopy*. J Biol Chem, 1990. **265**(32): p. 19434-40.
190. Sedlak, E. and N.C. Robinson, *Phospholipase A(2) digestion of cardiolipin bound to bovine cytochrome c oxidase alters both activity and quaternary structure*. Biochemistry, 1999. **38**(45): p. 14966-72.
191. Yue, W.H., et al., *Crystallization of mitochondrial ubiquinol-cytochrome c reductase*. Biochemistry, 1991. **30**(9): p. 2303-6.
192. Yankovskaya, V., et al., *Architecture of succinate dehydrogenase and reactive oxygen species generation*. Science, 2003. **299**(5607): p. 700-4.
193. Hoffmann, B., et al., *The reconstituted ADP/ATP carrier activity has an absolute requirement for cardiolipin as shown in cysteine mutants*. J Biol Chem, 1994. **269**(3): p. 1940-4.
194. Noel, H. and S.V. Pande, *An essential requirement of cardiolipin for mitochondrial carnitine acylcarnitine translocase activity. Lipid requirement of carnitine acylcarnitine translocase*. Eur J Biochem, 1986. **155**(1): p. 99-102.
195. Bisaccia, F. and F. Palmieri, *Specific elution from hydroxylapatite of the mitochondrial phosphate carrier by cardiolipin*. Biochim Biophys Acta, 1984. **766**(2): p. 386-94.
196. Nalecz, K.A., et al., *The monocarboxylate carrier from bovine heart mitochondria: partial purification and its substrate-transporting properties in a reconstituted system*. Biochim Biophys Acta, 1986. **851**(1): p. 29-37.
197. Ohtsuka, T., M. Nishijima, and Y. Akamatsu, *A somatic cell mutant defective in phosphatidylglycerophosphate synthase, with impaired phosphatidylglycerol and cardiolipin biosynthesis*. J Biol Chem, 1993. **268**(30): p. 22908-13.
198. Ohtsuka, T., et al., *Mitochondrial dysfunction of a cultured Chinese hamster ovary cell mutant deficient in cardiolipin*. J Biol Chem, 1993. **268**(30): p. 22914-9.
199. Jiang, F., H.S. Rizavi, and M.L. Greenberg, *Cardiolipin is not essential for the growth of Saccharomyces cerevisiae on fermentable or non-fermentable carbon sources*. Mol Microbiol, 1997. **26**(3): p. 481-91.
200. Jiang, F., et al., *Absence of cardiolipin in the crd1 null mutant results in decreased mitochondrial membrane potential and reduced mitochondrial function*. J Biol Chem, 2000. **275**(29): p. 22387-94.

201. Koshkin, V. and M.L. Greenberg, *Oxidative phosphorylation in cardiolipin-lacking yeast mitochondria*. *Biochem J*, 2000. **347 Pt 3**: p. 687-91.
202. Koshkin, V. and M.L. Greenberg, *Cardiolipin prevents rate-dependent uncoupling and provides osmotic stability in yeast mitochondria*. *Biochem J*, 2002. **364**(Pt 1): p. 317-22.
203. Bernardi, P. and G.F. Azzone, *Cytochrome c as an electron shuttle between the outer and inner mitochondrial membranes*. *J Biol Chem*, 1981. **256**(14): p. 7187-92.
204. Rytomaa, M., P. Mustonen, and P.K. Kinnunen, *Reversible, nonionic, and pH-dependent association of cytochrome c with cardiolipin-phosphatidylcholine liposomes*. *J Biol Chem*, 1992. **267**(31): p. 22243-8.
205. Nicholls, P., *Cytochrome c binding to enzymes and membranes*. *Biochim Biophys Acta*, 1974. **346**(3-4): p. 261-310.
206. Kawasaki, K., et al., *Isolation of a chinese hamster ovary (CHO) cDNA encoding phosphatidylglycerophosphate (PGP) synthase, expression of which corrects the mitochondrial abnormalities of a PGP synthase-defective mutant of CHO-K1 cells*. *J Biol Chem*, 1999. **274**(3): p. 1828-34.
207. Chang, S.C., et al., *Isolation and characterization of the gene (CLS1) encoding cardiolipin synthase in Saccharomyces cerevisiae*. *J Biol Chem*, 1998. **273**(24): p. 14933-41.
208. Paradies, G., et al., *Lipid peroxidation and alterations to oxidative metabolism in mitochondria isolated from rat heart subjected to ischemia and reperfusion*. *Free Radic Biol Med*, 1999. **27**(1-2): p. 42-50.
209. Paradies, G., et al., *Age-dependent decline in the cytochrome c oxidase activity in rat heart mitochondria: role of cardiolipin*. *FEBS Lett*, 1997. **406**(1-2): p. 136-8.
210. Paradies, G., et al., *The effect of reactive oxygen species generated from the mitochondrial electron transport chain on the cytochrome c oxidase activity and on the cardiolipin content in bovine heart submitochondrial particles*. *FEBS Lett*, 2000. **466**(2-3): p. 323-6.
211. Paradies, G., et al., *Reactive oxygen species affect mitochondrial electron transport complex I activity through oxidative cardiolipin damage*. *Gene*, 2002. **286**(1): p. 135-41.
212. Ushmorov, A., et al., *Nitric-oxide-induced apoptosis in human leukemic lines requires mitochondrial lipid degradation and cytochrome C release*. *Blood*, 1999. **93**(7): p. 2342-52.
213. Kirkland, R.A., et al., *Loss of cardiolipin and mitochondria during programmed neuronal death: evidence of a role for lipid peroxidation and autophagy*. *Neuroscience*, 2002. **115**(2): p. 587-602.
214. Kagan, V.E., et al., *Cytochrome c acts as a cardiolipin oxygenase required for release of proapoptotic factors*. *Nat Chem Biol*, 2005. **1**(4): p. 223-32.
215. Hardy, S., et al., *Saturated fatty acid-induced apoptosis in MDA-MB-231 breast cancer cells. A role for cardiolipin*. *J Biol Chem*, 2003. **278**(34): p. 31861-70.
216. Ostrander, D.B., et al., *Decreased cardiolipin synthesis corresponds with cytochrome c release in palmitate-induced cardiomyocyte apoptosis*. *J Biol Chem*, 2001. **276**(41): p. 38061-7.
217. Rytomaa, M. and P.K. Kinnunen, *Reversibility of the binding of cytochrome c to liposomes. Implications for lipid-protein interactions*. *J Biol Chem*, 1995. **270**(7): p. 3197-202.
218. Gorbenko, G.P., *Structure of cytochrome c complexes with phospholipids as revealed by resonance energy transfer*. *Biochim Biophys Acta*, 1999. **1420**(1-2): p. 1-13.
219. Cortese, J.D., A.L. Voglino, and C.R. Hackenbrock, *Persistence of cytochrome c binding to membranes at physiological mitochondrial intermembrane space ionic strength*. *Biochim Biophys Acta*, 1995. **1228**(2-3): p. 216-228.

220. Pereverzev, M.O., et al., *Cytochrome c, an ideal antioxidant*. *Biochem Soc Trans*, 2003. **31**(Pt 6): p. 1312-5.
221. Nomura, K., et al., *Mitochondrial phospholipid hydroperoxide glutathione peroxidase inhibits the release of cytochrome c from mitochondria by suppressing the peroxidation of cardiolipin in hypoglycaemia-induced apoptosis*. *Biochem J*, 2000. **351**(Pt 1): p. 183-93.
222. Shidoji, Y., et al., *Loss of molecular interaction between cytochrome c and cardiolipin due to lipid peroxidation*. *Biochem Biophys Res Commun*, 1999. **264**(2): p. 343-7.
223. Ott, M., et al., *Cytochrome c release from mitochondria proceeds by a two-step process*. *Proc Natl Acad Sci U S A*, 2002. **99**(3): p. 1259-63.
224. Garcia-Saez, A.J., et al., *Membrane-insertion fragments of Bcl-xL, Bax, and Bid*. *Biochemistry*, 2004. **43**(34): p. 10930-43.
225. Epand, R.F., et al., *The Apoptotic Protein tBid Promotes Leakage by Altering Membrane Curvature*. *J Biol Chem*, 2002. **277**(36): p. 32632-9.
226. Esposti, M.D., et al., *Proapoptotic Bid binds to monolysocardiolipin, a new molecular connection between mitochondrial membranes and cell death*. *Cell Death Differ*, 2003. **10**(12): p. 1300-9.
227. Liu, J., et al., *The interaction between tBid and cardiolipin or monolysocardiolipin*. *Biochem Biophys Res Commun*, 2005. **330**(3): p. 865-70.
228. Garcia Fernandez, M., et al., *Early changes in intramitochondrial cardiolipin distribution during apoptosis*. *Cell Growth Differ*, 2002. **13**(9): p. 449-55.
229. Aguilar, L., et al., *Phospholipid membranes form specific nonbilayer molecular arrangements that are antigenic*. *J Biol Chem*, 1999. **274**(36): p. 25193-6.
230. Esposti, M.D., et al., *Bid, a widely expressed proapoptotic protein of the Bcl-2 family, displays lipid transfer activity*. *Mol Cell Biol*, 2001. **21**(21): p. 7268-76.
231. Sorice, M., et al., *Cardiolipin and its metabolites move from mitochondria to other cellular membranes during death receptor-mediated apoptosis*. *Cell Death Differ*, 2004. **11**(10): p. 1133-45.
232. Iverson, S.L., et al., *Cardiolipin is not required for Bax-mediated cytochrome c release from yeast mitochondria*. *J Biol Chem*, 2004. **279**(2): p. 1100-7.
233. Polcic, P., et al., *Cardiolipin and phosphatidylglycerol are not required for the in vivo action of Bcl-2 family proteins*. *Cell Death Differ*, 2005. **12**(3): p. 310-2.
234. Rytomaa, M. and P.K. Kinnunen, *Evidence for two distinct acidic phospholipid-binding sites in cytochrome c*. *J Biol Chem*, 1994. **269**(3): p. 1770-4.
235. Kagan, V.E., et al., *The "pro-apoptotic genes" get out of mitochondria: oxidative lipidomics and redox activity of cytochrome c/cardiolipin complexes*. *Chem Biol Interact*, 2006. **163**(1-2): p. 15-28.
236. Hanahan, D. and R.A. Weinberg, *The hallmarks of cancer*. *Cell*, 2000. **100**(1): p. 57-70.
237. Daniel, P.T., et al., *The kiss of death: promises and failures of death receptors and ligands in cancer therapy*. *Leukemia*, 2001. **15**(7): p. 1022-32.
238. Reed, J.C., *Drug insight: cancer therapy strategies based on restoration of endogenous cell death mechanisms*. *Nat Clin Pract Oncol*, 2006. **3**(7): p. 388-98.
239. Hyer, M.L., et al., *Synthetic triterpenoids cooperate with tumor necrosis factor-related apoptosis-inducing ligand to induce apoptosis of breast cancer cells*. *Cancer Res*, 2005. **65**(11): p. 4799-808.
240. Li, L., et al., *A small molecule Smac mimic potentiates TRAIL- and TNFalpha-mediated cell death*. *Science*, 2004. **305**(5689): p. 1471-4.
241. Schimmer, A.D., et al., *Small-molecule antagonists of apoptosis suppressor XIAP exhibit broad antitumor activity*. *Cancer Cell*, 2004. **5**(1): p. 25-35.
242. Klasa, R.J., et al., *Oblimersen Bcl-2 antisense: facilitating apoptosis in anticancer treatment*. *Antisense Nucleic Acid Drug Dev*, 2002. **12**(3): p. 193-213.

243. Oltersdorf, T., et al., *An inhibitor of Bcl-2 family proteins induces regression of solid tumours*. Nature, 2005. **435**(7042): p. 677-81.
244. Johnston, J., et al., *Mutation characterization and genotype-phenotype correlation in Barth syndrome*. Am J Hum Genet, 1997. **61**(5): p. 1053-8.
245. Frey, T.G. and C.A. Mannella, *The internal structure of mitochondria*. Trends Biochem Sci, 2000. **25**(7): p. 319-24.
246. Cooper, C.E., P. Nicholls, and J.A. Freedman, *Cytochrome c oxidase: structure, function, and membrane topology of the polypeptide subunits*. Biochem Cell Biol, 1991. **69**(9): p. 586-607.
247. Landriscina, C., F.M. Megli, and E. Quagliariello, *Turnover of fatty acids in rat liver cardiolipin: comparison with other mitochondrial phospholipids*. Lipids, 1976. **11**(1): p. 61-6.
248. Kaufmann, S.H., et al., *Specific proteolytic cleavage of poly(ADP-ribose) polymerase: an early marker of chemotherapy-induced apoptosis*. Cancer Res, 1993. **53**(17): p. 3976-85.
249. Tewari, M., et al., *Yama/CPP32 beta, a mammalian homolog of CED-3, is a CrmA-inhibitable protease that cleaves the death substrate poly(ADP-ribose) polymerase*. Cell, 1995. **81**(5): p. 801-9.
250. Valianpour, F., et al., *Quantitative and compositional study of cardiolipin in platelets by electrospray ionization mass spectrometry: application for the identification of Barth syndrome patients*. Clin Chem, 2002. **48**(9): p. 1390-7.
251. Valianpour, F., et al., *Cardiolipin deficiency in X-linked cardioskeletal myopathy and neutropenia (Barth syndrome, MIM 302060): a study in cultured skin fibroblasts*. J Pediatr, 2002. **141**(5): p. 729-33.
252. Schlame, M., et al., *Deficiency of tetralinoleoyl-cardiolipin in Barth syndrome*. Ann Neurol, 2002. **51**(5): p. 634-7.
253. van Werkhoven, M.A., et al., *Monolysocardiolipin in cultured fibroblasts is a sensitive and specific marker for Barth Syndrome*. J Lipid Res, 2006. **47**(10): p. 2346-51.
254. Bissler, J.J., et al., *Infantile dilated X-linked cardiomyopathy, G4.5 mutations, altered lipids, and ultrastructural malformations of mitochondria in heart, liver, and skeletal muscle*. Lab Invest, 2002. **82**(3): p. 335-44.
255. Acehan, D., et al., *Comparison of lymphoblast mitochondria from normal subjects and patients with Barth syndrome using electron microscopic tomography*. Lab Invest, 2007. **87**(1): p. 40-8.
256. Xu, Y., et al., *A Drosophila model of Barth syndrome*. Proc Natl Acad Sci U S A, 2006. **103**(31): p. 11584-8.
257. Zhang, M., E. Mileykovskaya, and W. Dowhan, *Gluing the respiratory chain together. Cardiolipin is required for supercomplex formation in the inner mitochondrial membrane*. J Biol Chem, 2002. **277**(46): p. 43553-6.
258. Pfeiffer, K., et al., *Cardiolipin stabilizes respiratory chain supercomplexes*. J Biol Chem, 2003. **278**(52): p. 52873-80.
259. Brandner, K., et al., *Taz1, an outer mitochondrial membrane protein, affects stability and assembly of inner membrane protein complexes: implications for Barth Syndrome*. Mol Biol Cell, 2005. **16**(11): p. 5202-14.
260. Schwarz, E., et al., *Structure and transcription of human papillomavirus sequences in cervical carcinoma cells*. Nature, 1985. **314**(6006): p. 111-4.
261. Sedorf, K., et al., *Identification of early proteins of the human papilloma viruses type 16 (HPV 16) and type 18 (HPV 18) in cervical carcinoma cells*. Embo J, 1987. **6**(1): p. 139-44.
262. Werness, B.A., A.J. Levine, and P.M. Howley, *Association of human papillomavirus types 16 and 18 E6 proteins with p53*. Science, 1990. **248**(4951): p. 76-9.

263. Chou, J.J., et al., *Solution structure of BID, an intracellular amplifier of apoptotic signaling*. Cell, 1999. **96**(5): p. 615-24.
264. Chandra, D., et al., *Association of active caspase 8 with the mitochondrial membrane during apoptosis: potential roles in cleaving BAP31 and caspase 3 and mediating mitochondrion-endoplasmic reticulum cross talk in etoposide-induced cell death*. Mol Cell Biol, 2004. **24**(15): p. 6592-607.
265. Qin, Z.H., et al., *Pro-caspase-8 is predominantly localized in mitochondria and released into cytoplasm upon apoptotic stimulation*. J Biol Chem, 2001. **276**(11): p. 8079-86.
266. Boldogh, I.R. and L.A. Pon, *Interactions of mitochondria with the actin cytoskeleton*. Biochim Biophys Acta, 2006. **1763**(5-6): p. 450-62.
267. Milovic-Holm, K., et al., *FLASH links the CD95 signaling pathway to the cell nucleus and nuclear bodies*. Embo J, 2007. **26**(2): p. 391-401.
268. Juo, P., et al., *Essential requirement for caspase-8/FLICE in the initiation of the Fas-induced apoptotic cascade*. Curr Biol, 1998. **8**(18): p. 1001-8.
269. Tinel, A. and J. Tschopp, *The PIDDosome, a protein complex implicated in activation of caspase-2 in response to genotoxic stress*. Science, 2004. **304**(5672): p. 843-6.
270. Martinon, F., K. Burns, and J. Tschopp, *The inflammasome: a molecular platform triggering activation of inflammatory caspases and processing of proIL-beta*. Mol Cell, 2002. **10**(2): p. 417-26.
271. Tafani, M., et al., *Cytochrome c release upon Fas receptor activation depends on translocation of full-length bid and the induction of the mitochondrial permeability transition*. J Biol Chem, 2002. **277**(12): p. 10073-82.
272. Grinberg, M., et al., *tBID Homooligomerizes in the mitochondrial membrane to induce apoptosis*. J Biol Chem, 2002. **277**(14): p. 12237-45.
273. McDonnell, J.M., et al., *Solution structure of the proapoptotic molecule BID: a structural basis for apoptotic agonists and antagonists*. Cell, 1999. **96**(5): p. 625-34.
274. Hu, X., et al., *Helix 6 of tBid is necessary but not sufficient for mitochondrial binding activity*. Apoptosis, 2003. **8**(3): p. 277-89.
275. Wilson, K.S., et al., *Differential gene expression patterns in HER2/neu-positive and -negative breast cancer cell lines and tissues*. Am J Pathol, 2002. **161**(4): p. 1171-85.
276. Kobayashi, T., et al., *Microarray reveals differences in both tumors and vascular specific gene expression in de novo CD5+ and CD5- diffuse large B-cell lymphomas*. Cancer Res, 2003. **63**(1): p. 60-6.
277. Bleyl, S.B., et al., *Neonatal, lethal noncompaction of the left ventricular myocardium is allelic with Barth syndrome*. Am J Hum Genet, 1997. **61**(4): p. 868-72.
278. Stupack, D.G., et al., *Potentiation of neuroblastoma metastasis by loss of caspase-8*. Nature, 2006. **439**(7072): p. 95-9.
279. Stupack, D.G., et al., *Apoptosis of adherent cells by recruitment of caspase-8 to unligated integrins*. J Cell Biol, 2001. **155**(3): p. 459-70.